

**Preparation, Characterization and X-ray Crystal Structures of  
New Axially Functionalized Phthalocyanines and Phthalocyanine  
Modified SBA-15 Materials**

**Darstellung, Charakterisierung und Kristallstrukturen neuer  
axial funktionalisierter Phthalocyanine und Phthalocyanin-  
modifizierter SBA-15 Materialien**

**Dissertation**

Zur

Erlangung des Doktorgrades  
der Naturwissenschaften  
(Dr. rer. nat)

dem

Fachbereich Chemie  
der Philipps-Universität Marburg

Vorgelegt von

**Wael Mahmoud Ahmed Darwish**

aus Lekalyoubia

Marburg/Lahn 2006

Die vorliegende Arbeit entstand in der Zeit von Oktober 2001 bis Februar 2006 unter der Leitung von Herrn Prof. Dr. J. H. Sundermeyer am Fachbereich Chemie der Philipps-Universität Marburg.

Vom Fachbereich Chemie der Philipps-Universität Marburg als Dissertation angenommen am 15. Februar 2006

1. Gutachter: Prof. Dr. J. H. Sundermeyer

2. Gutachter: Prof. Dr. W. Massa

Tag der Disputation: 02 März 2006

*To my Parents, my Wife,  
my Daughter (Rawan),  
and every one taught me Chemistry  
To my Homeland  
Egypt*

## Acknowledgment

I wish to express my deepest thanks to Prof. Dr. J. H. Sundermeyer, Professor of Chemistry, Philipps-Universität Marburg, for supervision, valuable guidance and fruitful discussions.

I'm grateful to Dr. K. Steinbach for (MS) measurements, Dr. O. Burghaus (ESR), Dr. Weller and Mr. Schmock (RS), Mrs. Bahmann (FTIR), Mr. Lennick and Mr. Ulrich (EA), Dr. Xie (NMR-500 MHz), Mr. Beifus (GPC), and Dr. Schaper (TEM). I'm also grateful to Prof. Dr. W. Massa, Dr. K. Harms and Mrs. G. Geiseler for carrying out the X-ray crystallographic measurements of some isolated single crystals.

I would like to thank Prof. Dr. W. Rühle and his research group (Dr. S. Chatterjee and K. Hankte) at Physics Department, Philipps-Universität Marburg for carrying out the photoluminescence measurements of some compounds and together discussion of the results within a cooperation project. I'm very grateful to Prof. Dr. S. Schlecht, Professor of Chemistry, Freie-Universität, Berlin and Prof. M. Fröba, Professor of Chemistry, Justus-Liebig-Universität, Gießen for fruitful discussions in the field of mesoporous materials.

I would like also to thank Prof. Dr. Mahmoud A. Abd El-Ghaffar, Prof. of Polymers and Pigments, Dr. Elham A. Youssef, and Prof. Dr. A. S. Badran; National Research Centre, Cairo, Egypt for support and kind help.

My thanks are extended to my colleagues in AK Sundermeyer. I would like also to thank my colleagues at Philipps-Universität: Dr. S. Agarwal, M. Becker, S. Horst, and Frau M. Gerlach for kind help.

# Table of Contents

## 1. Introduction

1.1	History of Phthalocyanines .....	1
1.2	Structure of Phthalocyanines .....	1
1.3	Synthesis and Purification of Phthalocyanines .....	2
1.4	Mechanism of Phthalocyanine Formation .....	3
1.5	Crystal Structure of Phthalocyanines .....	5
1.6	The Electronic Structure of Metal Phthalocyanines .....	7
1.7	Applications of Phthalocyanines .....	7
1.8	Titanium Phthalocyanines	
1.8.1	Dichlorotitaniumphthalocyanine [PcTiCl <sub>2</sub> ] .....	8
1.8.2	Oxotitaniumphthalocyanine [PcTiO] .....	9
1.9	Titanium Porphyrins .....	13
1.10	Phthalocyanines and Porphyrins of Mo,W and Re .....	15
1.11	Phthalocyanine Polymers .....	17
1.12	Mesoporous Molecular Sieve Materials	
1.12.1	Preparation of SBA-15 and MCM-41 Materials .....	19
1.12.2	Preparation of Titanium Containing SBA-15 and MCM-41 .....	20
1.12.3	Properties of Mesoporous Molecular Sieves .....	21
1.12.4	Phthalocyanine Modified Mesoporous Molecular Sieves .....	22
1.12.5	Characterization of MPc Modified Mesoporous Molecular Sieves .....	27
1.12.6	Applications of MPc Modified Mesoporous Molecular Sieve Materials	27
1.13	Photoluminescence of Phthalocyanines .....	28
1.14	Phthalocyanines as Laser Pigments .....	29

## 2. Results and Discussions

### 2.1 Titanium Phthalocyanines

2.1.1	Synthesis of Imido-TiPc ( <b>2</b> ) and Ureato-TiPcs ( <b>3a-d</b> ) .....	30
2.1.2	Mechanism for the reaction of [PcTiO] ( <b>1</b> ) with the arylisocyanates .....	31
2.1.3	Characterization of the Imido-TiPc ( <b>2</b> ) and Ureato-TiPcs ( <b>3a-d</b> ) .....	33
2.1.4	Crystal Structure of [PcTi(NDip)] ( <b>2</b> ) .....	40

2.1.5	Crystal Structures of [PcTi(diarylyureato)] ( <b>3a</b> ) and ( <b>3b</b> ) .....	44
2.1.6	Reaction of [PcTi(diarylyureato)] with H <sub>2</sub> S .....	49
2.1.7	Crystal Structure of [PcTi( $\eta^2$ -S <sub>2</sub> )] ( <b>5</b> ) .....	50
2.1.8	Preparation of [PcTiS] ( <b>4</b> ) starting with [PcTiO] .....	53
2.1.9	Synthesis of [PcTi{(NH) <sub>2</sub> C <sub>6</sub> H <sub>4</sub> }] ( <b>6</b> ) .....	54
2.1.10	Synthesis of trans-[PcTi(OSiPh <sub>3</sub> ) <sub>2</sub> ] ( <b>7</b> ) .....	56
2.1.11	Crystal Structure of trans-[PcTi(OSiPh <sub>3</sub> ) <sub>2</sub> ] ( <b>7</b> ) .....	58
<b>2.2</b>	<b>Molybdenum Phthalocyanines</b>	
2.2.1	Synthesis of [PcMo(NR)Cl] ( <b>9a,b</b> ) .....	61
2.2.2	Characterization of [PcMo(NR)Cl] ( <b>9a,b</b> ) .....	63
2.2.3	ESR Spectra of [PcMo(NR)Cl] ( <b>9a,b</b> ) .....	65
2.2.4	Crystal Structure of [PcMo(NR)Cl] ( <b>9a</b> ) .....	68
<b>2.3</b>	<b>Tungsten Phthalocyanines</b>	
2.3.1	Synthesis of [PcW(NR)Cl] ( <b>11a,b</b> ) .....	72
2.3.2	Characterization of [PcW(NR)Cl] ( <b>11a,b</b> ) .....	72
2.3.3	ESR Spectra of [PcW(NR)Cl] ( <b>11a,b</b> ) .....	73
2.3.4	Synthesis of [(Cl <sub>2</sub> Pc)W(NR)] ( <b>13a-c</b> ) .....	77
2.3.5	Characterization of [(Cl <sub>2</sub> Pc)W(NR)] ( <b>13a-c</b> ) .....	79
<b>2.4</b>	<b>Rhenium Phthalocyanines</b>	
2.4.1	Synthesis of [PcRe(NR)Cl] ( <b>15a,b</b> ) .....	81
2.4.2	Characterization of [PcRe(NR)Cl] ( <b>15a,b</b> ) .....	82
<b>2.5</b>	<b>Phthalocyanine Polymers</b>	
2.5.1	Synthesis of Phthalocyanine Polymers ( <b>16-18</b> ) .....	84
2.5.2	Characterization of Phthalocyanine Polymers ( <b>16-18</b> ) .....	86
<b>2.6</b>	<b>Time-resolved Photoluminescence</b> .....	90
<b>2.7</b>	<b>Phthalocyanine Modified SBA-15 Mesoporous Silica Materials</b> .....	94
<b>3.</b>	<b>Summary</b> .....	105

## 4. Experimental Work

<b>4.1</b>	<b>Materials and Methods</b> .....	114
<b>4.2</b>	<b>Techniques of Characterization</b> .....	115
<b>4.3</b>	<b>Preparation of Titanium Phthalocyanines</b>	
4.3.1	Preparation of [PcTi(NDip)] ( <b>2</b> ) .....	118
4.3.2	Preparation of [PcTi(diarylureato)] ( <b>3a-d</b> ) .....	119
4.3.3	Preparation of [PcTiS] ( <b>4</b> ) .....	124
4.3.4	Preparation of [PcTi( $\eta$ -S <sub>2</sub> )] ( <b>5</b> ) .....	125
4.3.5	Preparation of [PcTi{(NH) <sub>2</sub> C <sub>6</sub> H <sub>4</sub> }] ( <b>6</b> ) .....	127
4.3.6	Preparation of trans-[PcTi(OSiPh <sub>3</sub> ) <sub>2</sub> ] ( <b>7</b> ) .....	127
<b>4.4</b>	<b>Preparation of Molybdenum Phthalocyanines</b>	
4.4.1	Preparation of [PcMo(N <sup>t</sup> Bu)Cl] ( <b>9a</b> ) .....	129
4.4.2	Preparation of [PcMo(NMes)Cl] ( <b>9b</b> ) .....	130
<b>4.5</b>	<b>Preparation of Tungsten Phthalocyanines</b>	
4.5.1	Preparation of [PcW(N <sup>t</sup> Bu)Cl] ( <b>11a</b> ) .....	131
4.5.2	Preparation of [PcW(NMes)Cl] ( <b>11b</b> ) .....	132
4.5.3	Preparation of [(Cl <sub>2</sub> Pc)W(NR)] ( <b>13a-c</b> ) .....	132
<b>4.6</b>	<b>Preparation of Rhenium Phthalocyanines</b>	
4.6.1	Preparation of [PcRe(N <sup>t</sup> Bu)Cl] ( <b>15a</b> ) .....	134
4.6.2	Preparation of [PcRe(NMes)Cl] ( <b>15b</b> ) .....	134
<b>4.7</b>	<b>Phthalocyanine Polymers</b>	
4.7.1	Preparation of Polyoxotitaniumphthalocyanine ( <b>16</b> ) .....	135
4.7.2	Preparation of Polyimidomolybdenumphthalocyanine ( <b>17</b> ) .....	136
4.7.3	Preparation of Polyimidotitaniumphthalocyanine ( <b>18</b> ) .....	137

<b>4.8</b>	<b>Time-resolved Photoluminescence Study of TiPcs .....</b>	<b>137</b>
<b>4.9</b>	<b>Preparation of Phthalocyanine Modified Silica Materials .....</b>	<b>139</b>
<b>5.</b>	<b>References .....</b>	<b>141</b>



## List of Abbreviations

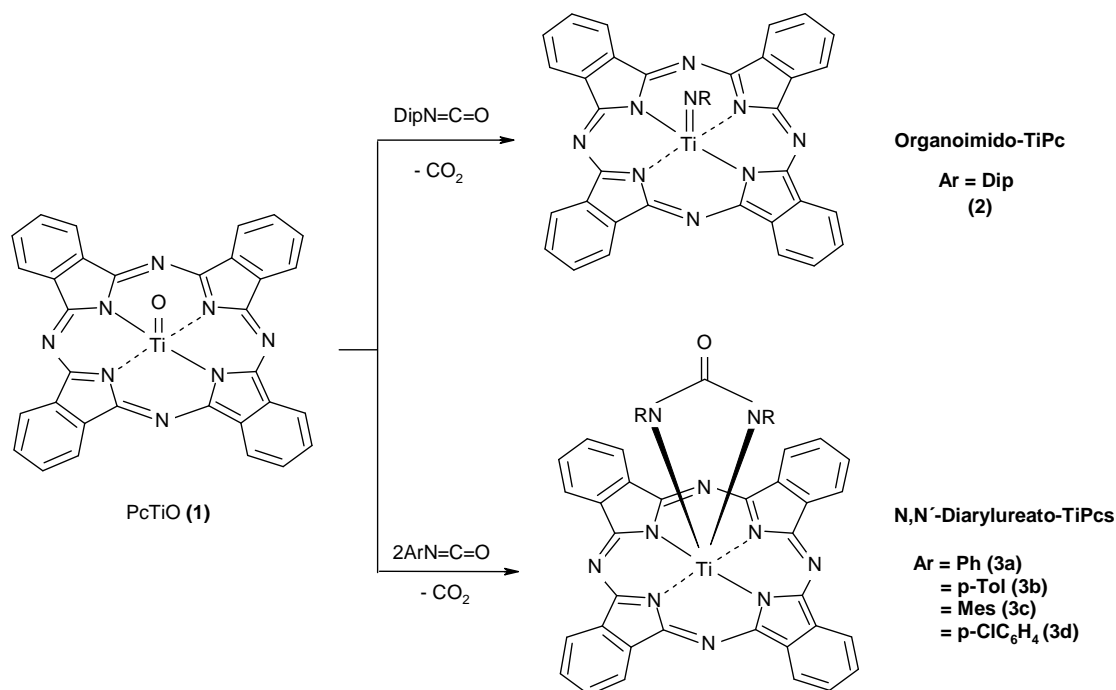
AAS	: Atom Absorption Spectroscopy
Calcd.	: Calculated
CHN	: Combustion analysis of mass %C, H, and N
CIB	: Chlorobenzene
CIN	: Chloronaphthalene
dme	: 1,2-Dimethoxyethane
DSC	: Differential Scanning Calorimetry
EA	: Elemental Analysis
EI-MS	: Electron Impact Mass Spectroscopy
EPR	: Electron Paramagnetic Resonance
ESI-MS	Electron Spray Ionization Mass Spectroscopy
ESR	: Electron Spin Resonance
GPC	: Gel Permeation Chromatography
M	mole L <sup>-1</sup>
M <sup>+</sup>	: Molecular ion peak
MALDI-TOF	Matrix Associated Laser Desorption Ionization (Time of Flight analyser)
MCM	: Mobil Composition of Matter
MPc	: Metal Phthalocyanine
MT	: MALDI-TOF
NMR	: Nuclear Magnetic Resonance
P	: Porphyrinato ligand
Pc	: Phthalocyanine ligand
PcH <sub>2</sub>	: metal-free phthalocyanine
PL	: Photoluminescence
PN	: 1,2- Dicyanobenzene or (1,2-Phthalodinitrile)
RS	: Raman Spectra
SBA-15	: Santa Barbara (15: mesoporous silica of hexagonal pore structure)
TCB	: 1,2,4,5-Tetracyanobenzene
TEM	: Transmission Electron Microscope
TGA	: Thermal Gravimetric Analysis
TTP	: Tetratolylporphrinato ligand

## **Aim of the Work**

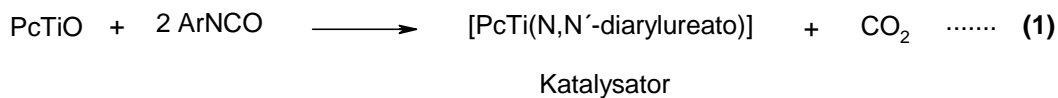
This work aimed at the development of new approaches to the building up of axially functionalized phthalocyanines of titanium, molybdenum, tungsten and rhenium, in which the organoimido or the diarylureato axial functionalities are capable to do further reactions with other reagents such as  $\text{H}_2\text{S}$ ,  $\text{Ph}_3\text{SiOH}$ , etc. Further we aimed at characterization of the prepared phthalocyanines using MS, UV/VIS, FTIR, AAS, TGA, DSC, etc. to get a close approach to the relation between their structure patterns and properties. Despite of the poor solubility of the prepared MPcs relative to the peripherally substituted MPcs, this work aimed at carrying out several attempts to grow up single crystals suitable for X-ray crystal structure measurements in order to identify the common arrangement patterns, which are seen among the different phthalocyanine structures. Crystal structures of the phthalocyanines are the fundament for the calculations or prediction of their properties. Different arrangements of the molecules in the lattice lead to materials with different physical properties such as photoconductivity and optical properties. Therefore, a great interest lies in the prediction of crystal structures from the molecular structure and calculations of physical properties there from. An important advantage of these axially functionalized metalphthalocyanines may be the possibility to anchor them covalently and in monomeric distribution in the pores of different silica templates, to prepare new MPc modified mesoporous silica materials. These materials have attracted the attention of many researchers in the last decade trying to understand the chemistry of these materials since the MPc/silica materials have found industrial applications. The chromophore-loaded inorganic hosts have been investigated in the last years for different properties, such as photocatalyst, novel pigments and nonlinear optical materials exhibiting optical bistabilities, frequency doubling, and spectral hole-burning or lasing.

## Zusammenfassung

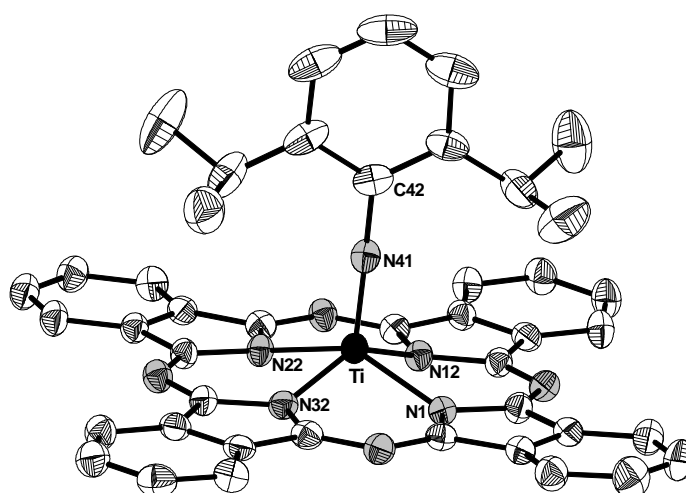
Ringsubstituierte Titanylphthalocyanine sind photoleitende Materialien im xerographischen Prozess von Fotokopierern oder Laser-Druckern, die im Sinne eines „green chemistry“ Konzeptes Selen als photoleitende Schicht ersetzt haben. Außerdem sind  $[(R_xPc)Ti=O]$  Verbindungen Laserpigmente der CD-ROM Technologie. Während organische Substitutionen am Ring im Fokus der gegenwärtigen Forschung stehen, sind Substitutionen an der axialen Titanylfunktion weitgehend unerforscht. Das Ziel der vorliegenden Arbeit war die Erforschung der Chemie der Titanylphthalocyanine. Es wurden Metathesereaktionen von  $[PcTiO]$  (**1**) untersucht, um isoelektronische Verbindungen des Typs  $PcTiX$  ( $X = S, Se, NR,$  usw) zu synthetisieren. Die Isocyanat-Metathesereaktion hängt stark von der Grösse der Arylisocyanate ab. Im Fall des sterisch anspruchsvollen 2,6-Diisopropylphenylisocyanats (DipNCO) scheint, dass nur eine Addition eines Isocyanates möglich ist. Der Angriff eines zweiten Isocyanat Moleküls an die  $[Ti=NAr]$  Funktion ist durch den hohen sterischen Anspruch der zwei Isopropylgruppen gehindert. Für kleine Gruppen, wie z.B.  $R = Phenyl$ , konnte der Imidokomplex nicht isoliert werden, da er breitwillig mit einem zweiten Äquivalent  $ArNCO$  in einer  $[2+2]$  Cycloaddition zu  $N,N'$ -Diarylureato-titan-phthalocyaninen (**3a-d**) reagiert. In diesen Fällen wurden die entsprechenden Diarylcarbodimide als weiße Nebenprodukte beobachtet.



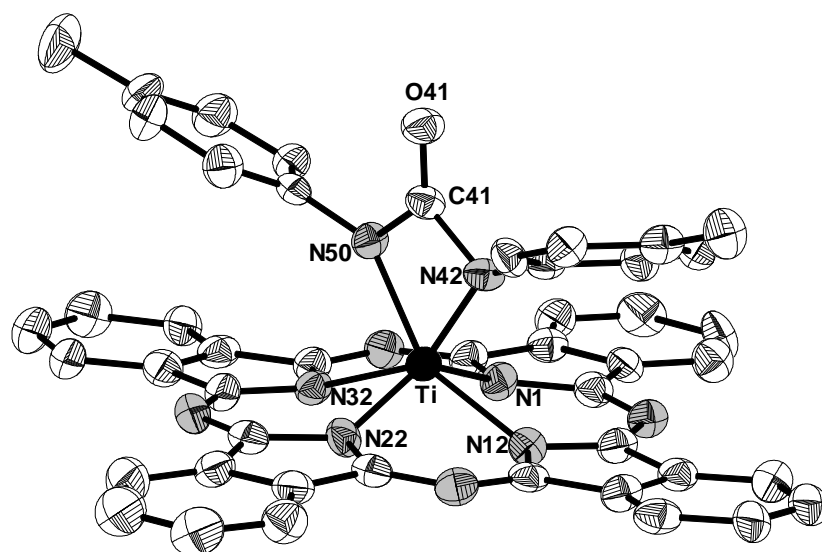
Die Reaktion von **(1)** mit Arylisocyanaten, die kleine Arylgruppen enthalten, konnte in der katalytischen Metathese von Arylisocyanaten zu Diarylcarbodiimiden und CO<sub>2</sub> angewendet werden.



Die Verbindung **(2)** kristallisiert in der zentrosymmetrischen Raumgruppe (P<sub>2</sub><sub>1</sub>/n) mit vier Molekülen in der Elementarzelle. Das Molekül enthält fünffach koordiniertes Ti (IV), welches von vier äquatorialen Isoindolin-Ringen des Pc Moleküls umgeben ist. Der Imidoligand steht in axialer Position. Das Titanatom liegt 0.594(1) Å oberhalb der Ebene der vier Stickstoffatome. Die Verbindung **(3a)** kristallisiert in der zentrosymmetrischen Raumgruppe (P<sub>2</sub><sub>1</sub>/n) mit vier Molekülen in der Elementarzelle. Die Verbindung **(3b)** kristallisiert in der zentrosymmetrischen Raumgruppe (P $\bar{1}$ ) mit zwei Molekülen in der Elementarzelle. In beiden Strukturen **(3a)** und **(3b)** enthält das Molekül fünffach koordiniertes Ti (IV), welches von vier äquatorialen Isoindolin-Ringen des Pc Moleküls umgeben ist. Der Ureatoligand steht in axialer Position. Das Titanatom liegt oberhalb der Ebene der vier Stickstoffatome in Richtung auf den Imidoligand mit einem Abstand von 0.791(1)Å in **(3a)** und 0.763(6)Å in **(3b)** zur Ebene.

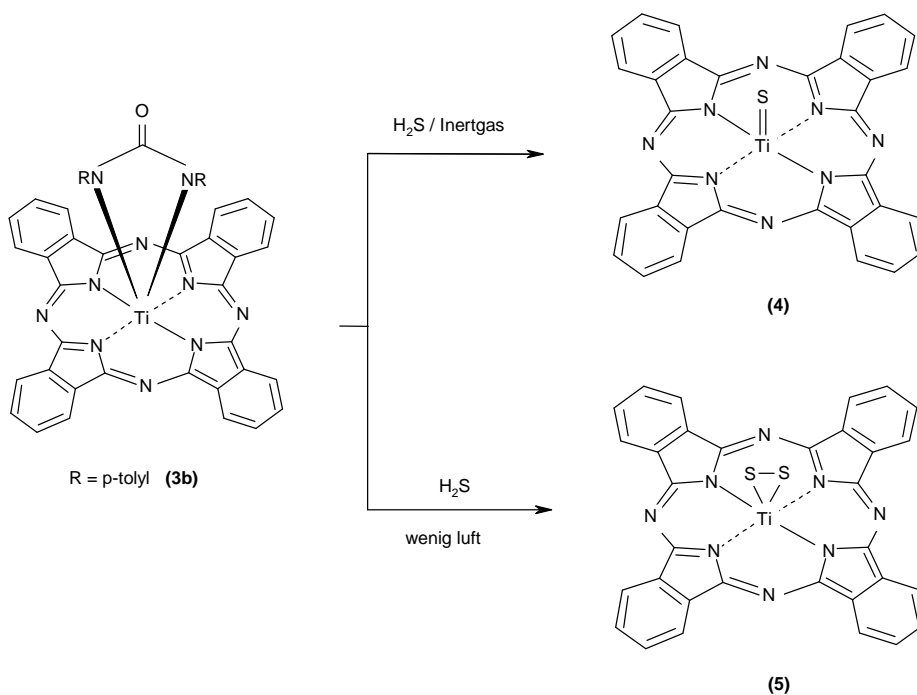


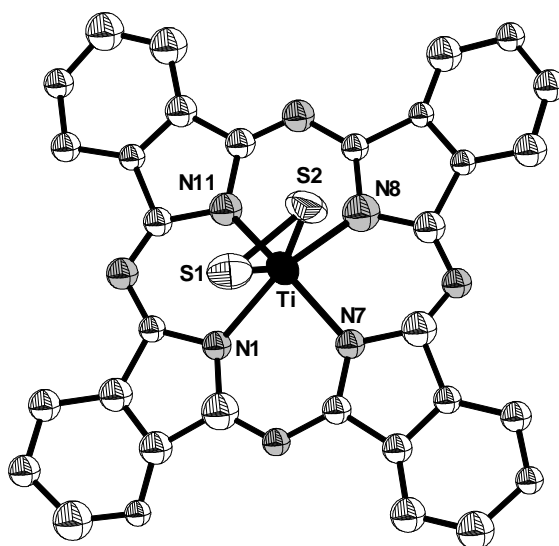
Die Molekülstruktur von [PcTi=NDip] **(2)**.



Die Molekülstruktur von [PcTi(N,N'-Ditoylureato)] (**3b**).

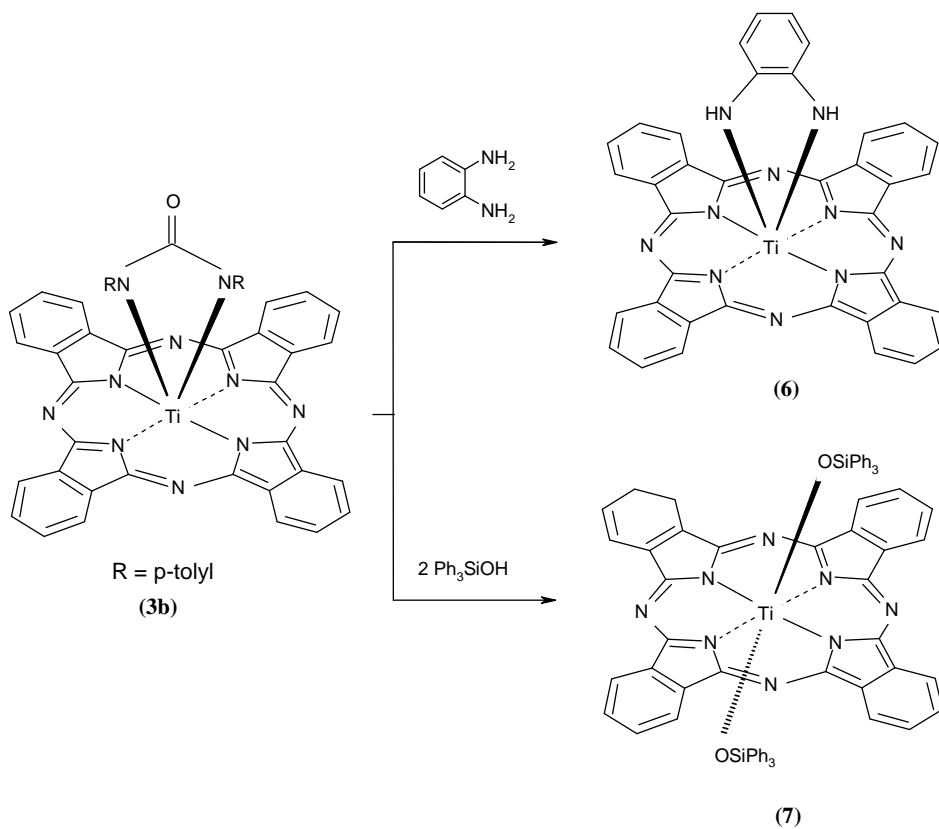
Die Reaktion von N,N'-Ditoylureato-(phthalocyaninato)-titan (**3b**) mit H<sub>2</sub>S Gas in Chlornaphthalin hängt sehr stark davon ab, ob sie unter Inertgas oder an Luft durchgeführt wird. Wird die Reaktion unter Inertgas durchgeführt, entsteht quantitativ Verbindung (**4**). Wird die Reaktion an Luft durchgeführt, entsteht quantitativ Verbindung (**5**). Die Kristallstruktur von (**5**) zeigt dass die  $\eta^2$ -S<sub>2</sub> Gruppe "side-on" in axialer Position koordiniert.

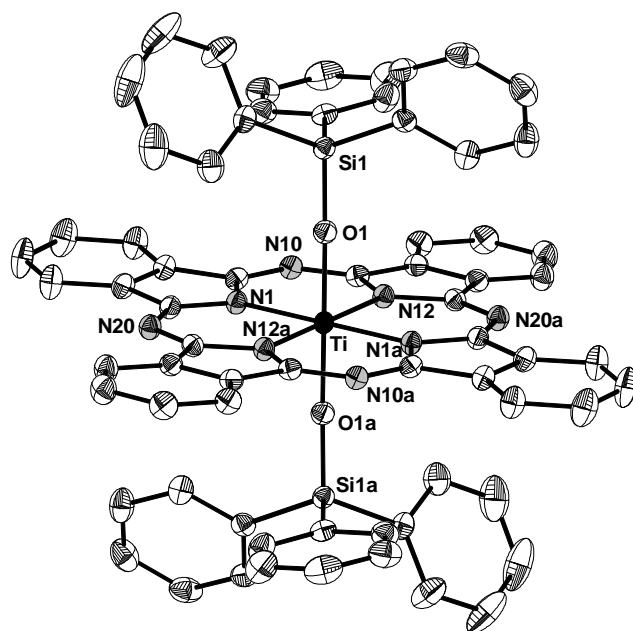




Die Molekülstruktur von  $[\text{PcTi}(\eta^2\text{-S}_2)]$  (**5**).

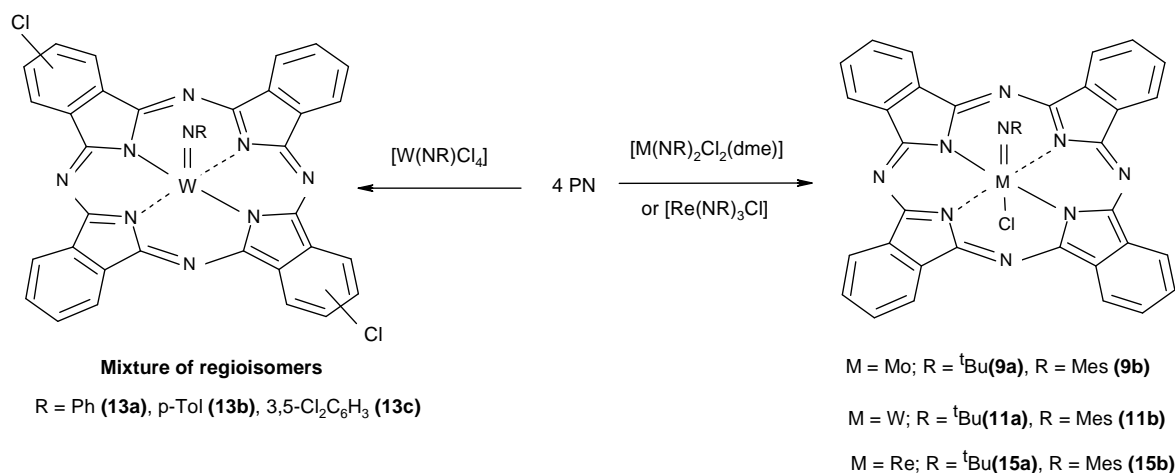
Die Reaktion von **(3b)** mit 1,2-Phenylendiamin führt zu  $[\text{PcTi}\{(\text{NH})_2\text{C}_6\text{H}_5\}]$  (**6**). Außerdem reagiert **(3b)** mit  $\text{Ph}_3\text{SiOH}$  zu  $\text{trans-}[\text{PcTi}(\text{OSiPh}_3)_2]$  (**7**). Diese Reaktion führt zu einer trans-Addition von zwei Triphenylsiloxy-Liganden am Titanatom. Die cis-Addition wird durch die starke sterische Hinderung der drei Phenylgruppen verhindert.



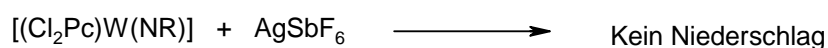
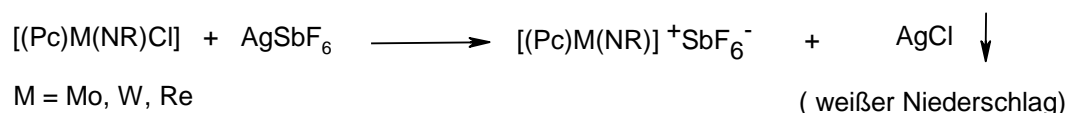


Die Molekülstruktur von *trans*-[PcTi(OSiPh<sub>3</sub>)<sub>2</sub>] (**7**).

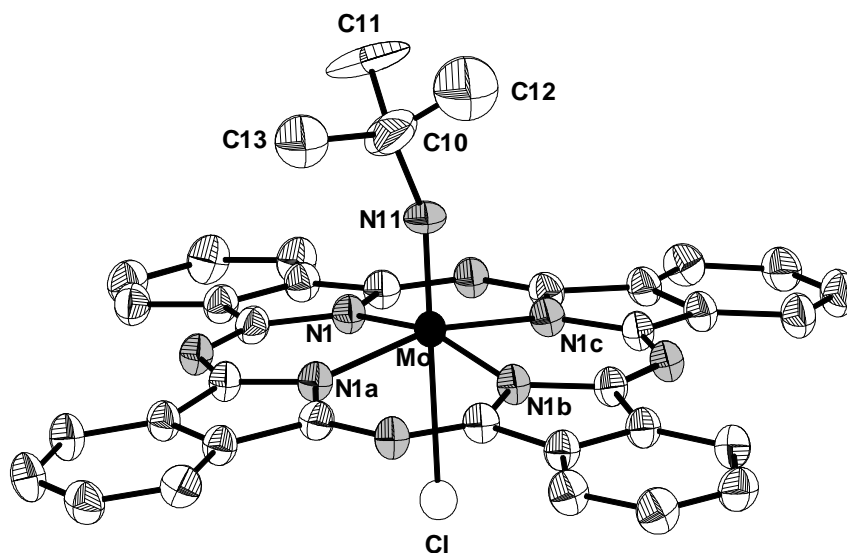
Neue Organoimidokomplexe der allgemeinen Summenformel [PcM(NR)Cl] (M = Mo, W, Re) (**9a,b**, **11a,b**, **15a,b**) wurden in der Schmelze von Phthalsäuredinitril (PN) mit Imidokomplexen [M(NR)<sub>2</sub>Cl<sub>2</sub>(dme)] (M = Mo, W; R = <sup>t</sup>Bu, Mes) bzw. [Re(NR)<sub>3</sub>Cl] (M = Re; R = <sup>t</sup>Bu, Mes) dargestellt. Als Produkt erhält man immer die Chloro-imido-phthalocyaninkomplexe. Erhitzt man andererseits Phthalsäuredinitril mit Wolframimidokomplexen der allgemeinen Summenformel [W(NR)Cl<sub>4</sub>] (R = Ph, *p*-Tol, 3,5-Cl<sub>2</sub>C<sub>6</sub>H<sub>3</sub>) (**13a-c**), so wurden immer die diamagnetischen Imido-wolfram(IV)-phthalocyanine mit zwei Chlorsubstituenten am aromatischen Ring des Phthalocyanins [(Cl<sub>2</sub>Pc)W(NR)] (**13a-c**) isoliert. Man kann dies auf die stark chlorierenden Eigenschaften von die d<sup>0</sup> Verbindungen [W(NR)Cl<sub>4</sub>] zurückführen. Die Chlorierung der aromatischen Ringe führt zu verschiedenen Isomeren, so dass keine einheitlichen Kristalle erhalten werden können.



Werden die Verbindungen **(9a,b)**, **(11a,b)**, **(15a,b)** mit  $\text{AgSbF}_6$  in Dichlormethan unter Rückfluss umgesetzt, beobachtet man einen weißen Niederschlag von  $\text{AgCl}$ . Das heißt, dass das Chloratom an dem Metall gebunden ist. Andererseits wird kein weißer Niederschlag beobachtet, wenn die Verbindungen **(13a-c)** mit  $\text{AgSbF}_6$  in Dichlormethan unter Rückfluss umgesetzt werden.



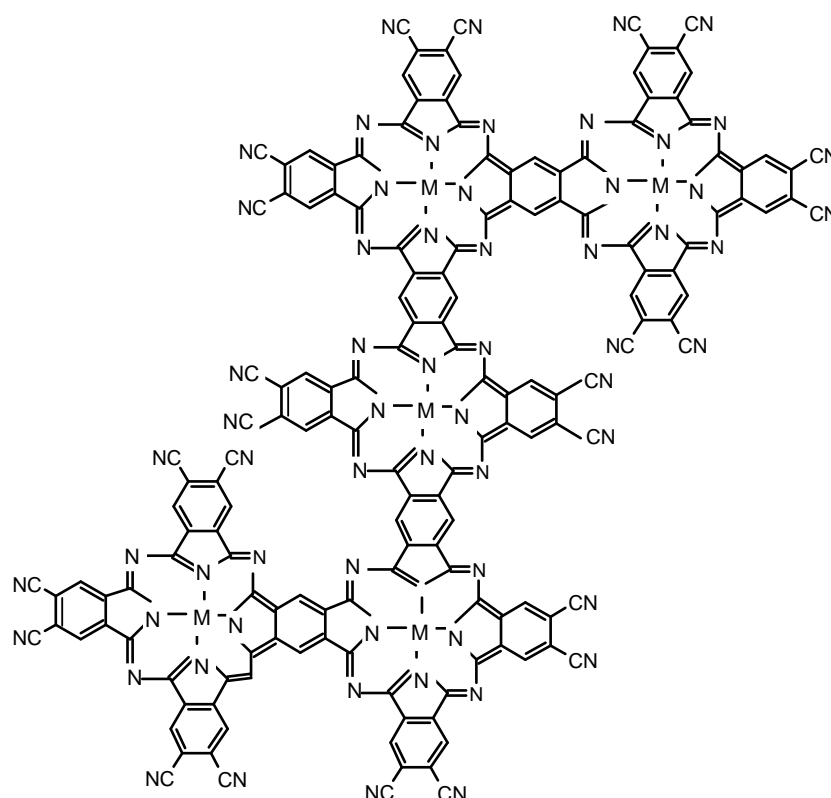
Die Verbindung **(9a)** kristallisiert in der zentrosymmetrischen Raumgruppe ( $P4/n$ ) mit vier Molekülen in der Elementarzelle. Das Molekül enthält ein sechsfach koordiniertes  $\text{Mo(V)}$  Atom, welches von vier äquatorialen Isoindolin-Ringen des Pc Liganden umgeben ist. Der Imidoligand und das Chloratom stehen in axialen Positionen in einer trans-Konfiguration. Das Molybdänatom liegt oberhalb der Ebene der vier Stickstoffatome mit einem Abstand von  $0.305(0)$  (Å) von der Ebene.



Die Molekülstruktur von  $[\text{PcMo}(\text{N}^t\text{Bu})]$  (**9a**).



Die Reaktion von 1,2,4,5-Tetracyanobenzol (TCB) mit  $\text{Ti}(\text{OBU})_4$  im Molverhältnis von 2:1 bei hohen Temperaturen von ca.  $220^\circ\text{C}$  führt zu einem Pentamer der idealisierten Summenformel  $\text{C}_{160}\text{H}_8\text{N}_{64}\text{O}_5\text{Ti}_5$ . Dieses Oligomer hat ein Molekulargewicht von 3145 g/mol. Wird dieses Oligomer mit 2,6-Diisopropylphenylisocyanat in DMF unter Rückfluss umgesetzt, erhält man das entsprechende Pentamer mit der Imidofunktionalität. Die Reaktion von TCB mit  $[\text{Mo}(\text{NMes})_2\text{Cl}_2(\text{dme})]$  führt zum Phthalocyanin-Pentamer mit  $[\text{Mo}(\text{NMes})\text{Cl}]$ -Funktionalität.



$\text{M}=[\text{TiO}]$  (**16**),  $\text{M}=[\text{Mo}(\text{NMes})\text{Cl}]$  (**17**),  $\text{M}=[\text{Ti}(\text{NDip})]$  (**18**).

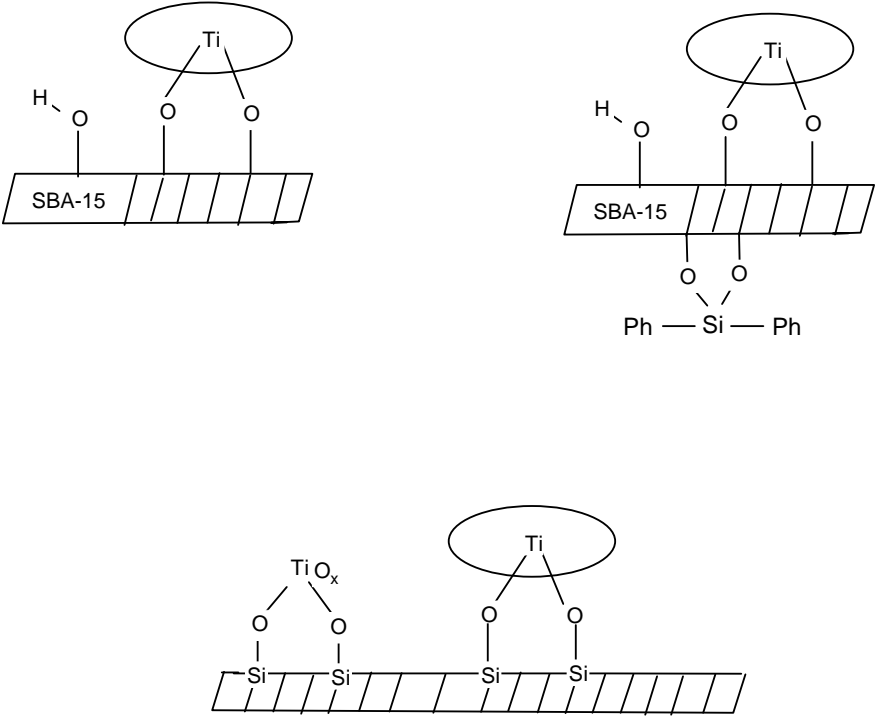
Die GPC Messungen der DMF Lösungen der Oligomere, bezogen auf Polystyrol, zeigen mit geringen Abweichungen die erwarteten Molekulargewichte der Pentamere. Allein durch die spektroskopischen Untersuchungen, lässt sich nicht herausfinden, wie die fünf PcM-Einheiten miteinander verbunden sind.

In einer Kooperation mit dem AK Prof. Rühle (FB Physik) wird die zeitaufgelöste Photolumineszenz von Phthalocyaninen (**1**) and (**3b**) untersucht. Das Sauerstoffatom des Titanylphthalocyanins wurde hierbei durch eine, dianionische N,N'-Ditolyureato-Baugruppe

ausgetauscht. Ziel dieser Funktionalisierung ist die Verbesserung der optischen Eigenschaften, insbesondere der Photoleitfähigkeit. Zum Vergleich werden beide Phthalocyanine fluoreszenzspektroskopisch untersucht. Die Untersuchungen an diesen Phthalocyaninen haben gezeigt, dass nur die Intensität der Emissionsbanden in den PL-Spektren und der Transienten konzentrationsabhängig ist, nicht aber deren qualitativer Verlauf. Beide Proben weisen ein ungewöhnliches zeitliches Abfallverhalten der PL-Intensität auf. Die Lebensdauer ist vergleichbar mit anderen experimentellen Ergebnissen zeitaufgelöster Fluoreszenzspektroskopie (4-6 ns) und bestätigt das Potential der Phthalocyanine auch für den medizinischen und biophysikalischen Bereich, z.B. in bildgebenden Verfahren, bei denen lebende Organismen mit Hilfe der Fluoreszenzspektroskopie auf der Nanosekunden-zeitskala untersucht werden oder im Bereich der Optical Limiting Materialien.

Materialien von Metallphthalocyaninen und Kieselgel sind Materialien in industriellen Anwendungen. So sind Materialien von  $\text{PcTiO/SiO}_2$  oder  $\text{PcTiO}$  mit anderen Metalloxiden in einem japanischen Patent als Materialien für optische Anwendungen beschrieben. Diese Materialien werden hergestellt, indem man  $[\text{PcTiO}]$  mit Metalloxiden wie  $\text{TiO}_2$  mit einer Partikelgröße von einem Durchmesser  $\leq 0.5 \mu$  oder amorphes  $\text{SiO}_2$  behandelt. Das erhaltene Material ist amorphes Titanylphthalocyanin, das keine klaren Reflexe bei Röntgenbeugungsuntersuchungen zeigt. Zuerst wurde  $\text{TiO}_x@\text{SBA-15}$  durch Einbringen von TBOT als Titan-Quelle in die Poren von SBA-15 erzeugt. Diese Methode führt zu einem Titangehalt von 2.66%. Anschließend wurde Ureato-TiPc (**3b**) in die Poren von SBA-15 und  $\text{TiO}_x@\text{SBA-15}$  eingebracht. Hierbei wurden folgende Faktoren ausgenutzt: (i) Der große Porendurchmesser von SBA-15 Materialien erlaubt die Einbindung von großen Molekülen, (ii) Die Harnstoffgruppe in (**3b**) ist eine gute, protolytisch leicht abspaltbare Abgangsgruppe, (iii) Die Passivierung der äußeren Oberfläche durch  $\text{Ph}_2\text{SiCl}_2$  vor der Behandlung mit Ureato-TiPc (**3b**). Der Ureatoligand von (**3b**) reagiert mit den Silanolgruppen der Oberfläche des SBA-15 Materials. Folglich ist TiPc zunächst kovalent an das SBA-15 Material gebunden, solange kein Wasser die  $[\text{Si-O-Ti}]$  Bindung hydrolisiert. Die UV/VIS Spektren der hergestellten Materialien stimmen mit den Spektren der einzeln verteilten Phthalocyanin-Moleküle in SBA-15 überein. TEM Aufnahmen zeigen die eingebundenen Phthalocyanine als verteilte kleine dunkle Flächen auf der Oberfläche des Trägermaterials. Auf den TEM Aufnahmen sind keine ausgedehnten Flächen der an SBA-15 Träger gebundenen Phthalocyaninmoleküle zu sehen. Dies stimmt sehr gut mit UV/VIS Spektren überein und

spricht für das Vorliegen einzelner, nicht assoziierter Phthalocyaninmoleküle. Daraus folgt, dass die in der TEM beobachteten dunklen Flächen nur auf den Wänden der Poren verteilt sind und nicht über das gesamte Volumen.



[PcTi] in den Poren von SBA-15 und TiO<sub>x</sub>@SBA-15.

# **1. Introduction**

## **1.1 History of Phthalocyanines**

The word phthalocyanine– from the Greek for naphtha (rock oil) and cyanine (blue) - was used about hundred years ago to describe a set of compounds of great importance in industrial and medical fields. Phthalocyanines (Pcs) were first observed in 1907 when Braun and Tscherniac observed a blue insoluble substance during heating phthalimide to prepare *o*-cyanobenzamide.<sup>1</sup> Similarly, in (1927), PcCu was prepared by heating 1,2-dibromobenzene with copper (I) cyanide in pyridine.<sup>2</sup> However, we owe the discovery of the structure of the phthalocyanines to an accident, which occurred at the right time and the right place, when a blue colored compound was detected in a reaction flask where only colorless materials were expected. Normally such an impurity is simply discarded, however, this accident occurred in (1928) in a dye company and the blue product attracted immediate interest which shows the material's potential as an exceptionally stable pigment.<sup>3</sup>

## **1.2 Structure of Phthalocyanines**

Linstead and co-workers<sup>4</sup> determined the molecular structure of phthalocyanines and reported the synthesis of many phthalocyanines and suggested that a phthalocyanine ligand consists of four isoindoline units and has a highly conjugated system. The structure of phthalocyanine was established later by Robertson and co-workers who reported the X-ray single-crystal structures of nickel -, copper -, and platinum- phthalocyanine.<sup>5</sup> Phthalocyanines (Figure 1) are systematically known as tetraazatetrabenzporphyrins (TABP) because of the apparent relation between the structure of the phthalocyanines and the well-known porphyrins.<sup>6</sup> Generally, phthalocyanine molecule is a hetero system contains four condensed isoindoline rings in a symmetrical planar 18  $\pi$ -electron aromatic macrocycle, closely related to the naturally occurring porphyrins. The dianionic ligand can play host to a metal ion in its central cavity. About 70 different elements could be coordinated with the Pc ligand, almost every metal, also some metalloids such as boron, silicon, germanium and arsenic. The coordination number of the square-planar phthalocyanine is four. In combination with metals, which prefer a higher coordination number, square-based pyramidal, tetrahedral or octahedral

structures result. In such cases, the central metal is coordinated with one or two axial ligands such as chlorine, water or pyridine. Together with lanthanides and actinides, complexes of a sandwich structure formed by two phthalocyanines and one central metal with eight coordinated nitrogen atoms result.<sup>7</sup> A lot of derivatives can be prepared by axial substitution at the central metal or peripheral substitution at the benzene rings. The substitution increases the solubility of the phthalocyanines due to sterical hindrance of  $\pi$ -stacking of the molecules such in [<sup>t</sup>Bu<sub>4</sub>Pc]M. Phthalocyanine polymers are also established either as coordination or network polymers.

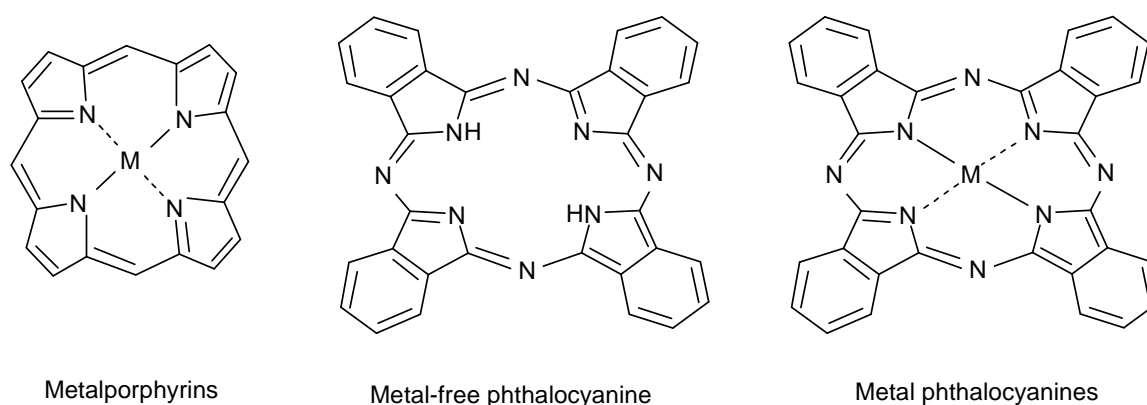
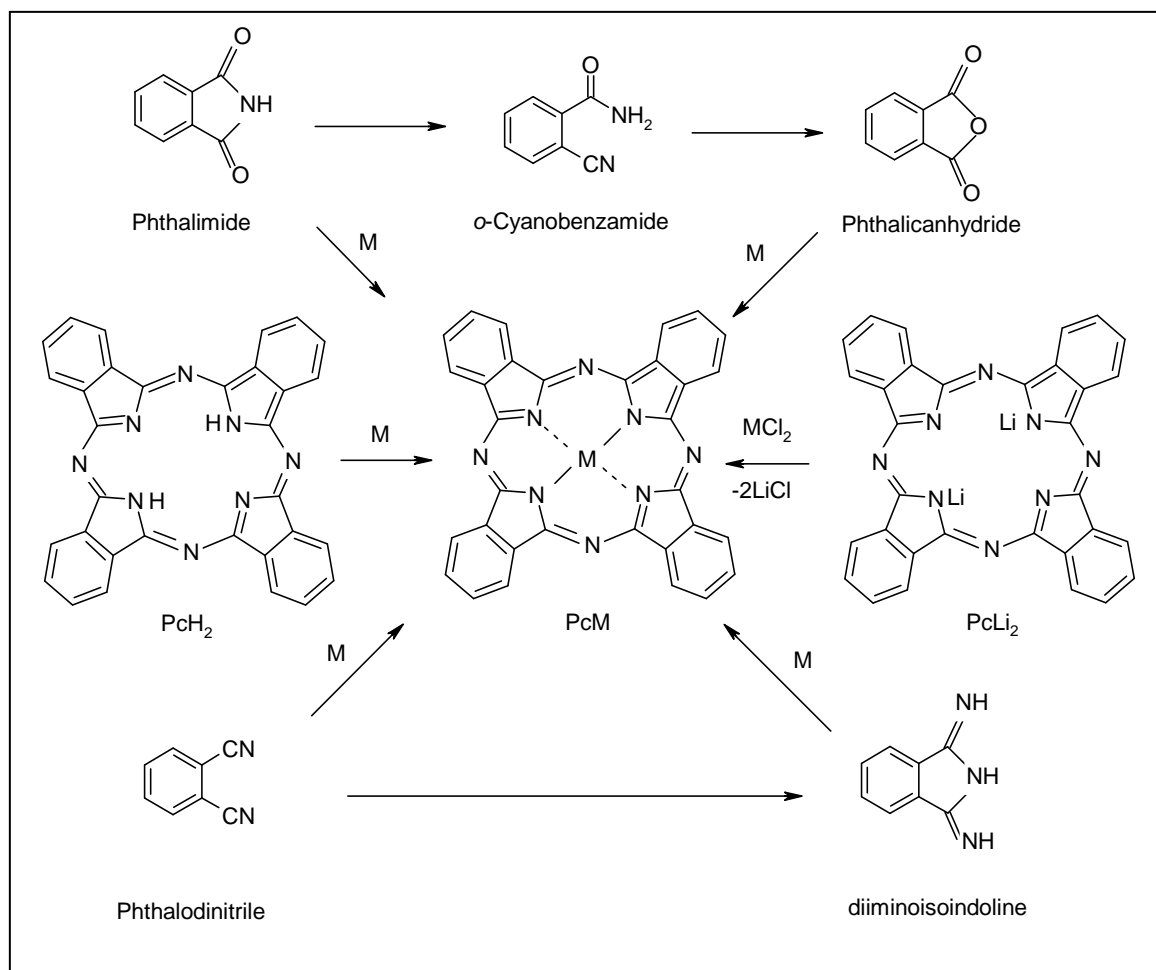


Figure 1: Structure of metalporphyrins, metal free and metalphthalocyanines.

### 1.3 Synthesis and Purification of Phthalocyanines

Phthalocyanines (Pcs) have been synthesized with nearly all metals of the periodic table. The metal-free phthalocyanines (PcH<sub>2</sub>) are normally formed as a one pot multiple-step reaction from derivatives of phthalic acid, phthalic anhydride, phthalimide, or phthalonitrile usually by fusion or in a high boiling solvent such  $\alpha$ -chloronaphthalene.<sup>8</sup> When the reaction is carried out in presence of metal salt the metal phthalocyanines PcM are formed (Scheme 1). Insoluble (unsubstituted) phthalocyanines can be mainly purified by sublimation at high temperature at 450°C under vacuum, by dissolution in concentrated acids followed by precipitation in water, or by extensive extraction with organic solvents. However, soluble (substituted) Phthalocyanines can be purified by recrystallization from organic solvents or by chromatography on alumina or silica gel. Wagner *et al*<sup>9</sup> reported the technical details of a simple train sublimation (carrier gas) system for purification of MPcs and studied the effect of sublimation on the physical properties of MPcs.

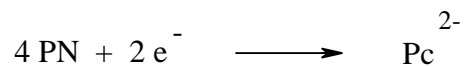


Scheme 1: Synthesis of metalphthalocyanines.

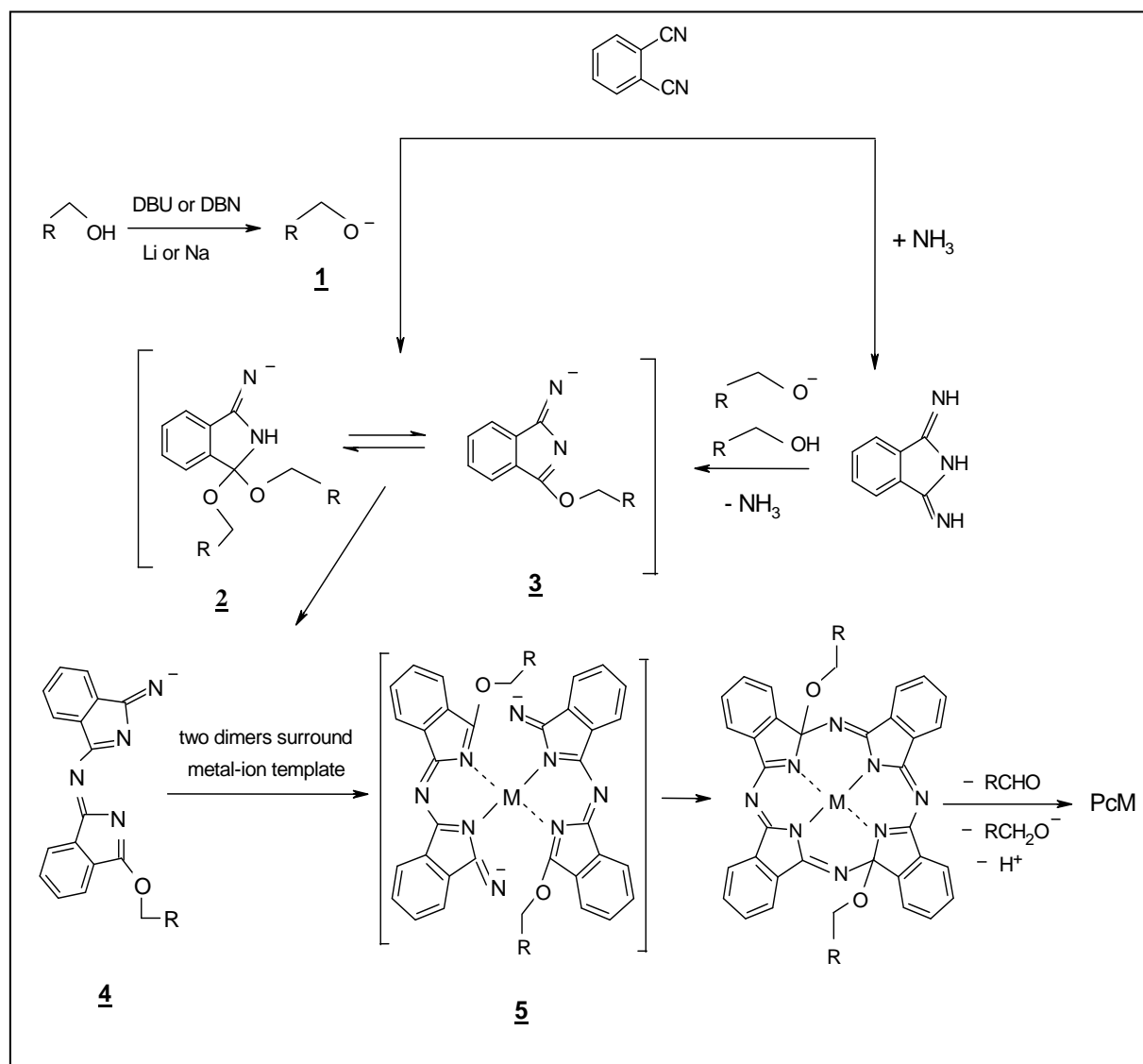
#### 1.4 Mechanism of Phthalocyanine Formation

Despite of all suggestions made for the reaction mechanism, the mechanism is not fully understood. There are generally different suggested mechanisms for the phthalocyanine formation depending on the starting materials and the reaction promoters.<sup>10</sup> For phthalocyanine synthesis in presence of an alcohol (Scheme 2), the alcohol is supposed to be firstly deprotonated by some basic promoters such as DBU or DBN resulting in strong nucleophilic alkoxide species **1** which attack the nitrile or the imide linkage in case of phthalonitrile and diiminoisoindoline respectively. This leads to formation of the intermediates **2** and **3** which are suggested to condense or add further PN in a template reaction forming the intermediate **4**. Two dimers of **4** surround metal-ion template to form the tetramer intermediate **5** which losses aldehyde and a hydride equivalent driven by the

aromatization of the formed phthalocyanine molecule (PcM). The same mechanism is also suggested for the reactions, which involve the use of Li or Na. In this case the metal serves as electron donor for the template cyclization according to the following equation:



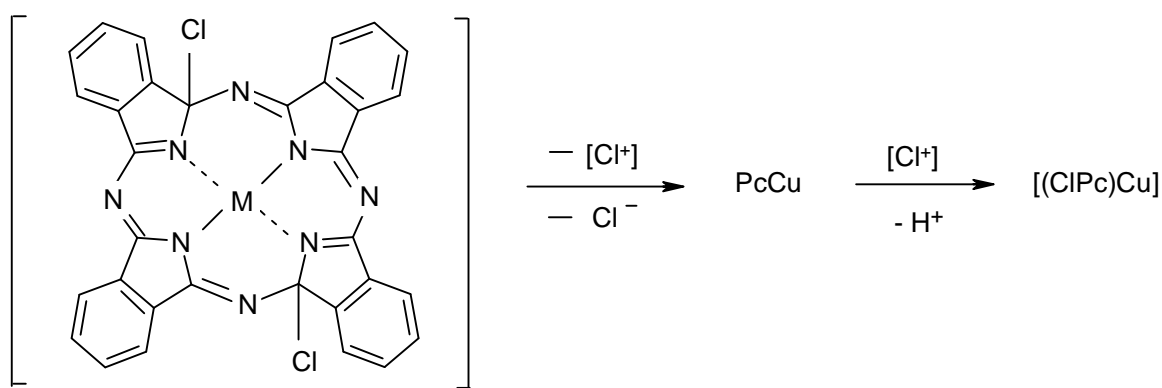
The phthalocyanine synthesis in presence of an alcohol is illustrated in (Scheme 2).



Scheme 2: Mechanism of phthalocyanine formation in the presence of an alcohol.<sup>10</sup>

The high temperature reactions of phthalonitrile with a metal or a metal salt, either neat or in a high boiling solvent, are likely to proceed by a similar mechanism to that shown in (Scheme 2). It has been observed that the reaction of phthalonitrile with copper bronze,

Cu(I) iodide does not occur under a nitrogen atmosphere.<sup>10</sup> This implies that at least some copper (II) ions are necessary for the formation of PcCu in a template mechanism. However, cyclotetramerization with  $\text{CuCl}_2$  results in  $[\text{ClPc}]\text{Cu}$  at  $260^\circ\text{C}$ . This can be explained by the chloride anions acting the role nucleophile instead of the alkoxide depicted in (Scheme 3). In order to provide the two electron reduction necessary for the  $18\pi$  electron aromaticity, a chloronium ion ( $\text{Cl}^+$ ) and a chloride ion ( $\text{Cl}^-$ ) are ejected from the dichloro intermediate. The chloronium ion then attacks the phthalocyanine in an electrophilic substitution reaction. The species that takes the role of nucleophile in the neat reaction with copper bronze must be a phthalonitrile anion (or radical anion) formed by reduction with the metal.



Scheme 3: Mechanism of phthalocyanine formation from metal chlorides.

### 1.5 Crystal Structures of Phthalocyanines

Crystal structures of the phthalocyanines are the fundament for the calculations or prediction of their physical properties. Different arrangements of the molecules in the lattice lead to materials with different physical properties. Polymorphic PcM modifications were therefore referred to as physical isomers.<sup>11</sup> Therefore, a great interest lies in the prediction of crystal structures from the molecular structure and calculations of physical properties there from. Recently, Kadish *et al*<sup>12</sup> gave an overview of all published crystal structures of phthalocyanine compounds and attempted to identify the common arrangement patterns which are seen among the different phthalocyanine structures. In the case of metal-free phthalocyanine,  $\text{PcH}_2$ , the two central atoms are hydrogen atoms, which are small enough to be both coordinated inside the central cavity. The two hydrogen atoms are either coordinated to one set of the centrosymmetrically related isoindoline nitrogen atoms (localized hydrogen atoms) or to both sets (disordered half-hydrogen atoms) and this means that every isoindoline



nitrogen atom is coordinated to 50% of one of the inner hydrogen atoms. In the case of a single central atom, coordination within the inner cavity depends on the size of the ion.<sup>13</sup> From geometrical considerations, it was calculated that the center- $N_i$  radius, ( $N_i$  denotes to nitrogen atoms of the isoindoline rings), with the minimized strain of the relatively rigid macrocycle is *ca.* 1.90 Å.<sup>14</sup> If the ion is smaller or larger than the optimum size, then insertion of the ion into the cavity introduces conformational stress, which the  $\pi$  macrocycle can be partially reduced by moving the isoindoline nitrogen atoms closer to or further away from the center accordingly. However, if the ion is too large, and is unable to enter the cavity it rests “atop” or “out of plane” coordinated, a situation that is sometimes referred to as extra-coordination.<sup>15</sup> The macrocycle adapts to this special bonding situation by deformation. In most of simple MPCs, the phthalocyanine molecule adopts a planar conformation in which the large metal ion is located between 0.1 Å and 1.8 Å from the plane defined by the four  $N_i$  isoindoline nitrogen atoms. (Figure 2) shows the molecular structure of a phthalocyanine complex with an out-of-plane coordinated central atom M and an axial ligand  $L_{ax}$ .<sup>12</sup> A review of the molecular structures of phthalocyanine complexes shows that they basically derive from two types of structures, either from molecules with an approximately planar macrocycle or from molecules with a bent macrocycle where the macrocycle takes the appearance of a saucer.<sup>16</sup>

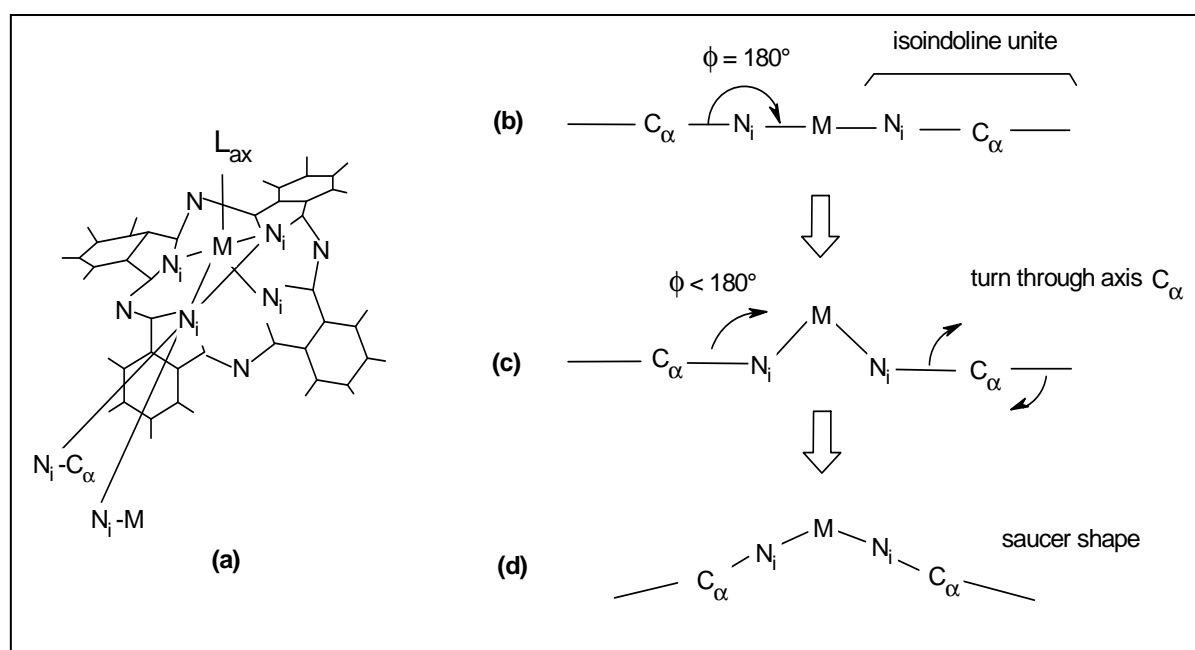


Figure 2: Rearrangement of the MPC macrocycle into a saucer-shaped form.

## 1.6 The Electronic Structure of Metal Phthalocyanines

When a molecule is irradiated with light ( $h\nu$ ), the electrons gain energy and undergo transition from the ground state ( $S_0$ ) to the first excited state ( $S_1$ ) or to higher excited states ( $S_2$ ) and ( $S_3$ ) (Figure 3). After certain time the deactivation process involves radiative and nonradiative processes. The radiative deactivation from  $S_1$  to  $S_0$  is called fluorescence and from a triplet excited state  $T_1$  to  $S_0$  is called phosphorescence. The nonradiative deactivation involves internal conversion (IC), intersystem crossing (ISC), vibrational and rotational processes. According to selection rule not all transitions are allowed, for example the transition from a singlet state to a triplet state is spin-forbidden because it involves change in the total spin multiplicity ( $M=2S+1$ ). Also the transition between two orbitals of the same symmetry in centrosymmetric molecules is called symmetry forbidden.

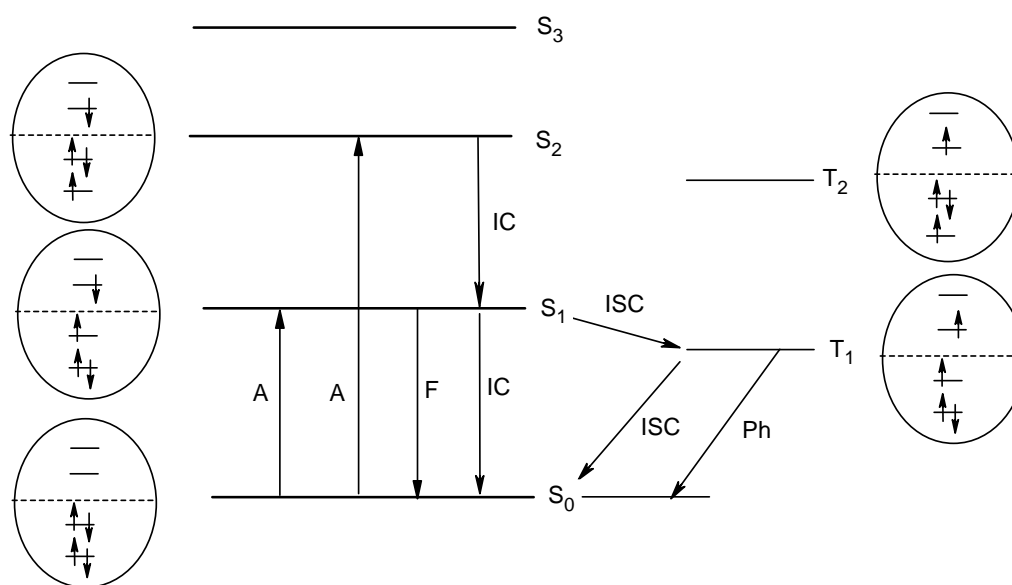


Figure 3: Jablonski diagram for energy levels and various electron transitions.<sup>17</sup>

## 1.7 Applications of Phthalocyanines

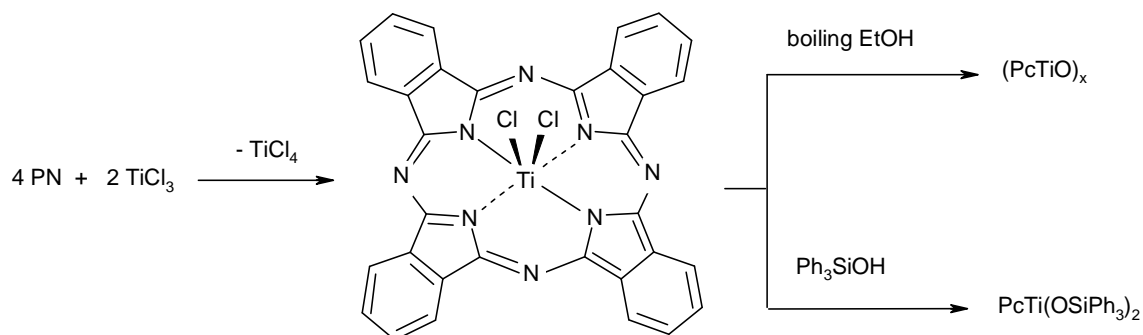
In recent years there has been a growth in the number of laboratories exploring the fundamental academic aspects of phthalocyanine chemistry. Interest has been focused, inter alia, on the synthesis of new types of soluble and unsymmetrical phthalocyanines, on the development of new approaches to the synthesis of polynuclear, bridged, and polymeric

species, on their electronic structure and redox properties, and their electro- and photocatalytic reactivity. Potential uses of phthalocyanines include nonlinear optical materials,<sup>18</sup> liquid crystals,<sup>19</sup> langmuir-Blodgett (LB) films,<sup>20</sup> applications to optical data storage (computer recordable DVDs),<sup>21</sup> as electrochromic substances,<sup>22</sup> as low dimensional metals,<sup>23</sup> gas sensors,<sup>24</sup> as photosensitizer,<sup>25</sup> and as NIR electrochromic materials,<sup>26</sup> in photoelectrochemical cells,<sup>27</sup> and in electrophotographic applications.<sup>28</sup> Certain substituted derivatives of phthalocyanines serve as photodynamic reagents for cancer therapy and other medical applications (e. g. Zn and AlPcs).<sup>29</sup>

## 1.8 Titanium Phthalocyanines

### 1.8.1 Dichlorotitaniumphthalocyanine [PcTiCl<sub>2</sub>]

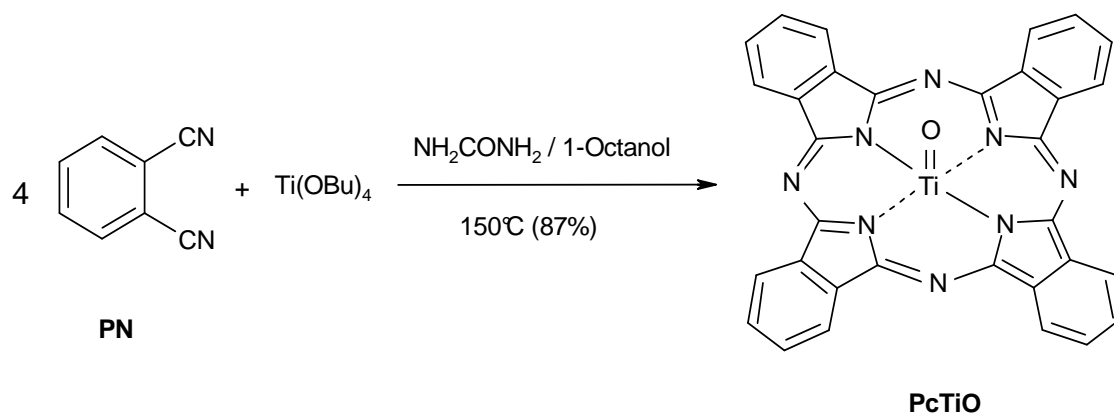
Taube<sup>30</sup> has prepared [PcTiCl<sub>2</sub>] by reaction of Li<sub>2</sub>Pc with TiCl<sub>3</sub> and subsequent oxidation. Block *et al*<sup>31</sup> prepared [PcTiCl<sub>2</sub>] by a more convenient route by reaction of PN with TiCl<sub>3</sub> (Scheme 4). This reaction is very convenient in that Ti(III) furnishes the electrons necessary, 2 electrons, to convert PN to the phthalocyanine anion. TiCl<sub>4</sub> is readily removed by evaporation. The author tested also the reactivity of [PcTiCl<sub>2</sub>] with different organic reagents (Scheme 4). Goedken *et al*<sup>32</sup> solved the X-ray crystal structure of PcTiCl<sub>2</sub> synthesized by reacting PN with TiCl<sub>4</sub> in 1-chloronaphthalene. The Ti atom was found to be displaced 0.84 Å above the N<sub>4</sub> plane toward the coordinated Cl atoms. The two chlorine atoms were proved to locate in a *cis* configuration. The author reported also several successful substitution reactions of the chloride ions of [PcTiCl<sub>2</sub>] producing new axially substituted titanium phthalocyanines.



Scheme 4: Synthesis and reactivity of [PcTiCl<sub>2</sub>].

### 1.8.2 Oxotitaniumphthalocyanine [PcTiO]

Titaniumphthalocyanine has been in commercial use as one of the most sensitive organic photoreceptors in electrophotographic printing.<sup>33</sup> Industrial production of [PcTiO] has been carried out by a reaction of 1,2-dicyanobenzene (PN) and  $\text{TiCl}_4$  at elevated temperature higher than  $210^\circ\text{C}$  in aprotic solvents.<sup>34</sup> High-yield synthesis of pure [PcTiO] has been conveniently achieved by heating a mixture of PN, Ti(VI)butoxide, urea, and 1-octanol at  $150^\circ$  for 6 hours (Scheme 5).<sup>35</sup> Two electrons are essentially needed for building up the  $\text{Pc}^{2-}$  macrocycle from 4 units of phthalonitrile (Figure 4). Ammonia can not be assumed as the source of these two electrons since the generation of ammonia in aprotic solvents, like chloronaphthalene, is only thermal which is slow at  $150^\circ\text{C}$ . Consequently it is supposed that  $[\text{Ti}(\text{OBu})_4]$  acts as a source of the two electrons. The reaction mechanism was suggested to involve a nucleophilic attack of 1-octanol which is facile enough to generate ammonia at sufficient steady state concentration. The in-situ generated ammonia activates  $[\text{Ti}(\text{OBu})_4]$  by formation of [2+2] adduct. The Bis(butoxide) complex is unstable and readily loses two units of 2-isobutene within an intermolecular arrangement to give the dihydroxy complex. The later loses a molecule of water forming [PcTiO] (Figure 4).



Scheme 5: Synthesis of [PcTiO].

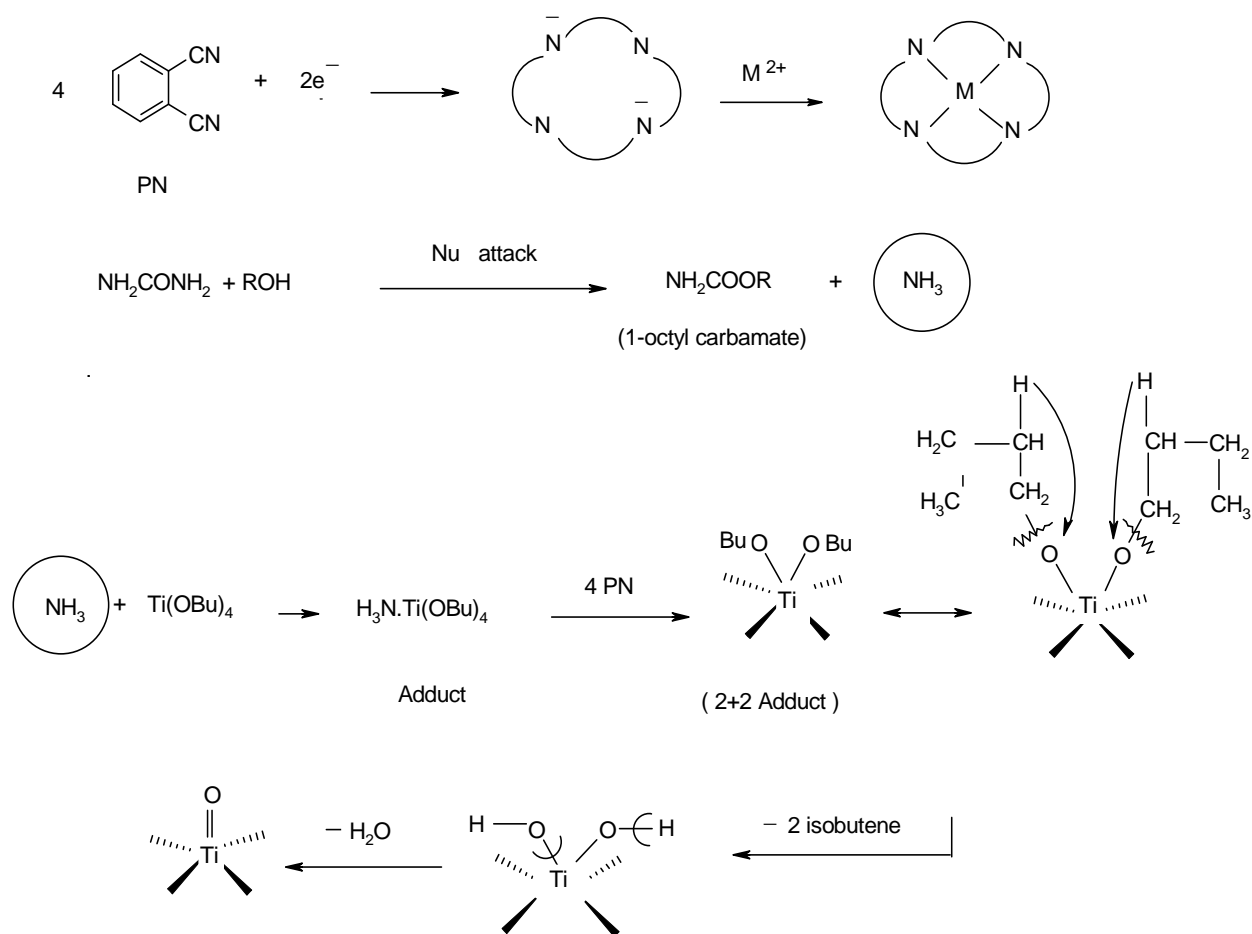


Figure 4: Mechanism of [PcTiO] formation.

Hiller *et al*<sup>36</sup> resolved the crystal structure of [PcTiO] and studied its monoclinic and triclinic modifications built up by the monomeric complexes (Figure 5 and Table 1). The titanium atom exhibits a square pyramidal coordination with a short Ti-O distance of 165.0(4) and 162.6(7) pm for monoclinic and triclinic phases respectively. Close contacts exist between the phthalocyaninato planes of neighboring molecules. Later an additional amorphous phase of [PcTiO] has been described by several authors.<sup>37</sup>

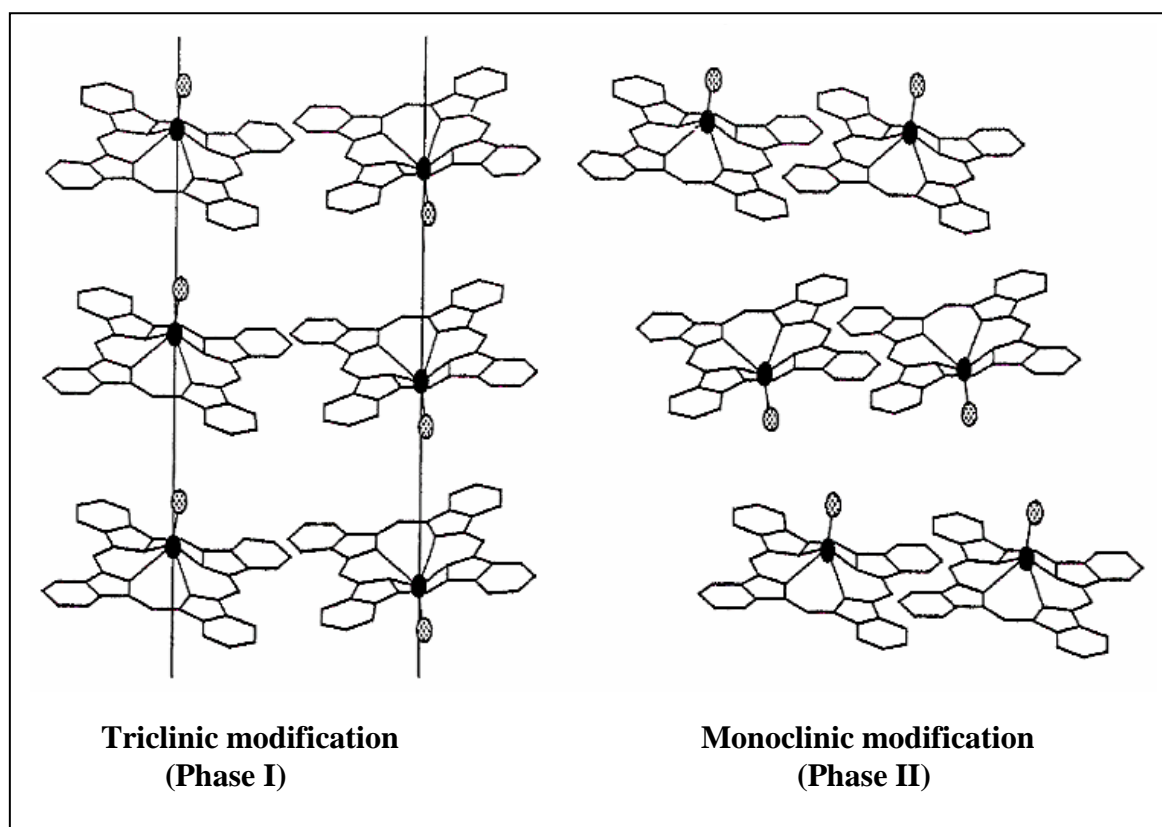


Figure 5: Triclinic and monoclinic modifications of [PcTiO].

Table 1: Cell Data of two different Modifications of [PcTiO]

	Phase I		Phase II
Space group	P2 <sub>1</sub> /c		P $\bar{1}$
Cell unit	Z = 4		Z = 2
Lattice constants			
a	1341.1 ± 0.6 pm	1343.1 ± 0.7 pm	1216.6 ± 0.4 pm
b	1323.0 ± 0.3 pm	1325.8 ± 0.3 pm	1216.6 ± 0.4 pm
c	1381.0 ± 0.4 pm	1390.5 ± 0.4 pm	1216.6 ± 0.4 pm
$\alpha$			96.28 ± 0.03
$\beta$	103.72 ± 0.03°	103.78 ± 0.03°	95.03 ± 0.04°
$\gamma$			67.86 ± 0.04°
Cell volume (pm <sup>3</sup> )	2381.2 · 10 <sup>6</sup>	2404.7 × 10 <sup>6</sup>	1216.4 × 10 <sup>6</sup>

Peripherally substituted phthalocyanines (Figure 6) were found to be more soluble in organic solvents than their unsubstituted analogues. The bulk peripherally substituents enhance the molecular stacking of the Pc molecules, which normally stack side by side. Soluble Tetra substituted titanylphthalocyanine [<sup>t</sup>Bu<sub>4</sub>PcTiO], as a mixture of structural isomers, are well known in the literature.<sup>38</sup> Also octa- alkyl-and alkoxy-substituted oxotitaniumphthalocyanines of general formula [R<sub>8</sub>PcTiO; R= C<sub>3</sub>H<sub>7</sub>, C<sub>4</sub>H<sub>9</sub>, C<sub>5</sub>H<sub>11</sub>, n-C<sub>7</sub>H<sub>15</sub> or OC<sub>5</sub>H<sub>11</sub>] have been also synthesized starting with alkyl and alkoxy disubstituted dinitriles.<sup>39</sup> Both symmetrically and asymmetrically peripherally substituted [PcTiO] were reported, the later was found to be more soluble in organic solvents due to the formation of four isomers.<sup>40</sup> New axially substituted titanium phthalocyanines were prepared by the reaction of the soluble titanylphthalocyanine with numerous bidentate ligands.<sup>41</sup> Thus, [PcTiO] reacts with strongly chelating oxygen or sulfur donor ligands leading to the formation of PcTiX complexes with X = oxalate (C<sub>2</sub>O<sub>4</sub><sup>2-</sup>), catecholate (C<sub>6</sub>H<sub>4</sub>O<sub>2</sub><sup>2-</sup>), dithiocatecholate (C<sub>6</sub>H<sub>4</sub>S<sub>2</sub><sup>2-</sup>). These new compounds possess an enhanced solubility in comparison to [PcTiO]. The replacement of oxo group with such bidentate ligands discards the stretching band ( $\nu_{\text{Ti=O}} = 970 \text{ cm}^{-1}$ ) in the IR spectra, but did not induce a significant change in the UV/VIS spectra.<sup>40</sup>

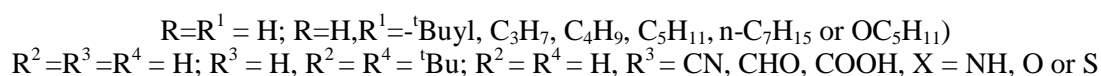
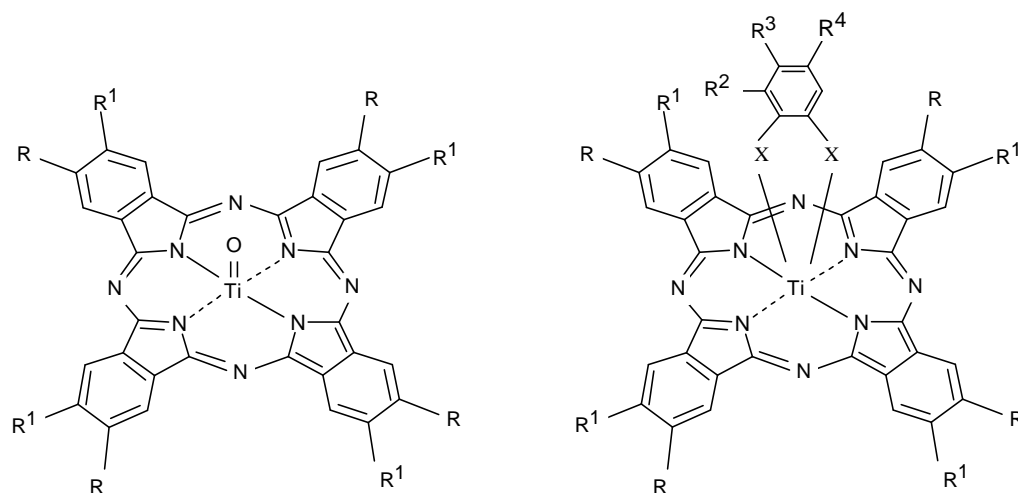


Figure 6: Soluble peripherally substituted titanium phthalocyanines.

Mountford<sup>42</sup> has studied the chemistry of dibenzotetraaza[14]annulene ligands which are tetraazamacrocycles related to porphyrins but have smaller N<sub>4</sub> coordination cavity (hole size) and typically possess a non-planar, saddle shaped confirmation. In this study, the author presented the reaction of titanium phenylimido complex with tolylisocyanate that results in the corresponding ureato derivative (N-phenyl, N-tolyl ureato derivative) (Figure 7).

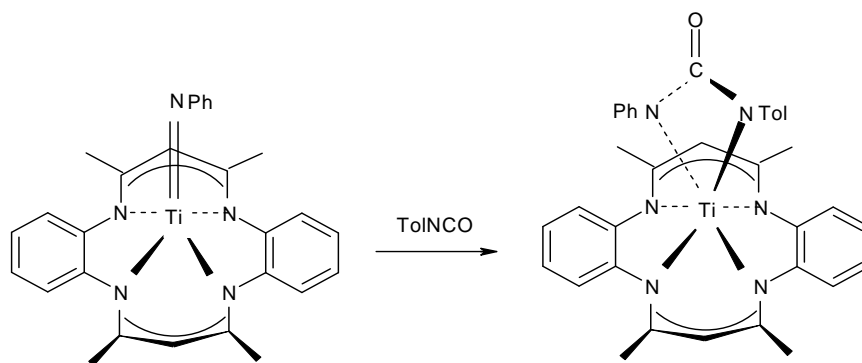


Figure 7: Synthesis of diaryluoreato derivative of titanium dibenzotetraaza[14]annulene.

Enokida *et al*<sup>43</sup> reported the synthesis of novel chalcogenido-TiPcs (Figure 8) (M = V, Ti, Mo; A = O, S, Se, Te) or (M = Si, Ge, Sn; A = SH, SeH, the). The R<sup>1-4</sup> groups are H, halogen, OH, NO<sub>2</sub>, CN, NH<sub>2</sub>, CO<sub>2</sub>H, alkoxy, (un)substituted alkyl, aryl, allyl; a, b, c, d = 0-6. The compounds were described as useful materials in charge-generating layers.

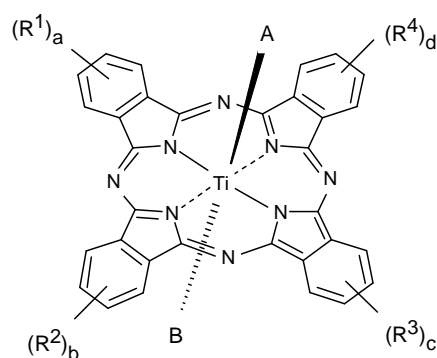


Figure 8: MPcs containing metal-chalcogen bonds as potential charge generation materials.

### 1.9 Titanium Porphyrins

Berreau *et al*<sup>44</sup> prepared [(TTP)Ti=NR], since R = C<sub>6</sub>H<sub>5</sub>, C<sub>6</sub>H<sub>4</sub>-*p*-CH<sub>3</sub>, or C<sub>6</sub>H<sub>11</sub>, by reaction of the corresponding dichloro complex with LiNHR (Scheme 6). The X-ray crystal structure of the product [(TTP)Ti=NPh] showed that titanium atom is displaced from the



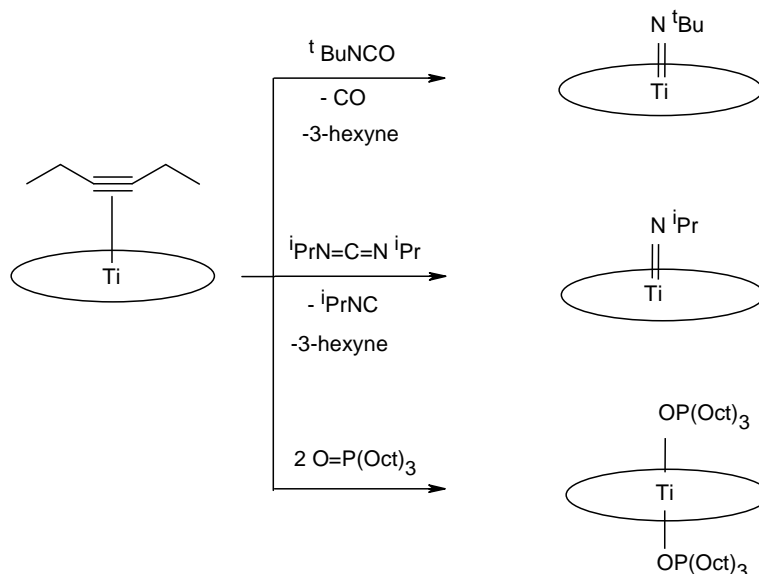
mean plane of the pyrrole nitrogen atoms toward the imido ligand by 0.52 Å. The imido complexes readily hydrolyzes to the corresponding free amines and [(TTP)Ti=O].



R = phenyl, p-tolyl, or cyclohexyl.

Scheme 6: Preparation of imidotitaniumporphyrins.

Gray *et al*<sup>45</sup> reported that reaction of [(TTP)TiCl<sub>2</sub>] with excess NaOR (R = Ph, Me, <sup>t</sup>Bu) affords the Bis (alkoxide) derivative [(TTP)Ti(OR)<sub>2</sub>]. The corresponding amido complexes [(TTP)Ti(NPh<sub>2</sub>)<sub>2</sub>] were prepared by reaction with LiNPh<sub>2</sub>. The imido derivatives [(TTP)TiNR] were prepared by reaction of [(TTP)TiCl<sub>2</sub>] with LiNHR. Thorman *et al*<sup>46</sup> have prepared [(TTP)Ti=NR]; (R = <sup>i</sup>Pr, <sup>t</sup>Bu) by reacting [(TTP)Ti(η<sup>2</sup>-3-hexyne)] with <sup>i</sup>PrN=C=N<sup>i</sup>Pr, <sup>i</sup>PrNCO, or <sup>t</sup>BuNCO (Scheme 7). The reaction between [(TTP)Ti(η<sup>2</sup>-3-hexyne)] and O=P(Oct)<sub>3</sub> resulted in formation of the paramagnetic Ti(II) derivative [(TTP)Ti{O=P(Oct)<sub>3</sub>}<sub>2</sub>]. The crystal structure of the later showed a *trans* configuration. Keith Woo *et al*<sup>47</sup> have prepared [(TTP)Ti{η<sup>2</sup>-RC≡CR'}] with different alkyl groups. The π-complex reacts with pyridine (py) and 4-picoline (pic) to afford the complexes *trans*-[(TTP)Ti(py)<sub>2</sub>] and *trans*-[(TTP)Ti(pic)<sub>2</sub>] respectively (Figure 9). The crystal structure of *trans*-[(TTP)Ti(py)<sub>2</sub>] shows that titanium atom resides in the centre of the 24 atom porphyrin plane. Guilard *et al*<sup>48</sup> prepared a series of disulfur and diselenium titanium (IV) porphyrins. Each compound was prepared by one of two methods. The first involves oxidative addition of S<sub>2</sub> generated from [Cp<sub>2</sub>TiS<sub>5</sub>] or [Cp<sub>2</sub>TiSe<sub>5</sub>] to [(P)TiF] leading to formation of [(P)Ti(η<sup>2</sup>-S<sub>2</sub>)] or [(P)Ti(η<sup>2</sup>-Se<sub>2</sub>)] derivatives, where (P) is the dianion of octaethylporphyrin (OEP) or other porphyrins. The second pathway involves substitution of fluoride at [(P)TiF<sub>2</sub>] with either [Cp<sub>2</sub>TiS<sub>5</sub>] or [Cp<sub>2</sub>TiSe<sub>5</sub>]. The S<sub>2</sub> entity is side-on bonded to the titanium atom.



Scheme 7: Synthesis of axially substituted titanium porphyrins (ring = TTP).

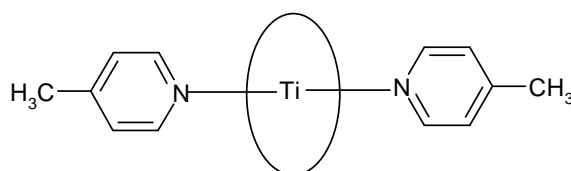
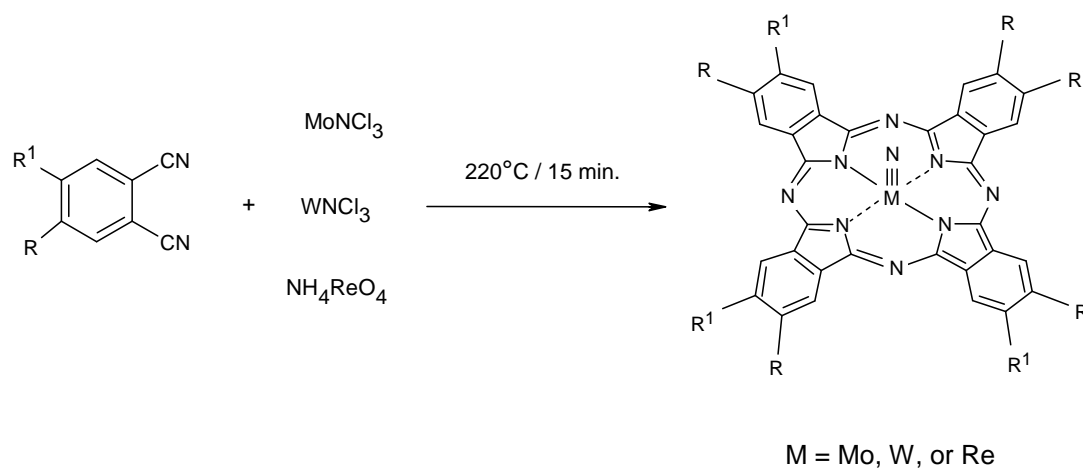


Figure 9: Structure of trans-[(TTP)Ti(pic)<sub>2</sub>].

### 1.10 Phthalocyanines and Porphyrins of Mo, W, and Re

[PcMoO] has been prepared by the reaction of phthalodinitrile with [Mo(CO)<sub>6</sub>] in toluene at 180°C in a sealed tube.<sup>49</sup> This compound has been also prepared by reacting phthalodinitrile and with ammonium heptamolybdate.<sup>50</sup> The paramagnetic compound [PcMo(O)(OH)] has been prepared by washing of [PcMoO] with 0.1M NaOH.<sup>51</sup> The compound [PcMo(O)<sub>2</sub>] has been prepared by heating a mixture of PcH<sub>2</sub> and [MoO<sub>2</sub>(acac)<sub>2</sub>] in chlorobenzene for 3 hours, and the product showed a good catalytic activity in epoxidation of olefins with alkyl hydroperoxides.<sup>52</sup> Blue diamagnetic [PcMoO] has been synthesized by reduction of [PcMo(O)<sub>2</sub>] with boiling triphenylphosphin.<sup>53</sup> Padilla *et al*<sup>54</sup> have prepared the compound [(ClPc)W<sup>V</sup>(O)OH] by reacting phthalodinitrile with tungsten hexachloride WCl<sub>6</sub> in air at 280°C. When this compound was extracted with aniline, the diamagnetic compound [(ClPc)W<sup>II</sup>] has been formed. The author proposed a structure of the type [(ClPc)W<sup>V</sup>(O)OH] with a W=O double bond in an axially compressed octahedral symmetry and chlorine atom

attached to the isoindoline unit. The preparation of unsubstituted and substituted [PcMoN] was found to be successful starting from the appropriate phthalonitrile and [MoNCl<sub>3</sub>] by melting them at 210°C for 20 min.<sup>55</sup> Unsubstituted and substituted nitrido(phthalocyaninato) metal (V) complexes [R<sub>4</sub>R'<sub>4</sub>PcMN] were prepared by the fusion of the corresponding phthalodinitrile with [MoNCl<sub>3</sub>], [WCl<sub>3</sub>] or [NH<sub>4</sub>ReO<sub>4</sub>] under an atmosphere of nitrogen (Scheme 8).<sup>56</sup>



Scheme 8: Different nitrido phthalocyanines of Mo, W, and Re.

The soluble nitridophthalocyanine [(<sup>t</sup>Bu<sub>4</sub>Pc)Re≡N] was used for preparation of new complexes with nitrido bridges between Rhenium and elements of the third main group. For example, it reacts with BX<sub>3</sub>, GaX<sub>3</sub>, AlCl<sub>3</sub>, InCl<sub>3</sub>, BPhCl<sub>2</sub>, BR<sub>3</sub>, and <sup>t</sup>BuMe<sub>2</sub>SiCl giving non-ionic, green nitrido-bridged compounds (Figure 10).<sup>57</sup>

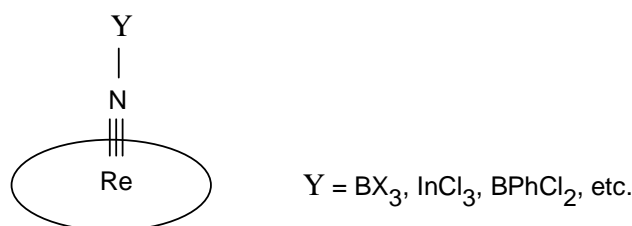
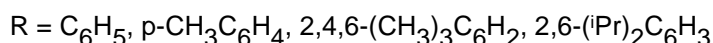
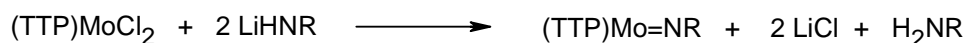


Figure 10: Nitrido-bridged RePcs.

The paramagnetic compound [PcRe≡RePc] has been prepared by the thermal decomposition of trans-Bis (triphenylphosphine)-phthalocyaninato (2-) rhenium (II), in boiling triphenylphosphine.<sup>58</sup>

Most of the imidomolybdenum porphyrin examples known in literature are Mo(V) complexes, and only one has been structurally characterized.<sup>59</sup> For example, the air stable organoimido molybdenum (V) porphyrin salt of formula [(TTP)Mo(NMe)(H<sub>2</sub>O)][I<sub>3</sub>] has been prepared by heating of [(TTP)MoN] with methyl iodide. The IR spectrum of this complex displays a strong absorption at 752 cm<sup>-1</sup>, partially overlapping one of the typical porphyrin bands, which was assigned to the molybdenum-imido stretching band. The ambient temperature ESR spectrum of this organoimido complex in toluene is typical for a d<sup>1</sup> configuration around the molybdenum atom. It consists of a strong central line (interaction among the *I* = 0 isotopes of Mo and the single electron) and six weak lines (interaction among <sup>95,97</sup>Mo (*I* = 5/2) and the electron). The strong central line is further split due to the interaction with four pyrrole nitrogen atoms and one axial nitrogen atom. The isotopic *g* value was found 1.9766. The crystal structure of this organoimido complex showed that the molybdenum atom is octahedrally coordinated by the four pyrrole nitrogen atoms and two axial ligands, methylimido and water. Berreau *et al*<sup>60</sup> have recently prepared a series of organoimidomolybdenum (IV) porphyrin complexes by reacting of [(TTP)MoCl<sub>2</sub>] with various lithium amides (Scheme 9). These Mo(IV) porphyrin complexes have been shown to exhibit both paramagnetic [(TTP)MoCl<sub>2</sub>]<sup>61</sup> and diamagnetic [(TTP)Mo=O] properties.<sup>62</sup>



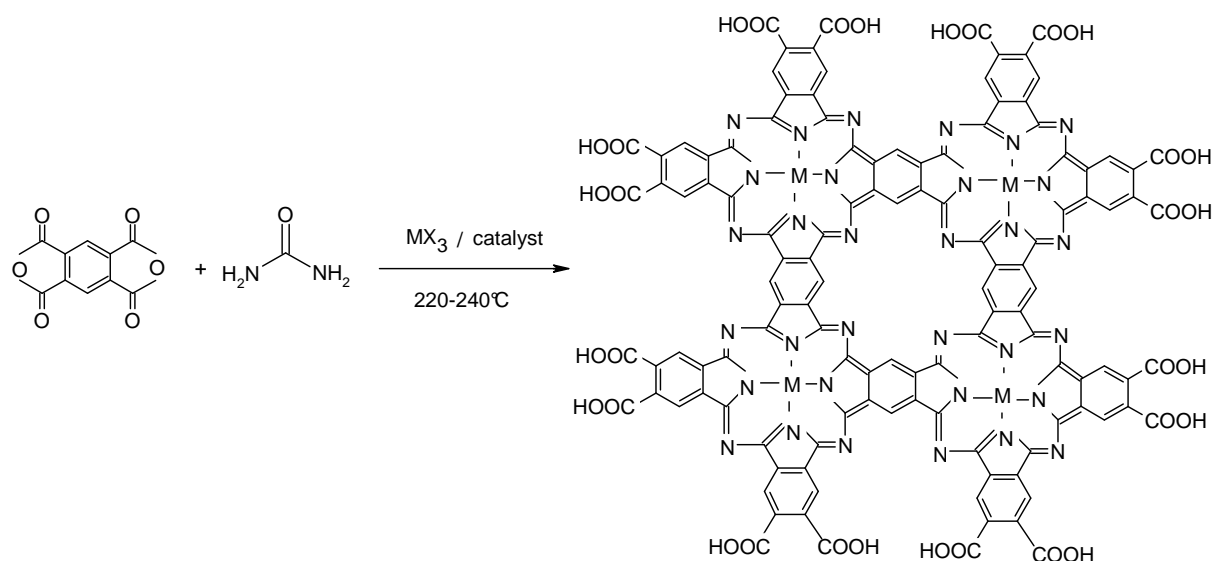
Scheme 9: Synthesis of imidomolybdenum (IV) porphyrins.

### 1.11 Phthalocyanine Polymers

Phthalocyanine polymers are important in many industrial fields such as catalysis, electrocatalysis, and manufacture of thermostable materials.<sup>63</sup> Phthalocyanine polymers have been prepared for the first time by Marvell and his coworkers.<sup>64</sup> They have prepared low molecular weight soluble polymeric phthalocyanines from mixtures of pyromellitic acid and phthalic anhydride and of 3,3',4,4'-tetracarboxy-diphenyl ether and phthalic anhydride. Generally, metal phthalocyanine polymers are synthesized by polycyclotetramerization of tetra functional building blocks such as 1,2,4,5-benzene-tetracarboxylic dianhydride or 1,2,4,5-benzenetetracarbonitrile. The reaction pathway is far more complex when

benzenetetracarboxylic acid derivatives instead of benzenetetracarbonitrile derivatives are used as starting materials. For conversion of benzenetetracarboxylic acid derivatives, urea as a source of ammonia, and a suitable catalyst such as boric acid or ammonium molybdate, have to be present. In absence of metal salts the reaction leads to the production of metal-free phthalocyanine polymers, and in the presence of the metal salt, the corresponding metal phthalocyanine polymers are obtained. The reactions can be carried out either in bulk<sup>65</sup> or in high-boiling solvents such as nitrobenzene.<sup>66</sup> A polymeric "CuPc" has been produced by the reaction of pyromellitic dianhydride, copper (II) chloride, urea and catalyst at 180°C. Molecular weights and equivalent weights have been determined by elemental analysis and by potentiometric titration and the shapes of the molecules have been determined. Average molecular weights as high as 4000 have been identified.<sup>67</sup> Structurally uniform polymeric phthalocyanines of Cu, Co, Ni, and Fe and containing imido end groups were synthesized by reaction of different derivatives of 1,2,4,5-benzenetetracarboxylic acid with the corresponding metal salt, urea and a catalyst.<sup>68</sup>

Abd El-Ghaffar *et al*<sup>69</sup> have prepared a series of phthalocyanine polymers either metal-free or containing the transition metal Cu, Co, Cr, and Fe from pyromellitic dianhydride by the conventional urea fusion method (Scheme 10). Abd El-Ghaffar *et al*<sup>70</sup> have also prepared fluorinated phthalocyanine and phthalocyanine enamionitrile polymers. The synthesis of novel titanium phthalocyanine polymers has been also reported by Block and his coworkers<sup>71</sup> by replacing the chloride ions in the moisture sensitive [PcTiCl<sub>2</sub>] to give (TiPcO)<sub>x</sub>, or an oligomer of formula {TiPc(OPPhO<sub>2</sub>)<sub>x</sub>}. Lo *et al*<sup>72</sup> have prepared a series of silicon (IV) phthalocyanines with two axial poly (ethylene glycol) chains [PcSiX<sub>8</sub>{(OCH<sub>2</sub>CH<sub>2</sub>)<sub>n</sub>OCH<sub>3</sub>}<sub>2</sub>] (X=H, Cl, Br; n=16). The prepared materials showed enhanced photosensitizing properties as the periphery of the macrocycle is substituted with heavier halogens. Van der Pol *et al*<sup>73</sup> have prepared coaxially polymerized, peripherally substituted derivatives of phthalocyanine by heating of dihydroxy silicon octaalkoxy-phthalocyanine under vacuum at 210°C for 24 hours. The reaction results in the formation of oxygen-bridged siliconphthalocyanine polymer. Gel Permeation Chromatography (GPC) was used to estimate the degree of polymerization.



Scheme 10: Synthesis of phthalocyanine polymers.

## 1.12 Mesoporous Molecular Sieve Materials

### 1.12.1 Preparation of Mesoporous Molecular Sieves (SBA-15 and MCM-41 Materials)

Mesoporous materials locate a middle position between the macroporous and microporous materials according to the pore size and diameter (Table 2).

Table 2: Pore Size and Diameter of Molecular Sieves

Definition	Pore size ( $\text{\AA}^3$ )	Pore diameter ( $\text{\AA}$ )
Macroporous	> 500	15-100
Mesoporous	20-500	
Microporous	< 20	

The MCM family of mesoporous silica has been discovered in 1992 by researchers at Mobil as materials prepared from surfactant-containing gels.<sup>74</sup> The family includes MCM-41, MCM-48 and MCM-50.<sup>75</sup> Among the wide variety of silica mesophases, SBA-15<sup>76</sup> and MCM-41<sup>77</sup> have been the most extensively investigated. Though both of them exhibit two dimensional hexagonal structures ( $p6mm$ ), they have some notable differences: (i) SBA-15 is endowed with larger pores and thicker pore walls than MCM-41;<sup>76</sup> (ii) MCM-41 is purely mesoporous in nature, whereas typical SBA-15 silica contains a significant amount of

micropores within the pore walls;<sup>78</sup> while the channels of MCM-41 are not connected to each other, those of SBA-15 are interconnected via micropores or secondary mesopores.<sup>79</sup> An extensive work was devoted to the morphological control of the mesoporous silicas.<sup>80</sup> As far as SBA-15 is concerned, the most common morphology consists of bundles of fibers several tens of micrometers in length obtained by coupling short rodlike particles.<sup>81</sup> Zaho *et al*<sup>76</sup> have firstly used the amphiphilic triblock copolymers to direct the organization of polymerizing silica species has resulted in the preparation of well-ordered hexagonal mesoporous silica structures SBA-15 with uniform pore sizes up to approximately 300 angstroms. The SBA-15 materials are synthesized in acidic media to produce highly ordered, two dimensional hexagonal (space group *p6mm*) silica-block copolymer mesophases. Calcination at 500°C gives porous structures with unusually large interlattice *d* spacing of 74.5 to 320 angstroms between the (100) planes, pore sizes from 46 to 300 angstroms, pore volume fractions up to 0.85, and silica wall thicknesses of 31 to 64 angstroms. SBA-15 can be readily prepared over a wide range of uniform pore sizes and pore wall thicknesses at low temperature (35° to 80°C), using a variety of poly(alkylene oxide) triblock copolymers and by the addition of cosolvent organic molecules. Especially, mesoporous host materials of the SBA-15 type can provide pore diameters up to 10 nm and relatively thick walls.<sup>82</sup> Covalent Grafting of the guest molecules onto the functionalized interior surface of the host is a well known method to achieve the fixation process.<sup>83, 84</sup>

### **1.12.2 Preparation of Titanium Containing SBA-15 and MCM-41**

Titanium-containing SBA-15 and MCM-41 materials have been prepared by two different techniques.<sup>85a</sup> The first is called *in situ* incorporation and involved incorporation of Ti onto Si-MCM41 material during the hydrothermal synthesis. The second technique involved impregnation of titanium in siliceous MCM-41 either with tetrabutylorthotitanate or with titanyl acetylacetonate. A perfect ordering of the hexagonal structures was revealed from XRD patterns and nitrogen adsorption isotherm. Uniform of titanium in the pores was demonstrated by UV/VIS diffuse reflectance spectra (DRS).

Aguado *et al*<sup>85b</sup> obtained TiO<sub>2</sub>/SBA-15 (TiO<sub>2</sub> ~20 wt%) by stirring a mixture of SBA-15 with (TTIP) in (*i*-PrOH) followed by addition of water. Segura *et al*<sup>85c</sup> prepared Ti-SBA-15 by heating solution of TiO(acac)<sub>2</sub> in toluene with SBA-15 followed by calcinations of the product. TiO(acac)<sub>2</sub> was found to covalently bound to most of the OH

groups on SBA-15 surface. The product did not show the typical Raman absorption bands of anatase  $\text{TiO}_2$  (638-519, 399, 147  $\text{cm}^{-1}$ ). Luan *et al*<sup>85d</sup> studied the impregnation of Ti in SBA-15 via incipient-wetness method using titanium isopropoxide as titanium precursor. It was revealed that low titanium loading of 1 atom 5 results in monoatomic dispersion of Ti ions in SBA-15. These titanium species reach a maximum of 6 atom % relative to silicon. A higher Ti loading leads to formation of anatase. Raman spectra showed absorption bands at 790, 830  $\text{cm}^{-1}$  assigned to (Si-OSi) linkage, and 485 and 603  $\text{cm}^{-1}$  (assigned to four and three membered siloxane rings), and 981  $\text{cm}^{-1}$  (assigned to surface silanol groups). With Ti present, the band at 981  $\text{cm}^{-1}$  is not observable even at low titanium loadings. As titanium loading increases the Raman spectra resemble one reported for fumed silica coated with  $\text{TiO}_2$  at 397, 515 and 639  $\text{cm}^{-1}$ . UV-spectra for the low titanium loaded samples show absorption at 230 nm like tetrahedral titanium in TS-1 which represents charge transfer between  $\text{Ti}^{4+}$  and oxygen ligand. The high titanium loaded samples show absorption band at 290 nm ( $\text{TiO}_2$  anatase, blue shifted from 335 nm of the bulk  $\text{TiO}_2$  anatase). Landau *et al*<sup>85e</sup> achieved  $\text{TiO}_2$  loading of (30-80%) inside the pores of SBA-15 silica by chemical solution decomposition (CSD) or internal hydrolysis (IH) of  $\text{Ti}[\text{n-BuO}]_4$  producing composites with high  $\text{TiO}_2$  (anatase). Perathoner *et al*<sup>85f</sup> reported that in case of titanium loadings up to 12-13 wt%, the XRD patterns are in agreement with the model of a guest phase layer uniformly covering the inner part of SBA-15 walls, while higher titanium loadings leads to patterns like that of separate  $\text{TiO}_2$  nanoparticles. Calleja *et al*<sup>85g</sup> studied the grafting of Ti(1-3 wt%) in SBA-15 using titanocene dichloride  $(\text{Cp})_2\text{TiCl}_2$ . DR UV-VIS of the prepared Ti-SBA-15 showed the presence of titanium isolated species tetrahedrally coordinated and the absence of bulky  $\text{TiO}_2$  Phase. Peng Wu *et al*<sup>85h</sup> studied the post synthesis of Ti-SBA-15 by titanation of pure SBA-15 with TBOT in glycerol containing quaternary ammonium hydroxide. Brutchey *et al*<sup>85i</sup> achieved (0.17 and 2.64 wt%) loading of Ti into SBA-15 and the grafting yielded mostly isolated Ti(IV) sites. Srivastava *et al*<sup>85j</sup> functionalized Ti-SBA-15 to Ti-SBA-15-pr-Cl and Ti-SBA-15-pr- $\text{NH}_2$  using the corresponding isopropyl derivatives. Afterwards adenine was grafted in these active sites to result in an active catalyst for the synthesis of cyclic carbonates.

### **1.12.3 Properties of Mesoporous Molecular Sieves**

The discovery of mesoporous molecular sieves was followed by a variety of reports on the inclusion chemistry of these materials with respect to the surface silanol groups.<sup>86</sup> Zhao *et al*<sup>87</sup> distinguished three types of silanol groups (Figure 11) and determined the



number of the silanol groups of the MCM-41 by means of NMR and found 2.5 to 3 silanol groups per  $\text{nm}^2$ . The silanol groups are not acidic and Bronsted-acid bridging OH groups are formed only after modification with aluminum.<sup>88</sup>

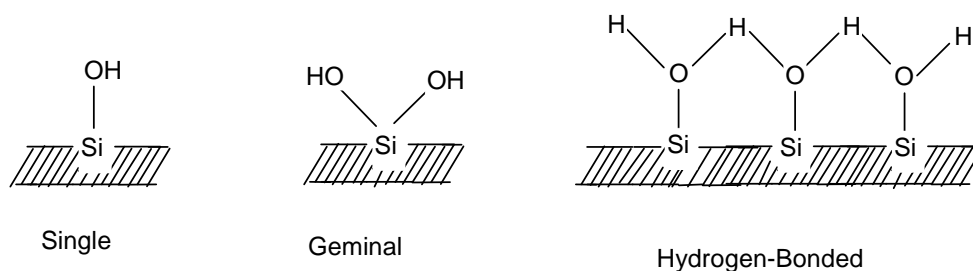


Figure 11: Types of silanol groups in M41S materials.

#### 1.12.4 Phthalocyanine Modified Mesoporous Molecular Sieves

The high density of surface silanol groups of mesoporous materials opened the way for manifold inclusion chemistry.<sup>88</sup> However, here as in the clays the problem of fixation occurs. Some complexes are impossible to be encapsulated inside the cages of zeolites because of their too large dynamic diameters (e.g. the ligand of  $[\text{Co}^{\text{II}}\text{Pc}]$  with a diameter of  $15 \text{ \AA}$  cannot be encapsulated by NaY zeolite). All of these drawbacks can be overcome by taking advantage of MCM-41, as shown in (Figure 12), because the advantages of MCM-41.

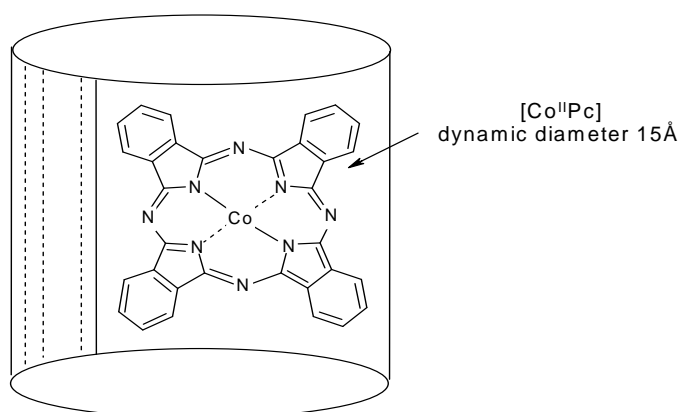


Figure 12: Schematic representation of  $[\text{Co}^{\text{II}}\text{Pc}]$  trapped in MCM-41 channels.

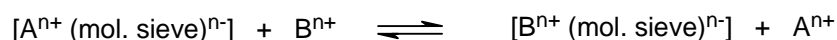
Schulz-Ekloff *et al*<sup>75</sup> reported the synthesis and optical properties of various molecular-sieves-based materials. Synthetic methods for the inclusion of dyes in molecular sieves include the following methods:

**(i) Dye loading by sorption**

The sorption of the dye is carried out from solutions or from gas phase. The size of the dye molecule must be smaller than the free diameter of the channels in order to give access to the pore system.<sup>89</sup> The dye molecules are physically adsorbed and can be therefore relatively extracted. The diffusion depends also on the strength of the guest-host interaction. An inhomogeneous distribution may occur. Example for this method is the sorption of CuPc into mesoporous Al-MCM-41.<sup>90</sup>

**(ii) Dye loading by ion exchange**

Cation exchange of ions originally present in negatively charged molecular sieves is an important strategy in their inclusion chemistry.<sup>89</sup> The process is usually occurs from solutions according to the following equation:

**(iii) Covalent anchoring of the dye onto pre-synthesized calcined mesoporous silica****(a) Covalent anchoring after modification of the surface:**

One possibility to overcome leaching of the dye in wide-pore mesoporous materials is their covalent bonding at pore walls.<sup>88</sup> In the first step the external surface must be passivated through the reaction with  $\text{Ph}_2\text{SiCl}_2$  whereas selective modification of the internal surface can be achieved by reaction of the silanol groups in the pores with different reagents such as 3-aminopropyltriethoxysilane or 3-chloropropyltriethoxysilane (Figure 13). The dye to be anchored must have a functional group, which is capable to react with the amino group or the chlorine, and consequently can be fixed onto the pores of the M41S materials. RuPc was incorporated into a Si-MCM-41 modified with 3-amino-propyltriethoxysilane.<sup>91</sup> Also  $[(\text{NH}_2)_4\text{Pc}\{\text{Fe}\}]$  has been immobilized in chloro-modified silica (Cl-MCM-41).<sup>92</sup> Similarly,  $[\text{ClAlPc}(\text{SO}_2\text{Cl})_2]$  was grafted onto amino-modified MCM-41 silica.<sup>93</sup> Bartels *et al*<sup>94a</sup> immobilized tetrasulfo-phthalocyanine in SBA-15 (Scheme 11a). The extraction stable fixation was achieved by either covalent or ionic bonding in the pores of differently modified hosts. Modification of the host material with N-trimethoxysilyl-propyl-N,N,N-trimethylammonium chloride provides a material that is suitable for ionic grafting of negatively charged dyes with less aggregation compared with covalently grafted dyes.

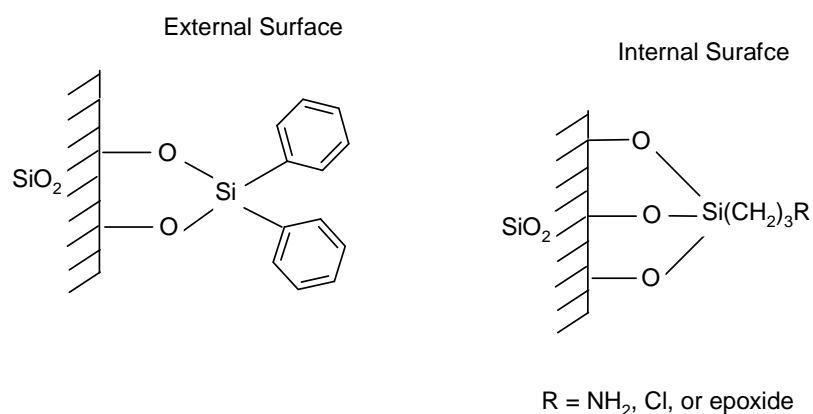
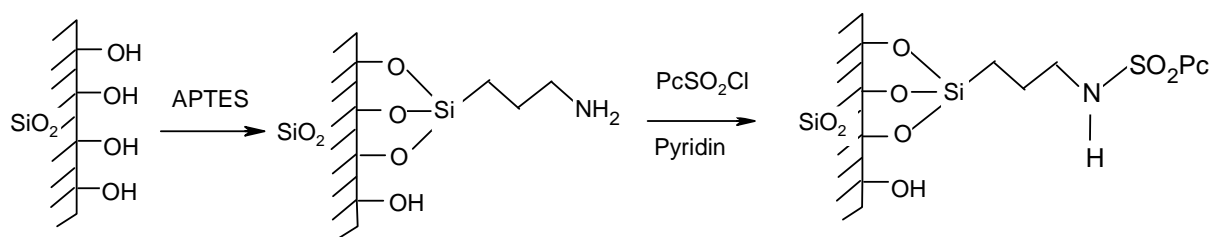


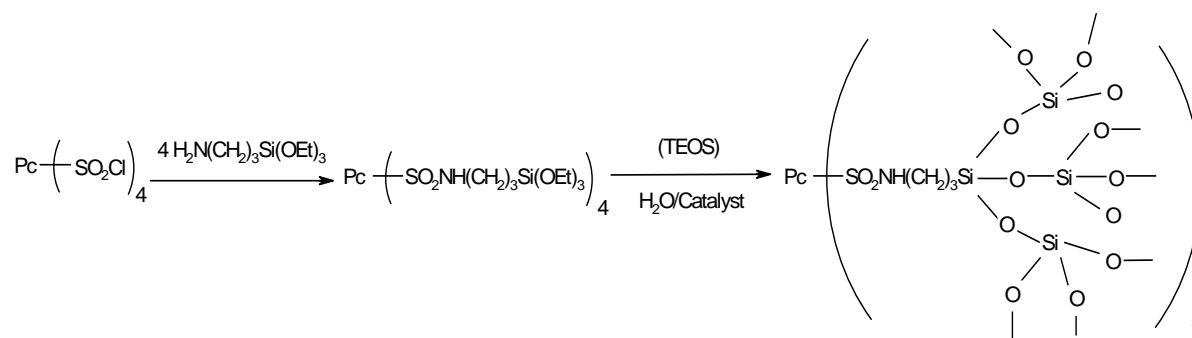
Figure 13: Modification of the surface of M41S materials.



Scheme 11a: Immobilization of Pc in SBA-15 or MCM-41 by covalent bonding.

(b) Phthalocyanine covalently bonded to an inorganic network:

Ribeiro *et al*<sup>94b</sup> described the preparation phthalocyaninosilica, where the phthalocyanine is covalently bonded to an inorganic network (Scheme 11b). The synthesis consists of the reaction between tetrachlorosulfonylphthalocyanine (PcSO<sub>2</sub>Cl) and 3-amino-propyltriethoxysilane (APTES) under reflux in dry dichloroethane. After that, ethanol, tetraethoxysilane, water and 1 M HCl or 1 M NH<sub>4</sub>OH were added to the reaction mixture. In this method the phthalocyanine molecules are incorporated into the silica network and the product was described as hybrid material, whereas the covalent bonded phthalocyanines to the modified surface of mesoporous silica was described as composite material.<sup>94a</sup>



Scheme 11b: Preparation of phthalocyaninosilica hybrid materials.

**(iv) Coordinative anchoring**

Recently, Wark *et al*<sup>95</sup> has provided a method to impregnate ZnPc onto Ti-MCM-41 by heating with ZnPc in dried DMF (Figure 14).

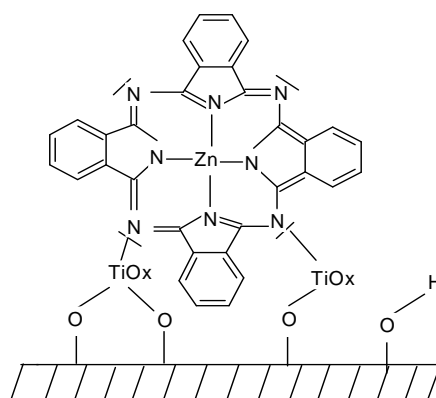
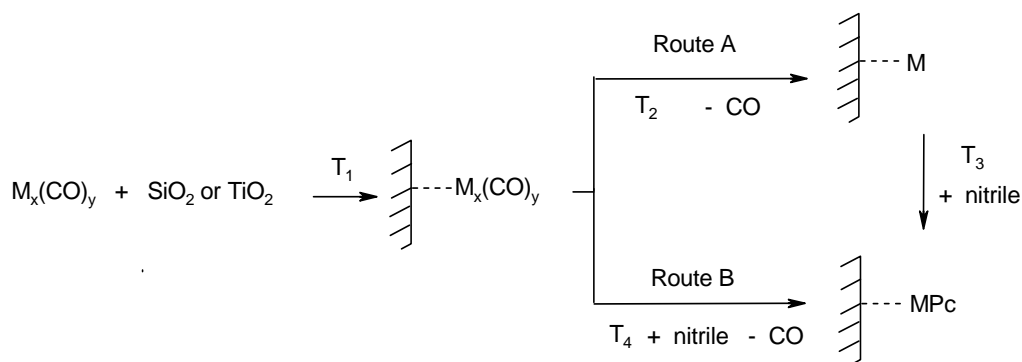


Figure 14: Coordinative anchoring of ZnPc onto Ti-MCM-41.

**(v) Dye synthesis in nanopores (ship in the bottle synthesis)**

In this method the dye is synthesized from two precursors. The first precursor is incorporated by diffusion and fixed by host-guest-interaction. Addition of the second precursor results in synthesis of the dye inside the cages. Wöhrle *et al*<sup>96</sup> have used this method for synthesis of polymeric and low molecular weight phthalocyanines from nitriles and metal carbonyls (Scheme 12) and used the produced matrices as catalysts in the sulfide oxidation. Also [CuPc] and [F<sub>16</sub>PcCo] have been prepared inside the pores of MCM-41 by heating a mixture of phthalonitrile and Cu<sup>2+</sup> or Co<sup>2+</sup> ion exchanged MCM-41 materials.<sup>97</sup>

Scheme 12: Synthesis of MPc on SiO<sub>2</sub> and TiO<sub>2</sub>.

### **(vi) Encapsulation of the dye during the preparation of the host**

The dye must be acid stable and soluble in the gel matrix in order to achieve a monomolecular encapsulation. CuTsPc-silica-sono-xerogel composites can be obtained by hydrolysis and polycondensation of tetramethoxysilane (TMOS) with [CuTsPc] in an aqueous solution<sup>98</sup> Sol-gel polymerization of tetraethoxysilane in the presence of some phthalocyanine polymers has been successfully achieved producing composites with the rod-like phthalocyanine polymers incorporated within ordered hexagonal channels.<sup>99</sup>

The axial ligand is also employed to anchor the dye to the nanocrystalline particles and to prevent the aggregation of the macrocycle. Ruthenium phthalocyanine pigment bearing pyridine-4-carboxaldehyde as an axial ligand has been prepared and the carboxaldehyde group of the apical ligand has been used to link the complex to the chemically modified surface.<sup>100</sup> Palomares *et al*<sup>101</sup> described a titanium phthalocyanine (Figure 15) and anchored it in nanocrystalline TiO<sub>2</sub> films through the axial carboxylate ligand without the use of co-adsorbents. The choice of titanium as a central metal allows axial ligation to the metal centre. State selective electron injection into the TiO<sub>2</sub> was demonstrated resulting in efficient photocurrent generation in dye sensitized solar cell.

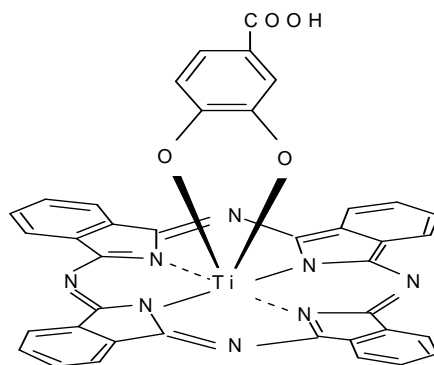


Figure 15: Axially substituted TiPc.

### **1.12.5 Characterization of MPc Modified Mesoporous Molecular Sieves**

Kadish *et al*<sup>102</sup> has summarized the recent developments in the design of composites based on porphyrins or phthalocyanines and inorganic hosts and discussed their most important applications. The Characterization of MPc@MCM-41 materials includes mostly powder X-ray diffraction, UV/DSR, FTIR, XAS, TEM, STM, nitrogen physisorption, and fluorescence excitation spectra. The stepwise decrease of the pore size could be precisely shown by nitrogen adsorption measurements e.g. shrinkage of 0.9 nm in case of functionalization with quaternary ammonium alkoxysilane. The powder XRD patterns of the obtained composites, as well as the fact that these reflections disappear upon calcinations point to a lamellar structure of the mesoporous material. In UV/VIS spectra a drastic change in the intensity ratio of the Soret bands and the Q-bands is often observed in comparison to the ratio in solution.

### **1.12.6 Applications of MPc Modified Mesoporous Molecular Sieve Materials**

The chemical stability of phthalocyanine chromophores is often drastically enhanced after inclusion.<sup>102</sup> The applications of such composite materials are reported in literature in the last decade and include the development of optical devices, improved and high stereo- and regioselective catalysts, etc. For optical applications embedding in polymers might be necessary<sup>103</sup>, requiring refractive index matching or chemical modifications at the external surface of the mineral crystals to improve the wetting by the polymer material. Methods for the production of colored composites as pigments on a large scale might be required. The coupling of molecular sieve based host-guest composites to external devices is essential for

fully exploiting their potential.<sup>88</sup> The realization of devices consisting of guest sieve assemblies interacting with other components constitute a challenging field of research in which considerable progress can be expected in the future.<sup>88</sup> Molecular sieve pigments where dyes are encapsulated in molecular sieves they exhibit better stability against photobleaching, chemical degradation and thermal decomposition.<sup>88</sup> Phthalocyanines with loading of (~ 1wt%) are mentioned as dyes with high extinction coefficients for normal absorption coloring.<sup>104,105</sup> A series of studied molecular sieves pigments, where the chromophores could be encapsulated without degradation, exhibited perfect migration stability. In most cases, high dye loadings were achieved for sufficient color intensity.

### **1.13 Photoluminescence of Phthalocyanines**

In the last decade, titanylphthalocyanine [PcTiO] was found to have excellent photoconductive response at the near-infrared GaAsAl laser wavelength and consequently its Y-form crystal has acquired a leading status as a photoreceptor in laser printing system.<sup>106</sup> Moreover, some substituted phthalocyanines compounds are used as CD-R dyes.<sup>107</sup> In addition some recent reports<sup>108,109</sup> on the electroluminescence (EL) of phthalocyanines compounds offer a new potential application as light-emitting materials. Most of these functions are generated through the excited states of solid phase phthalocyanines. Therefore, knowledge of their excited electronic states and relaxation processes is important to understand these functions. Photoluminescence (PL) is a powerful probe for the excited states, because it supplies important information by measuring its properties such as quantum yields, spectra, time decay, and temperature dependence. Photoluminescence of phthalocyanines molecules in solution (and in vapor) has been investigated extensively and many fluorescence spectra and quantum yields are reported in the literature.<sup>110,111</sup> However, PL properties in the solid or crystalline phases have been only studied for a limited number of phthalocyanines materials such as PcH<sub>2</sub>,<sup>112</sup> [ZnPc],<sup>113</sup> [PcAlCl],<sup>114</sup> [PcVO],<sup>115</sup> [PcTiO].<sup>116</sup> Sakakibara and his coworkers<sup>117</sup> have measured the photoluminescence properties for vacuum-deposited thin films of magnesium, chloroaluminum, bromoaluminum, and metal-free phthalocyanines (MgPc, AlClPc, AlBrPc, and H<sub>2</sub>Pc). The authors observed an increase of the fluorescence intensity with decreasing temperatures in all samples, but the extent of the increase was at most as large as 10 times, even at the liquid helium temperature, indicating that nonradiative relaxation is still dominant. The spectral features were very difficult depending on the crystal phases and the materials. The as-deposited AlBrPc and H<sub>2</sub>Pc films showed broad emission

bands at approximately 1000 and 900 nm. This feature was interpreted by the very weakly allowed transition from the forbidden lowest-lying exciton state to the vibronic sublevel of the ground state. The appearance of new bands was ascribed to the change of the crystal packing.<sup>114</sup> The expanded  $\pi$  orbitals of the phthalocyanines and metal phthalocyanines create the large oscillator strength in the Q band ( $S_1$ ) region and result in high quantum yields of fluorescence. Pigments, dyes, nonlinear optics, and optical data storage devices are important applications of phthalocyanines. Phthalocyanines are also important for applications in electronic conduction because of their extra stabilization of electrons/holes in their large  $\pi$ -electronic frameworks.<sup>118</sup>

#### **1.14 Phthalocyanines as Laser Pigments**

Sakaguchi *et al*<sup>119</sup> reported the manufacture of a material, which shows excellent electrophotographic characteristics containing a titanium-phthalocyanine pigment and a charge-transporting layer containing a hydrazone while the charge-transporting layer is prepared by coating with a solution containing a polycarbonate resin and a dioxane-containing solvent. The image formation was claimed by reversal development using a photoreceptor containing composite particles of a phthalocyanine and a polycyclic quinone pigment or a polycyclic anhydride.<sup>120</sup> The photoreceptor shows high sensitivity to near-IR ray, i.e., of a semiconductor laser, and stable potential at the first charging. Kim *et al*<sup>121</sup> prepared a polyoxymethylene resin composition for laser marking, which has improved thermal stability, durability, and abrasion-, chemical-, and fatigue-resistance comprising 100 parts polyoxymethylene, 0.01-3.0 parts carbon black coated with OH group, 0.01-5.0 parts dihydrazide compounds, such as oxalic dihydrazide and malonic dihydrazide,  $TiO_2$ , inorganic pigment and phthalocyanine blue as an organic pigment. Shimomura *et al*<sup>122</sup> utilized CuPc pigment in the manufacture of ink cartridges free of problems associated with precipitation. The cartridges contain microporous absorbing materials (polyurethanes) filled with CuPc pigment dispersion and displayed improved ink storage stability.

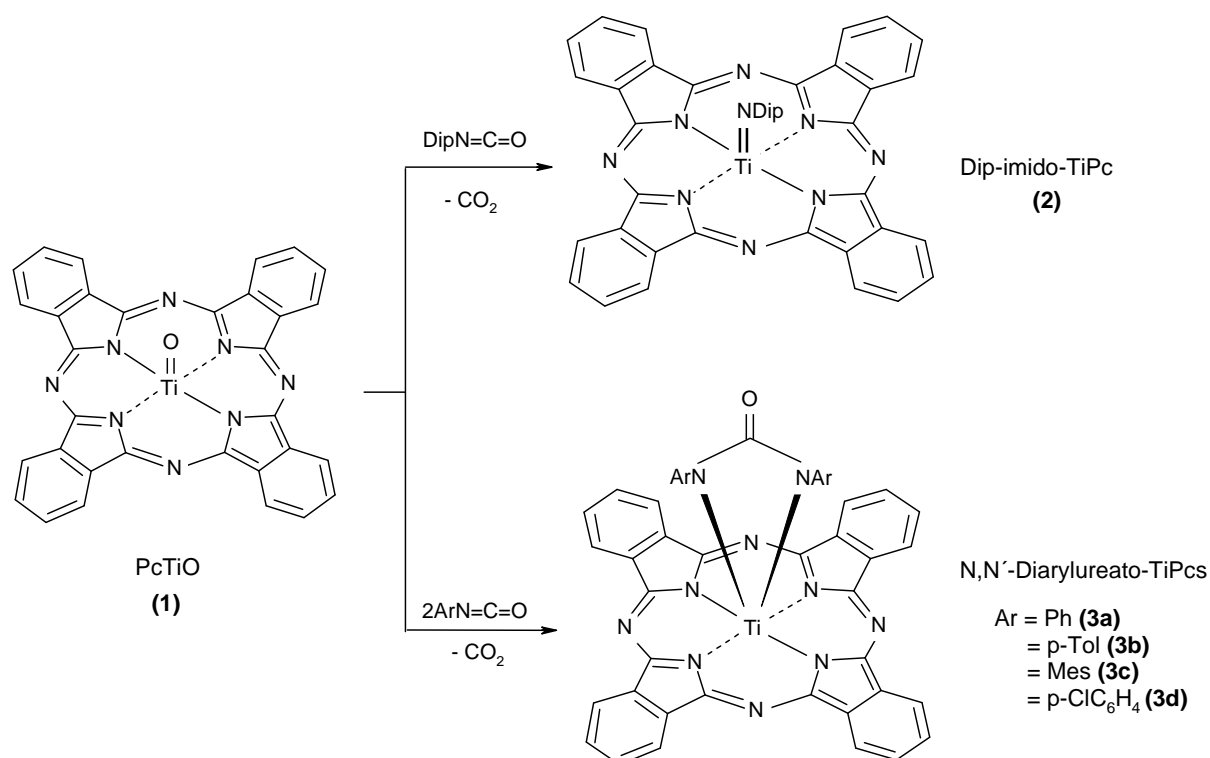


## 2. Results and Discussions

### 2.1 Titanium Phthalocyanines

#### 2.1.1 Synthesis of Imido-TiPc (2) and Ureato-TiPcs (3a-d)

We became interested to investigate the typical reaction patterns of [PcTiO] (**1**) aiming at the synthesis of its isoelectronic derivatives PcTiX (X = S, Se, NR, etc) that have not been isolated in a pure form up to date. As one of the synthetic strategies for the replacement of the oxo functionality and generating an organoimido group, we chose the metathesis of [PcTiO] (**1**) with several organic isocyanates (Scheme 13). This metathetical transformation was found to depend largely on the size of the aryl group. For the large group, 2,6-diisopropylphenyl, the imido complex (**2**) was the final product. For small groups such as R = phenyl, the imido complex could not be isolated in an analytically pure form since it reacts readily with a second equivalent of the arylisocyanate in a [2+2] cycloaddition forming the N,N'-diarylureato complexes (**3a-d**).



Scheme 13: Reaction of [PcTiO] (**1**) with different arylisocyanates.

In the last case the molecular ion peaks of the corresponding diarylcarbodiimide were detected in MS measurements of the crude samples. The ureato products were purified from these white byproducts by extraction with the organic solvents. These byproducts were not detected in the reaction of [PcTiO] with 2,6-diisopropylphenyl isocyanate since the final product is the imido complex.

### **2.1.2 Mechanism of the reaction of [PcTiO] with arylisocyanates**

The suggested mechanism of reaction of [PcTiO] with the arylisocyanates containing small aryl groups is illustrated in (Figure 16). The mechanism involves a [2+2] cycloaddition of an isocyanate molecule with the titanyl group forming the cyclic intermediate **(I)**. This unstable metallocycle readily loses a molecule of CO<sub>2</sub> forming the corresponding imido complex [PcTi(NR)] **(II)**.

In the case of sterically demanding 2,6-diisopropylphenyl isocyanate only one addition (cycloreversion step) seems to be possible and the imido complex is the final product. Any further addition of a second isocyanate molecule to the [Ti=NAr] functionality is supposed to be hindered because of the high steric occupation caused by the two isopropyl groups around the reacting Ti=N bond. In case of arylisocyanates with aryl groups having less steric hindrance, ArN=C=O (Ar = phenyl, 4-tolyl, mesityl or 4-ClC<sub>6</sub>H<sub>4</sub>) another [2+2] addition of an isocyanate molecule at the [Ti=N] bond is observed leading to the formation of the corresponding ureato complex **(III)**.

The carbodiimide byproduct **(V)** was not observed in the reaction of titanylphthalocyanine with 2,6-diisopropylphenyl isocyanate, since the formation of the corresponding carbodiimides is essentially depending on the second addition of an arylisocyanate molecule and formation of the cyclic intermediates **(III)** and **(IV)**. This second addition is completely hindered in the case of 2,6-diisopropylphenyl isocyanate. It is noteworthy to mention, that all attempts made trying to react tert-butyl isocyanate, with [PcTiO] were unsuccessful. Also, vanadylphthalocyanine [PcVO] seemingly does not react with the aryl isocyanates under the same conditions applied for the reaction of [PcTiO].

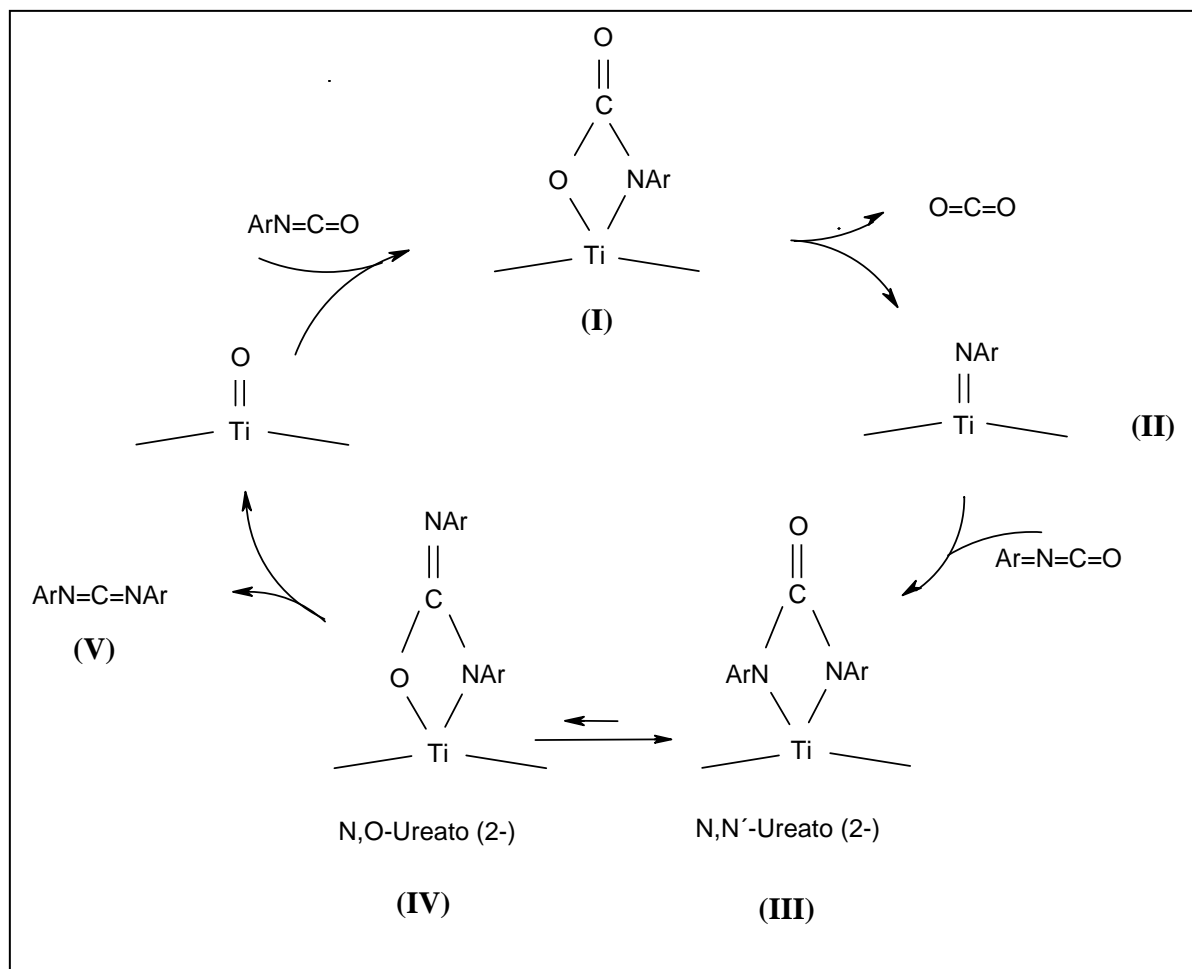
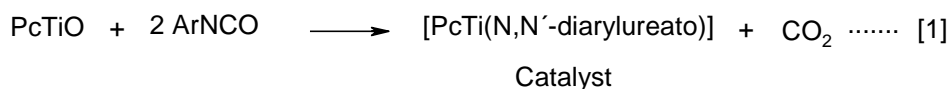


Figure 16: The suggested mechanism for the reaction of [PcTiO] (1) with different arylisocyanates.

Thus, the reaction of [PcTiO] (1) with arylisocyanates containing small aryl group can be used in the catalytic metathesis of the arylisocyanates into the corresponding arylcarbodiimides and carbon dioxide. The general catalytic reaction can be summarized as follows:



### 2.1.3 Characterization of Imido-TiPc (2) and Ureato-TiPcs (3a-d)

#### Mass Spectra and Elemental Analysis

The  $m/z$  values of the molecular ions of the prepared imido- and ureato-TiPcs in EI, MALDI-TOF, and ESI measurements were observed with the expected isotopic patterns as illustrated in (Figure 17). There are five naturally abundant isotopes of Ti ( $^{45}\text{Ti}$ ,  $^{46}\text{Ti}$ ,  $^{47}\text{Ti}$ ,  $^{48}\text{Ti}$  and  $^{49}\text{Ti}$ ) with the following natural abundance 8%, 7.3%, 73.8%, 5.5%, and 5.4% respectively. The absence of  $M^+ = 576$  of  $[\text{PcTiO}]$  was observed for the pure ureato-TiPcs. The structures of (2) and (3a-d) were confirmed also by the elemental analysis of %C, %H, and %N in addition to determination of the titanium content using AAS technique.

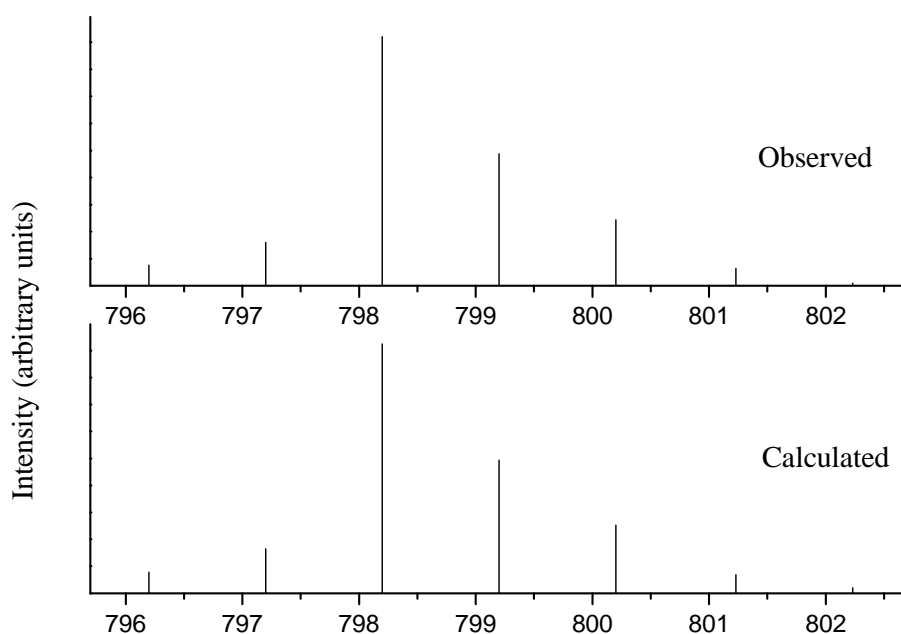


Figure 17: MALDI-TOF spectrum of (3b) and the isotopic pattern of the molecular ion.

#### UV/VIS

UV/VIS spectra of the prepared imido- and ureato-TiPcs show the characteristic metalphthalocyanine absorptions.<sup>4</sup> (Figure 18) shows the UV/VIS spectra of compounds (1), (2) and (3b). The Q band at ( $\lambda_{\text{max}} \sim 698$ ) nm is attributed to an allowed ( $\pi$ - $\pi^*$  transition).

A second allowed  $\pi$ - $\pi^*$  transition (B band), near 340 nm, extending to the blue of the visible spectrum is also observed.<sup>8</sup> The shoulders at  $\lambda_{\text{max}} \sim 665$  nm and 628 nm are vibronic transitions.<sup>56b</sup> The intense Q band arises from the doubly degenerated transition between the  $A_{1g}$  ( $a^2_{1u}$ ) ground state to the first excited singlet state which has  $E_u(a^1_{1u}e^1_g)$  symmetry.<sup>8,17</sup> Generally, no significant changes have been induced in the absorption positions in the UV/VIS spectra as the titanyl group replaced with the imido- or ureato-ligand. This is attributed to the fact that the absorption positions and patterns arise mainly from the phthalocyanine basic moiety and are only slightly affected by the nature of the axial ligands.<sup>4</sup> The absorption measurements were carried out in both of chloronaphthalene and chloroform (cut-off point at 240 nm) and no significant difference was observed.

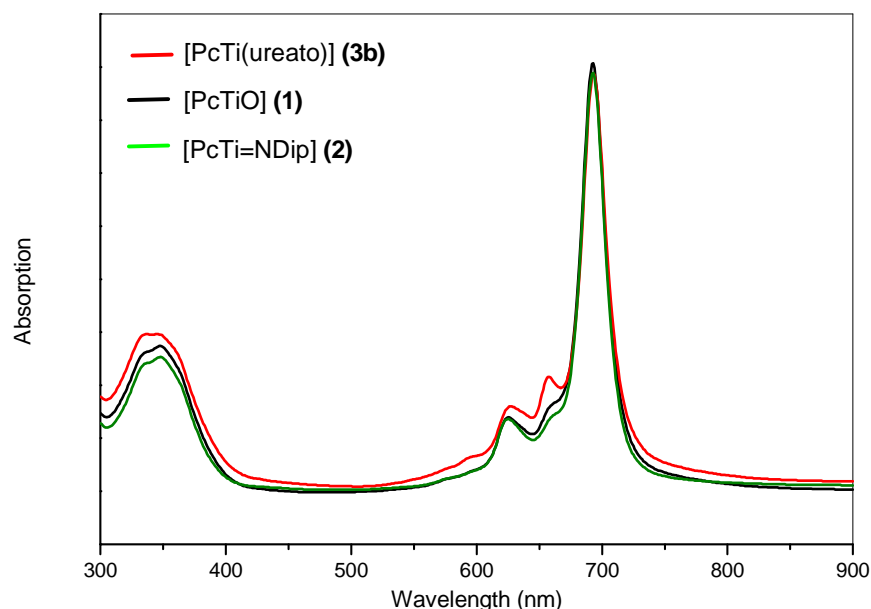


Figure 18: UV/VIS spectra of the compounds (1), (2) and (3b) in  $\text{CHCl}_3$ .

### IR Spectra

The vibration spectra are dominantly internal vibrations of the  $\text{Pc}^{2-}$  ligand. The IR absorptions common to the spectra of the basic Pc moiety, such as  $\nu_{\text{C}=\text{C}}$  arom. at  $1608 \text{ cm}^{-1}$ , were observed (Figure 19). New bands, which are not observed in the spectra of  $\text{PcH}_2$ ,  $\text{PcTiO}$ ,  $\text{PcTiCl}_2$ , or  $\text{PcMnCl}$ , were observed in the spectra of imido- and ureato-TiPcs. These new vibrations, underlined in IR data of (2) and (3a-d) in the experimental work, include the  $\nu_{\text{C}=\text{O}}$  vibrations at  $(1675\text{-}1690 \text{ cm}^{-1})$ . Other new signals at different values along the finger print region of the spectra ( $800\text{-}1400 \text{ cm}^{-1}$ ) are also observed. However, unambiguous

assignment to stretching of the [Ti=N] bond in imido and the [Ti-N] in ureato-TiPcs bonds can not be assumed because of the well known multiplicity of IR absorptions of Pcs in this region. This is also known in imidoporphyrins whose similar IR spectra.<sup>44</sup> One of the important features in IR spectra of the prepared imido- and ureato-TiPcs is the absence of  $\nu_{\text{Ti=O}}$  at  $965\text{ cm}^{-1}$ .

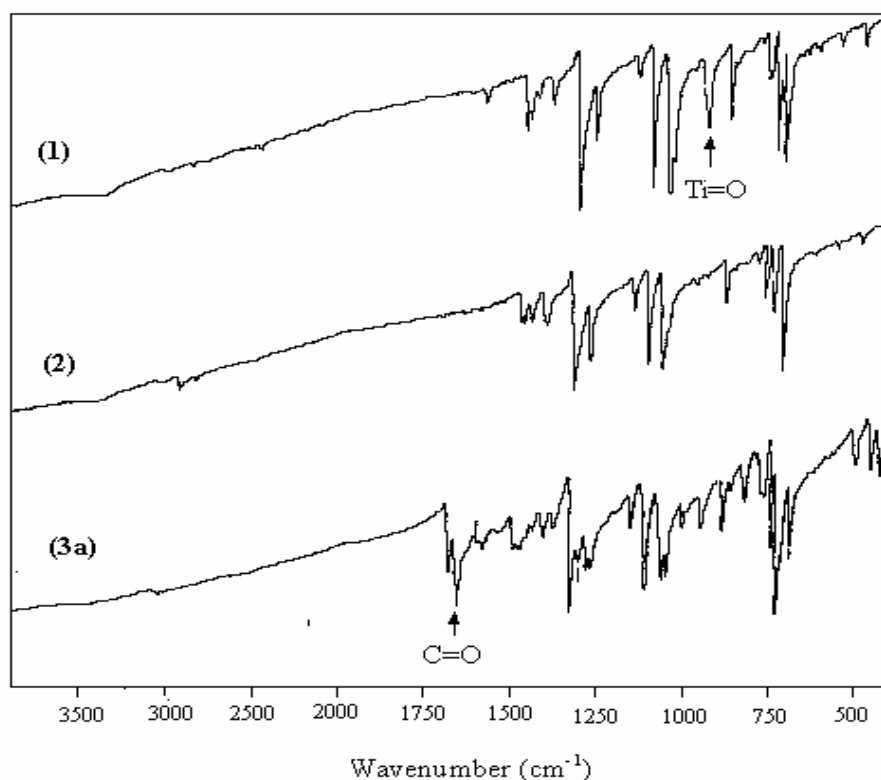


Figure 19: IR spectra (KBr pellets) of [PcTiO] (**1**), [PcTi(NDip)] (**2**), and [PcTi(N,N'-diphenylureato)] (**3a**).

### <sup>1</sup>H-NMR Spectra

The <sup>1</sup>H-NMR spectra of Pcs are known to show large diamagnetic ring-current effects due to the macrocyclic 18- $\pi$ -system.<sup>8,39,41</sup> Thus, the signals of the aromatic protons of phthalocyanines appear at lower field than in PN. Protons of the axially bonded ligands show a large shift to higher field. The shift to high field depends on the distance and relative position of the protons to the macrocycle. Planar phthalocyanines exhibit a large shift of the aromatic and central ring protons at different concentrations and temperatures due to aggregation phenomena.<sup>123</sup> When the aggregation is prevented by additional axial ligands or

by long side chains in the 1,4-position, this influence should be reduced. The  $^1\text{H-NMR}$  spectra of arylimido-TiPc (**2**) and diarylureato-TiPcs (**3a-d**) show the expected resonance patterns and integration values for the suggested structures (spectrum of **3a**) is shown in Figure 20). Moreover, the spectra display pure compounds free from any signals of [PcTiO], unreacted arylisocyanate, and the diarylureato byproducts. The phthalocyanine unit shows in the aromatic region the characteristic AA'BB' spin pattern for an unsubstituted Pc, with two multiplets, the first multiplet found generally in the region 9.46-9.93 ppm for eight protons in the 1,4-positions and the second multiplet in the region 8.21-8.47 ppm for eight protons in the 2,3-positions. The protons of the axial ligand show upfield-shifted signals due to the well-known current effect of the phthalocyanine rings. The aromatic protons of the axial ligand appear in the region 4.95-6.60 ppm and the methyl groups in the region 0.74-2.07 ppm. The CH and CH<sub>3</sub> protons of the isopropyl group in (**2**) show a typical upfield shift, the methyl group at (0.03 ppm,  $J = 4.9$  Hz) and CH group at 0.27-0.39 ppm. This upfield shift may be attributed to two factors; the first is the low distance between the (*Dip* substituent, and the Pc macrocycle, the second may be the higher extent of planarity in (**2**) compared to (**3a-d**) which increases the aggregation and the ring-current effect.<sup>123</sup>

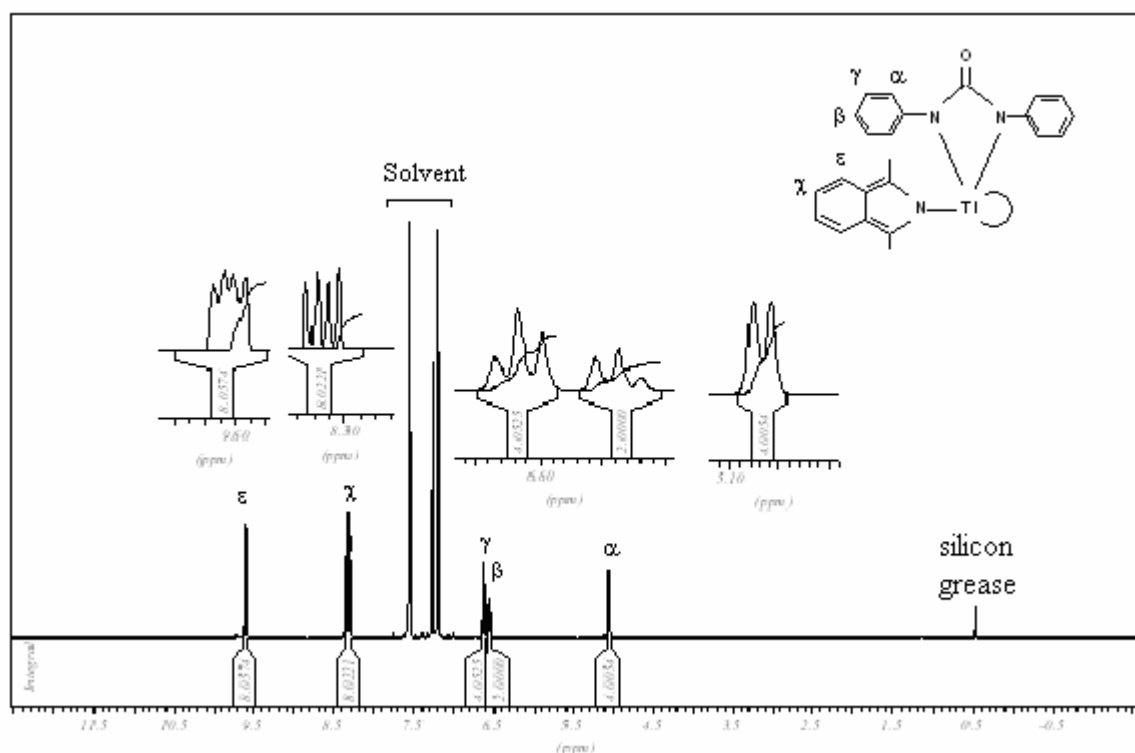


Figure 20:  $^1\text{H-NMR}$  spectrum of (**3a**) (500 MHz, at 373 K, in  $\text{C}_6\text{D}_5\text{Br}$ ).

## Fluorescence Measurements

The expanded  $\pi$  orbitals of Pcs create the large oscillator strength in the Q band ( $S_1$ ) region and result in high quantum yields of fluorescence and therefore they are efficient pigments.<sup>120-122</sup> Room temperature fluorescence measurements of **(1)** and **(3b)** (Figure 21) show that the emission intensities are comparable. A red shift in the emission spectrum is observed as the axial group is replaced from oxo to the ureato group (B-band excitation at  $\lambda_{exc} = 230$  nm). Consequently **(1)** displays a higher radiative energy-deactivation than **(3b)**. The fluorescence which results from Q-band excitation occurs at higher wavelength (lower energy) in **(3b)** than in **(1)** (at  $\lambda_{exc} = 630$  nm and 650 nm respectively) but the radiative deactivation and the fluorescence quantum yield is more in **(1)** than in **(3b)**.

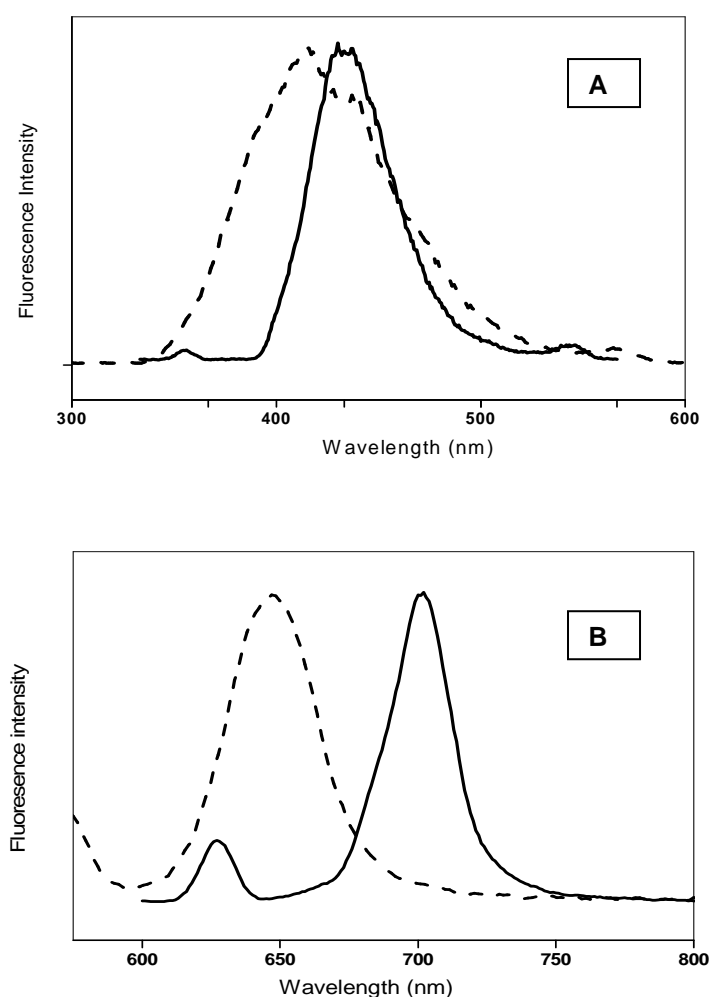


Figure 21: Fluorescence spectra of [PcTiO] **(1)** (dotted line) and **(3b)** (solid line).

[A] excitation at 280 nm; [B] excitation of **(1)** at 630 nm and **(3b)** at 650 nm.



## TGA&DSC

### (i) [PcTi(NDip)] (2)

Although the MPcs are generally robust at ambient temperature, most of axially substituted Pcs underwent axial bonds cleavage at elevated temperatures. Generally, two successive thermal decompositions are characteristic for the axially substituted MPcs. The first one occurs in the temperature range (250–450 °C) and represents the destruction of the axial ligand and the second occurs at about 600°C and represents the destruction of the Pc macrocycle<sup>124</sup>. The thermal gravimetric pattern of [PcTi(NDip)] is illustrated in (Figure 22). Generally, [PcTi(NDip)] (2) shows a high thermal stability since no weight loss is observed up to 300°C. Afterwards, the compound shows two endothermic effects (as shown from DSC measurements), the first weight loss occurs in the temperature range of (300-420 °C) and is attributed to the thermal destruction of the axial moiety that represents the loss of the imido ligand (NDip, C<sub>12</sub>H<sub>17</sub>N) (Figure 23). The second one starts at about 600°C and is attributed to the thermal destruction of the basic skeleton of the phthalocyanine. This TGA profile is common for most of the axially substituted phthalocyanines. Calculations made for the TGA diagrams matched well with those experimentally observed for compound (2).

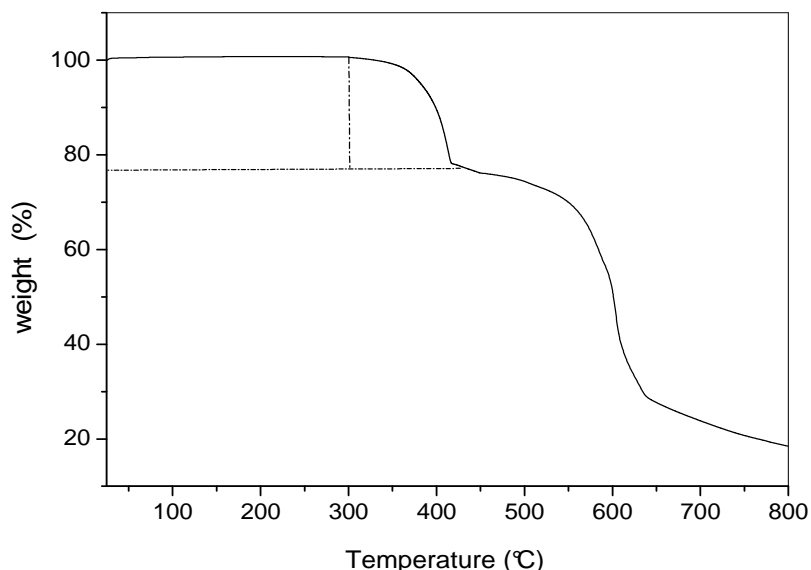


(Figure 22): TGA Diagram of (2).

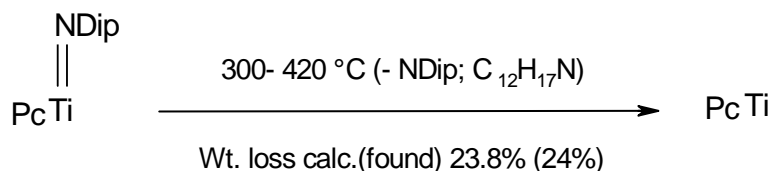


Figure 23: Thermal decomposition of the axial moiety of (2).

**(ii) Diarylureato-TiPcs (3a-d)**

The [PcTi(N,N'-diarylureato)] compounds are thermally stable up to 220°C since no weight loss is observed before this temperature. At higher temperature a different TGA profile, a three steps thermal decomposition, was observed for the ureato-TiPcs. The decomposition of the axial (ureato) ligand occurs in the temperature range of (220-300 °C) and involves two successive weight losses associated with two endothermic effects (Figure 24). The first weight loss represents the loss of ArN=C=O molecule via a [2+2] cyclo reversion and formation of an imido complex and the second represents the loss of nitrene fragment [ArN] (**I**) and consequently the formation of the fragments [PcTi] (**II**) (Figure 25). This is in addition to the third step at about 600°C, which represents the complete decomposition of The Pc macrocycle. Quantitative calculations for the thermal destruction of diarylureato-TiPcs have been made and the values match well with the calculated values (Table 3).

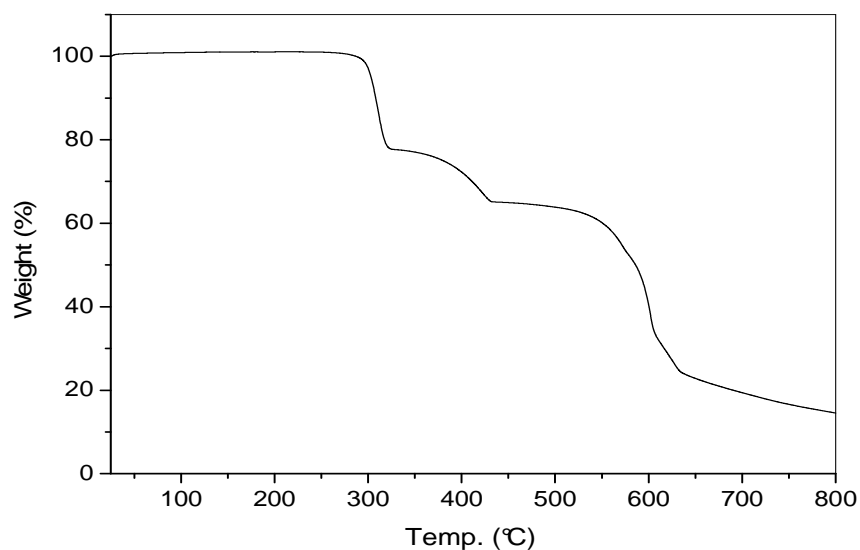


Figure 24: TGA diagram of (3c).

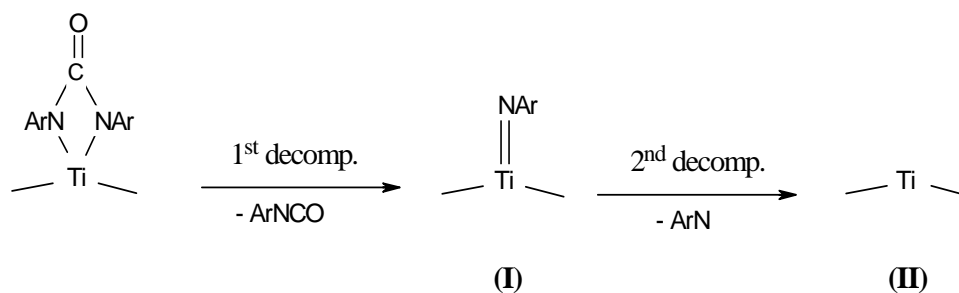


Figure 25: Stepwise thermal decomposition of the axial moiety in (3a-d).

Table 3: Thermal Analysis Data of Diarylimido-TiPcs (3a-d)

R	Weight loss (%) at the end of the 1 <sup>st</sup> stage			Weight loss (%) at the end of the 2 <sup>nd</sup> stage		
	Temp. (°C)	Calcd.	Found	Temp. (°C)	Calcd.	Found
Ph	220-250	15.5	19	250-300	27.3	28
4-tolyl	212-260	16.8	18	260-520	30	30
mesityl	317-320	19	22	320-435	34.4	35
4-ClC <sub>6</sub> H <sub>4</sub>	266-300	18.3	---	300-330	33.2	35

#### 2.1.4 Crystal Structure of [PcTi(NDip)] (2)

The crystal structure of (2) (Figure 26) was solved and its crystallographic data are reported. It crystallizes in the centrosymmetric space group  $P2_1/n$  with 4 molecules per the unit cell (P: primitive cell;  $2_1$ : two fold screw axis; n: diagonal glide plane “according to International Tables for Crystallography: Volume A”). The molecule consists of a five-coordinate titanium (IV) atom surrounded by four equatorial isoindoline rings of the Pc molecule and the imido group in the axial position. Therefore, the geometry about the titanium atom is square-pyramidal with the four isoindoline nitrogen atoms forming the basal plane and the imido group at the apical site. Titanium atom is too large and unable to enter the cavity of the Pc macrocycle, so it sits “atop” or “out-of-plane” from the  $N_4$  plane. Such situation called extra-coordination and the macrocycle adapts to this special situation by deformation and the macrocycle takes the appearance of a saucer with  $\varphi = 156.28(1)$ , since  $\varphi$  is the angle between the plane of isoindoline unit and the Ni-M bond.<sup>12</sup> Since the angle  $\varphi$  is less than  $180^\circ$  the molecule suffers from conformational stress particularly for the  $sp^2$  isoindoline nitrogen atoms.

Titanium atom is displaced from the plane defined by the four  $N_i$  isoindoline nitrogen atoms toward the imido ligand by 0.594 Å. This distance is 0.70-0.72 Å in [PcTiO]<sup>36</sup> and 0.84 Å in [PcTiCl<sub>2</sub>].<sup>32</sup> The imido group is nearly linear with a C42–N41–Ti angle 178.20(3)°. The slight deviation from 180° may be due to the interaction with the two adjacent isopropyl groups. The bond length of [Ti–N<sub>imido</sub>] is 1.707(3) Å, therefore a Ti–N triple bond character can be suggested. Compound **(2)** belongs to the *cis* complexes which have two different molecular sides, a “phthalocyanines only” side, and a side, which is dominated by the central atom and the axial ligand, Due to the resemblance with optical lenses, Iyechika<sup>125</sup> first adopted the terms “concave side” to represent the phthalocyanines only side, and “convex side” to describe the “metal-axial-ligand side”. Crystal structure of the imido TiPc **(2)** is very similar to that of its analogue phenylimido-Ti tetratoloylporphyrine [(TTP)TiN=Ph].<sup>44</sup> Selected bond distances (Å) and bond angles (deg.) of **(2)** are given in (Table 4).

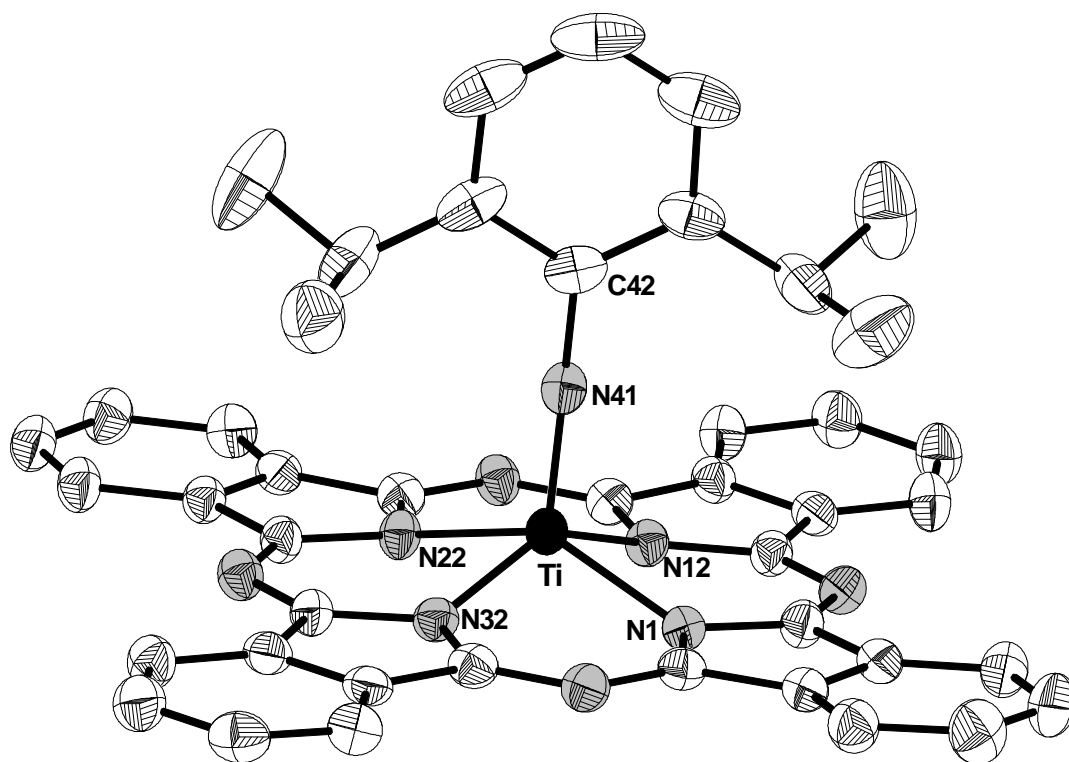


Figure 26: The molecular structure of **(2)**. Displacement ellipsoids at the 50% probability level. (H atoms are omitted for clarity)

Table 4: Selected Bond Distances for (2)

Bond Distances (Å)			
Ti–N1	2.062(3)	Ti–N12	2.057(3)
Ti–N22	2.059(3)	Ti–N32	2.069(3)
Ti–N41	1.707(3)	N41–C42	1.396(3)
Bond Angles (deg)			
C42–N41–Ti	178.20(3)	N41–Ti–N12	105.89(15)
N41–Ti–N22	107.85(14)	N12–Ti–N22	85.54(12)
N41–Ti–N1	105.67(13)	N12–Ti–N1	85.13(12)
N22–Ti–N1	146.48(13)	N41–Ti–N32	107.58(14)
N12–Ti–N32	146.52(13)	N22–Ti–N32	84.83(13)
N1–Ti–N32	85.44(13)		

### **The Molecular Packing and the Arrangement in the Crystal Lattice of (2)**

From studying the molecular packing and the arrangement of the molecules in the unit cells of (2) (Figure 27), it can be concluded that the presence of the axial imido group at the central titanium atom results in increasing of the steric demand in the face-to-face lattice more than that observed in some isoelectronic phthalocyanines such as [PcTiO].<sup>36</sup> Due to  $\pi$ - $\pi$  interaction of the basal faces of the pyramidal molecular structure the crystal lattice consists in a close packing of face-to-face dimers. A crystallographic inversion centre relates the two molecules of the dimer with respect to each other. The imido moieties are stacked in the crystal lattice in a trans-arrangement to minimize the interaction between each two neighboring phthalocyanine molecules. This modifies drastically the molecular packing of the phthalocyanine in the solid state relative to the molecular packing of [PcTiO]. Therefore, relevant consequences for the electronic and NLO properties would be expected for the prepared [PcTi(NDip)] (2).

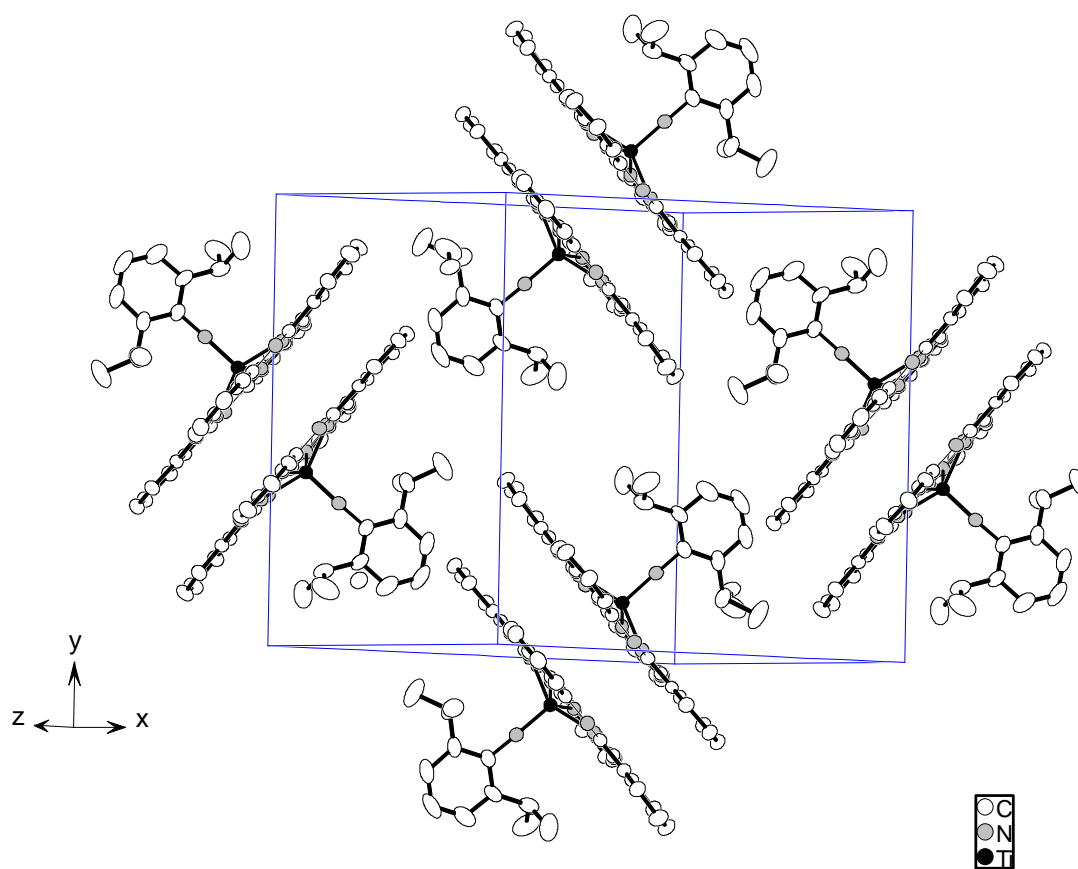


Figure 27: The molecular packing of (2) View along [101] diagonal.

### 2.1.5 Crystal Structures of Ureato-TiPcs (3a) and (3b)

The crystal structures of **(3a)** and **(3b)** were solved and their crystallographic data are given (Figures 28, 29). Compound **(3a)** crystallizes in the centrosymmetric space group  $P2_1/n$  with 4 molecules per unit cell (P: primitive cell;  $2_1$ : two fold screw axis; n: diagonal glide plane). Compound **(3b)** crystallizes in the centrosymmetric space group  $P\bar{1}$  with 2 molecules per unit cell ( $P\bar{1}$ : primitive cell containing an inversion centre). The inversion centre in **(3b)** is the titanium atom. In both structures the molecule consists of a six-coordinate titanium (IV) atom surrounded by four equatorial isoindoline rings of the Pc molecule and the ureato group in the axial position. Therefore, the geometry about the titanium atom is square-pyramidal with the four isoindoline nitrogen atoms forming the basal plane and the ureato group at the apical site.

The titanium atom is too large and unable to enter the cavity of the phthalocyanine macrocycle, so it sits “atop” or “out-of-plane” from the  $N_4$  plane. Such situation is called extra-coordination and the macrocycle adapts to this special situation by deformation and the phthalocyanine macrocycle takes the appearance of the saucer.<sup>12</sup> Titanium atom is displaced from the plane defined by the four  $N_i$  isoindoline nitrogen atoms toward the imido ligand by 0.791 Å in **(3a)** and 0.763 Å in **(3b)**.

Selected bond distances (Å) and bond angles (deg.) of **(3a)** and **(3b)** are given in (Tables 5 and 6). A comparison of bonding parameters of the compounds **(2)**, **(3a)** and **(3b)** with [PcTiO] and [PcTiCl<sub>2</sub>] is also reported in (Table 7). From this comparison, it can be concluded that the titanium atom in all known titanium phthalocyanines is displaced above the  $N_4$  mean plane. The distance in which the titanium atom is displaced out of the  $N_4$  plane follows the order: [PcTiCl<sub>2</sub>] > **(3a)** > **(3b)** > [PcTiO] > **(2)**. Consequently, the [Ti-N<sub>iso</sub>] bonds lengths follow the same previous order.

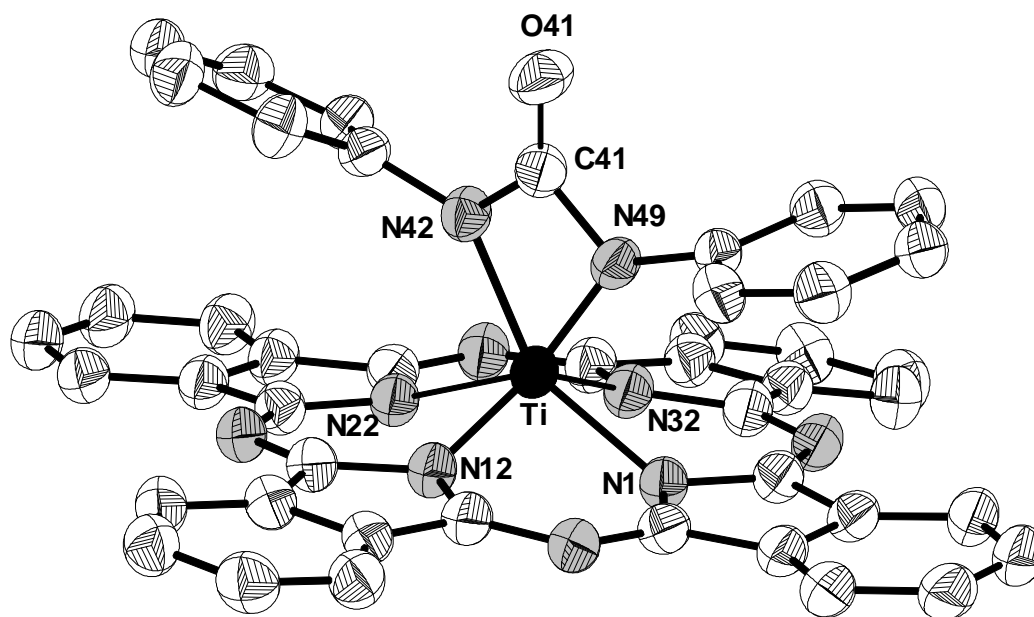


Figure 28: The molecular structure of **(3a)**.

Displacement ellipsoids at the 50% probability level. (H atoms are omitted for clarity)

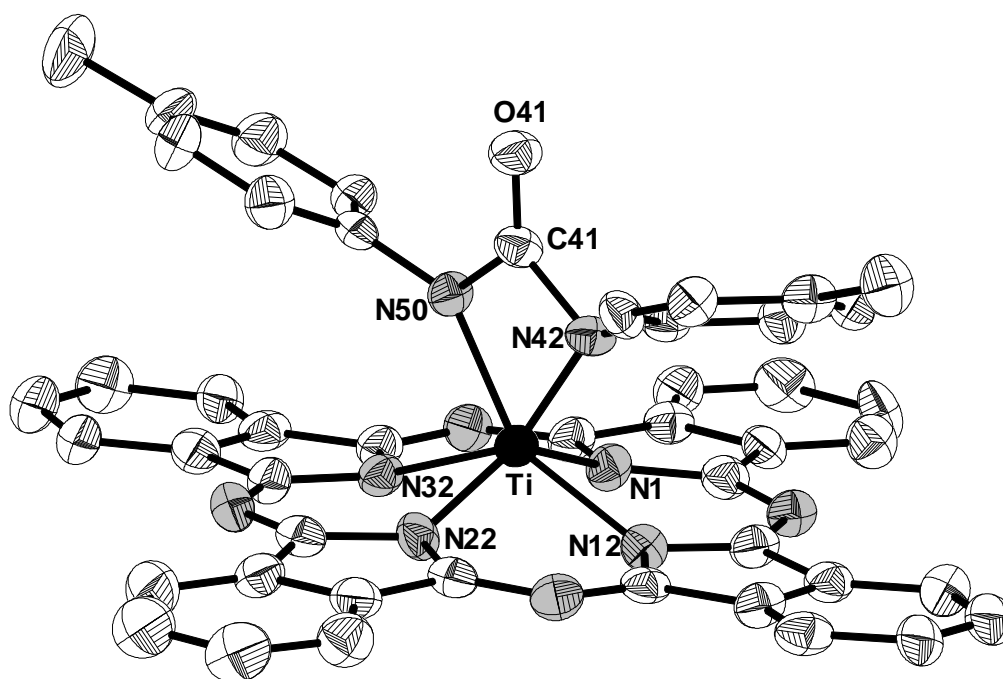


Figure 29: The molecular structure of **(3b)**.

Displacement ellipsoids at the 50% probability level. (H atoms are omitted for clarity)



Table 5: Selected Bond Distances (Å) of **(3a)** and **(3b)**

<b>(3a)</b>		<b>(3b)</b>	
C41–N42	1.389(3)	C41–N42	1.396(7)
C41–O41	1.217(3)	C41–O41	1.221(7)
C41–N49	1.393(3)	C41–N50	1.402(7)
N1–Ti	2.113(2)	N1–Ti	2.060(5)
N12–Ti	2.069(3)	N12–Ti	2.111(5)
N22–Ti	2.105(2)	N22–Ti	2.066(5)
N32–Ti	2.060(2)	N32–Ti	2.104(5)
N42–Ti	2.001(2)	N42–Ti	1.982(4)
N49–Ti	1.972(2)	N50–Ti	1.990(9)

Table (6): Selected Bond Angles (deg.) in **(3a)** and **(3b)**

<b>(3a)</b>		<b>(3b)</b>	
N49–Ti–N42	65.42(8)	N42–Ti–N50	65.59(18)
O41–C41–N42	130.0(3)	O41–C41–N42	130.6(5)
N42–C41–N49	101.1(2)	N42–C41–N50	100.5(5)
N12–Ti–N22	81.50(9)	N22–Ti–N12	82.30(18)
N32–Ti–N1	81.73(9)	N1–Ti–N32	82.89(18)
N12–Ti–N1	81.60(9)	N1–Ti–N12	81.97(18)
N22–Ti–N1	131.86(8)	N1–Ti–N22	140.26(19)
C41–N42–Ti	96.02(16)	C41–N42–Ti	97.1(3)
C41–N49–Ti	97.17(16)	C41–N50–Ti	96.5(3)

Table 7: Comparison of Bonding Parameters in **(2)**, **(3a)**, **(3b)**, [PcTiCl<sub>2</sub>], and [PcTiO]

Complex	Av. Ti–N (Å)	Ti from N <sub>4</sub> plane (Å)	Reference
[PcTiCl <sub>2</sub> ]	2.087	0.84	32
[PcTiO]	2.067	0.63	36
<b>(2)</b>	2.062	0.594	this work
<b>(3a)</b>	2.086	0.791	this work
<b>(3b)</b>	2.085	0.763	this work

### The Molecular Packing and the Arrangement in the Crystal Lattice of (3a) and (3b)

From studying of the molecular packing and the arrangement of the molecules in the unit cells of **(3a)** and **(3b)** (Figures 30, 31), we noticed that two molecules of the solvent of crystallization (chlorobenzene) are included in the centre of the unit Cell of **(3b)**. The presence of the prism-shaped axial ureato group at the central titanium atom results in increasing of the steric demand in the lattice more than that of the [PcTi(NDip)] and [PcTiO].<sup>36</sup> Due to  $\pi$ - $\pi$  interaction of the basal faces of the pyramidal molecular structure the crystal lattice consists in a close packing of face-to-face dimers. A crystallographic inversion centre relates the two molecules of the dimer with respect to each other. The ureato groups are stacked in the crystal lattice in a trans-arrangement relative to the other ureato ligands to minimize the expected high interaction among the molecules in the crystal lattice. This modifies drastically the molecular packing of the phthalocyanine in the solid state relative to the molecular packing of [PcTiO] (**1**). Therefore, relevant consequences for the electronic and NLO properties would be expected for the prepared [PcTi(N,N'-diaryluato)] (**3a-d**).

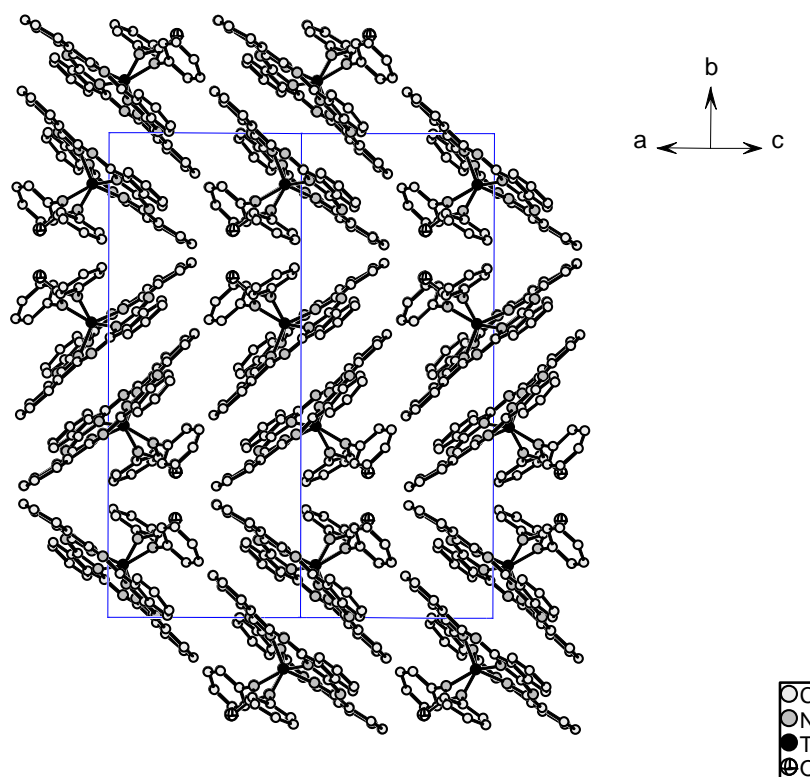


Figure 30: The molecular packing of **(3a)**. View along [101] diagonal.

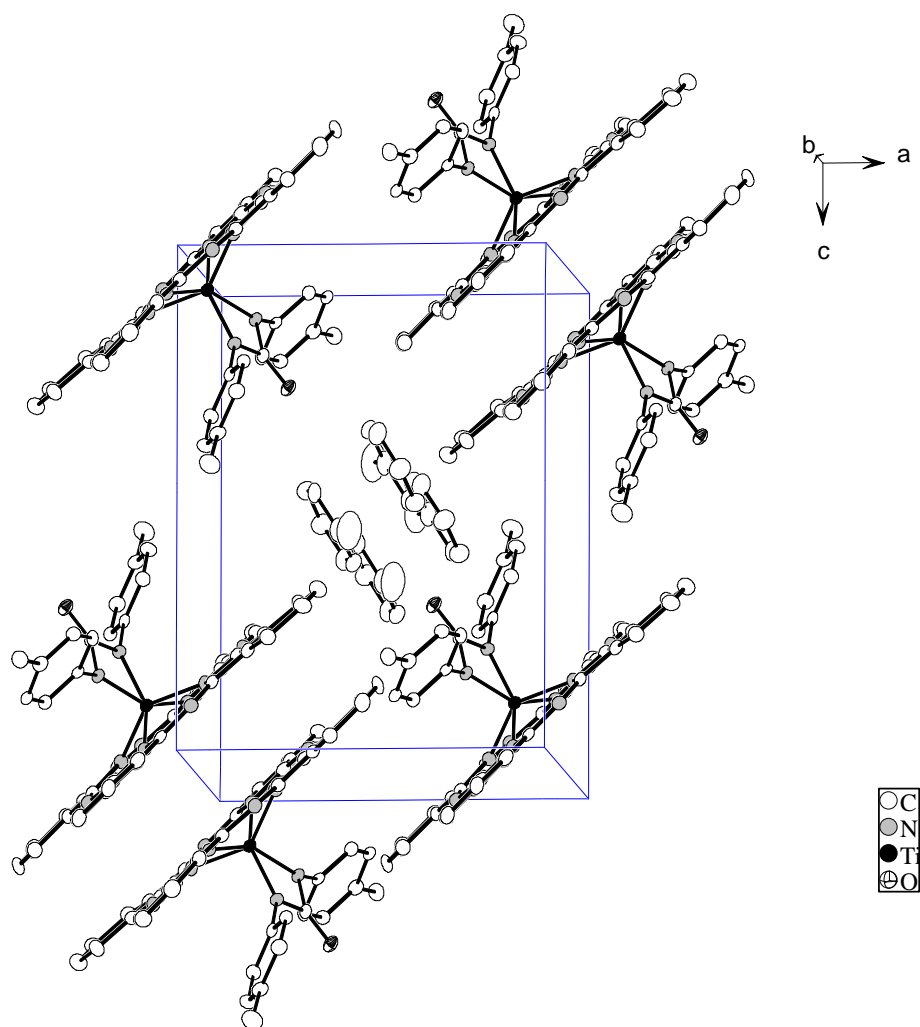
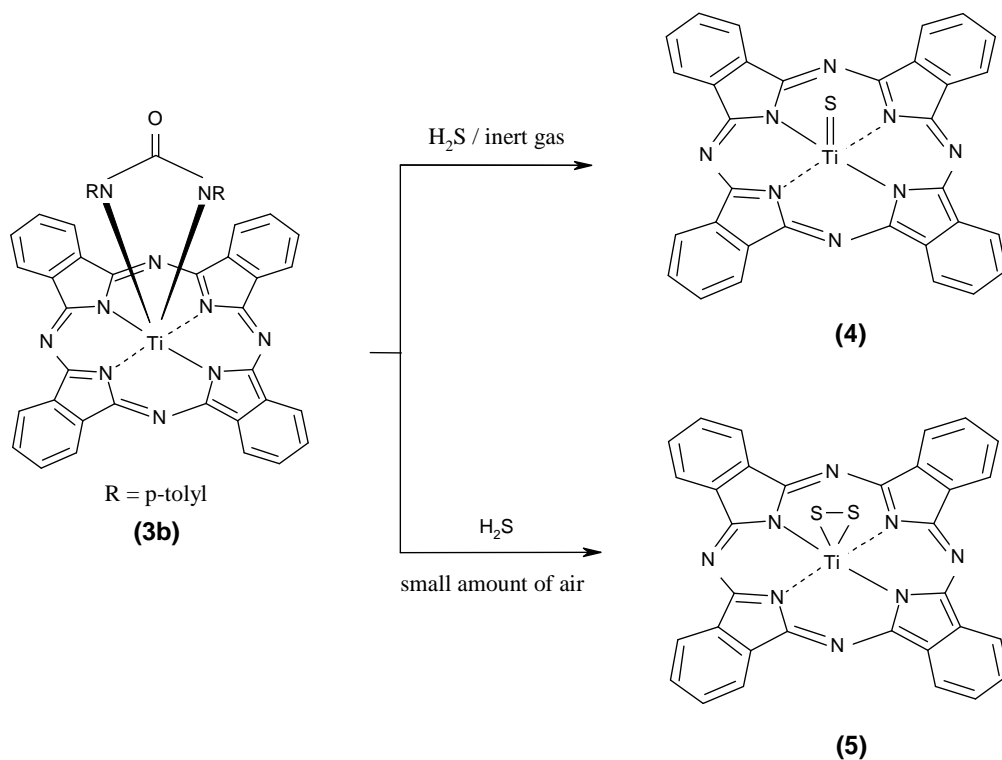


Figure 31: The molecular packing of **(3b)**, View along approx. [010] diagonal. Two molecules of solvent of crystallization (chlorobenzene) are shown in the middle of the unit cell.

### 2.1.6 Reaction of Diaryllureato-TiPcs with H<sub>2</sub>S

The solution of **(3b)** in chloronaphthalene reacts with H<sub>2</sub>S gas in absence of the air yielding the compound [PcTi=S] **(4)**. IR spectrum of **(4)** shows ( $\nu_{\text{Ti-S}}$ ) at 563 cm<sup>-1</sup> and in Raman spectrum at 560 cm<sup>-1</sup> which is in agreement with values reported for the analogue porphyrins.<sup>47</sup> The presence of slight amount of air in the reaction vessel leads to formation of perchalcogenido species [PcTiS<sub>2</sub>] **(5)** (Scheme 14). The reaction mechanism (Figure 32) involves forming of the intermediate [PcTi(SH)<sub>2</sub>], which is probably oxidized by the air forming [PcTiS<sub>2</sub>]. The m/z values of the molecular ions of **(5)** together with its analytical data confirm the structure of [PcTiS<sub>2</sub>]. Raman spectrum of **(5)** shows ( $\nu_{\text{Ti-S}}$ ) at 424.6 cm<sup>-1</sup> and ( $\nu_{\text{S-S}}$ ) at 548.4 cm<sup>-1</sup> and this in accord with the values reported for the analogue porphyrins at (426.0) and (549-553 cm<sup>-1</sup>) respectively.<sup>48a</sup> Comparison of ( $\nu_{\text{S-S}}$ ) in **(5)** with that in free S<sub>2</sub> (725 cm<sup>-1</sup>), ionic S<sub>2</sub><sup>-</sup> (589 cm<sup>-1</sup>), and S<sub>2</sub><sup>2-</sup> (446 cm<sup>-1</sup>)<sup>47, 48</sup> indicates that the S-S bond strength of **(5)** lies between that of the S<sub>2</sub><sup>-</sup> and S<sub>2</sub><sup>2-</sup>. <sup>1</sup>H-NMR spectrum of **(5)** shows two multiplets at 8.38-8.32 and 9.82-9.72 ppm which prove the presence of only one complex [PcTiS<sub>2</sub>]. The electronic absorption spectrum of [PcTiS<sub>2</sub>] **(5)** is similar to that of [PcTiO] **(1)** with a small blue shift of Q<sub>1.0</sub> and Q<sub>2.0</sub>. The Q<sub>3.0</sub> band is not present in [PcTiS<sub>2</sub>] **(5)**.



Scheme 14: Reaction of **(3b)** with H<sub>2</sub>S gas.

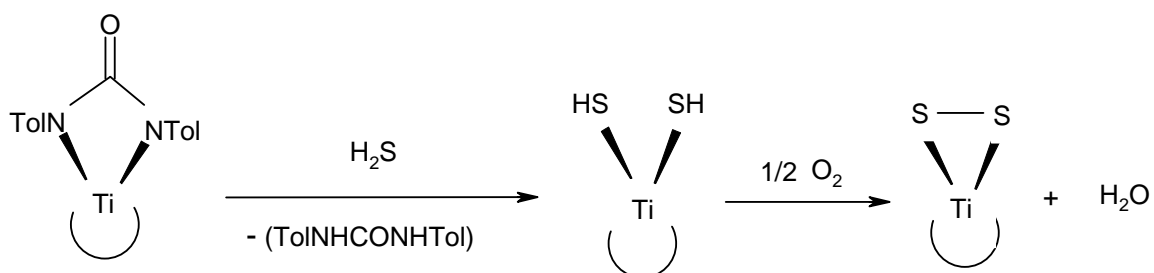


Figure 32: Reaction mechanism suggested for formation of (5).

### 2.1.7 Crystal Structure of [PcTi( $\eta^2$ -S<sub>2</sub>)] (5)

The crystal structure of (5) was solved and its crystallographic data are reported. The molecular structure is shown in (Figure 33).

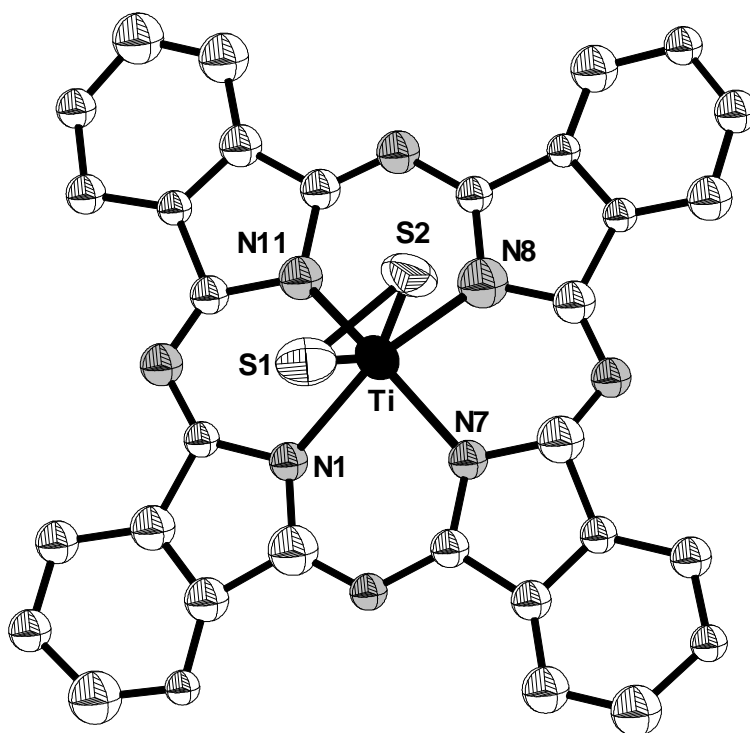


Figure 33: Side view of the [PcTi( $\eta^2$ -S<sub>2</sub>)] (5) illustrating the position of the titanium and chalcogen atoms relative to the Pc ring.

Displacement ellipsoids at the 50% probability level. (H atoms are omitted for clarity)

The prominent features of the molecular structure of compound **(5)** are:

The molecule crystallizes monoclinic in the centrosymmetric space group  $P2_1/n$  with 4 molecules per unit cell. The molecule consists of a six-coordinate titanium (IV) atom surrounded by four equatorial isoindoline rings of the phthalocyanine macrocycle. The  $S_2$  group is  $\eta^2$  “side-on” bonded to the titanium atom in an axial position. Therefore, the geometry at the titanium atom is square-pyramidal with the four isoindoline nitrogen atoms forming the basal plane and the dichalcogen group at the apical site. This coordination scheme is similar to that of the  $[(OEP)Ti(\eta^2-O_2)]^{48b}$  and  $[(TpTP)Ti(\eta^2-S_2)]^{48a}$ . The titanium atom is located 0.702 Å above the plane of the four nitrogen atoms. This out-of-plane displacement drives the macrocycle to adapt to this special situation by deformation.<sup>12</sup> This distance is comparable to the corresponding distance of 0.658 Å observed for the analogue porphyrin  $[(TpTP)Ti(\eta^2-S_2)]^{46}$ . The titanium (VI) atom and the two sulfur atoms of  $[PcTi(\eta^2-S_2)]$  fit into a triangular structure. Similar coordination patterns are documented in the literature for the peroxy-, disulfur-, and diselenium analogues.<sup>48a</sup> It was noticed for  $[PcTi(\eta^2-S_2)]$  (**5**), as expected for such coordination patterns, that four different bond distances between the titanium atom and the  $N_4$  atoms are present:  $Ti-N1 = 2.1412(2)$  Å,  $Ti-N7 = 2.0542(2)$  Å,  $Ti-N8 = 2.091(2)$  Å and  $Ti-N11 = 2.0292$  Å. These values are similar to those found in  $[(OEP)Ti(\eta^2-O_2)]^{48b}$  and  $[(TpTP)Ti(\eta^2-S_2)]^{48a}$ . The S-S distance of 2.029(2) Å is close to those found in the other  $\eta^2-S_2$  compounds<sup>126</sup> and are comparable with values found for free  $S_2$  (1.89 Å) or ionic  $S^{2-}$  (2.00 Å) and  $S_2^{2-}$  (2.13 Å).<sup>126</sup> Selected bond distances (Å) and bond angles (deg.) of  $[PcTi(\eta^2-S_2)]$  (**5**) are given in (Table 8). A comparison between some structural parameters of  $[PcTi(\eta^2-S_2)]$  (**5**) and  $[(TpTP)Ti(\eta^2-S_2)]$  is shown in (Table 9).

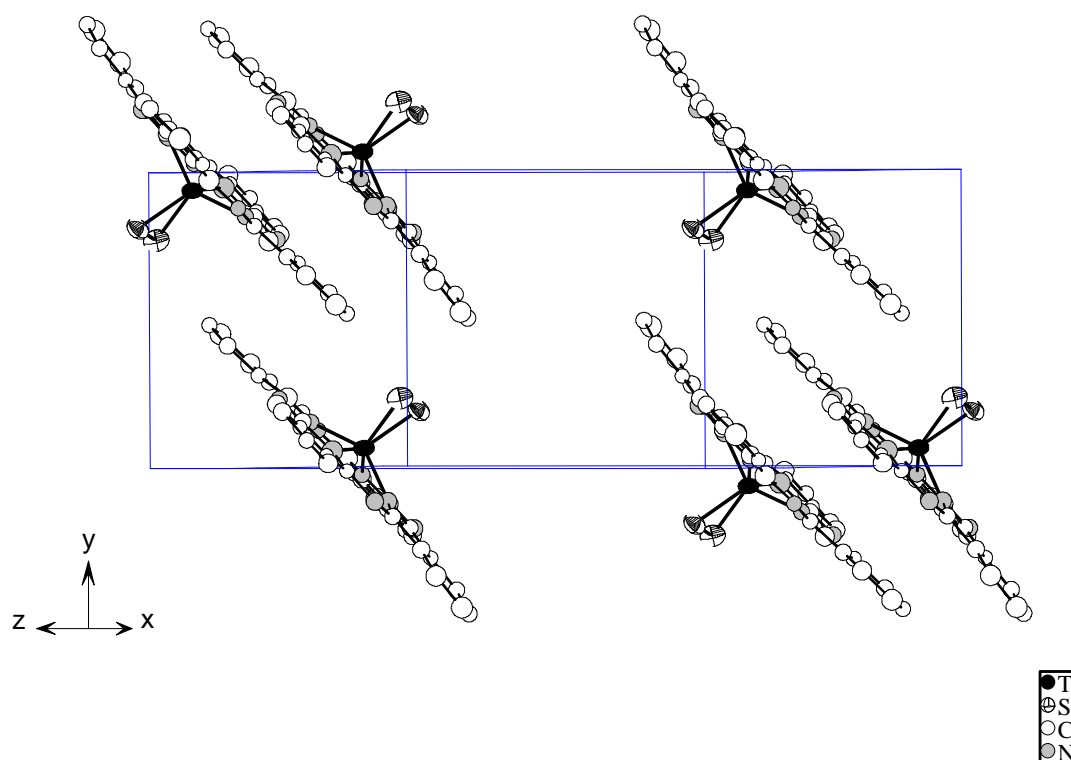
Table 8: Selected Structural Parameters [Å and °] of **(5)**. The low precision is due to the very small crystal.

Ti-N1	2.141(2)	N1-Ti-N7	81.63(7)	S1-Ti-S2	51.90(3)
Ti-N7	2.054(2)	N1-Ti-N11	85.05(8)	Ti-S1-S2	64.38(3)
Ti-N8	2.091(2)	N7-Ti-N8	83.05(8)	Ti-S2-S1	63.72(3)
Ti-N11	2.029(2)	N8-Ti-N11	84.19(9)	N8-Ti-S2	81.90(7)

Table 9: Structural Parameters Å / ° of  $[\text{PcTi}(\eta^2\text{-S}_2)]$  (**5**) in comparison to  $(\text{TpTP})\text{Ti}(\eta^2\text{-S}_2)^{48}$ 

Structural parameters	$\text{PcTi}(\eta^2\text{-S}_2)$ ( <b>5</b> )	$(\text{TpTP})\text{Ti}(\eta^2\text{-S}_2)$
Ti–S1	2.312(10)	2.283(2)
Ti–S2	2.325(10)	2.311(2)
S1–S2	2.029(2)	2.042(2)
S1–Ti–S2	51.90(3)	52.78(6)
S2–S1–Ti	64.38(3)	64.30(7)
S1–S2–Ti	63.72(3)	62.92(8)

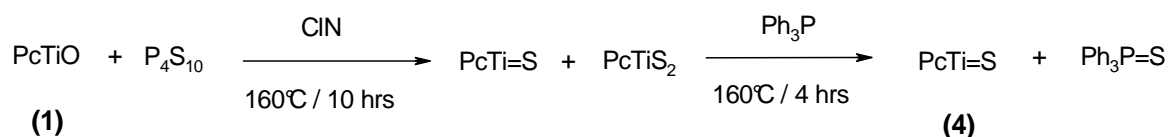
### Molecular Packing and Arrangement in the Crystal Lattice of (**5**)

Figure 34: The molecular packing of  $[\text{PcTiS}_2]$  (**5**).

From studying of the molecular packing and the arrangement of the molecules in the molecular cells of [PcTi( $\eta^2$ -S<sub>2</sub>)] (Figure 34), it can be concluded that the presence of the axial disulfur group does not display a similar steric demand in the face-to-face lattice as it is observed in imido-TiPc (**2a**) and ureato-TiPcs (**3a,b**). Consequently, the  $\pi$ - $\pi$  interaction of the basal faces of the pyramidal molecular structure the crystal lattice is low in comparison to these compounds and this leads to more dense molecular packing in the unit cell. A crystallographic inversion centre relates the two molecules of the dimer with respect to each other. The disulfur moieties are stacked in the crystal lattice in a trans-arrangement to minimize the interaction between each two neighboring phthalocyanine molecules.

### 2.1.8 Preparation of [PcTi=S] (**4**) starting with [PcTiO] (**1**)

The compound [PcTiS] (**4**) could be prepared alternatively by the reaction of [PcTiO] (**1**) with phosphorus P<sub>4</sub>S<sub>10</sub>. This reaction results firstly in formation of a mixture of [PcTiS] (M<sup>+</sup> = 592) and [PcTiS<sub>2</sub>] (M<sup>+</sup> = 624) (Scheme 15). However, reduction of the [PcTiS<sub>2</sub>] portion was achieved successfully by reaction of the mixture with melted Ph<sub>3</sub>P at 160°C yielding a homogeneous product of [PcTiS] (**4**). The byproduct Ph<sub>3</sub>P=S had to be removed by extraction with different organic solvents.



Scheme 15: Synthesis of [PcTiS] (**4**) from [PcTiO].

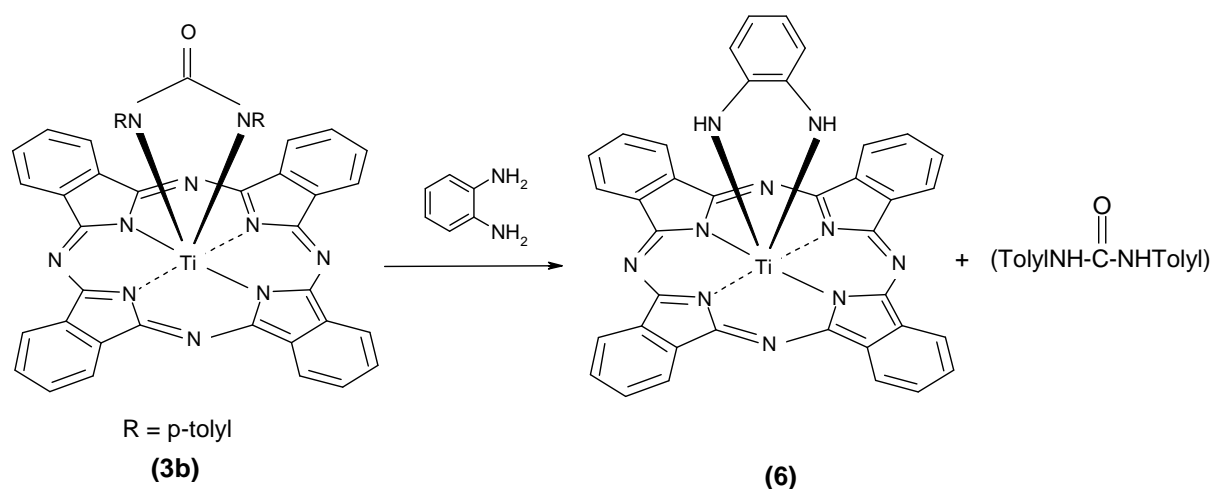
EI-mass spectroscopic measurements were used to monitor the homogeneity of the product. After the first reaction both the molecular peaks of [PcTiS] and [PcTiS<sub>2</sub>] were observed, however after completeness of the reduction with triphenylphosphine, only the molecular peak (M<sup>+</sup>=592) of [PcTiS] was observed in MS measurements under the same conditions. The analysis of sulfur content matched well with the thio- compound rather than the perthio- compound. The stretching vibration of (Ti=S) is detected in IR spectrum at 563 cm<sup>-1</sup> and in Raman spectrum at 560.0 cm<sup>-1</sup>.<sup>47</sup> Identical spectroscopic data were obtained for the [PcTi=S] (**4**) prepared in this way and that prepared by the reaction of (**3b**) with H<sub>2</sub>S gas in



absence of air. However, starting with [PcTiO] (**1**) results in a reduced yield of (**4**) because of the essential need of successive extraction to eliminate the byproducts in the two reaction steps.

### 2.1.9 Preparation of N, N'-(1,2-phenylenediimino) phthalocyaninato titanium (IV) (**6**)

Donor ligands such as catechol were proved to possess reactivity toward the [PcTiO]<sup>41</sup> and [PcTiCl<sub>2</sub>].<sup>32</sup> Therefore, a similar or higher reactivity toward these donor ligands was expected from the ureato group, since reaction with [PcTiCl<sub>2</sub>] yields HCl and with [PcTiO] yields H<sub>2</sub>O which is supposed to hinder the completion of the reaction. Compound (**3b**) was found to react with 1,2-phenylenediamine to produce N, N'-(1,2-phenylenediimino)-phthalocyaninato titanium (IV) (**6**) in a quantitative yield. The corresponding urea derivative is formed as perfect leaving group. The reaction is illustrated in (Scheme 16).



Scheme 16: Synthesis of (**6**).

The new axially substituted titanium phthalocyanine (**6**) was characterized with MS, UV, IR, TGA and CHN analysis. The mass spectrometric data and elemental analysis values of (**6**) match well with the calculated values of the suggested product. UV/VIS and IR spectra are characteristic for a metal phthalocyanine and are in agreement with those of the analogue

compounds such as catecholato and thiocatecholato-titanium phthalocyanines.<sup>41</sup> IR spectrum of **(6)** shows the expected absorption of the N-H group ( $\nu_{\text{N-H}} = 3450 \text{ cm}^{-1}$ ). Thermal gravimetric analysis of **(6)** (Figures 35) show that the compound is thermally stable up to 350°C. Afterward, two weight losses can be observed. The first loss occurs in the temperature range (350-450 °C) and is attributed to the loss of the axial ligand ( $\text{C}_6\text{H}_4(\text{NH})_2$ ) moiety, weight loss calcd./found 14/14% (Figures 36). The second one starts at about 600°C and is attributed to the thermal destruction of the basic skeleton of the phthalocyanine macrocycle.

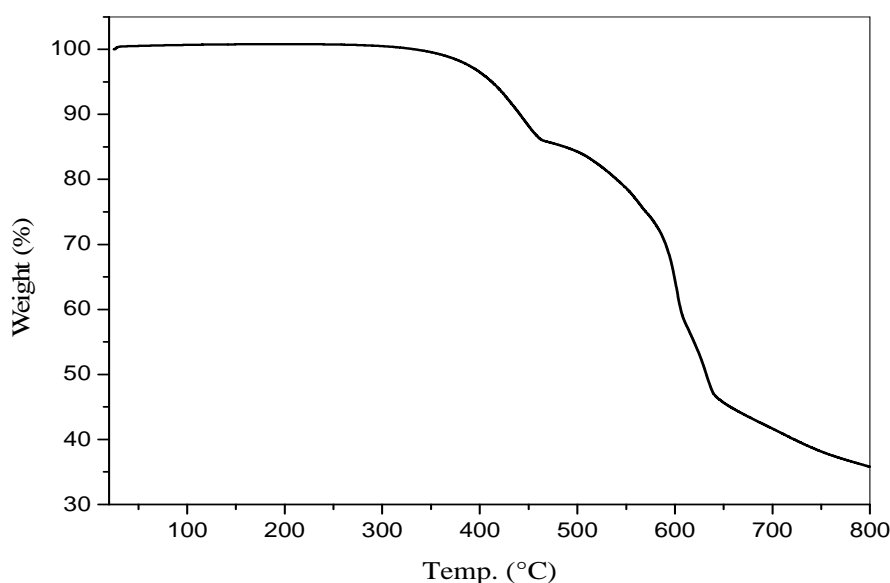


Figure 35: TGA Diagram of **(6)**.

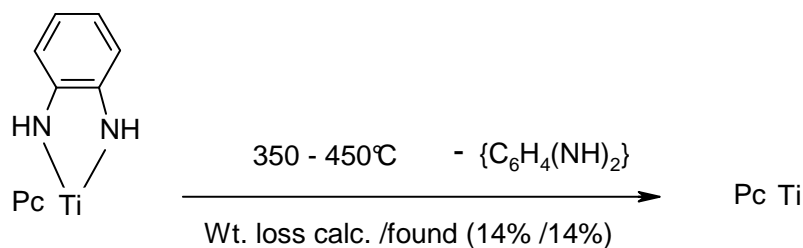
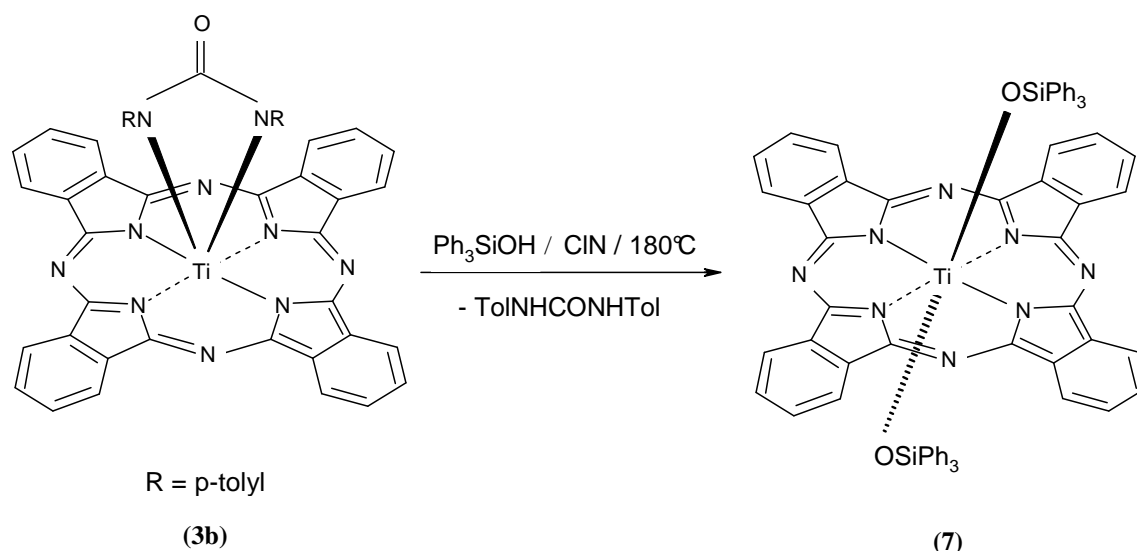


Figure 36: Thermal decomposition of the axial moiety of **(6)**.

### 2.1.10 Preparation of trans- Bis (triphenylsiloxy) phthalocyaninato (2-) titanium (IV) (7)

Compound (3b) was found to react with two molecules of  $\text{Ph}_3\text{SiOH}$  forming trans- Bis (triphenylsiloxy) phthalocyaninato (2-) titanium (IV) (7) (Scheme 17). The blue green compound is air sensitive; it turns readily into  $[\text{PcTiO}]$  (1) in air as indicated by mass and IR spectroscopic measurements.



Scheme 17: Synthesis of (7).

The UV/VIS spectrum of (7) in chloronaphthalene (Figure 37) shows splitted ( $Q_{0.0}$ ) absorption band at  $\lambda_{\text{max}} = 741 \text{ nm}$  and  $698.0 \text{ nm}$ . Another allowed  $\pi$ - $\pi^*$  transition at  $\lambda_{\text{max}} = 356.5 \text{ nm}$  (B-band) is observed. The shoulders at  $\lambda_{\text{max}} = 663.5 \text{ nm}$  and  $630.0 \text{ nm}$  are observed and attributed to the ( $Q_{1.0}$ ) and ( $Q_{2.0}$ ) vibronic transitions. The broadening and splitting of the Q band into two maxima at  $\lambda_{\text{max}} = 741 \text{ nm}$  and  $698.0 \text{ nm}$ , which is not observed in spectra of  $\text{PcTiO}$  or ureato-TiPcs, may be attributed to the exciton interaction between the Pc ligand and the two triphenylsiloxy groups in the axial positions.<sup>127</sup> The IR spectrum of (7) is very similar to that shown by the same product obtained starting from  $[\text{PcTiCl}_2]$ .<sup>31</sup> The small absorption band at  $821 \text{ cm}^{-1}$  in the IR spectrum of (7) is attributed to the antisymmetric stretching of (O-Si-O) group.<sup>31,32</sup>

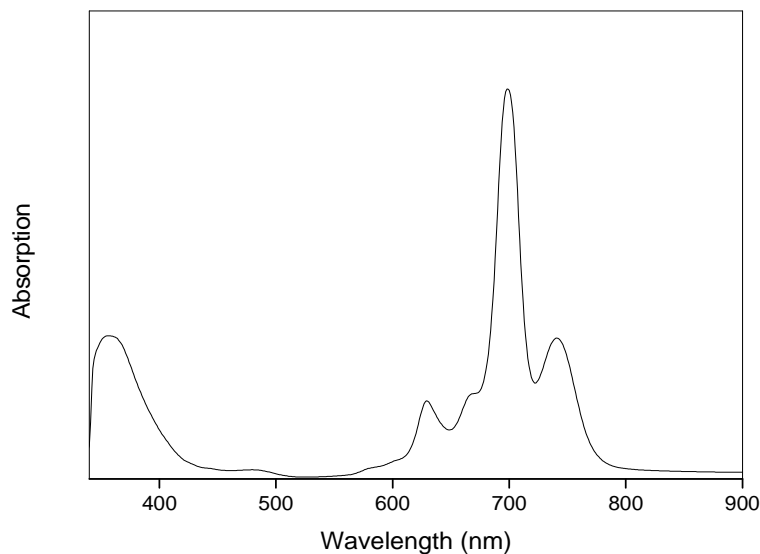


Figure 37: UV/VIS spectrum of **(7)** (CIN,  $10^{-5}$  M).

The  $^1\text{H}$ NMR spectrum of **(7)** (Figure 38) shows the typical expected resonance patterns and integration values for the pure compound **(7)**. The phthalocyanine unit shows in the aromatic region a characteristic resonance pattern for an unsubstituted phthalocyanine, with two multiplets. The first multiplet in the region 9.62-9.70 ppm for eight protons in the 1,4-positions and the second multiplet in the region 8.25-8.32 ppm for eight protons in the 2,3-positions. The protons of the axial ligand show upfield-shifted signals due to the well known ring current effect of the phthalocyanine macrocycle.<sup>123</sup> The aromatic protons of the axial ligand are found in the region 5.23-6.87 ppm.

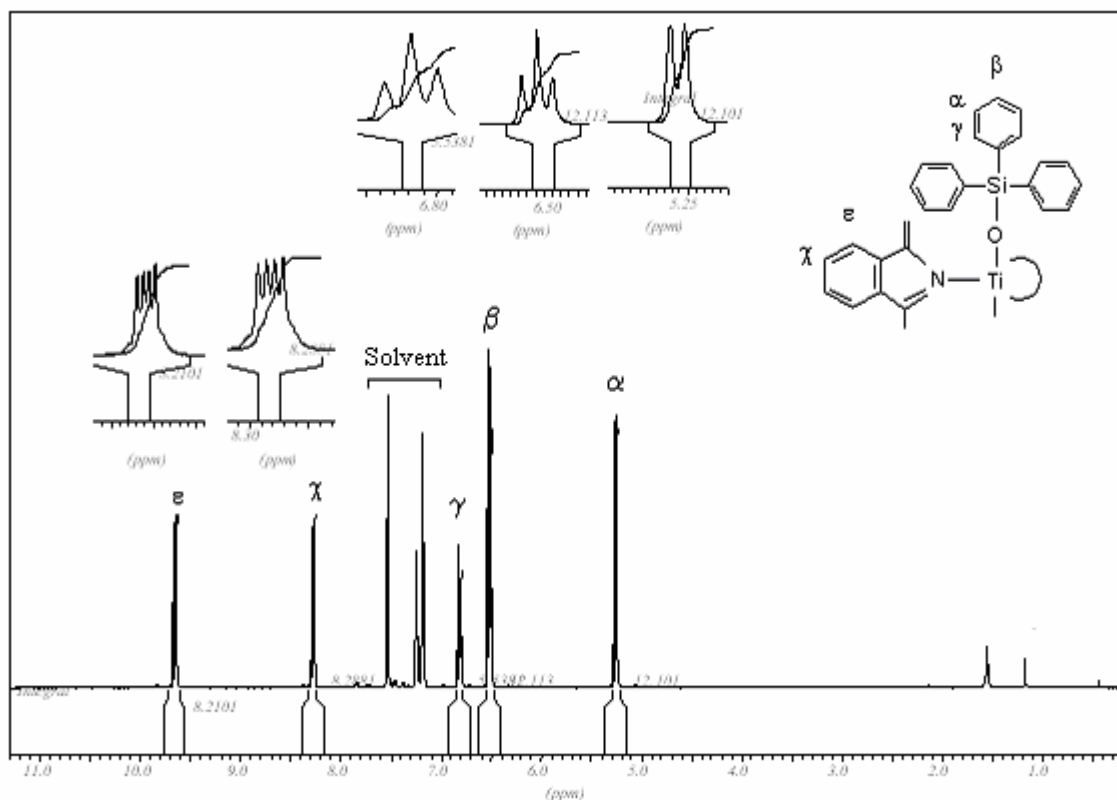


Figure 38:  $^1\text{H-NMR}$  spectrum of (**7**), 500 MHz, in  $\text{C}_6\text{D}_5\text{Br}$ , 373K.

### 2.1.11 Crystal Structure of (**7**)

The X-ray crystal structure of (**7**) (Figure 39) revealed that the reaction proceeds via *trans* addition of two of triphenylsiloxy ligands on the titanium atom. After the first addition of a triphenylsiloxy group the high steric demand around the titanium atom hinders any *cis* addition of another triphenylsiloxy group. Consequently, the titanium atom fits into the core of the  $\text{N}_4$  plane and the saucer shape is not regarded in this molecule in contrast to most of titanium phthalocyanines. Compound (**7**) crystallizes in the centrosymmetric space group  $\text{P}\bar{1}$  with one molecule per unit cell ( $\text{P}\bar{1}$ : primitive cell containing an inversion centre). The titanium atom represents a crystallographic centre of inversion symmetry in the molecule of  $\text{trans-}[\text{Ti}(\text{OSiPh}_3)_2\text{Pc}^{2-}]$  (**7**). Compound (**7**) belongs to the group  $(\text{CN}6_{\text{tr}})$ , since the coordination number of the metal is six and the two axial substituents are located in a *trans* configuration relative to the central metal.<sup>12</sup> This unusual geometry of the octahedral titanium atom in the compound  $\text{trans-}[\text{Ti}(\text{OSiPh}_3)_2\text{Pc}^{2-}]$  (**7**) between the upside and the down side

siloxo groups affords a high strain of the axial moiety of the molecule and this is supposed to affect largely the properties of the produced phthalocyanine molecule such as its high air instability.

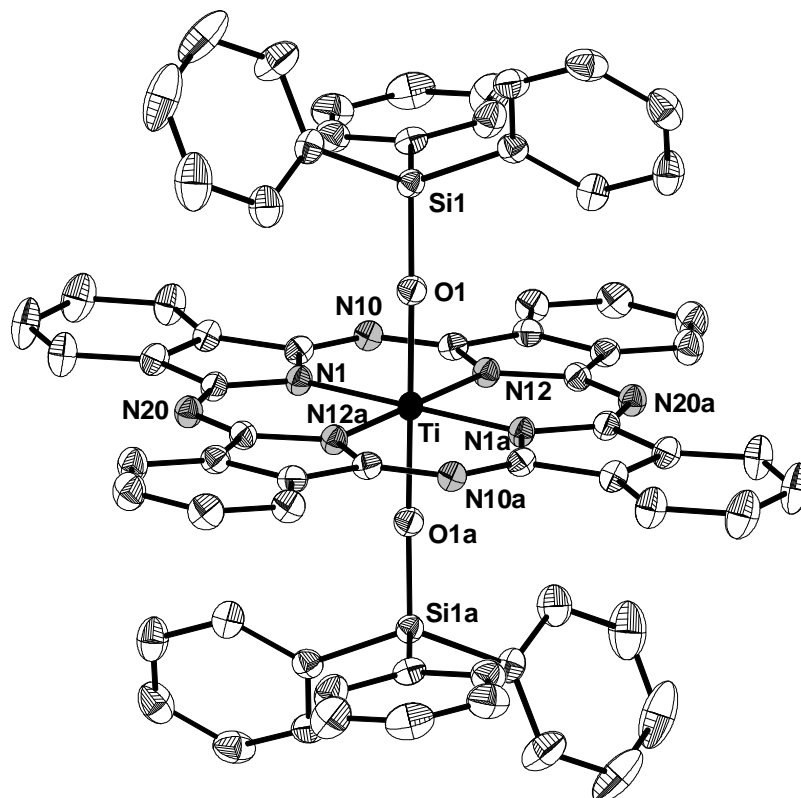


Figure 39: The molecular structure of  $[\text{PcTi}(\text{OSiPh}_3)_2]$  (**7**).

Displacement ellipsoids at the 40% probability level. (H atoms are omitted for clarity)

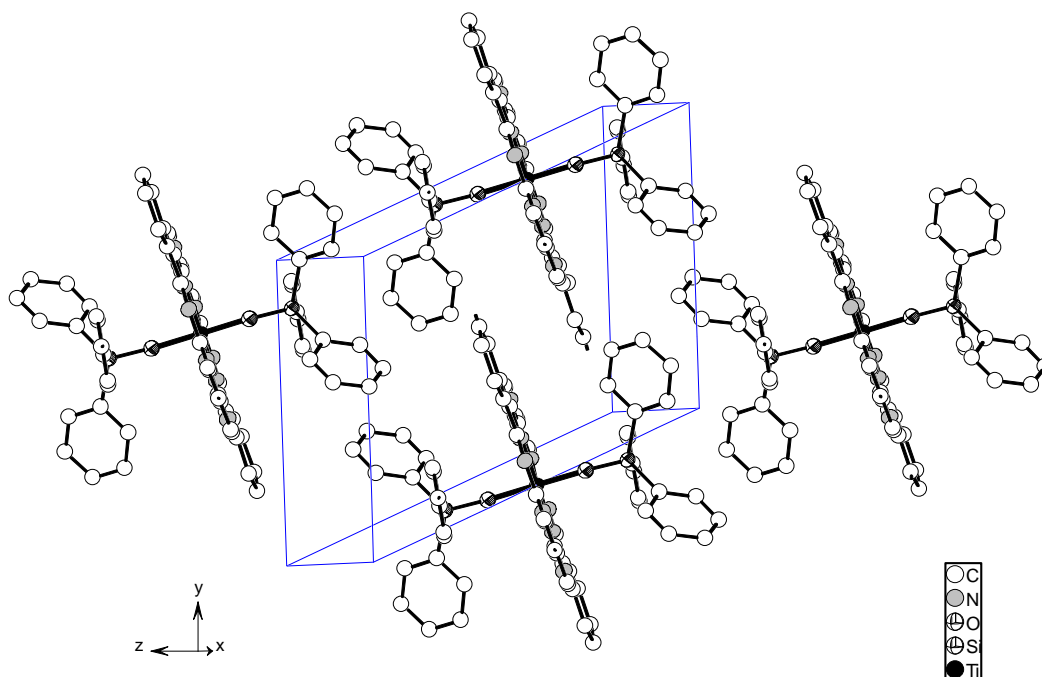
The molecule  $\text{trans-}[\text{Ti}(\text{OSiPh}_3)_2\text{Pc}^{2-}]$  (**7**) crystallizes in the space group  $P\bar{1}$ . The structure of (**7**) is very similar to that of  $[(\text{TTP})\text{Ti}[\text{OP}(\text{Oct})_3]_2]$ .<sup>46</sup> The titanium atom resides in an octahedral environment with the four nitrogen atoms of the four isoindole rings in the equatorial plane and the two  $(\text{OSiPh}_3)$  groups occupying the axial positions. Owing to a center of symmetry at titanium, the  $[\text{TiN}_4]$  unit is planar and the  $\text{OSiPh}_3$ -groups adopt a staggered *trans* conformation. A *cis* configuration is not possible because of the high steric demand of the triphenylsiloxy groups. A *cis* orientation like that given for  $[\text{PcTiCl}_2]$  in the literature<sup>32</sup> is not possible in the case of  $[\text{PcTi}(\text{OSiPh}_3)_2]$  (**7**) because of the high steric demand of the triphenylsiloxy groups. The angle  $(\text{O1-Ti-O1a})$  is  $180.00^\circ$  but the angle between the titanium and the two silicon atoms is  $(\text{Si1-O1-Ti})$  is  $162.9(8)^\circ$ . Selected bond distances and angles of (**7**) are given in (Table 10).

Table 10: Selected bond distances /Å and angles /° of (7)

Ti–N1	2.0227(13)	Ti–O1	1.8521(11)
Ti–N12	2.00235(14)	Si1–O1	1.6272(11)
Si1–O1–Ti	162.9(8)	O1–Ti–N1	89.6(5)
O1a–Ti–O1	180	O1–Ti–N12	90.2(5)
O1a–Ti–N1	90.4(5)	N1–Ti–N12a	89.4(6)
N1–Ti–N12	90.6(6)	N12–Ti–N12a	180

### The Molecular Arrangement of the Crystal Lattice of (7)

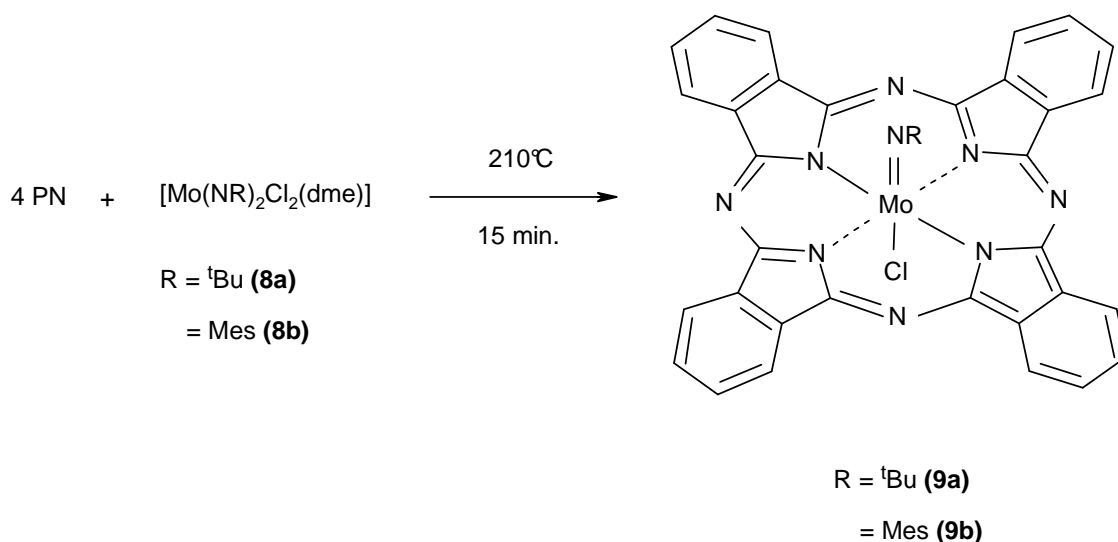
The molecular stacking of trans-[Ti(OSiPh<sub>3</sub>)<sub>2</sub>Pc<sup>2-</sup>] (7) is shown in (Figure 40). Four molecules are packed in the unit cell. The presence of the two bulk triphenyl- siloxy groups in a trans orientation influences the molecular packing in the unit cell. In comparison to the compounds (2), (3a) and (3b), the molecules in the lattice are not stacked face to face as most of phthalocyanines but the Pc faces are packed with greater distances due to the bulky trans triphenylsiloxy groups. This reduced molecular stacking in the unit cell enhances the solubility of the product in most of organic solvents such as 1,2-dichloroethane.

Figure 40: View of the molecular packing of trans-[PcTi(OSiPh<sub>3</sub>)<sub>2</sub>] (7) in the crystal lattice.

## 2.2. Molybdenum Phthalocyanines

### 2.2.1 Synthesis of [PcMo(NR)Cl] (**9a,b**)

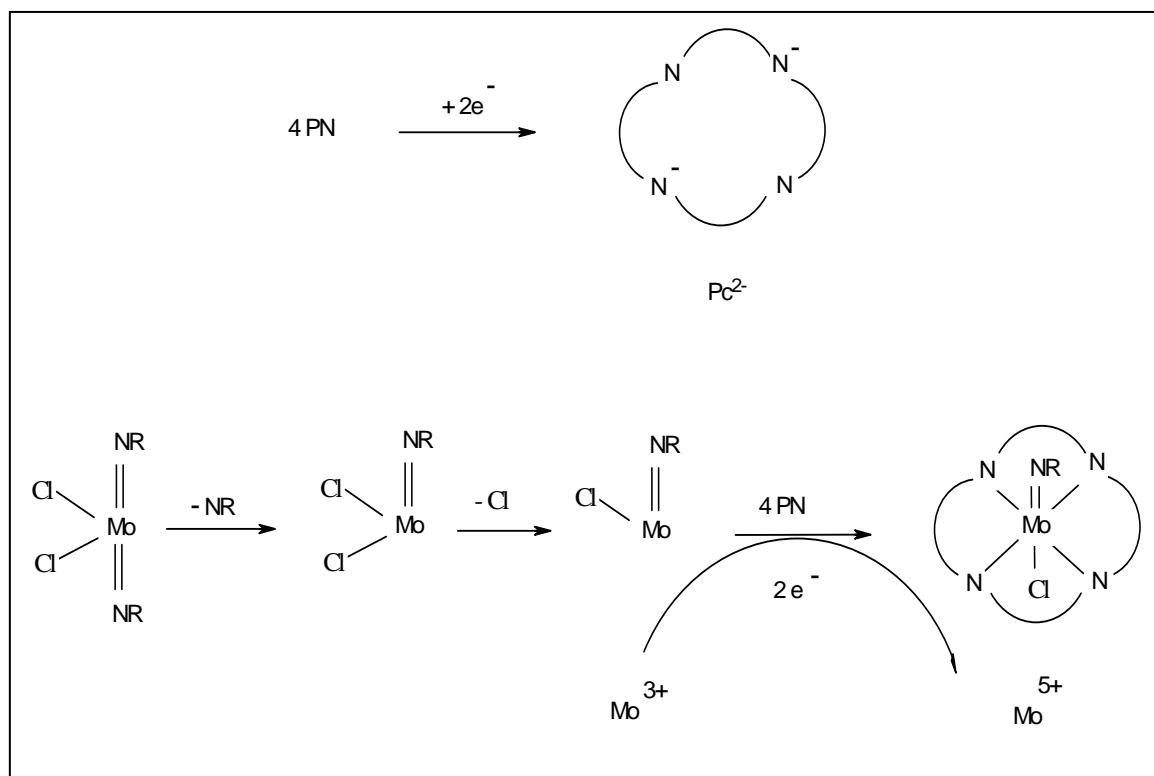
We aimed in this part to prepare new axially substituted molybdenum phthalocyanines, definitely the organoimido Mo(V)Pcs. We did not try to react [PcMoO] with the corresponding isocyanate, since no reasonable synthetic procedure for preparation of a pure [PcMoO] is documented in literature as in the case of [PcTiO]. Therefore, we suggested another strategy for preparation of [PcMo(NR)], starting from phthalonitrile and building up the phthalocyanine molecule in the presence of a proper imido molybdenum complex (**8a,b**) as a precursor of the imido functionalities (Scheme 18a). Thus, if about four equivalents of PN are thoroughly mixed with one equivalent of (**8a**) or (**8b**) and the mixture was put in a preheated oil bath at 210°C for 15 minutes, a paramagnetic air stable organoimido compound (**9a**) or (**9b**) respectively is formed. Elevated temperatures more than 210°C have been avoided since it may cause a partial thermal decomposition of the imido complex into the corresponding nitrido complex (PcMN). The formation of the nitrido complex [PcMoN] can be safely ruled out depending on the absence of its molecular ion peak ( $M^+ = 622.5$ ) in mass spectra, and the absence of the medium absorption  $\nu_{\text{Mo}=\text{N}}$  at 953  $\text{cm}^{-1}$  in the IR spectra.<sup>55, 56</sup>



Scheme 18a: Synthesis of [PcMo(NR)Cl] (**9a,b**).



The suggested reaction mechanism (Scheme 18b) involves the generation of the two electrons, essential for reduction of four phthalonitrile units to the phthalocyanines dianion, from oxidation of molybdenum in its diimido-dichloro- precursor from  $\text{Mo}^{6+}$  to  $\text{Mo}^{3+}$  by losing of a nitrene and chlorine at elevated temperature followed by the reaction of  $\text{Mo}^{3+}$  with four units of phthalonitrile forming  $[\text{PcMo}(\text{NR})\text{Cl}]$  in which molybdenum is  $\text{Mo}^{5+}$ .



(Scheme 18b): The suggested reaction mechanism for formation of  $[\text{PcMo}(\text{NR})\text{Cl}]$  (**9a,b**).

In case of carrying out the reaction in chloronaphthalene, the compounds (**9a**) and (**9b**) are formed at 190-210°C with a lower yield even in the presence of ammonium molybdate as a reaction promoter. The use of urea as promoter had to be avoided because the presence of urea promotes the formation of the metal free phthalocyanine ( $\text{PcH}_2$ ) rather than the slower process involving the cyclotetramerization of four PN units at the imido metal template. The compound was recrystallized from chloronaphthalene in presence of few drops of water, this means that the complex is stable against hydrolysis. This stability against hydrolysis is characteristic for  $d^1$ -Mo complexes rather than for  $d^0$  complexes.

## 2.2.2 Characterization of [PcMo(NR)Cl] (**9a,b**)

### Mass Spectra

The  $m/z$  values of the  $(M-Cl)^+$  ions of the prepared compounds (**9a,b**) were obtained in MALDI-TOF measurements with the expected isotopic patterns. We could not detect the molecular ion peak ( $M^+$ ) of all compounds containing inorganic chlorine (M-Cl bond) with or without using of different matrices to assist the energy transfer. This is the first indication that the Mo-Cl bond is rather weak.

### UV/VIS

UV/VIS spectrum of [PcMo(N<sup>t</sup>Bu)Cl] (**9a**) is shown in (Figure 41). The spectrum shows characteristic metalphthalocyanine absorptions as indicated in the literature.<sup>8,17</sup> The observed bands arise from an isolated band (Q band) at the far-red end of the visible spectrum of light near 871 and 730 nm. A second allowed  $\pi-\pi^*$  transition (B band), near 326 nm, extending to the blue of the visible spectrum is also observed if the solvent (CIN) is compensated by the base line correction. Additional bands, which appear in the spectrum, can be assigned to ligand-to-metal charge transfer.<sup>8,17</sup> There are no remarkable differences between the UV/VIS spectra of (**9a**) and (**9b**).

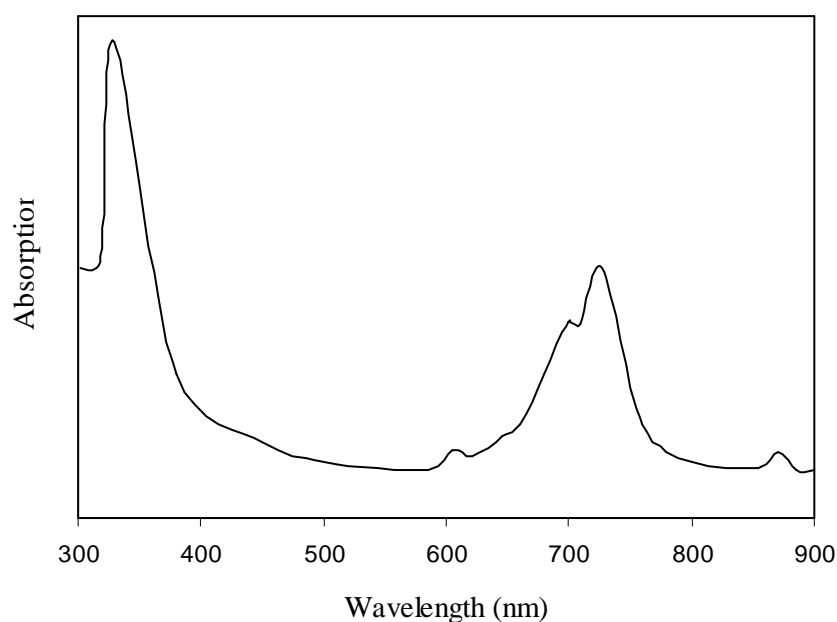


Figure 41: UV/VIS spectrum of (**9a**) (CIN,  $10^{-5}$  M).

## IR Spectra

IR absorptions common to the spectra of the basic Pc moiety (e.g.  $\nu_{C=C}$  arom. at nearly  $1602\text{ cm}^{-1}$ ) were observed for **(9a,b)** (Figure 42). New absorptions, which are not observed in most of the other phthalocyanines such as  $\text{PcH}_2$  and  $[\text{PcTi}(\text{NR})]$ , were observed in the spectra of **(9a)** and **(9b)**. A shoulder at about  $1260\text{ cm}^{-1}$  was observed in the IR spectra of both **(9a)** and **(9b)** which can be assigned to  $\nu_{(\text{Mo}=\text{N})}$  in the  $(\text{Mo}=\text{N}-\text{C})$  system. On the other hand, the characteristic absorption for  $\nu_{(\text{Mo}=\text{N})}$  in  $[\text{PcMoN}]$  at  $953\text{ cm}^{-1}$ <sup>55, 56</sup> were not observed in both spectra. The IR spectra of **(9a)** and **(9b)** are remarkably similar, and they match well with those of other metal phthalocyanines.

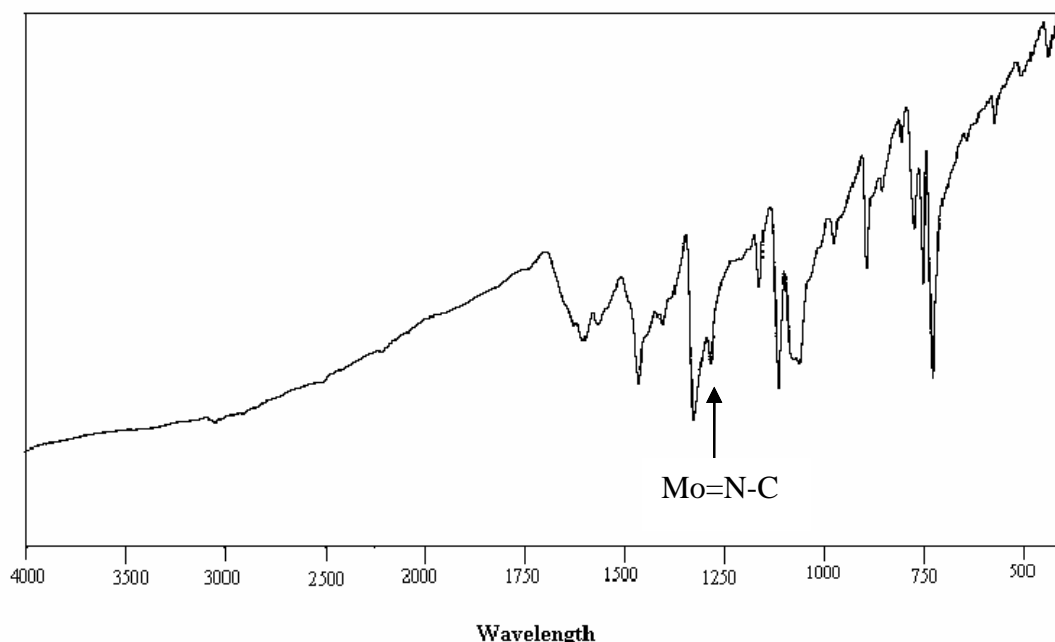


Figure 42: IR spectrum of **(9b)**.

## TGA:

The thermal analysis diagram of **(9a,b)** is typical for a metal phthalocyanine. The compound is thermally stable without any weight loss up to about  $250^\circ\text{C}$ .

## Raman Spectra (RS)

The metal-phthalocyanine skeletal vibrations are observed in the frequency range  $1300\text{-}1610\text{ cm}^{-1}$ . (Figure 43) shows the high-frequency region of the Raman spectra for the organoimido molybdenum phthalocyanines **(9a,b)** obtained with excitation at  $432\text{ nm}$ . The

extreme complexity of these molecules has precluded us from performing complete, high-frequency region normal-mode analysis. The most important feature is the absence of the characteristic absorption of ( $\nu_{\text{Mo-Mo}}$ ) at  $310\text{ cm}^{-1}$  and consequently the formation of a  $d^1-d^1$  M-M bonded molybdenum phthalocyanine dimer can be safely ruled out.<sup>128,55</sup>

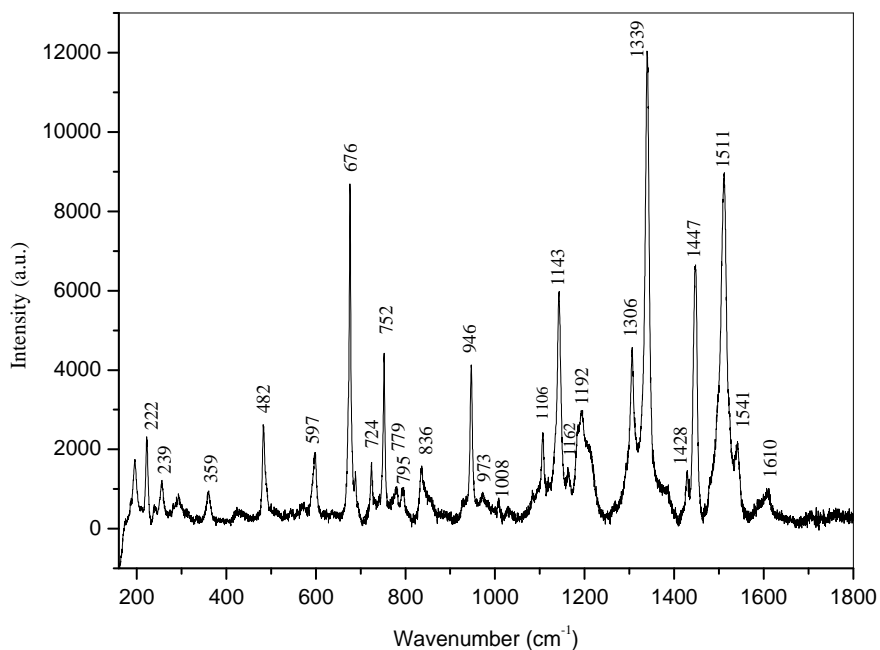


Figure 43: Raman spectrum of **(9b)**.

### 2.2.3 ESR Spectra of (9a,b)

Molybdenum is an element of the group (6), consequently Mo of oxidation state (5+) such as in  $[\text{PcMo}(\text{N}^t\text{Bu})\text{Cl}]$  (**9a**), has one unpaired electron ( $d^1$ -system). Therefore, ESR measurements may give a lot of information about the chemistry of the central metal atom and its ligand regime such as the estimation of the average metal hyperfine coupling. Molybdenum has 6 naturally occurring isotopes, four of them are ESR inactive ( $^{94}\text{Mo}$ ,  $^{96}\text{Mo}$ ,  $^{98}\text{Mo}$ , and  $^{100}\text{Mo}$ ;  $I = 0$  and natural abundance 74.82%), while the other two isotopes  $^{95}\text{Mo}$  and  $^{97}\text{Mo}$  are ESR active with  $I = 5/2$  and natural abundance  $^{95}\text{Mo}$ : 15.72%;  $^{97}\text{Mo}$ : 9.46%.<sup>129</sup> ESR measurements of  $[\text{PcMo}(\text{N}^t\text{Bu})\text{Cl}]$  (**9a**) in toluene and in a mixture of toluene and chloronaphthalene at ambient temperature are illustrated in (Figures 44-46). The ESR spectra of **(9a)** are similar to that of the corresponding phthalocyanines, such as  $[\text{PcMo}\equiv\text{N}]$ , given in the literature.<sup>55, 130</sup> The following facts can be concluded:

- The high sensitivity (low resolution) scan ESR spectra (Figure 44) of a solution of **(9a)** in toluene show the hyperfine structure of molybdenum which contains one strong central peak and six satellite peaks. The large central line is due to the interaction of the unpaired electron with the molybdenum isotopes of  $I = 0$  which account for 75% of the integrated intensity “zeeman effect since  $2nI+1 = 2 \times 1 \times 0 + 1 = 1$ ”. The six satellite peaks (hyperfine structure of molybdenum) are due to splitting with the isotopes of  $I = 5/2$  (since  $2nI+1 = 2 \times 1 \times 5/2 + 1 = 6$ ). The nuclear gyromagnetic ratio of the two  $I = 5/2$  isotopes  $^{95}\text{Mo}$  and  $^{97}\text{Mo}$  are very similar and are not usually distinguished by ESR spectroscopy.

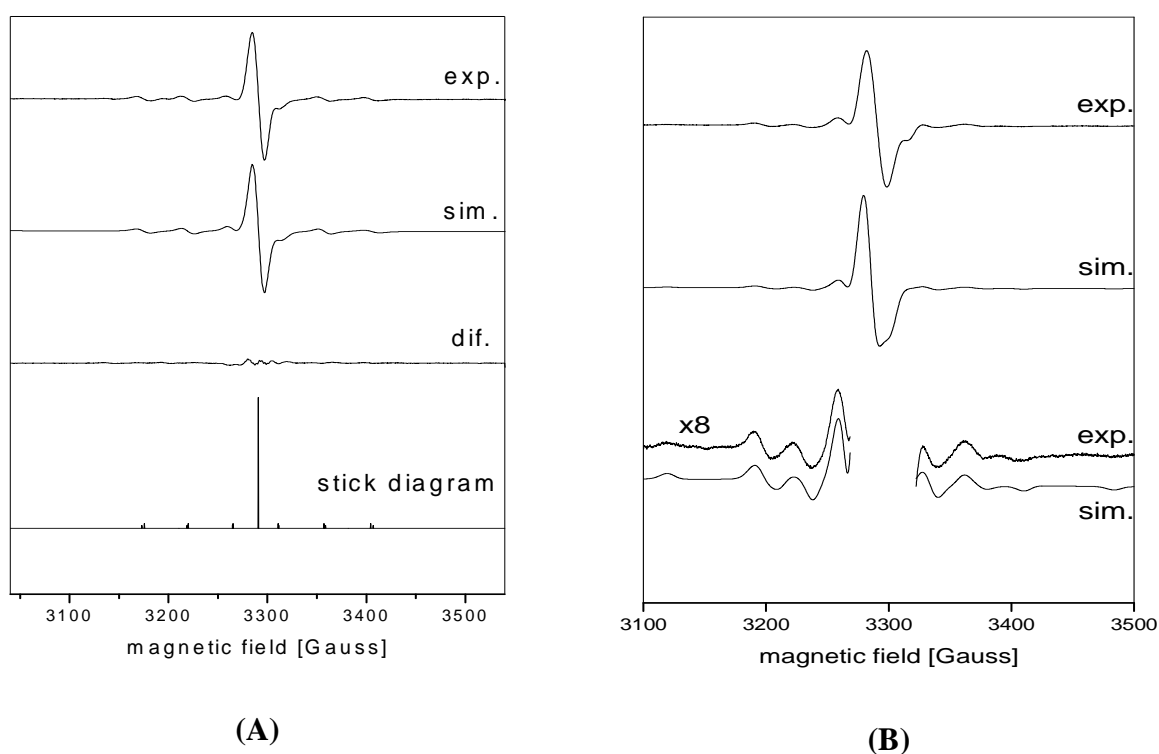


Figure 44: The hyperfine structure of molybdenum in ESR spectra of **(9a)** (toluene/CIN)

A: at 330 K; B: at low temperature (130 K) and magnified eight times (X8).

- The high resolution scan ESR spectra of **(9a)** are shown in (Figures 45, 46). One of the most relevant features of the spectra is the rich superfine structure of molybdenum resulted from the hyperfine coupling of two magnetically nonequivalent nitrogen atoms (4 equatorial vs. 1 axial N). The most abundant nitrogen isotope is  $^{14}\text{N}$  with  $S=1$ . Splitting of the central peak, due to interaction of the unpaired electron with the four nitrogen atoms, leads to formation of nine lines or resonances ( $2 \times 1 \times 4 + 1 = 9$ ). Every line of these nine resonances splits further with

the fifth nitrogen atom resulting in 27 lines. Because these lines are similar and relatively broad, only 12 lines are observed. However, in the stick diagram (Figure 46), in which the peaks are replaced with sharp lines, the expected 27 lines can be observed. If the compound (**9a**) could be prepared containing the  $^{15}\text{N}$  isotope regardless the high costs, only 10 lines would be obtained because the  $^{15}\text{N}$  isotope has  $I = 1/2$ , and the spectra would be less complicated. The experimental diagram (top) fits with the simulated one (bottom). The modulation amplitude was 1 Gpr. Three g factors can be distinguished at 130K, because the anisotropic effect is highly reduced, and the  $g_{\text{iso}}$  was found to be 1.9799. The g value of the free electrons is 2.0023, consequently the deviation from the value of the free electrons is ( $\Delta g = (g_e - g) = 0.0224$ , which is comparable to  $g = 0.0313$  of  $\text{MoO}(\text{TTP})\text{Cl}$ .<sup>129</sup> The following values were determined:  $^{95}\text{Mo}$  ( $A_{\text{iso}} = 45.7$  G),  $^{97}\text{Mo}$  ( $A_{\text{iso}} = 46.7$  G),  $4x\text{N}_{\text{eq}}$  ( $A_{\text{iso}} = 2.6$  G),  $1x\text{N}_{\text{eq}}$  ( $A_{\text{iso}} = 3.7$  G). (Figure 45) shows the super hyperfine structure of the molybdenum central line with  $I=0$  with the five nitrogen atoms ( $4\text{N}_{\text{eq}}$  and  $1\text{N}$ ).

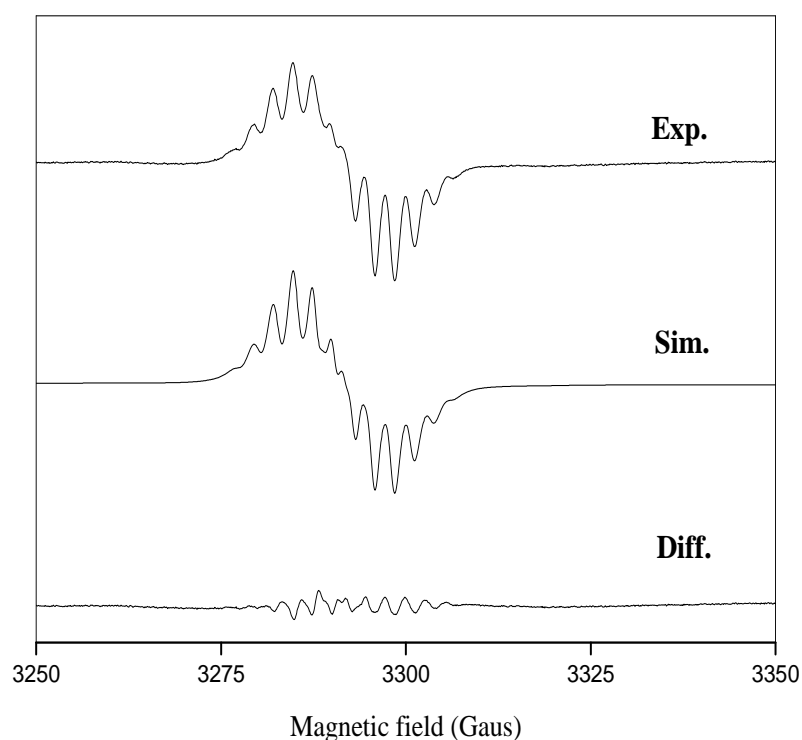


Figure 45: The super hyperfine structure of molybdenum in ESR spectra of (**9a**) in (toluene/CIN), high resolution scan (at 220 K), (modulation amplitude 1 Gpr).

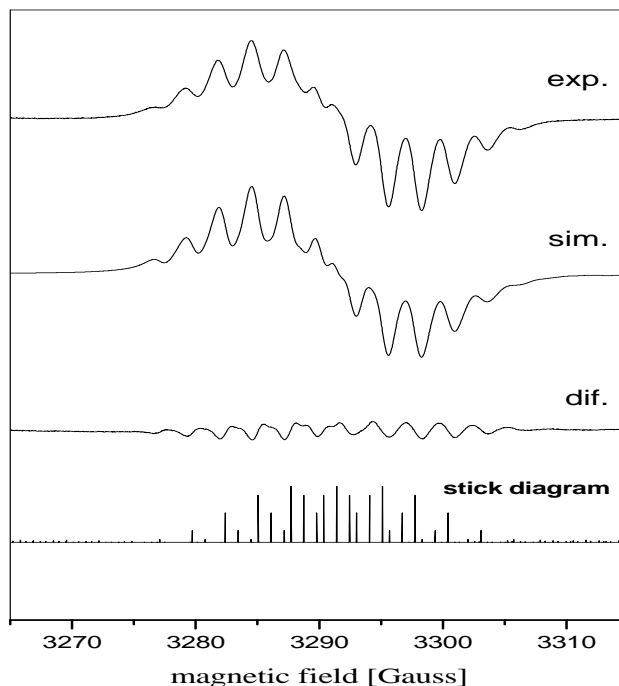


Figure 46: The super hyperfine structure of molybdenum with 5N atoms ( $4N_{\text{eq}}$  are equal) in ESR spectra of **(9a)** in (toluene/CIN) and the stick diagram.

#### 2.2.4 Crystal Structure of [PcMo(N<sup>t</sup>Bu)Cl] (9a)

Single crystals of **(9a)** were obtained by dropping water to its heated chloronaphthalene solution. The crystal structure of **(9a)** was solved and its crystallographic data are given in (Figures 47, 48) and (Table 11). It crystallizes in the centrosymmetric space group P4/n with 4 molecules per unit cell (P: primitive cell containing a four fold rotation axis; n: diagonal glide plane). Eight disordered molecules of water per molecule **(9a)** are observed and omitted for simplicity. The molecule consists of six-coordinate molybdenum atom surrounded by four equatorial isoindoline rings of the Pc molecule whereas the chlorine atom and the imido group are located in the axial positions in a *trans* configuration. Therefore, the geometry around the molybdenum atom is octahedral with the four isoindoline nitrogen atoms forming the basal plane and two axial ligands, the chlorine atom and the imido group. The compound **(9a)** belongs to the group ( $CN_{6_{\text{tr}}}$ ), since the coordination number of the metal is six and the two axial substituents are located in a *trans* configuration relative to the central metal.<sup>12</sup> The molybdenum atom is too large and consequently unable to enter the cavity of the phthalocyanine macrocycle, so it sits “atop” or “out-of-plane” from the  $N_4$  plane.<sup>12</sup> The molybdenum atom is displaced from the mean plane defined by the four

$N_i$  isoindoline nitrogen atoms toward the imido ligand by a distance of 0.305 Å. This distance is shorter than that of molybdenum atom in [PcMoO] (0.69 Å)<sup>49</sup> and that of titanium atom in the compounds (**2**, **3a**, and **3b**). This can be attributed to the presence of chlorine atom that is bonded to the molybdenum atom at the other side of the  $N_4$  plane. The out-of-plane distance is 0.334 Å in methylimido molybdenum (V) porphyrins.<sup>59b</sup> On the other side, the distance between the chlorine atom and the  $N_4$  plane is 2.295 Å which is much longer than that of molybdenum atom and this is attributed to the thermodynamic trans effect of the imido functionality. The (Mo-Cl) bond is 2.600(2) Å. This unexpected weak interaction gives this bond ionic character which may explain the solubility of the complex in the most of the polar solvents such as THF. The imido rest is not perfectly linear with a C10–N11–Mo angle of 161.93(6)°. An angle of 160–180° has been found in many other N-organoimido complexes. The bond length of [Mo–N<sub>imido</sub>] is 1.704(7) Å which compares well with that of 1.689(6) Å in [Mo(NMe)(TPP)(H<sub>2</sub>O)][I<sub>3</sub>].<sup>59b</sup> Selected bond distances and angles of (**9a**) are given in (Table 11). (Figure 48) shows clearly the  $sp^3$  hybridization and the high displacement observed for the <sup>t</sup>butyl group. In (Figure 47) only one of these displaceable positions is shown for clarity. Also (Figure 47) shows clearly the bending deformation of the phthalocyanine macrocycle in the saucer shape.<sup>12</sup>

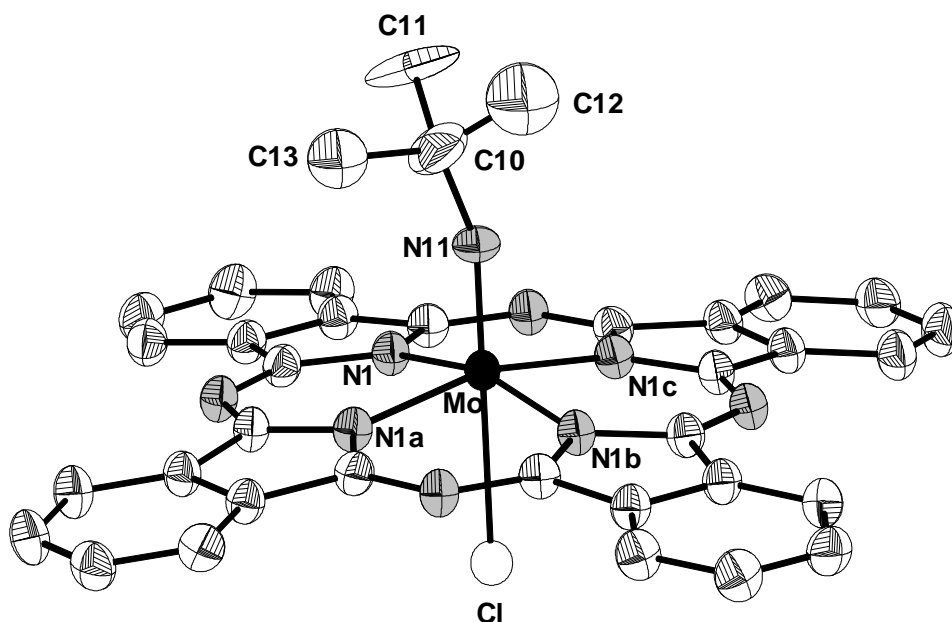


Figure 47: The molecular structure of (**9a**).

Displacement ellipsoids at the 50% probability level. (H atoms are omitted for clarity)



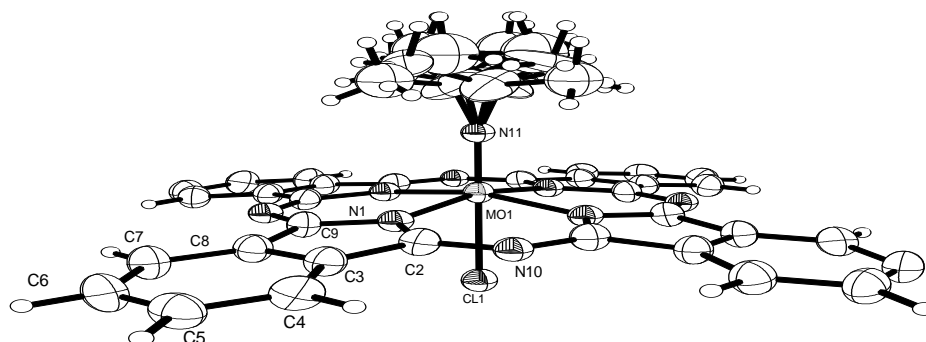


Figure 48: The four fold displacement of the <sup>t</sup>butyl group and the deformation of the Pc macrocycle in a saucer appearance in compound (**9a**).

Table 11: Selected Bond Distances and Angles of (**9a**)

Bond distances (Å)		Bond angles (deg)	
Mo–N11	1.704(7)	Cl–Mo–N11	179.99(14)
Mo–N1	2.053(3)	Mo–N11–C10	161.93(58)
Mo–N1a	2.053(3)	C5–Mo–C5	101.00(5)
Mo–N1b	2.053(3)	N1–Mo–N1	88.74(11)
Mo–N1c	2.053(3)	N11–C10–C11	113.87(150)
Mo–Cl	2.600(2)	N11–C10–C12	108.99(175)
N11–C42	1.403(16)	N11–C10–C13	115.06(148)

### Molecular Packing and Arrangement in the Crystal Lattice of (**9a**)

From studying of the molecular packing and the arrangement of the molecules in the unit cell of [PcMo(N<sup>t</sup>Bu)Cl] (**9a**) (Figure 49), it can be concluded that the presence of two axial substituents (chlorine atom and imido group) at the central molybdenum atom results in a reduction of the stacking degree of the molecules in the unit cell. Due to the molecules shape the crystal lattice consists not in a close packing of face-to-face dimers. The phthalocyanines rings in the lattice are close to coplanar, however only half-faces of the

phthalocyanines rings may interact as  $\pi$ -star due to the trans-axial substituents. Thus a layered lattice of coplanar Pc-rings with short interlayer distances separated by chlorine atoms (and water molecules) and with large interlayer distance separated by the bulky tert-butylimido groups is observed.

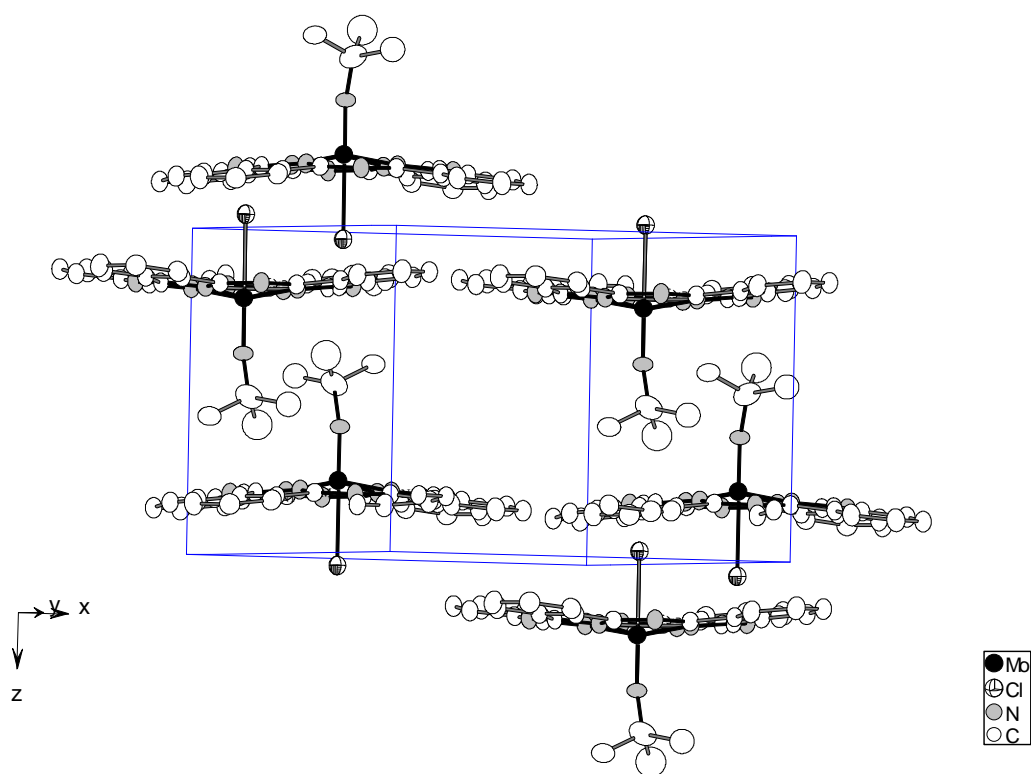
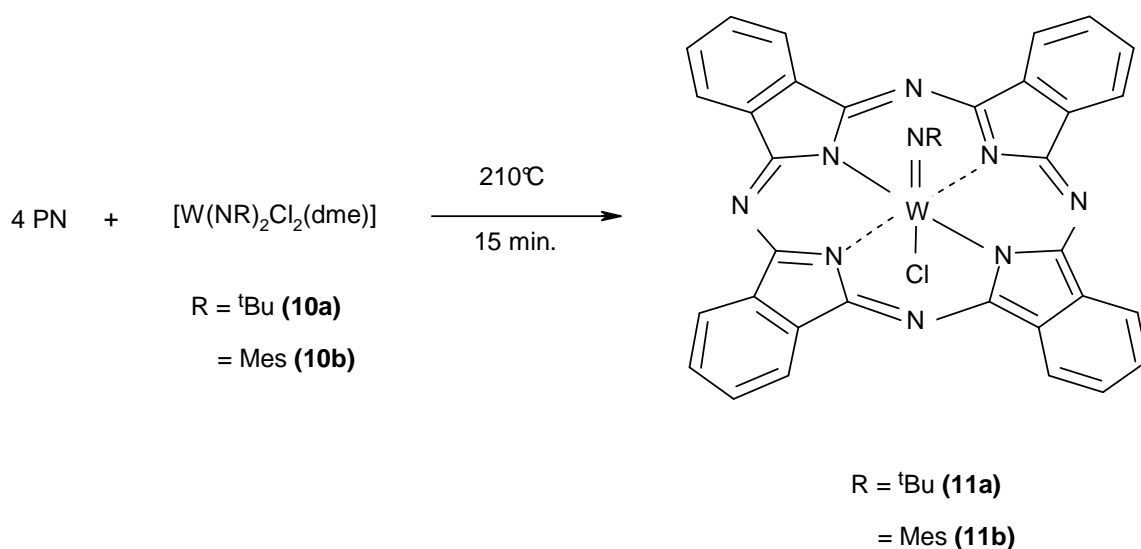


Figure 49: View of the molecular packing in the lattice of **(9a)** along the  $N_4$  planes.

## 2.3 Tungsten Phthalocyanines

### 2.3.1 Synthesis of [PcW(NR)Cl] (**11a,b**)

Aiming to prepare the imido-WPcs, the analogue tungsten compounds to the imido-TiPcs and imido-MoPcs, we applied the typical fusion reaction of PN in the presence of a proper imido tungsten compound [W(N<sup>t</sup>Bu)<sub>2</sub>Cl<sub>2</sub>(dme)] (**10a**) or [W(NMes)<sub>2</sub>Cl<sub>2</sub>(dme)] (**10b**) as a precursor of the imido ligand. The reaction product was identified as the paramagnetic organoimido species [PcW(NR)Cl] (**11a,b**) (Scheme 19).

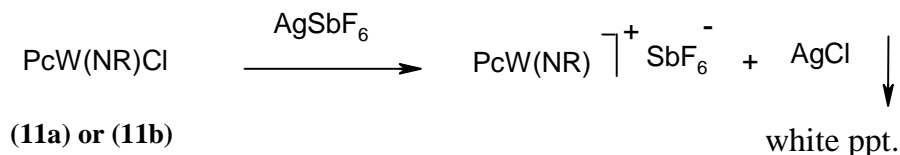


Scheme 19: Synthesis of (**11a,b**).

### 2.3.2 Characterization of [PcW(NR)Cl] (**11a,b**)

The  $m/z$  values of the ions  $[\text{M}-\text{Cl}]^+$  of (**11a,b**) were obtained in MALDI-TOF measurements with the expected isotopic patterns. Again, the molecular ion peaks ( $\text{M}^+$ ) could not be detected in MALDI-TOF measurements with or without use of an additional energy transfer matrix. This is typical for the phthalocyanines with weakly coordinated inorganic chlorine. However, the elemental analysis of C, H, N, and Cl together with the ESR measurements emphasizes the presence of inorganic chlorine linked to the tungsten central

atom. When an equimolar mixture of **(11a)** or **(11b)** and  $\text{AgSbF}_6$  was refluxed for 2 hours in dichloroethane, a white precipitate of  $\text{AgCl}$  was observed after few minutes according to the following reaction:



The formation of this precipitate is evidence that a weakly bonded chloride ligand is attached to the tungsten atom and not to the aromatic rings. The formation of metal-free phthalocyanines can be also ruled out according to the absence of ( $M^+ = 514$ ) of  $\text{PcH}_2$ . UV/VIS spectra of **(11a,b)** show characteristic metal phthalocyanine absorptions.<sup>8</sup> A small blue shift of the ( $Q_{0,0}$ ) and the broadening of the B band is observed in the UV/VIS spectra of **(11a,b)** in comparison to that of the molybdenum analogues **(9a,b)**.

### IR Spectra

IR absorptions common to the spectra of the basic Pc moiety (e.g.  $\nu_{\text{C=C}}$  arom. at nearly  $1602 \text{ cm}^{-1}$ ) were observed. The IR spectra of **(11a,b)** are very similar to that of **(9a)**. The absence of the characteristic bands of ( $\text{W}\equiv\text{N}$ ) and ( $\text{W}=\text{O}$ ) at  $978$  and  $953 \text{ cm}^{-1}$  respectively, ensures that the product is free of  $[\text{PcWN}]$  and  $[\text{PcWO}]$ .<sup>54,55</sup> New absorptions, which are not observed in the spectra of  $\text{PcH}_2$  or  $[\text{PcWN}]$  were observed in the spectra of **(11a,b)** (see the experimental work). The formation of  $\text{PcH}_2$  as a byproduct can be again ruled out according to absence of its characteristic IR absorption at  $1007 \text{ cm}^{-1}$ .<sup>35</sup>

### 2.3.3 ESR Spectra of $[\text{PcW(NR)Cl}]$ (**11a,b**)

Tungsten in the compounds **(11a,b)** has the oxidation state (+V) and since it is an element of group (VI), it has one unpaired electron ( $d^1$ -electronic configuration). Therefore the ESR spectroscopic measurements are possible and may confirm the structure around the central tungsten atom. ESR spectrum of  $[\text{PcW(NMes)Cl}]$  (**11b**) in a mixture of toluene and

chloronaphthalene (3:1) at 220 K is shown in (Figure 50). The spectrum displays one strong central signal with  $g_{\text{iso}} = 1.914$ ,  $g_1 = 1.927$ ,  $g_2 = 1.908$ , and  $g_3 = 1.911$ ; but with poorly resolved super hyperfine structure. This strong signal is attributed to the unpaired electron of the tungsten isotopes of  $I = 0$  ( $W^{180}$ ,  $W^{182}$ ,  $W^{184}$  and  $W^{186}$ ). The coupling with the isotope  $W^{183}$  ( $I = 1/2$ ) was observed as doublet. Both of these two signals have a relative intensity of 7% of the main signal which is comparable to the calculated values. ESR spectrum of (**11b**) at 240 K is shown in (Figure 51). The spectrum shows that both of the first and the second derivatives fit well with the simulated ones. The super hyperfine coupling of the nitrogen atoms are  $[(4x^{14}\text{N})A_{\text{iso}} = 3 \text{ Gauss}$  and  $(1x^{14}\text{N})A_{\text{iso}} = 3.5 \text{ Gauss}$ . The  $A_{\text{iso}}$  of ( $^{183}\text{W}$ ) was found to be 84 Gauss.

The first derivative ESR spectrum of (**11b**) at 130 K (Figure 52) fits with the simulated spectrum and delivers the nitrogen anisotropic hyperfine values (goodness of fit = 0.16). ESR spectrum of (**11b**) is comparable to that of  $[(\text{CIPc})\text{W}^{\text{V}}(\text{O})\text{OH}]$ <sup>54</sup> and that obtained for  $[\text{PcWN}]$  in which tungsten displays also  $d^1$ -configuration.<sup>55</sup> The second derivative of the spectrum was made mathematically aiming at enhancing the resolution of the spectrum.

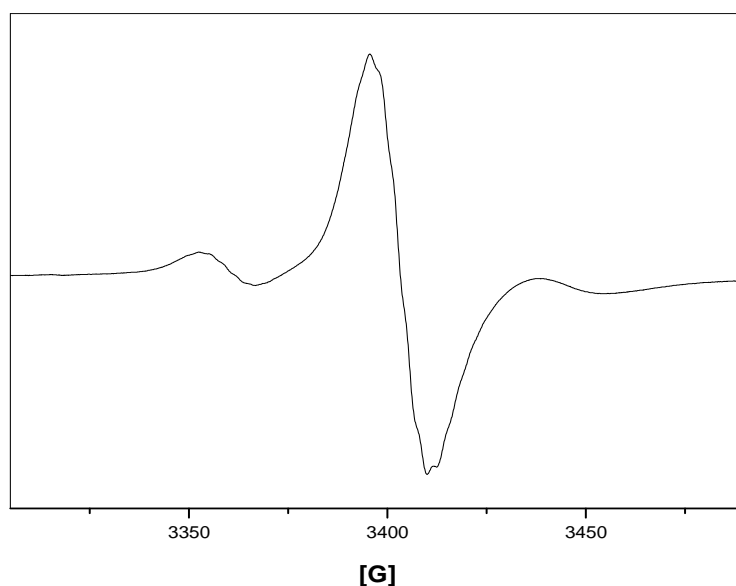


Figure 50: ESR spectrum of (**11b**) at 220 K, in toluene/CIN (3:1).

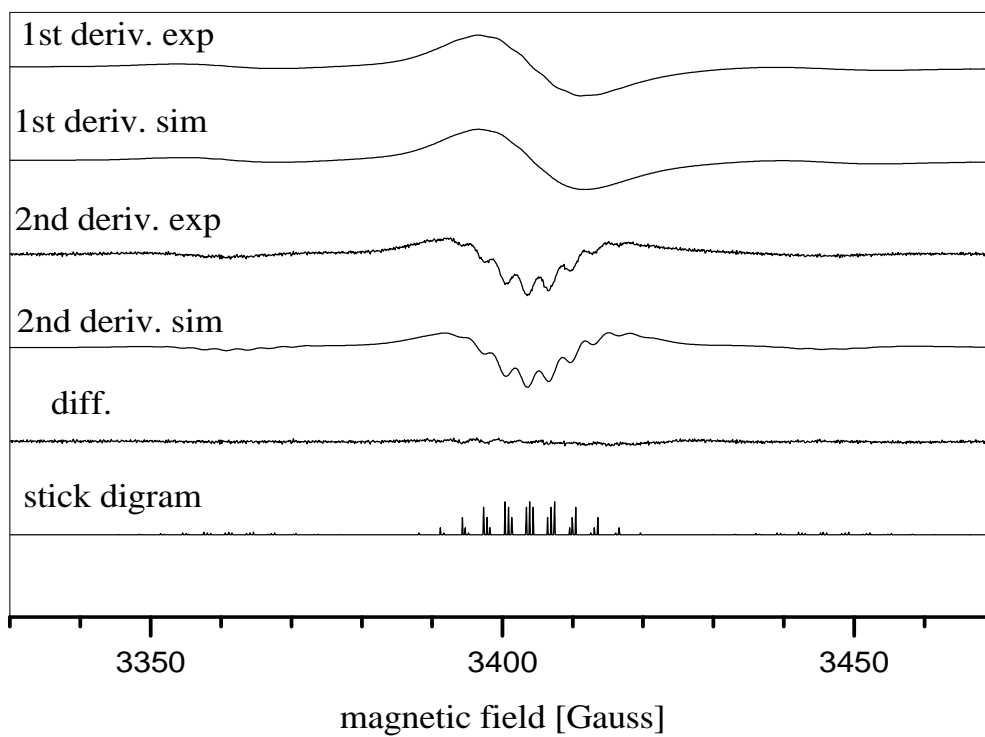


Figure 51: ESR spectra of **(11b)** at 240 K in toluene/CIN (3:1).

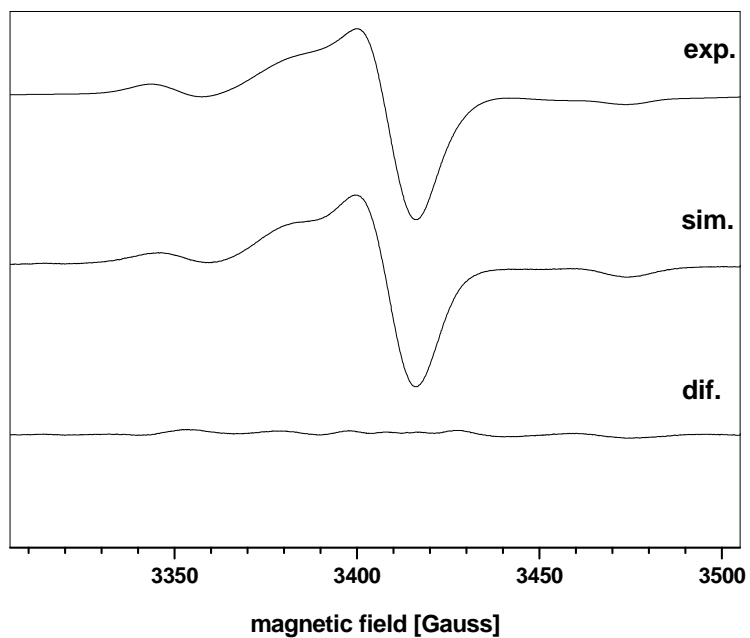


Figure 52: The first derivative in ESR spectra of **(11b)** at 130 K.

### Raman Spectra of (11a,b)

The Raman spectrum of **(11b)** is shown in (Figure 53). The spectra of **(11a,b)** display typical absorptions of MoPc. The spectra are rich with intense absorptions in the phthalocyanines finger print region 500-1500  $\text{cm}^{-1}$ . The absence of the characteristic absorption of W-W bond at 275  $\text{cm}^{-1}$  emphasizes that no tungsten phthalocyanine dimer is formed<sup>128</sup> as a result of high temperature synthesis.

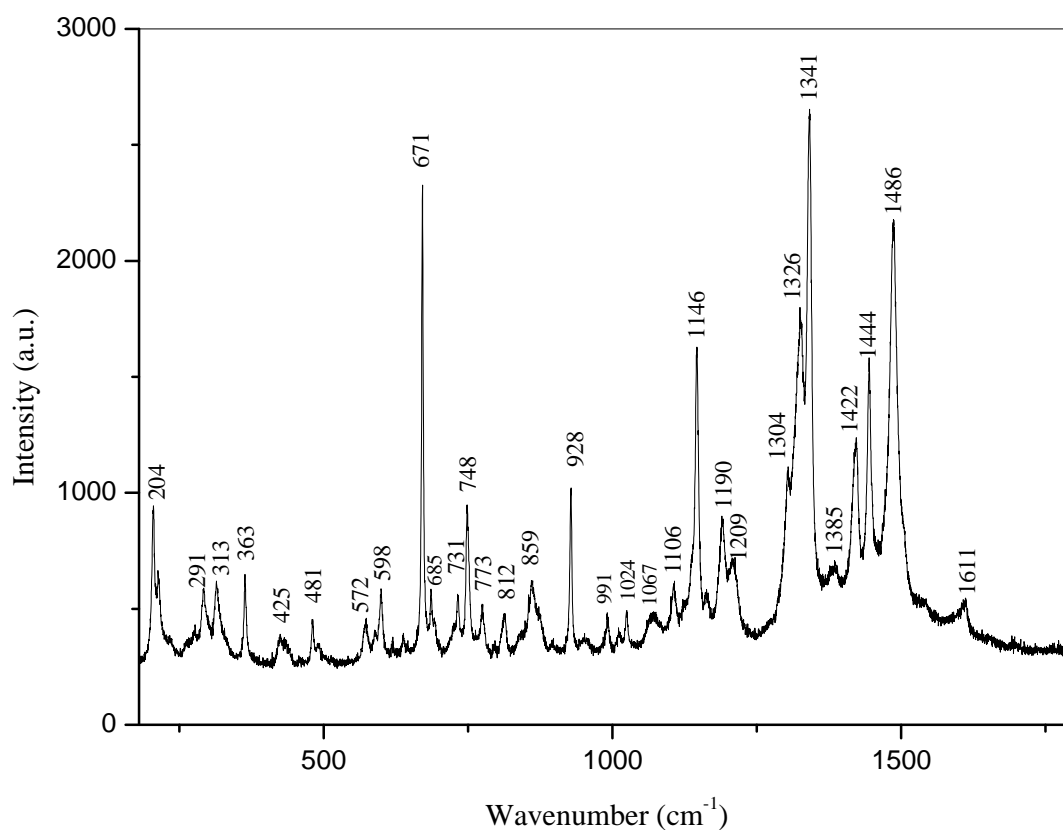
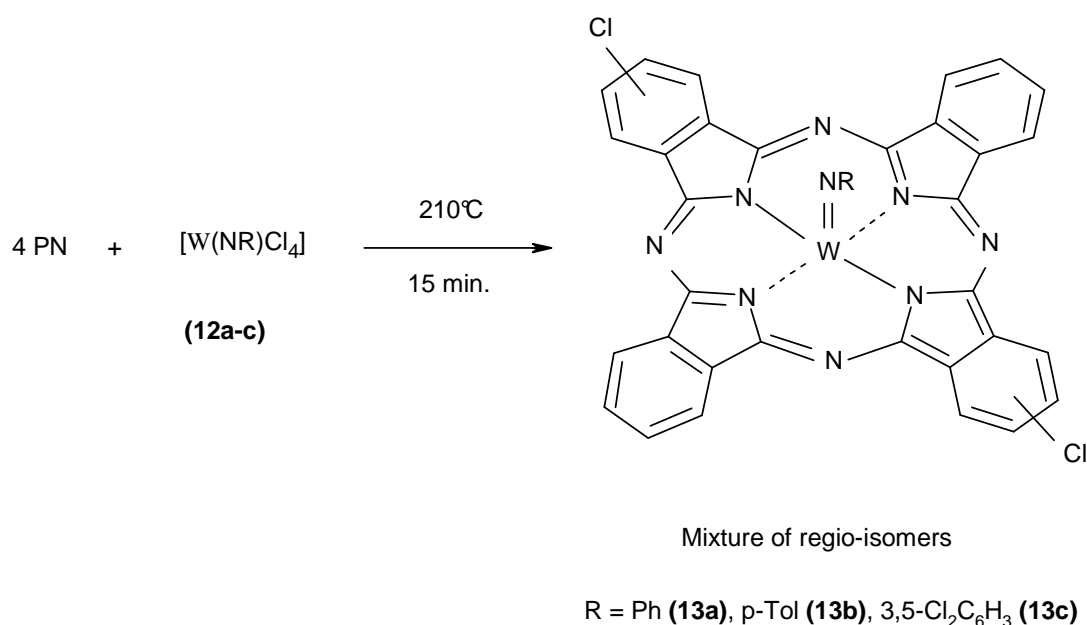


Figure 53: Raman spectrum of **(11b)**.

### 2.3.4 Synthesis of $[(Cl_2Pc)W(NR)]$ (**13a-c**)

The typical fusion reaction of PN was also studied in the presence of other imido tungsten complexes of general formula  $[W(NMes)Cl_4]$  as a precursor of the imido ligand. Thus when PN was heated at melt with  $[W(NMes)Cl_4]$  ( $R = \text{phenyl, } p\text{-tolyl, or } 3,5\text{-}Cl_2C_6H_3$ ) (**12a-c**), the corresponding compounds  $[(Cl_2Pc)W(NR)]$  (**13a-c**) were obtained (Scheme 20). The products were crystallized by layering hexane slowly to their solutions in 1,2-dichloroethane. Despite this crystallization provides feather-like crystals which were not suitable for X-ray structure determination, they afford analytically pure samples.



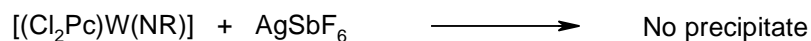
Scheme 20: Synthesis of  $[(Cl_2Pc)W(NR)]$  (**13a-c**).

The two chlorine atoms are suggested to be bonded to the aromatic rings of the phthalocyanine molecule and not to the central tungsten atom according to the following points:

- A molecular ion containing two chlorine atoms is observed implying that chlorine is covalently bonded to carbon not to the tungsten atom.
- The  $m/z$  values, of the highest intensity, obtained in MALDI-TOF measurements for ( $M^+$ ,  $M^+-Cl$ , and  $M^+-2Cl$ ) corresponded always to the chlorine ring substituted molecule whose molecular mass is lower than that of the ionic chloride compound by two mass units.



- We have detected some molecular ions of the tri and tetrachloro substituted complex in the crude samples that could be eliminated within the extensive extraction from different organic solvents. The appearance of such species gives rise to believe that the chlorine atoms are bonded to the aromatic rings of the Pc molecule and not to the central tungsten atom; otherwise the later would reach impossible oxidation states (7+ and 8+).
- $[W(NR)Cl_4]$  as  $d^0$  species are strong chlorination reagents and consequently are capable for chlorination of the aromatic rings. Similar case has been observed in literature, when PN was heated with  $[WCl_6]$  in which tungsten has  $d^0$  configuration, compounds of formula  $[(ClPc)W]$  and  $[(ClPc)W(O)OH]$  were obtained.<sup>54</sup>
- Ring chlorination gives chance to different isomers and this may explain the failure of all attempts made to obtain crystals of the products (**13a-c**) even under the same conditions applied successfully with analogue compounds such (**9a**).
- When the complexes  $[(Cl_2Pc)W(NR)]$  (**13a-c**) were refluxed with  $AgSbF_6$  in dichloromethane for several hours, no white precipitate of  $AgCl$  was observed and the  $m/z$  values after the reaction corresponded also to the *dichloro* species. Therefore, the two chlorine atoms are supposed to be bonded to aromatic carbon atoms.



- The mechanism of such phthalocyanine formation, which involves fusion of the reactants at elevated temperatures in absence of urea, alcohols, or reaction promoters such as ammonium heptamolybdate, is given in the literature (Scheme 3).<sup>10</sup> The mechanism suggested that the chlorine anion plays the role of the nucleophile (ammonia in synthesis procedures which include urea). Thus, chlorine is supposed to attack the  $\alpha$ -position in the isoindoline hetero ring and later at high temperature the chlorinum ion is formed and attacks the benzene ring in an electrophilic substitution reaction forming the aromatic chlorine substituted metal phthalocyanine. A similar mechanism is to be supposed for the reaction of PN with the strong chlorination reagents of formula  $[W(NR)Cl_4]$  (Scheme 20).

### 2.3.5 Characterization of [(Cl<sub>2</sub>Pc)W(NR)] (13a-c)

Firstly, the formation of the nitrido complexes as a result of an expected thermal degradation of the produced imido compound, can be safely ruled out according to the absence of its molecular ion peak ( $M^+ = 710$ ) and the absence of its characteristic IR stretching absorption at  $\nu_{W=N} = 953 \text{ cm}^{-1}$ .<sup>55</sup> Further, solutions of different concentrations of the product were found to be ESR silent; this varnishes the possibility of formation of the monochloro ( $W^{5+}$ ) species. Other known complexes of W(IV) and Mo(VI) such as [(ClPc)W=O]<sup>54</sup> and [PcMo=O]<sup>49</sup> have been reported to be ESR silent.

#### Mass Spectra

The  $m/z$  values of the molecular ions ( $M^+$ ,  $M^+-Cl$ ,  $M^+-2Cl$ ) of the prepared compounds (**13a-c**) were obtained in MALDI-TOF measurements with the expected isotopic patterns. The formation of metal-free phthalocyanines can be also ruled out according to the absence of ( $M^+ = 514$ ) of PcH<sub>2</sub>.

#### Elemental Analysis

Elemental analysis of C, H, N, and Cl together with the estimation of %W using AAS of the prepared compounds (**13a-c**) confirm the suggested structure of the dichloro substituted phthalocyanines ring. Chlorine analysis was important to ensure the presence of chlorine in addition to estimation of the number of chlorine atoms labeled in the produced complex.

#### UV/VIS and IR Spectra

The UV/VIS spectra of [(Cl<sub>2</sub>Pc)W(NR)] (**13a-c**) in chloronaphthalene (Figure 54) display both B and Q band absorptions of metal phthalocyanines around 320-330 nm and 640-720 nm respectively.<sup>8,55</sup> A small blue shift relative to the analogue compounds (**2**) and (**3a-d**) is observed. The splitting of the Q-band may be attributed to the lower molecular symmetry in (**13a-c**) relative to the peripherally unsubstituted Pcs because of presence of different regio-isomers. This may result in different dipolemoment interactions between the Pc macrocycle and the axial imido ligand and consequently lower degeneration of the first excited state. The different aryl groups in the imido groups do not result in remarkable differences in the electronic spectra. IR absorptions common to the spectra of the basic Pc moiety (e.g.  $\nu_{C=C}$  arom. at nearly  $1602 \text{ cm}^{-1}$ ) were observed. New

absorptions (underlined in the experimental work), which are not observed in the spectra of PcH<sub>2</sub>, [PcWO] and [PcWN], were observed in the spectra of **(13a-c)**. The formation of PcH<sub>2</sub> as byproduct can be again ruled out according to absence of its characteristic IR absorption at 1007 cm<sup>-1</sup>.<sup>35</sup>

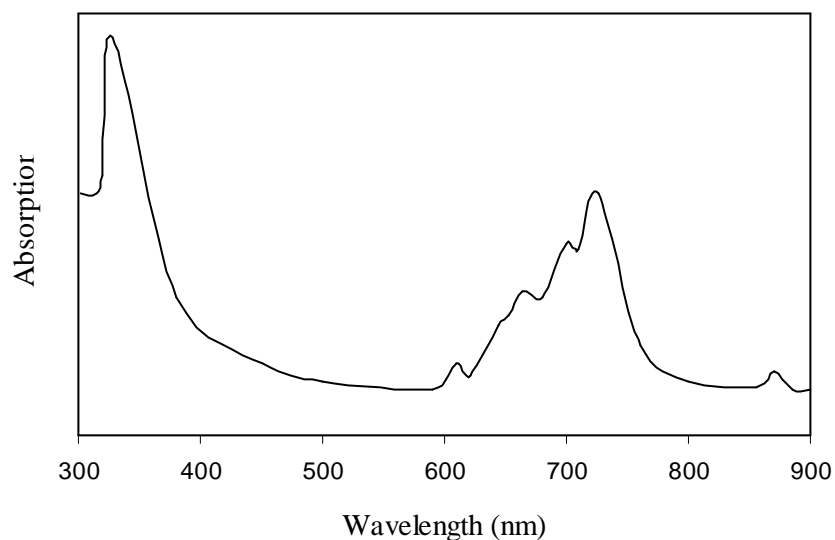


Figure 54: UV/VIS spectrum of **(13c)** (CIN, 10<sup>-5</sup> M).

### TGA

TGA of **(13a-c)** show that they are highly thermal stable since no weight loss is observed up to about 350°C. Further at 500°C about 60% of the material has not yet thermally decomposed. TGA of compound **(13a)** is shown in (Figure 55)

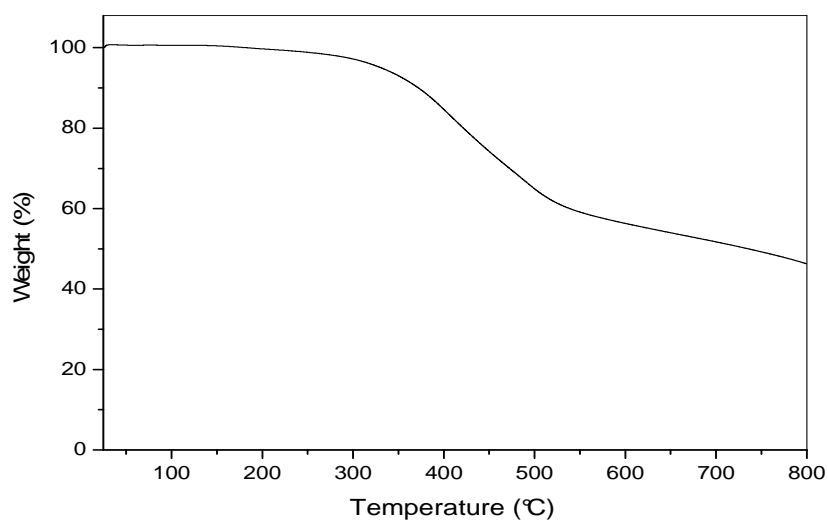
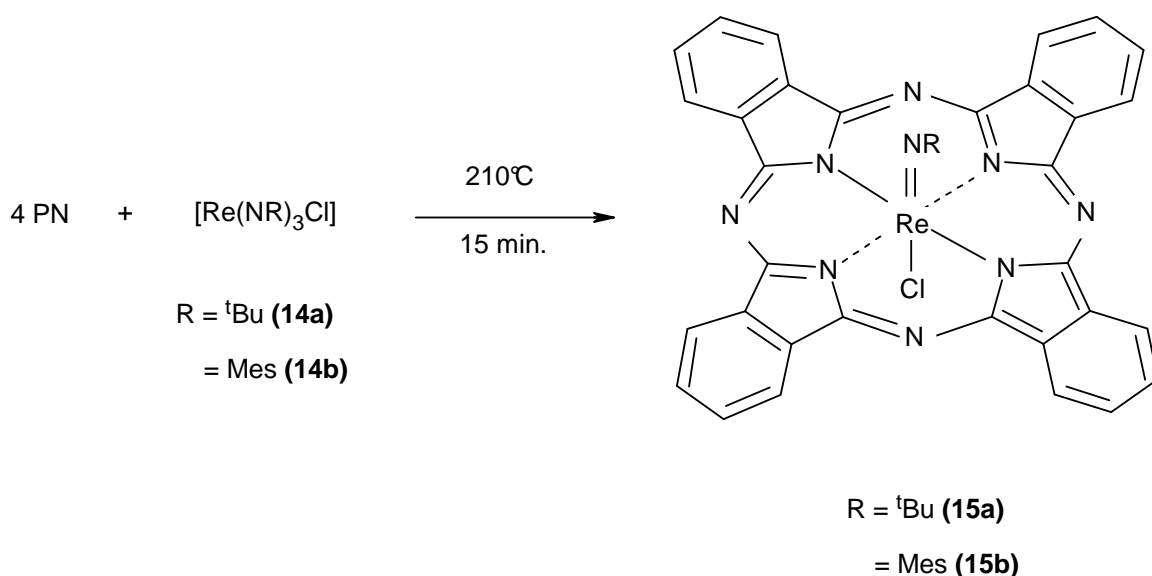


Figure 55: TGA of **(13a)**.

## 2.4. Rhenium Phthalocyanines

### 2.4.1 Synthesis of [PcRe(NR)Cl] (**15a,b**)

With the goal to prepare novel imido rhenium phthalocyanines we applied the typical fusion reaction of PN with complexes of the general formula  $[\text{Re}(\text{NR})_3\text{Cl}]$ , R = <sup>t</sup>butyl (**14a**) or mesityl (**14b**), as precursors for the (Re=NR) bond (Scheme 21). The corresponding chloro (organoimido) phthalocyaninato Re (V) complexes (**15a,b**) were obtained in good yields. Elevated temperatures were avoided to avoid any thermal degradation of the imido complexes into the nitrido complex [PcReN].



Scheme 21: Synthesis of [PcRe(NR)Cl] (**15a,b**).

Despite of the complex and unknown mechanism involving loss of a nitrene radicals [Cl] at the metal, this fusion reaction has been successfully applied for the preparation of similar 4d- and 5d-phthalocyanine species such as nitrido phthalocyanines [PcMN], M = Mo, W and Re.<sup>55</sup> All attempts done to obtain crystals suitable for X-ray structure analysis of the imido rhenium compounds (**15a,b**) were unsuccessful because of the poor solubility. However, utilizing the crystal structure data obtained for the analogue compound (**9a**) we suggest an isotype structure to (**9a,b**). Because of the large radius of the rhenium atom, it can not be inserted in the mean plane identified by the four isoindoline nitrogen atoms but displaced above this equatorial plane toward the imido group. The formation of the nitrido

complex [PcReN] as a result to an expected thermal degradation of the produced imido-complex, can be safely ruled out in accord with the absence of its molecular peak ( $M^+=712$ ) and the absence of its characteristic IR stretching absorption of ( $\text{Re}\equiv\text{N}$ ) at  $953\text{ cm}^{-1}$ .

#### **2.4.2 Characterization of Imido-RePcs**

##### **Mass Spectra**

The  $m/z$  values of the molecular ions of the prepared complexes [PcRe(NR)Cl] (**15a,b**) were obtained in both EI and MALDI-TOF measurements with the expected isotopic patterns. There was no need for using of a special matrix for energy transfer since a lot of metal phthalocyanines serve as LASER-energy transfer materials. The molecular ion peak ( $M^+$ ) could not be detected as the case of the previously discussed complexes containing a M-Cl bond.

##### **Elemental Analysis**

The CHN elemental analysis of (**15a,b**) matched fairly with the suggested structure. However, lower values of %C than expected were obtained. This may be attributed to the formation of the extreme thermally stable rhenium carbides at elevated temperatures. Chlorine analysis confirms the monochloro rhenium complex.

##### **$^1\text{H-NMR}$ Spectra**

The  $^1\text{H-NMR}$  spectra of (**15a,b**) show the expected resonance patterns of the diamagnetic Re(V) organoimido complexes. The phthalocyanine unit shows in the aromatic region two multiplets, the first multiplet in the region 9.42-9.63 ppm for eight protons in the 1,4-positions and the second multiplet in the region 8.13-8.38 ppm for eight protons in the 2,3-positions. The protons of the axial ligand show upfield-shifted signals due to the current effect of the phthalocyanine rings.<sup>8,39,41</sup> The aliphatic protons, tert-butyl group in (**15a**) and methyl groups in (**15b**) show a drastic upfield-shift (-1.48:-1.54 ppm) and (-0.75:-1.95 ppm) respectively. Because of the well known ring current effect of the phthalocyanine macrocycle, the aromatic protons of the axial ligand in (**15a,b**) suffer an expected upfield shift as to they are found in the region (5.06-5.13) ppm.

## UV/VIS

The electronic absorption measurements of the prepared (**15a,b**) in chloronaphthalene display characteristic absorption patterns of a monomeric metalphthalocyanine.<sup>8,17</sup> The B-bands in solution measurements of (**15a,b**) show unexpectedly sharp absorptions and are splitted into two main absorptions at  $\lambda_{\max} = 341$  nm and 323 nm.

## IR Spectra

The IR absorption spectrum of [PcRe(NMes)Cl] (**15b**) is shown in (Figure 56). The spectra of (**15a,b**) display the usual pattern common to the spectra of the basic Pc moiety (e.g.  $\nu_{\text{C}=\text{C}}$  arom. at nearly  $1602\text{ cm}^{-1}$ ).<sup>8</sup> The medium strong stretching band at  $1288\text{ cm}^{-1}$ , which is not observed in [PcReO] and [PcReN],<sup>56-59</sup> can be assigned to the (Re=N-C) stretching. Also disappearance of the stretching band of (Re $\equiv$ N) at  $953\text{ cm}^{-1}$ <sup>55,56</sup> rules out the thermal degradation of the imido complex into the nitrido complex.

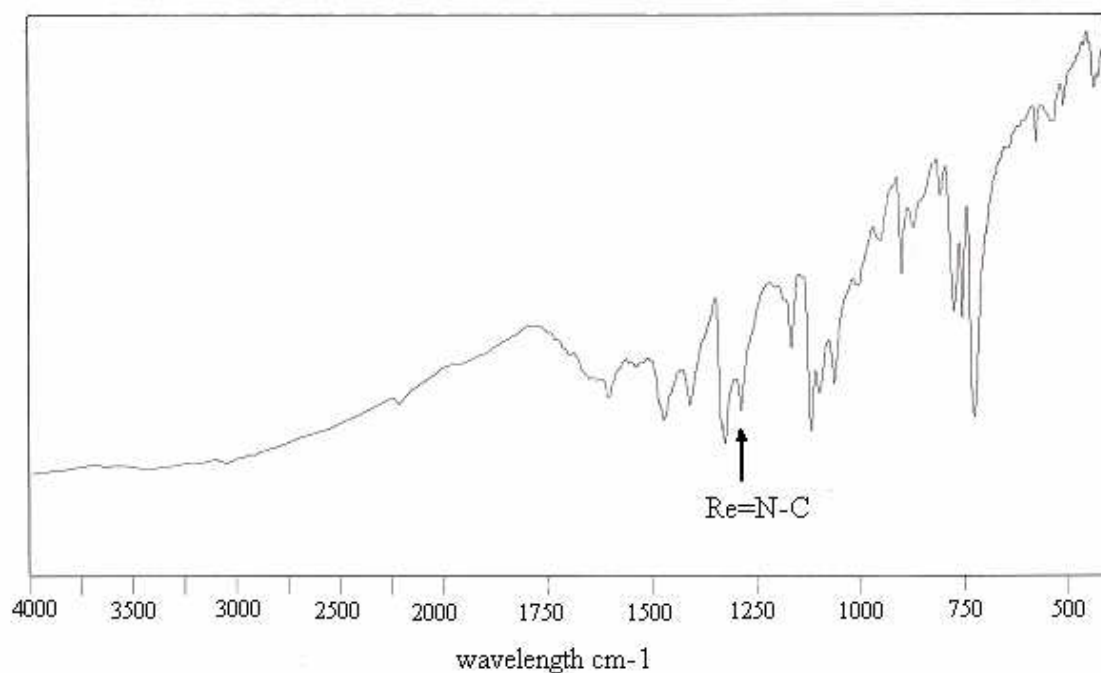


Figure 56: IR spectrum of [PcRe(NMes)Cl] (**15b**); KBr pellets.

## 2.5 Phthalocyanine Polymers

### 2.5.1 Synthesis of Phthalocyanines Polymers (16-18)

The typical reaction of pyromellitic acid dianhydride with anhydrous Cu (II) chloride in 2:1 ratio has been found to produce MPC oligomers having average molecular weight of 4000.<sup>67</sup> Other synthetic procedures of metal and metal-free phthalocyanines polymers have been reported in the literature by reaction of pyromellitic acid derivatives with a metal salt and urea in presence of a catalyst<sup>68,69</sup> or by reaction of 1,2,4,5-tetracyanobenzene (TCB) with a metal or a metal salt.<sup>65,66,131</sup> Wöhrle *et al*<sup>132</sup> have prepared metal-free phthalocyanineoctacarbonitrile  $[(CN)_8PcH_2]$  monomer by the cyclotetramerization of 1,2,4,5-tetracyanobenzene (TCB) in which two of the nitrile groups react. Complexation with a metal was accomplished by treating the product with a metal salt in DMF at 100°C. We applied this method to prepare the metal-free octacyanophthalocyanine as low molecular weight model compound for structurally uniform, nitrile group containing polymeric phthalocyanines.

Planar and ladder phthalocyanine polymers, because of their interesting long  $\pi$ -electron conjugation system and high thermal stability, display very interesting thermal and photoelectrical properties. However, the poor solubility in the common organic solvents increases the difficulties of their purification and processing schemes. We aimed in this part to prepare low molecular phthalocyanine planar oligomers (Figure 57a) which possess both the relatively enhanced solubility of the axially substituted Pc monomers (e.g. organoimido complexes) and the extended long-range conjugation and the high thermal stability of the Pc-polymers. To best of our knowledge, the titanium phthalocyanines planar-oligomers have not been yet reported in the literature despite of the success of a large number of titanium phthalocyanines monomers and dimers in many industrial fields.

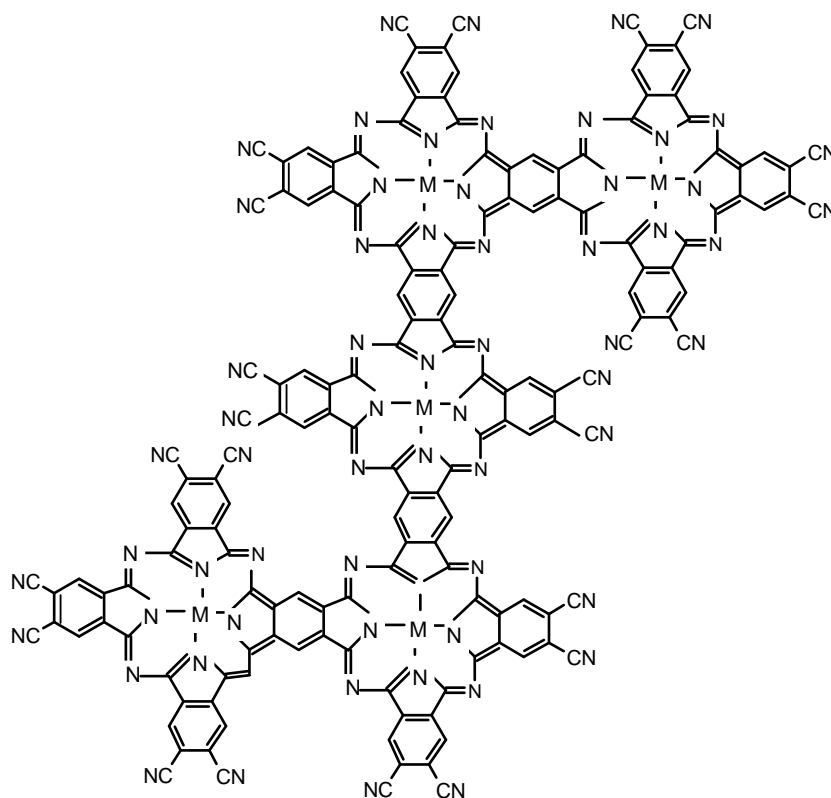


Figure 57a: Idealized systematic structure of the pentamer involving TCB as building blocks; M=[TiO] (**16**), M=[Mo(NMes)Cl] (**17**), M=[Ti(NDip)] (**18**).

Reaction of 1,2,4,5-tetracyanobenzene (TCB) with a proper titanium source e.g.  $\text{Ti}(\text{O}i\text{Bu})_4$  under certain conditions e.g. molar ratio 2:1 and 4 hour heating at  $220^\circ\text{C}$  was found to produce high molecular weight phthalocyanine including the pentamer,  $\text{C}_{160}\text{H}_8\text{N}_{64}\text{O}_5\text{Ti}_5$ , molecular weight = 3145.59. This is in agreement to the previous schemes reported in the literature for synthesis of Pc-oligomers having four to nine phthalocyanine units. Four of the possible isomers for the pentamer (Figure 57b) can be postulated. On the basis of the spectroscopic data, it can not be excluded that the connectivity of the five PcM building blocks differs from the idealized structure shown in (Figure 57a). After formation of the trimer, two TCB molecules may attack the cyano groups of this trimer in three different ways (B, C, and D in Figure 57b). According to steric factors the attack which leads to formation of the structure (B) has the highest probability compared to the others (A and C), and consequently should be more predominant. The structure (C) has the lowest probability on basis of the steric hindrance caused by the cyano groups of the trimer.



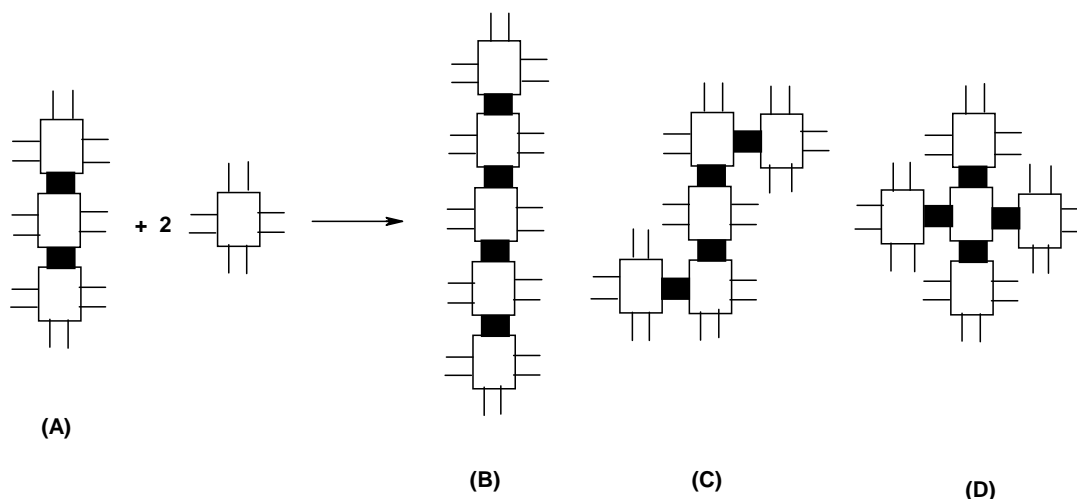




Figure (57b): Four of the possible isomers of the phthalocyanines pentamer.

 refers to Pc unit and  
 refers to cyano group.

### 2.5.2 Characterization of Phthalocyanines Polymers (16-18)

The prepared phthalocyanines oligomers ( $n = 5$ ) were characterized using elemental analysis, GPC measurements, UV/VIS, FT-IR, TGA, etc. The formation of the octacyanophthalocyanine monomers can be safely ruled out since their molecular peaks were not detected in several mass spectroscopic measurements (EI, FAB, and MALDI-TOF). Moreover, the values obtained by analysis of C, H, N, and estimation of the metal content using the atom absorption spectroscopy (AAS), support the formation of Pc-oligomer rather than the octacyanophthalocyanine monomers. The most reasonable suggestion for the reaction mechanism of Pc-Polymer formation from TCB has been reported by Wöhrle *et al*<sup>131,132</sup> who expected from the high reactivity of the nitrile groups of TCB in ortho position, compared with those of metal-free  $(CN)_8Pc$  monomer, that TCB reacts partially to form the metal free  $(CN)_8Pc$  monomer at first. This monomer is supposed to react with itself or with TCB molecules to form products of high molecular weights.

### GPC

Partially soluble (PolyMPc) in DMF are known in the literature.<sup>133</sup> The prepared (PolyMPcs) were found to be soluble in DMF. Since the DMF soluble (**3b**) can be considered as a low molecular weight model compound for the prepared (polyMPcs), we carried out the

GPC measurements for this monomer under the same conditions as the prepared (polyMPcs). The molecular weight of the monomer, calculated as (~800), was determined by GPC as ( $M_n=1012$ ). This means that the GPC measurements for the analogue oligomers are reasonable and can be taken in account. The difference between the theoretical and the obtained molecular weights are considered as experimental error. The GPC of the oligomers showed unimodal curves and the molecular weights obtained with respect to polystyrene standards could be taken in consideration as a rough estimation of the molecular weights of the prepared poly Pcs.

### **Elemental Analysis**

The values obtained by C and N analysis are comparable to the calculated values for the planar phthalocyanines oligomer of ( $n=5$ ) (Figure 57a). Additionally, the metal analysis using AAS supports the assumption of formation of MPc oligomers.

### **FTIR**

For both TiPc oligomers, the resolution of the IR-spectra are relatively good and exhibits the typical absorptions of the phthalocyanine polymers at 1500, 1308, 1082, 1028, 790  $\text{cm}^{-1}$ .<sup>133b</sup> The absence of  $\delta_{oop}$  (N-H) vibration at 700  $\text{cm}^{-1}$  ensured the complete metalation of the oligomer.<sup>68</sup> IR spectra permit conclusion on the nature of the end groups in the Pc-polymers. Because of the reaction conditions and working up method e.g. dry conditions, all the prepared Pc-oligomers possess only nitrile end groups ( $\nu_{C\equiv N}$ ) at 2221-2225  $\text{cm}^{-1}$ . The presence of (C=N) containing structure element (X) is demonstrated by the absorption bands at 1582-1578, 1522-1520, 1310-1308, 1082-1080, and the band at 2225-2221  $\text{cm}^{-1}$  (Figure 58).<sup>68, 130</sup> The formation of triazine structure (Y) from nitriles is possible in the presence of metal chlorides acting as Lewis acids and can be excluded in case of the prepared MPC-oligomers depending on absence of its characteristic absorption band at 1360  $\text{cm}^{-1}$ .<sup>68,130</sup> The resolution of the IR-spectrum of the MoPc-oligomer is bad and shows only few phthalocyanines frame vibrations and this well known in the literature for some analogue Pc-polymers.

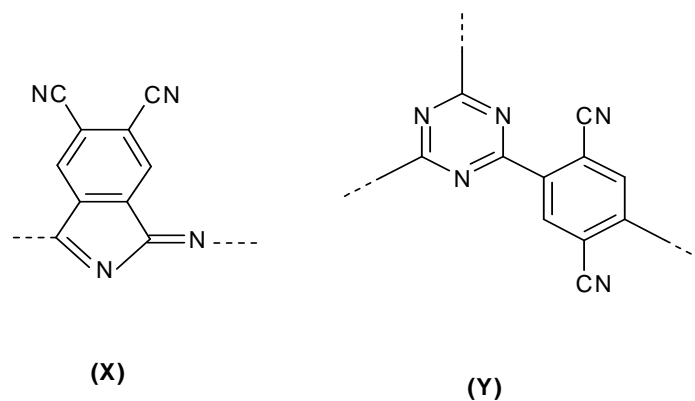


(Figure 58): The possible bonding schemes in MPC polymers.

### UV/VIS

The UV/VIS spectra of the prepared oligomers (**16-18**) in DMF show the expected absorption patterns of a high molecular weight phthalocyanine (Q and B bands).<sup>68, 130, 132</sup> The strong absorptions begin at 312 nm and extending to the 742 nm. By comparison of these spectra with those of the analogue monomers (**1**), (**2**) and (**9b**) it can be concluded that the planar Pc-oligomer contains the main skeleton of a phthalocyanines unit but with a poor resolution (broadening) of the Q-bands which indicate the high aggregation and high  $\pi$ - $\pi$  interaction in the MPC-oligomers in DMF. UV/VIS spectrum of (**16**) in DMF is shown in (Figure 59).

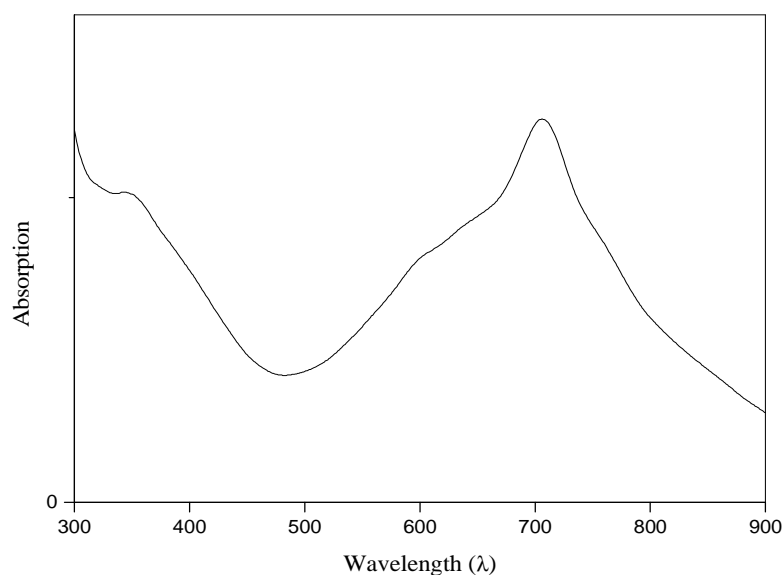


Figure 59: UV/VIS. spectrum of (Poly PcTiO) (**16**) in DMF.

## TGA

Polymers with a Pc ring are resistant to thermal oxidation.<sup>69, 70</sup> The prepared (Poly MPcs) show high thermal stability and no weight loss is observed below 250°C. The stability of (Poly PcTiO) is much higher than that of the other polymers which show degradation of the axial moiety in the temperature range (380-400 °C). Generally, about 70% of the material is maintained up to 500°C. TGA diagram of (PolyPcTiO) is shown in (Figure 60).

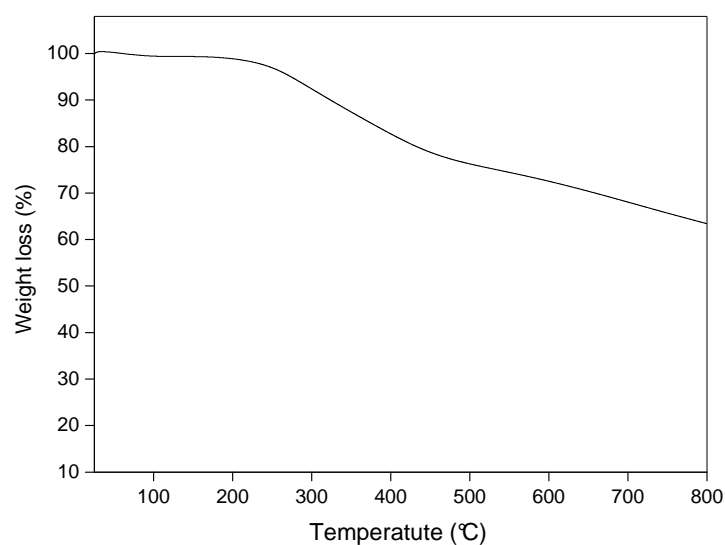


Figure 60: TGA diagram of (Poly PcTiO) (16).

## XRD

X-ray diffraction measurements of the prepared (Poly MPcs) show broad diffuse peaks. This is characteristic for low molecular weight (Poly MPcs), since they show broad bands and by increasing the molecular weight the diffuse peaks become more intense.<sup>67</sup>

## 2.6 Time-resolved Photoluminescence

PcTiO (**1**) has been successfully used to compensate the toxic and hard disposable selenium as photoconductor in xerography.<sup>6,28</sup> The aim of this part was studying the effect of the chemical modification on the optical properties of these materials specially the photoconductivity. The transient photoluminescence (PL) measurements were carried out for solutions in chloronaphthalene ( $10^{-3}$  M) of [PcTiO] (**1**) and [PcTi(N,N'-ditolylureato)] (**3b**). Afterwards the solutions were microfiltered for some samples prior to the measurements to avoid the presence of any solid particles. Such solid fine particles must be eliminated to avoid the dimer aggregation of the phthalocyanine molecules in the solid state which retards the fluorescence process. This effect was indicated by comparison of the PL properties of the filtered and not filtered samples. The spectro-temporal streak camera images for [PcTiO] (**1**) and [PcTi(N,N'-ditolylureato)] (**3b**) are shown in (Figure 61).

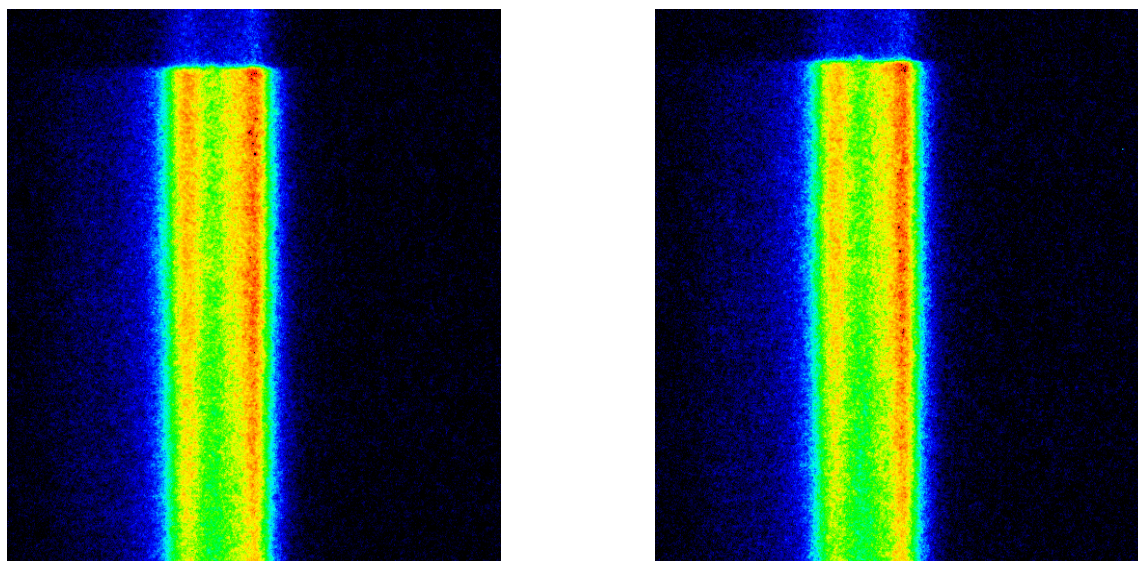


Figure 61: Spectro-temporal streak camera images for (**1**) left and (**3b**) right.

The fluorescence spectra of [PcTiO] (**1**) and [PcTi(N,N'-ditolylureato)] (**3b**) were measured to study the effect of replacing the axial oxo group with the ureato group in the optical properties. The measurements were carried out as part of this work in a cooperation project with the research group of Prof. Dr. Wolfgang Rühle, Physics Department, Philipps-Universität, Marburg. For this purpose a Ti:Saphir-Laser with an excitation light of

doubled frequency ( $\lambda = 380 \text{ nm}$ ,  $\rho_{\text{exc}} \sim 120 \text{ W/cm}^2$ ) was applied. We carried out preliminary investigations at these phthalocyanines and found that only the intensity of the PL spectra and the transient ones is concentration dependent, but not their qualitative process. (Figure 61) shows a typical photo recorded on a streak camera for room temperature measurements of [PcTiO] (**1**) and [PcTi(N,N'-ditolylureato)] (**3b**). The corresponding time-integrated PL-spectra of both samples are shown in (Figure 62). Several maxima are observed in both spectra and the most two sharp maxima are lettered as A and B. Similar PL-spectra were obtained and reported in the literature for the other phthalocyanines derivatives.<sup>134</sup>

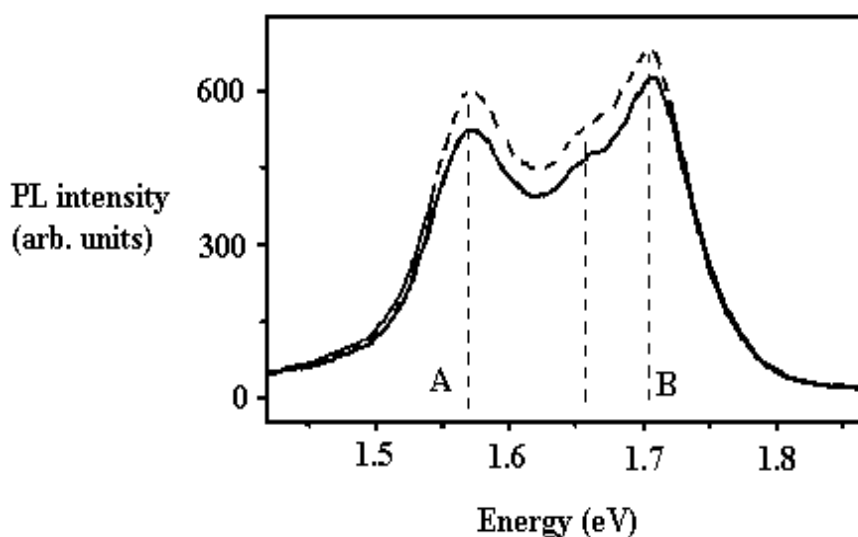


Figure 62: Comparison of the Time integrated PL of [PcTiO] (**1**) solid line and [PcTi(N,N'-ditolylureato)] (**3b**) dashed line. ( $T = 290 \text{ K}$  and  $\rho_{\text{exc}} \sim 120 \text{ W/cm}^2$ ).

Although the exact electronic configuration and the location of the energy transitions are not known, it must be nevertheless concluded that the observed emission bands in case of the investigated phthalocyanines are caused by the basic structure of the phthalocyanine molecule. Otherwise the relative strength or the energetic situation of the individual signatures would have to change. [PcTi(N,N'-ditolylureato)] (**3b**) seems to have a lower photoconduction than [PcTiO] (**1**). This statement is based on the circumstance that the transition of an electron from the excited state LUMO-S1 to the ground state HOMO-S0 is a competitive process to the photoconduction process. This depends on the fact that when an organic photoconductor shows higher fluorescence or PL this means that it processes lower photoconductivity. It is noteworthy to mention that higher PL density leads to a less effective photoconductivity but to enhanced optical limiting properties.

To discuss the dynamics of the emission of the investigated compounds, we measured the spectral integrated PL-transients of both samples (Figure 63). It can be concluded that both samples show unusual time-decay behavior. At the first 750 ps the strength of the signal is fast unchanged and then decreases with time constant of  $\tau \sim 3.9$  ns. The life time values are comparable with the other values of the time-resolved fluorescence spectra (4-6 ns)<sup>135</sup> and confirms the potential of the phthalocyanines also for the medical and biophysical range, e.g. in imaging procedures, with which living organisms are examined with the help of the fluorescence spectroscopy on NS time scales. The constant PL intensity in the first time period can not be definitely explained.

The decay time ( $\tau$ ) is calculated according to the equation:

$$I_{PL} = I_0 \cdot e^{-t/\tau} \quad (t = \tau \text{ when } I_{PL} = I_0/e = I_0/2.71)$$

(Figure 63) shows the spectral resolved emission-dynamic of [PcTiO] (**1**) and [PcTi(N,N'-ditolylureato)] (**3b**) for the energy transitions marked in (Figure 62). Up to the PL intensity the qualitative process of the PL loss curves depends neither on the kind of the metal complex nor on the detection energy. This explains again that the fundamental optical properties such as absorption and emission dynamics of the studied compounds depend mainly on the basic organic building block. Due to the expanded  $\pi$ -electron system the phthalocyanine compounds possess very strong, nonlinear optical characteristics.

Experiments for optical limitation show typical flow densities of  $100 \text{ mJ/cm}^2$ ,<sup>136</sup> with which the transmission coefficient reaches approximately a minimum saturation value. Then a (Nd:YAG-laser with puls time of  $\Delta t$  puls  $\sim 7$  ns) is generally applied so that the pulse maximum performance decisive for the delimitation process lies within the range of  $10\text{-}20 \text{ GW/cm}^2$ . The energy pro puls in case of using (Ti:Saphir-Lasers) is actually smaller than ( $\sim 1.5 \times 10^{-6} \text{ J/cm}^2$ ) but within the short puls (puls-period  $\sim 80$  fs) this can be compensated.

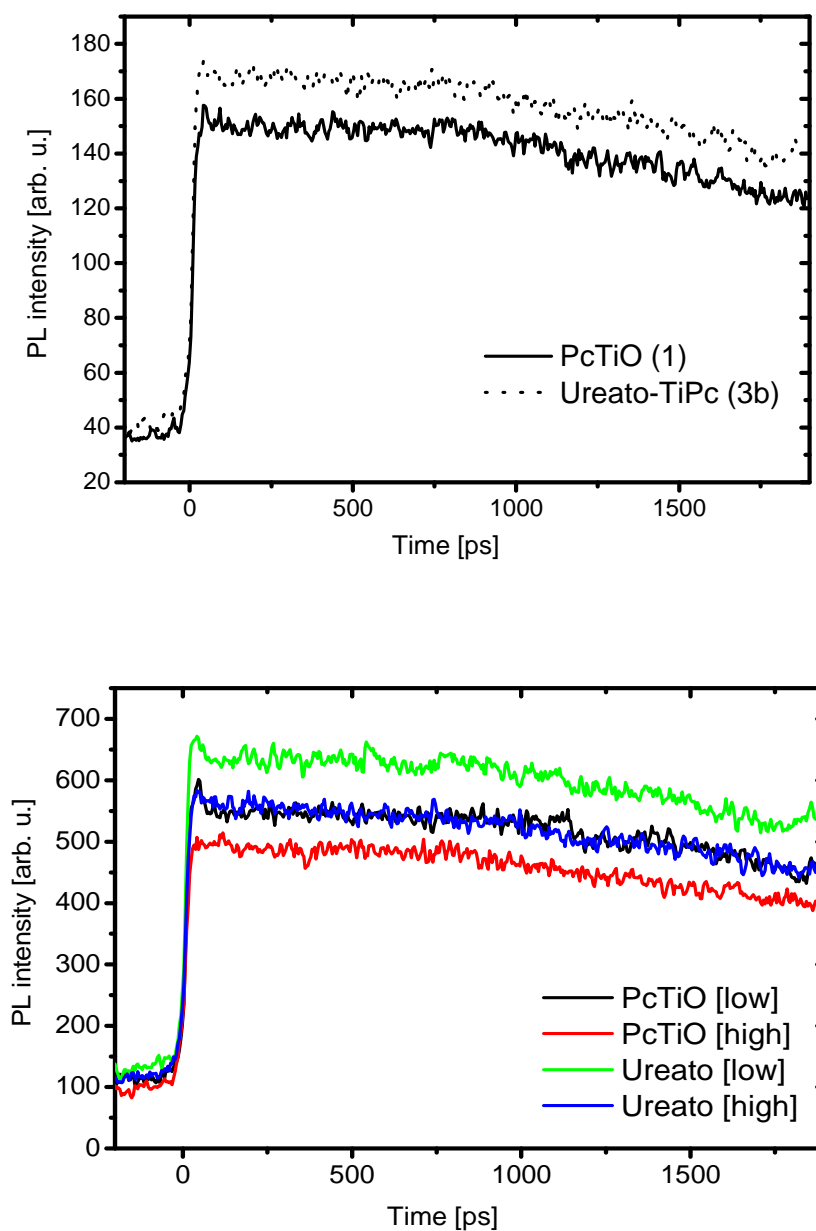


Figure 63: Top: The spectral integrated PL-transient of [PcTiO] (**1**) and (**3b**).  
Bottom: Transient PL-decay at energy  $E(A) = 1.57$  eV and  $E(B) = 1.705$  eV.

Generally, it can be concluded from this study that the new prepared compound (**3b**) shows higher PL density than PcTiO (**1**). This suggests that compound (**3b**) is expected to display relatively less effective photoconductivity but enhanced optical limiting properties in comparison to the well known photoconductor and optical limiting material [PcTiO] (**1**).



## **2.7 Phthalocyanine Modified SBA-15 Mesoporous Silica Materials**

Systems combining inorganic host and organic guest molecules provide a source of new materials with challenging properties.<sup>137a</sup> Chromophore- loaded zeolites have been investigated for different properties, such as photocatalyst,<sup>137b</sup> novel pigments<sup>137c-e</sup> and nonlinear optical materials exhibiting optical bistabilities,<sup>137f</sup> frequency doubling,<sup>137g-h</sup> spectral hole-burning<sup>137i</sup> or lasing.<sup>137j</sup> Dye molecules adsorbed on the surface of TiO<sub>2</sub> Nano crystals were found to inject electrons into the empty states of the TiO<sub>2</sub> from a photo excited state of the dye (dye sensitization).<sup>137k-l</sup> This photoinduced electron transfer via a single-photon process is the basis of the remarkable photosensibilisation cells introduced by Grätzel and coworkers<sup>137m</sup> and can be used to realize a photochemical hole burning, as shown recently by Machida and coworkers for a titania-encapsulated derivative of zinc tetrabenzoporphine.<sup>137n</sup> In this work, we aimed at studying the impregnation of titanium phthalocyanine in SBA-15 and TiO<sub>x</sub>@SBA-15 utilizing the reactivity and better solubility of the diaryl titanium phthalocyanines, relative to [PcTiO], to entrap monomeric TiPc molecules in close contact with SBA-15 and with titanium centers highly dispersed inside the pore system of the SBA-15.

In this work SBA-15 template has been prepared according to the schemes reported in the literature.<sup>138</sup> SBA is an abbreviation of Santa Barbara and 15 for hexagonal structure.<sup>139</sup> For preparation of TiO<sub>x</sub>@SBA-15, we used a method similar to that previously used for impregnation of titanium species.<sup>85a, 85h, 95, 140</sup> Thus titanium species were impregnated in a previously synthesized calcined siliceous SBA-15 using tetrabutylorthotitanate (TBOT) as a precursor of titanium species. It is known, that TBOT interacts with the surface silanol groups of SBA-15.<sup>85a</sup> In our experiments, unreacted TBOT was removed by extraction with dried solvents under inert conditions. During the following calcination in air at 600°C, the remaining butoxy ligands are assumed to be burned off while the TiO<sub>x</sub> species remained fixed via a Si-O-Ti linkage at the surface of SBA-15 (Figure 64). According to AAS we obtained a Ti-loading of about 2.66 wt.% and this value is comparable to that achieved applying this method for MCM-41 materials where loadings of 1.7-8.6% were reported.<sup>85a</sup> The lower Ti loading in the pores compared with that achieved for MCM-41 using TiO(acac)<sub>2</sub> may be attributed to the weaker interaction of TBOT with the OH groups because of its hydrophobic hydrocarbon chain.<sup>85a</sup> While high loadings (30-80%) of TiO<sub>2</sub> in SBA-15 led to the presence

of anatase,<sup>85e</sup> the material  $\text{TiO}_x\text{@SBA-15}$  prepared in this work having relatively low titanium loading displays monodispersed isolated Ti(IV) sites. This is in agreement with other reports of SBA-15 materials of low titanium loading.<sup>85c,f,g</sup> Raman spectrum of the prepared  $\text{TiO}_x\text{@SBA-15}$  shows absorption bands at 789, 832  $\text{cm}^{-1}$  assigned to the Si-O-Si linkage, and at 488 and 601  $\text{cm}^{-1}$  assigned to four and three membered siloxane rings.<sup>85d</sup> The absence of the typical Raman absorption bands of anatase  $\text{TiO}_2$  (638, 519, 399, 147  $\text{cm}^{-1}$ ) ensures the absence of the anatase.<sup>85c</sup> It is suggested that due to the strong extraction of the unreacted TBOT under inert atmosphere and low titanium content Ti(IV) is only covalently bonded to the surface of SBA-15 via 1-3 Ti-O-Si links forming thin layer of  $\text{TiO}_x$ .

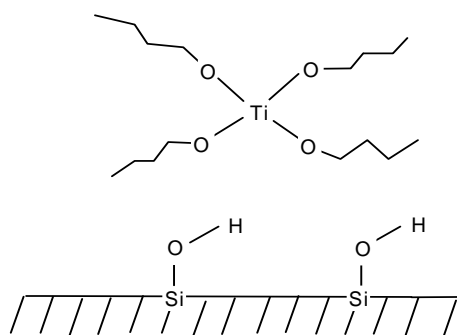
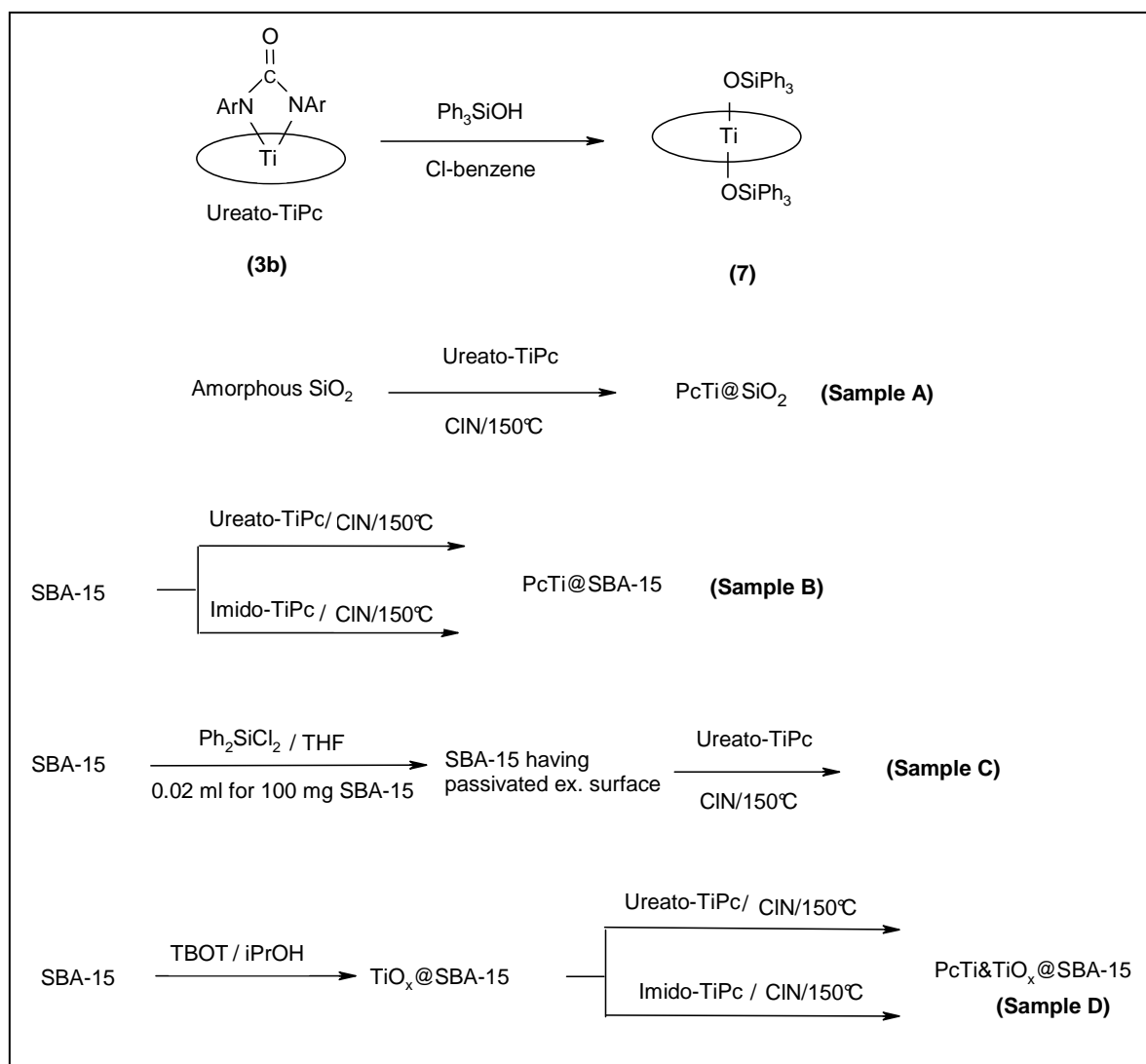


Figure 64: Interaction of TBOT with the pore walls of SBA-15.

### Interaction of Titanium Phthalocyanines with SBA-15 and $\text{TiO}_x\text{@SBA-15}$

The large pore size of SBA-15 offers the possibility to tether sizeable and complex catalytically reactive sites within the silica framework. As we previously mentioned in the synthesis of compound (7), the good ureato leaving group in N,N'-di-4-tolylureato (phthalocyaninato) titanium (IV) (3b) results in smooth reaction with the silanol groups of  $\text{Ph}_3\text{SiOH}$ . In the following part, compound (3b) was used to anchor and fix the TiPc dye in the pores of SBA-15 and  $\text{TiO}_x\text{@SBA-15}$  where the titanium atom in (3b) can smoothly link to the silanol groups in SBA-15 molecular sieves (Figures 65a,b). Several samples were included in this study (Scheme 22). In (Sample A) silica ( $\text{SiO}_2$ ) was heated with a dilute solution of the phthalocyanine dye. In (Sample B) the SBA-15 material was heated with a dilute solution of the phthalocyanine dye. Consequently, the TiPc species is expected to be immobilized predominantly inside the channels to give the modified material

shown in (Figure 65b). In (Sample C) the SBA-15 was firstly treated with  $\text{Ph}_2\text{SiCl}_2$  (0.01 equivalent) on the assumption that the most kinetically available silanol groups were those at the outside surfaces of the silica particles (about  $1\mu\text{m}$  in diameter) and hence, these would be silylated and deactivated prior to heating with **(3b)**.<sup>141</sup> Thus in (Sample C), only the inner surface of the host SBA-15 is decorated with [PcTi] species. In (Sample D) the prepared  $\text{TiO}_x\text{@SBA-15}$  (Ti 2.66 wt.%) was heated with a diluted solution of **(3b)** and since some surface silanol groups are still unreacted, the hypothetical monolayer coverage of SBA-15 with  $\text{TiO}_x$  is about 35 wt.%<sup>85f</sup>, the dye molecules are presumably covalently bound via the remaining silanol groups or via the Ti-OH groups which may be present at the  $\text{TiO}_x(\text{OH})_y$  sites (Figure 65a).



Scheme 22: Reaction of **(3b)** with triphenylsilanol and preparation of PcTi@silica, PcTi@SBA-15, and PcTi& $\text{TiO}_x\text{@SBA-15}$  materials.

In all samples the physically adsorbed phthalocyanine dye was supposed to be removed by intensive extraction of all samples with different organic solvents such as toluene, MeCN and chlorobenzene. Finally, the samples were dried under reduced pressure. This study further included the impregnation using imidoTiPc (**2**) which was found to lead to the same results as (**3b**) but lower load because of lower solubility and lower diffusion of (**2**) relative to (**3b**). For comparison, we also impregnated PcTiO (**1**) in SBA-15, however lower dye content and higher dye aggregation was obtained because the mostly interaction is physical adsorption. No remarkable differences were detected in the spectroscopic data of (Samples B and C). However, (Sample C) allows selective anchoring of the dye into the internal surface and may also offer a better view of the Pc molecules in the pores in TEM investigations. In another experiment, we passivated both the internal and external surfaces of SBA-15 by with excess amount of  $\text{Ph}_2\text{SiCl}_2$ . When this material, whose both internal and external surfaces are passivated by silylation, is heated with a solution of (**3b**) a very low dye loading was obtained.

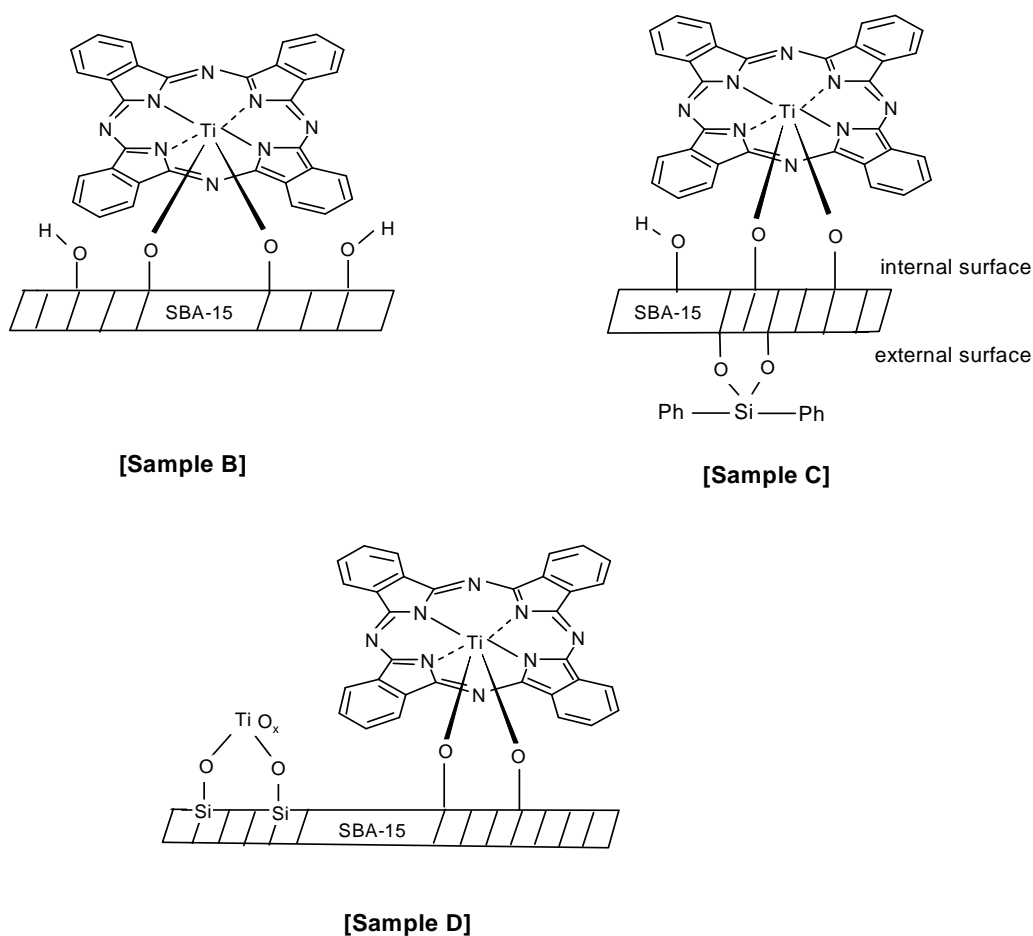


Figure 65a: Covalent anchoring of [PcTi] onto different SBA-15 materials.

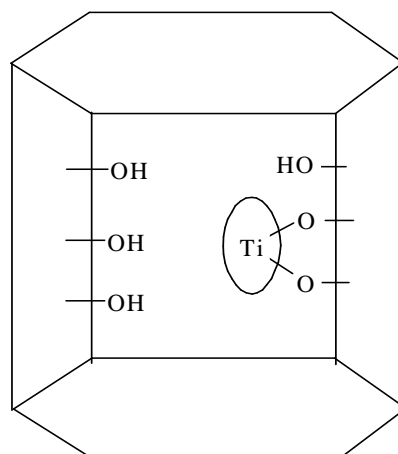


Figure 65b. Fixation of (TiPc) in the hexagonal porous of SBA-15 (Sample B).

### Mass Spectroscopy

In mass spectra measurements (MALDI-TOF) of all prepared samples the ion peak of  $[\text{PcTi}^+]$   $m/z = 560$  instead of the molecular ion peak of *N,N*-di-4-tolylureato (phthalocyaninato) titanium (IV) (**3b**) or the imido-TiPc (**2**) has been detected. This gives rise to the assumption that the ureato complex reacted with the silanol groups on the surface of the SBA-15 material. The formed urea derivative (ToINHCONHTol) was extracted from the produced materials by successive washing by several organic solvent such as boiling acetonitrile.

### Titanium Analysis

The amounts of the loaded titanium in  $\text{TiO}_x\text{@SBA-15}$  and  $\text{PcTi}\&\text{TiO}_x\text{@SBA-15}$  were determined using Atom Absorption Spectra (AAS) and the following results were obtained:

$$\% \text{Ti in } \text{TiO}_x\text{@SBA-15} = 2.66$$

$$\% \text{Ti in PcTi}\&\text{TiO}_x\text{@SBA-15 (Sample D)} = 3.44$$

$$\% \text{Ti because of PcTi dye} = 0.78 \text{ (consequently content of PcTi-dye} = 9.13\%).$$

### UV-VIS/NIR Transmission Spectra of the Prepared Materials

The analysis of the UV-VIS transmission spectra of the pure mesoporous SBA-15, conventional silica and the products of immobilization of N,N'-di-4-tolylureato-(phthalocyaninato) titanium (IV) (**3b**) by different techniques in silica matrices can be used to give an idea about the nature of the interaction between the dye and the inorganic template and to reveal if the dye is aggregated at the template surface or monomeric encapsulates in its pores.<sup>85a, 94, 95</sup>

The UV-VIS/NIR transmission spectra (200-2000 nm) of pure N,N'-di-4-tolylureato (phthalocyaninato) titanium (IV) (**3b**), dye/silica, dye@SBA-15 and a mechanical mixture of dye and silica are shown in (Figure 66). It is apparent that the spectral patterns are different and this is attributed to different interactions of the dye with the silica when the components are mechanically grounded in a mortar and when the dye is covalently anchored onto the pore walls by heating the SBA-15 or silica with the dye solution.

The UV-VIS/NIR transmission spectra of the prepared materials (Figure 66) and (Table 12) display sharp Q-band absorptions. This absorption behavior which is very close to that of (**3b**) dissolved in chloronaphthalene (Figure 18) and this indicates that the titanium phthalocyanine dye in the two materials is molecularly dispersed in the silica and SBA-15 matrices. The absorption band at 698 nm for PcTi@SBA-15 material and at 700 nm for the PcTi@silica is the monomer absorption corresponding to (0-0) transition from the HOMO to the LUMO. The second absorption band at 640 nm for PcTi@SBA-15 and at 612 nm for the PcTi@silica is the (0-1) transition from the HOMO to the first overtone of the LUMO<sup>142</sup> and its presence is a strong indication for the absence of aggregated phthalocyanines dye.<sup>142</sup>

On the other side, the two spectra of solid N,N'-di-4-tolylureato (phthalocyaninato) titanium (IV) (**3b**) and the mechanical mixture of PcTi/silica (Figure 66) show an absorption Q-band around 820 nm which is attributed to the dimeric stacking in the solid phthalocyanines since this band is not observed in the solution spectrum of the dye in chloronaphthalene (Figure 18). The monomer band around 700 nm in both samples shows only a weak intensity and overtone signal can be identified.<sup>95</sup> These are evidences for the presence of high degree of aggregation in solid PcTi(ureato) (**3b**) and PcTi/silica (mechanical mixing). We resolved the crystal structure of (**3b**) and discussed the molecular packing

of the molecules in the unit cell. We identified that **(3b)** exists in the solid state as dimeric species in a face-to-face configuration which results in UV-VIS absorption band at about 800 nm. In the case of PcTi&TiO<sub>x</sub>@SBA-15 the chemical and physical properties would be slightly different as documented in literature in case of impregnation of ZnPc into the pores of the calcined Ti-MCM-41 and TiO<sub>2</sub>@MCM-41.<sup>85a, 95</sup> The high dispersion of both components and their close contact enables a charge transfer from the titanium phthalocyanines to the titanium centers.

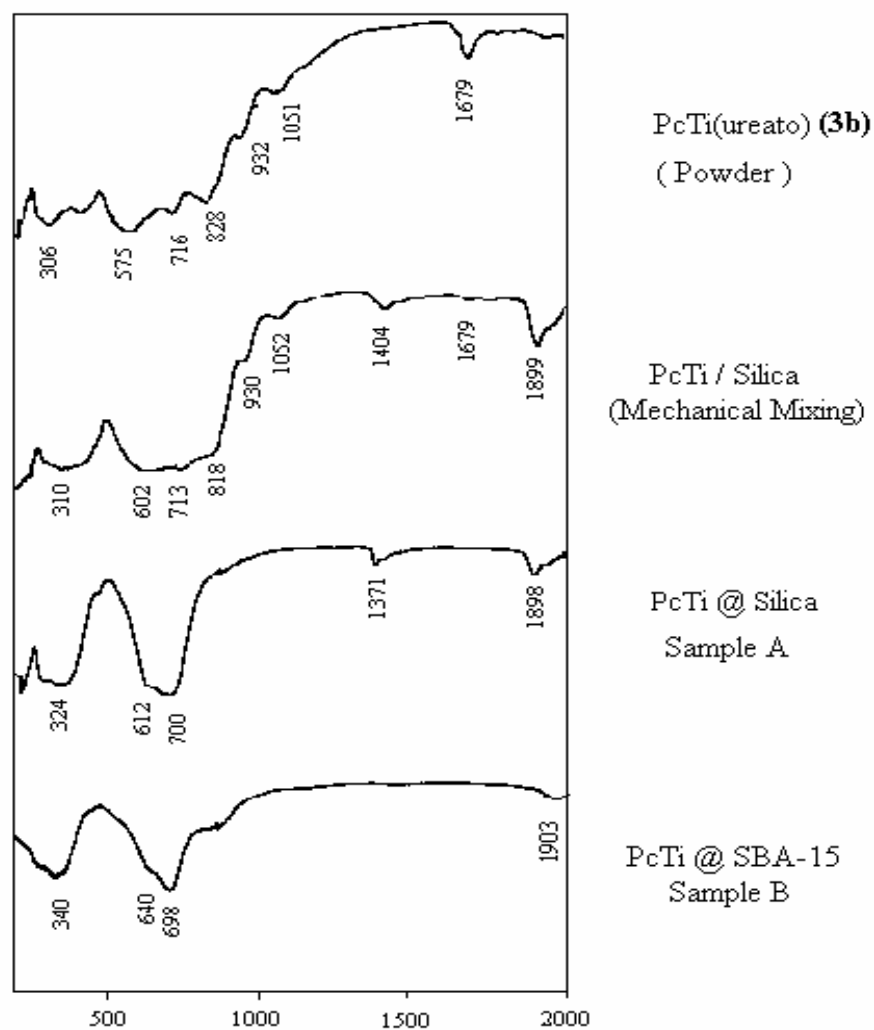


Figure 66: UV-VIS/NIR transmission spectra of **(3b)** and some prepared materials.

Table 12: UV/VIS Spectroscopic Data of (**3b**) and Pc-modified SBA-15 Materials

Material	$\lambda$ max (nm)				
PcTi(ureato) ( <b>3b</b> ) solid	306	575	716	828	932
PcTi(ureato)/SiO <sub>2</sub> (mechanical mixing)	310	602	713	818	930
PcTi(ureato)/SBA-15 (mechanical mixing)	329	586	702 ( <i>w</i> )	793	-----
PcTi(ureato)@SiO <sub>2</sub> (Sample A)	324	612	700	-----	-----
PcTi@SBA-15 (Sample B)	340	640	698	-----	-----
PcTi(ureato) ( <b>3b</b> ) Solution in ClN	347	629	697	-----	-----

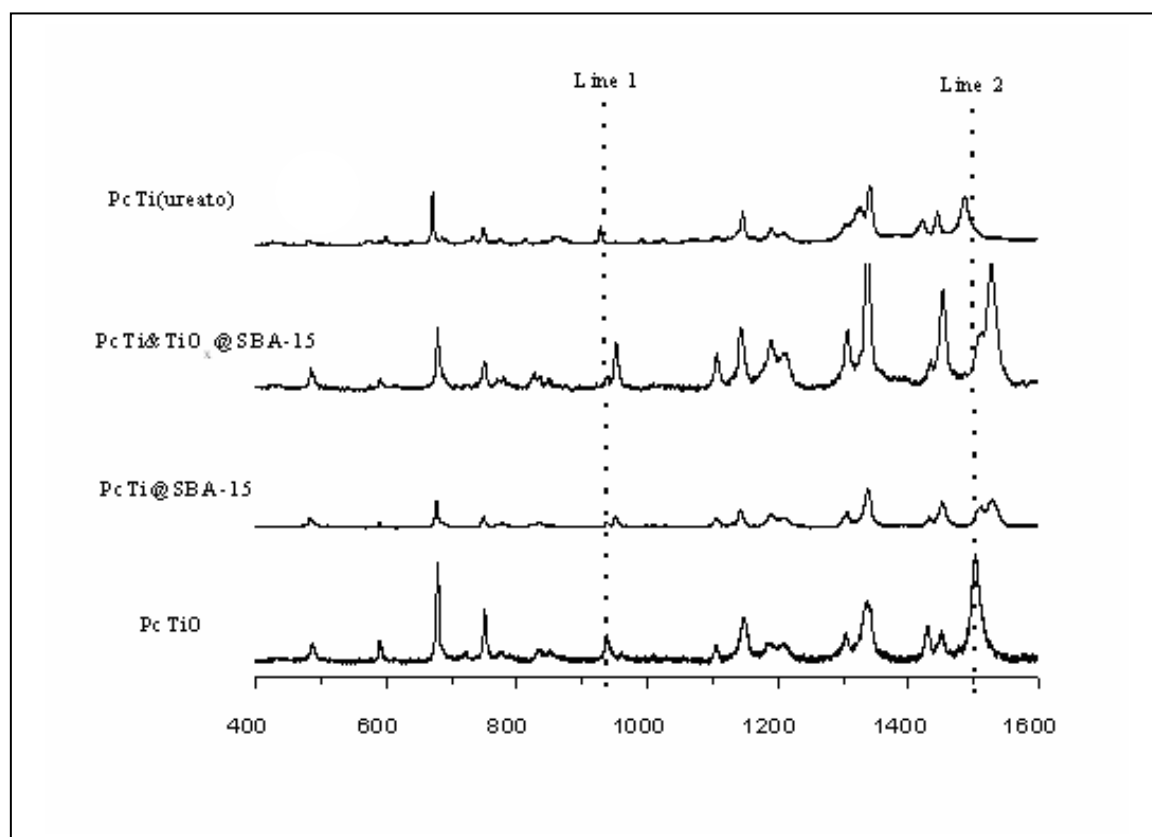
### Raman Spectra

Raman spectra (RS) of N,N'-di-4-tolylureato (phthalocyaninato) titanium (IV) (**3b**), PcTi@SBA-15, and PcTi&TiO<sub>x</sub>@SBA-15 at  $\lambda(\text{exc}) = 632$  nm are shown in (Figure 67) and the band positions are reported in (Table 13). (Line 1 and 2) in (Figure 67) are made for comparison of the most important band positions in the spectra of the prepared materials. There are remarkable differences in the spectra of (**3b**) and the two prepared materials due to the different compositions of each material. The appearance of the basic absorptions of the titanium-phthalocyanine dye emphasizes the inclusion of the dye in the impregnated materials. The absence of ( $\nu_{\text{Ti=O}}$  at  $965 \text{ cm}^{-1}$ )<sup>35</sup> rules out the assumption that [PcTiO] (**1**) may be formed and hydrogen bonded to the OH groups at the pores surface.



Table 13: Raman Bands of the prepared Materials

Material	Wavenumber (cm <sup>-1</sup> )
PcTi(ureato) ( <b>3b</b> )	1506, 1491, 1449, 1433, 1338, 1303, 1212, 1192, 1142, 1104, 1009, <u>971</u> , 938, 835, 751, 677, 591, 484, 308, 254, 235, 216, 188.
PcTi@SBA-15 (Sample B)	<u>1611</u> , <u>1529</u> , 1511, 1451, 1432, 1338, 1304, 1210, 1190, 1142, 1104, <u>952</u> , 937, 835, 778, 749, 677, 589, 483, 215.
PcTi&TiO <sub>x</sub> @SBA-15 (Sample D)	1528, 1514, 1453, 1433, 1338, 1307, 1210, 1190, 1143, 1105, <u>953</u> , 938, 837, 825, 780, 751, 679, 599, 485, 236, 217.

Figure 67: Raman spectra of PcTiO (**1**), PcTi(ureato) (**3b**), PcTi@SBA-15, and PcTi&TiO<sub>x</sub>@SBA-15.

**TEM investigations on the PcTi@SBA-15 material**

The PcTi@SBA-15 material obtained from interaction of **(3b)** with SBA-15 mesoporous silica was investigated by electron microscopy. Transmission electron microscopy (TEM) images were taken for the on-top view and a cross-section of the pore system (Figures 68a,b). The TEM micrographs show small and very distributed dark contrasts from the metal-containing dye anchored on the wall surface. No extended areas of accumulated dye molecules are found on the micrographs, which is in good accordance with the UV/VIS spectroscopic data indicating the presence of individual non-aggregated phthalocyanine molecules anchored to the pore walls. Consequently, the observed dark spots in the TEM micrographs are evenly spread over the pore walls but are not found in the pore volume.

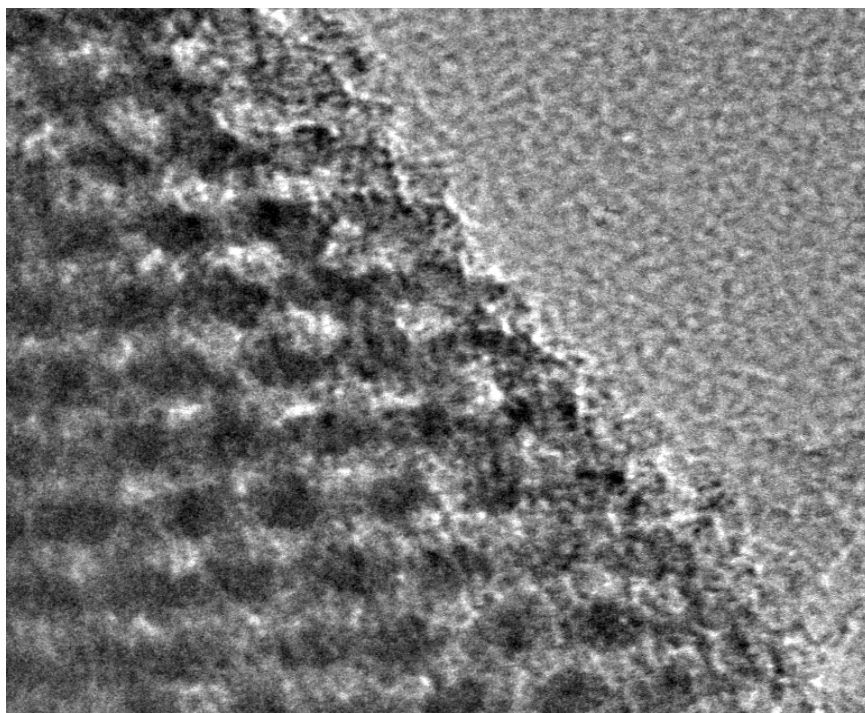


Figure 68a: On-top view of the hexagonal pore array with dark contrast showing the presence of titanium phthalocyanine in the pores.

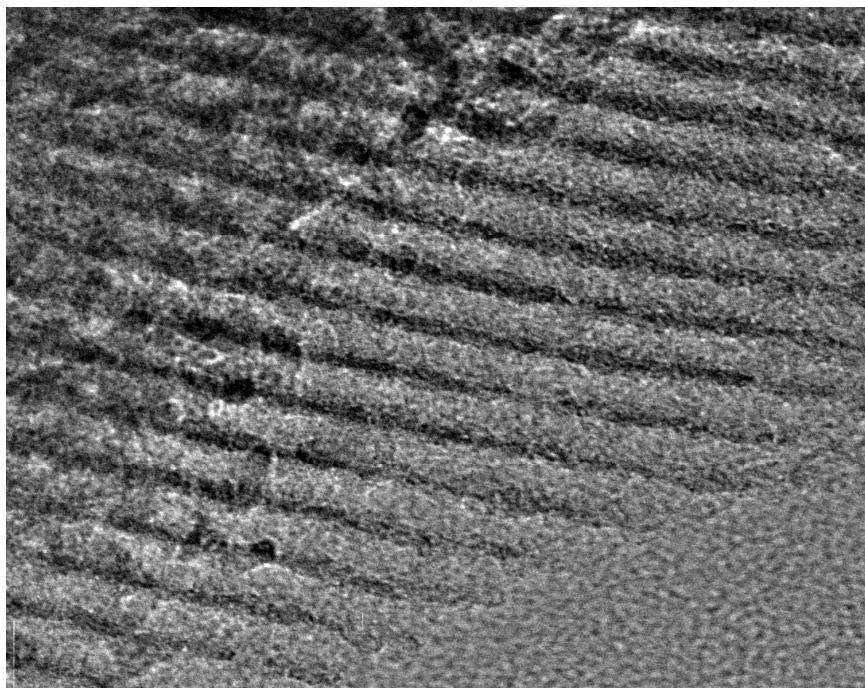
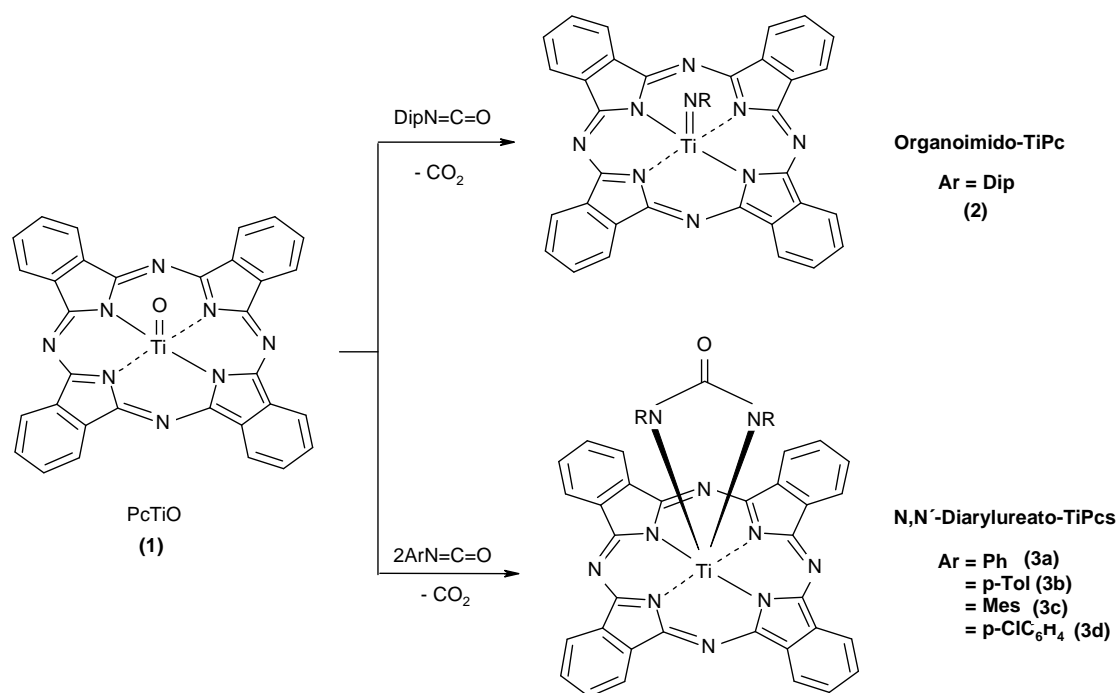


Figure 68b: Cross-section of the ordered pore system where dark spots originating from the dye can be seen on the pore wall system where dark spots originating from the dye can be seen on the pore wall.

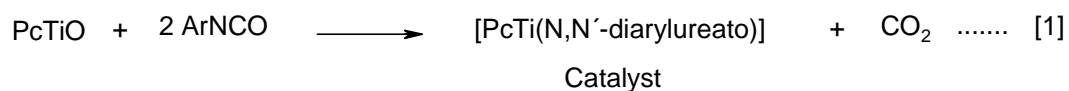
After studying the chemical and physical properties including the molecular arrangement of the prepared MPc molecules (**2**) and (**3b**), the (PcTi) dye were successfully grafted in the pores of SBA-15 and  $\text{TiO}_x\text{@SBA-15}$  materials. As indicated by the different analytical and spectroscopic techniques, the applied methods offer two advantageous: (i) the monomolecular dispersion of the dye molecules since no aggregation of the dye molecules was observed and (ii) the covalent fixation of the dye. Consequently, the applied methods can be further used to overcome the common problems in the dye/molecular sieve inclusion chemistry. The prepared materials were characterized using MS, AAS, Raman spectra, UV/VIS-NIR absorption spectra and TEM. The prepared materials are expected to retain the physical and optical properties of both silica and titanium phthalocyanines such as [PcTiO]. A lot of studies concerned this inclusion chemistry after the discovery of these mesoporous materials in the last decade. Systems combining inorganic host material and organic guest molecules processing interesting optical properties (PcTi) are expected to provide a source of new materials with challenging properties for several application such as optical application, photochemical hole burning<sup>137a-n</sup> and use as molecular sieve pigments.<sup>75</sup>

### 3. Summary

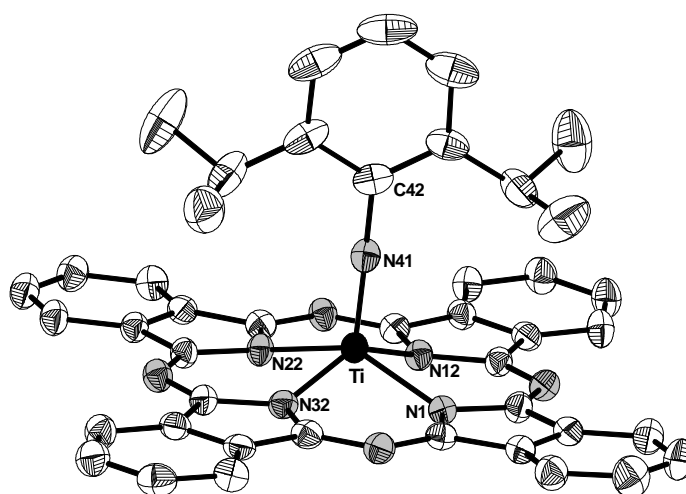
Ring substituted titanylphthalocyanines are green chemistry photoconducting materials in the xerographic process of photocopy machines or laser printers that have replaced selenium as photoconducting layer. Furthermore  $[(R_xPc)Ti=O]$  is the laser pigment of CD-ROM disc technology. While organic transformations of the ring-substituents are the focus of most recent and current research efforts, the axial transformation at the titanyl functionality were largely unexplored. The aim of this work was to develop the chemistry of titanylphthalocyanine. We investigated the typical metathetical reaction patterns of  $[PcTiO]$  (**1**) with arylisocyanates aiming at the synthesis of its isoelectronic compounds  $(PcTiX ; X = S, Se, NR, \text{etc.})$ . This metathetical transformation was found to depend largely on the size of the aryl group. In the case of sterically demanding 2,6-diisopropylphenyl isocyanate only one addition cycloreversion step seems to be possible and the imido complex  $[PcTi=NDip]$  (**2**) is the final product. Any further addition of a second isocyanate molecule to the  $[Ti=NAr]$  functionality is hindered because of the high steric occupation caused by the two isopropyl groups. For small groups such as  $R = \text{phenyl}$ , the imido complex could not be isolated in an analytically pure form since it reacts readily with a second equivalent of  $ArNCO$  in a  $[2+2]$  cycloaddition forming the  $N,N'$ -diaryllureato-TiPc (**3a-d**). In these cases, the corresponding diarylcarbodiimides were observed as white byproducts. Whereas the carbodiimide was not observed in the reaction of (**1**) with 2,6-diisopropylphenyl isocyanate.



The reaction of **(1)** with the arylisocyanates containing small aryl groups may be applied in the catalytic metathesis of arylisocyanates into diarylcarbodiimides and carbon dioxide.

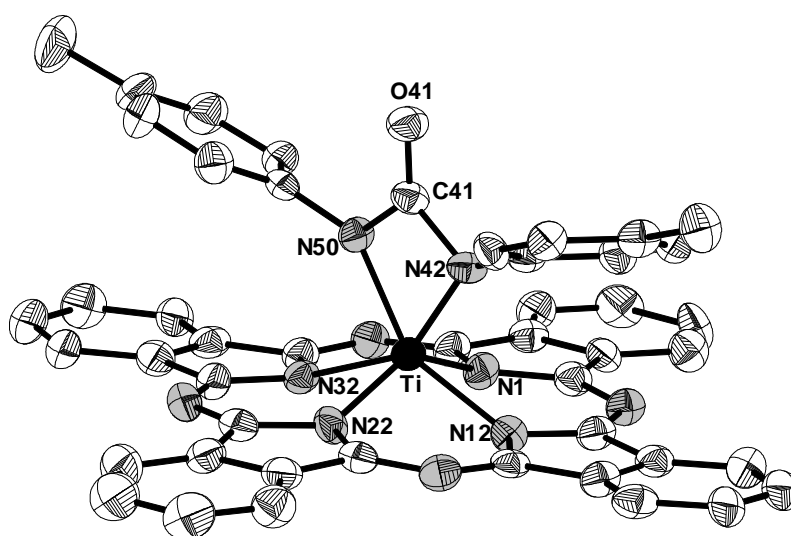


Compound **(2)** crystallizes in the centrosymmetric space group  $P2_1/n$  with 4 molecules per the unit cell. The titanium is displaced above the mean plane of the four isoindoline nitrogen atoms toward the imido ligand by 0.594(1) Å. Due to  $\pi$ - $\pi$  interaction of the basal faces of the pyramidal molecular structure the crystal lattice consists in a close packing of face-to-face dimers. The two molecules of a dimer are related with respect to each other by a crystallographic inversion centre.



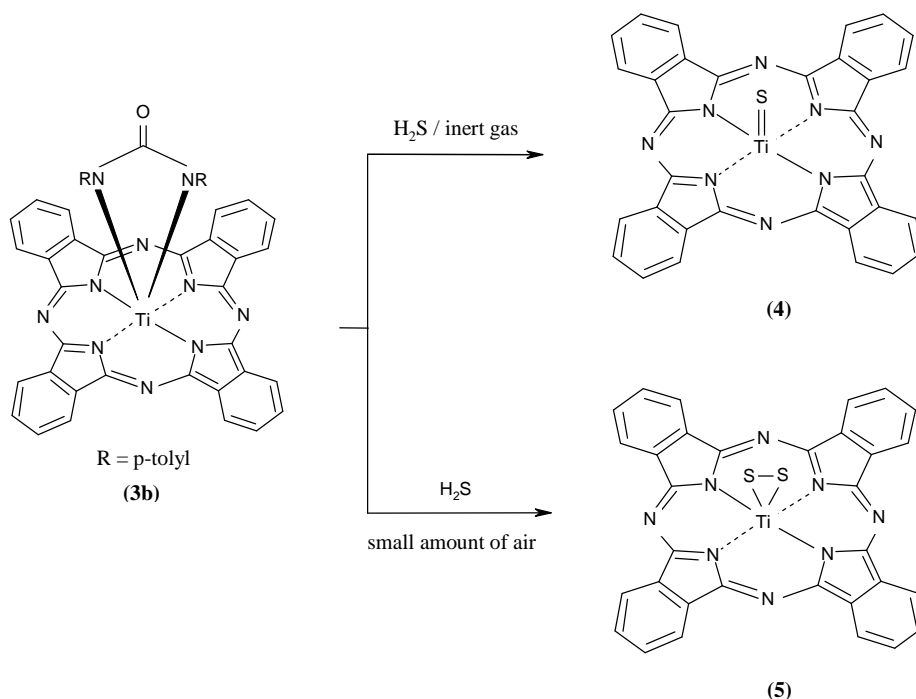
The molecular structure of  $[\text{PcTi}=\text{NDip}]$  (**2**).

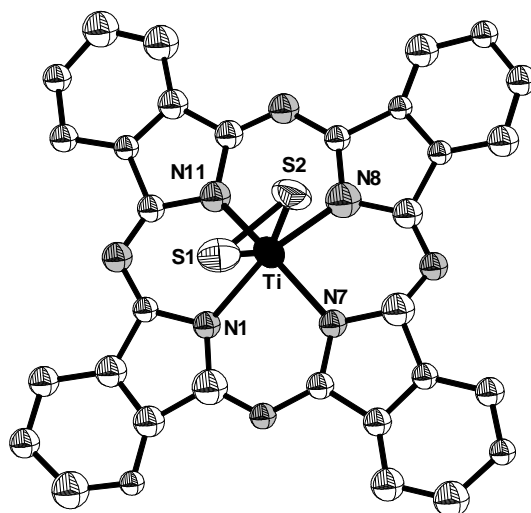
The compound **(3a)** crystallizes in the centrosymmetric space group  $P2_1/n$  with 4 molecules per unit cell, whereas the compound **(3b)** crystallizes in the centrosymmetric space group  $P\bar{1}$  with two molecules per unit cell. The titanium atom is displaced from the mean plane of the four isoindoline nitrogen atoms toward the ureato ligand by 0.791(1)Å in **(3a)** and 0.763(6)Å in **(3b)**.



The molecular structure of **(3b)**.

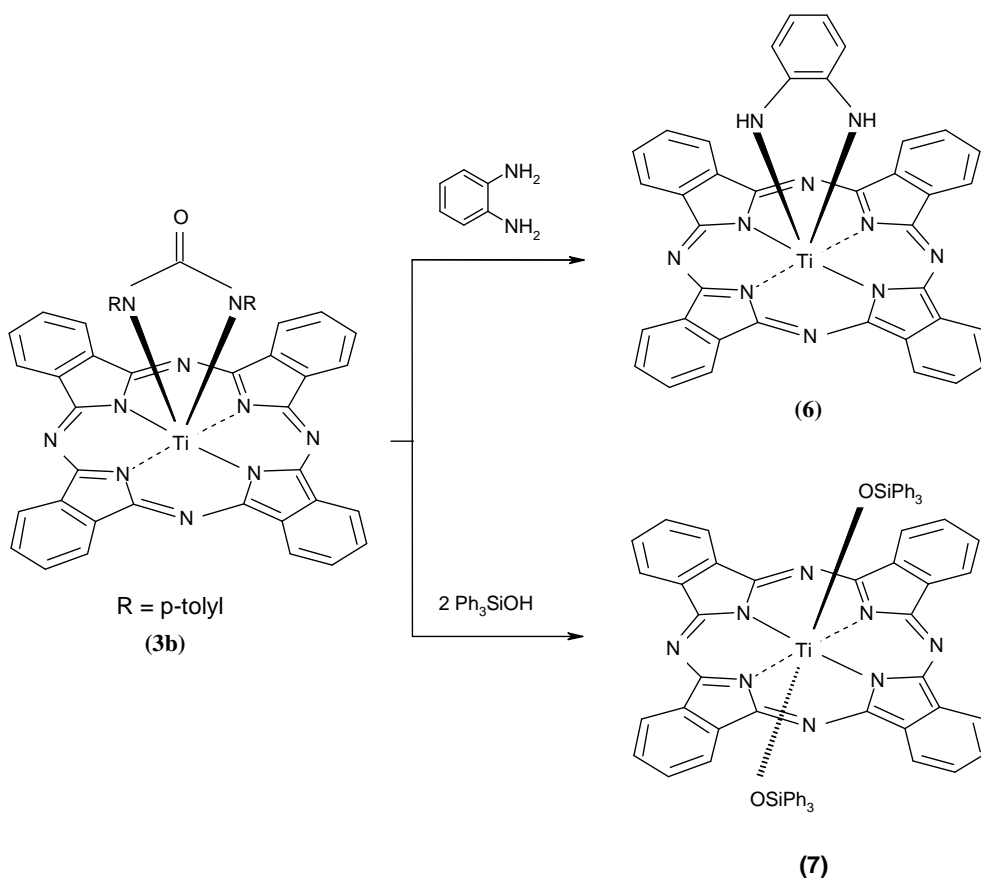
The reaction of *N,N'*-di-4-tolylureato (phthalocyaninato) titanium (IV) **(3b)**, dissolved in  $\text{ClN}$ , with  $\text{H}_2\text{S}$  gas was found to be largely affected by presence of air. When the reaction is carried out under inert atmosphere the compound  $[\text{PcTi}=\text{S}]$  **(4)** is formed in quantitative yield. However, in presence of air the disulfido compound  $[\text{PcTiS}_2]$  **(5)** is the main product. The reaction mechanism of formation of  $[\text{PcTiS}_2]$  involved the oxidation of the intermediate  $[\text{PcTi}(\text{SH})_2]$  with the oxygen of the air. The crystal structure of **(5)** revealed that the  $\text{S}_2$  group is  $\eta^2$  “side-on” bonded to the titanium atom in the axial position.

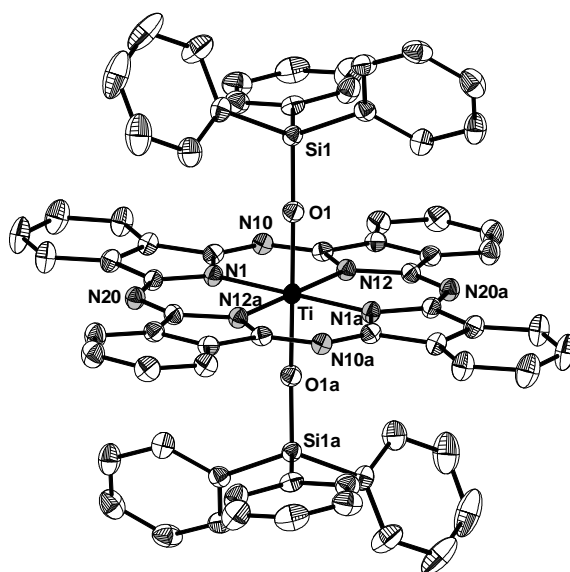




The molecular structure of  $[\text{PcTi}(\eta^2\text{-S}_2)]$  (**5**).

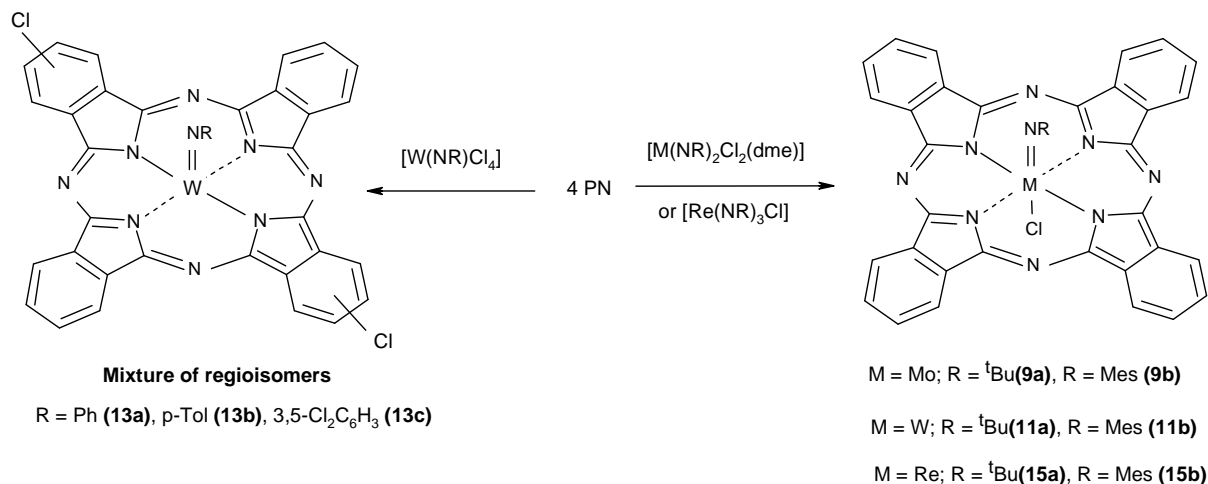
Compound (**3b**) was found to react with 1,2-phenylenediamine forming  $[\text{PcTi}\{(\text{NH})_2\text{C}_6\text{H}_3\}]$  (**6**). Furthermore (**3b**) was found to react with  $\text{Ph}_3\text{SiOH}$  forming  $[\text{PcTi}(\text{OSiPh}_3)_2]$  (**7**). The reaction proceeds via a *trans* addition of two of triphenylsiloxy ligands on the titanium atom.





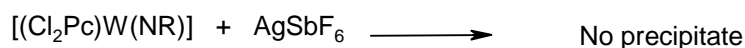
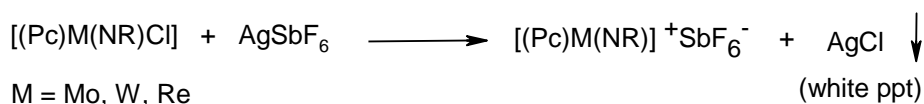
The molecule structure of *trans*-[PcTi{(NH)<sub>2</sub>C<sub>6</sub>H<sub>3</sub>}] (**7**).

Novel organoimido compounds of the general formula [PcM(NR)Cl] (M = Mo, W, Re; R = <sup>t</sup>Bu, Mes) (**9a,b**; **11a,b**; **15a,b**) were prepared using the typical fusion reaction of phthalonitrile (PN) in the presence of a proper metal complex [M(NR)<sub>2</sub>Cl<sub>2</sub>(dme)], M = Mo, W or [Re(NR)<sub>3</sub>Cl], respectively, as imido ligand precursor. The products have been always the chloro (imido) metalphthalocyanines. On the other hand, when phthalonitrile was heated with other tungsten imido complexes [W(NR)Cl<sub>4</sub>]; R = Ph, *p*-Tol, 3,5-Cl<sub>2</sub>C<sub>6</sub>H<sub>3</sub>, the products have been always the corresponding imido tungsten phthalocyanines with two chlorine atoms bonded to the aromatic rings of the phthalocyanine [(Cl<sub>2</sub>Pc)W(NR)] (**13a-c**). This can be attributed to the fact that the compounds [W(NR)Cl<sub>4</sub>] as d<sup>0</sup> species are strong chlorination reagents and are capable for chlorination of the aromatic rings. Ring chlorination results in formation of different regioisomers.

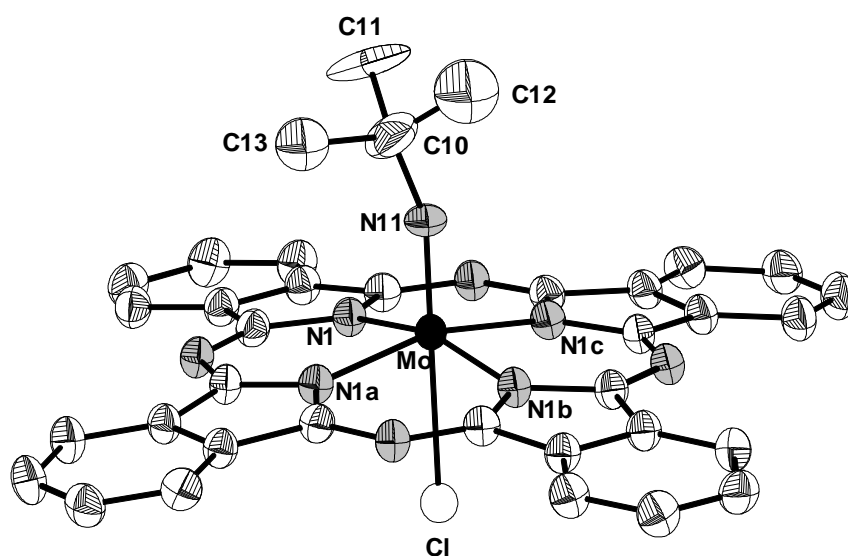




The compounds **(9a,b)**, **(11a,b)** and **(15a,b)** form a white precipitate of AgCl when refluxed with AgSbF<sub>6</sub> in dichloromethane and consequently we suggested that the chlorine atom is bonded to the central metal atoms. On the other side, no precipitate of AgCl was observed when the complexes **(13a-c)** were refluxed with AgSbF<sub>6</sub> in dichloromethane for several hours and therefore the two chlorine atoms are supposed to be bonded to aromatic carbon atoms.

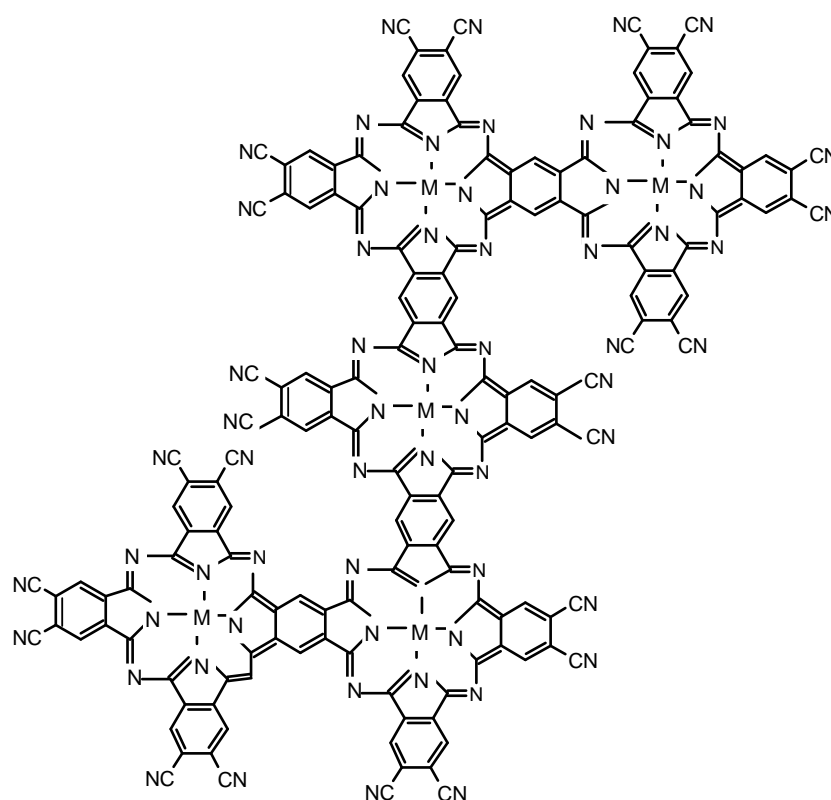


The compound **(9a)** crystallizes in the centrosymmetric space group P4/n with 4 molecules per unit cell. The molecule consists of a six-coordinate molybdenum atom surrounded by four equatorial isoindoline rings of the Pc molecule, whereas the chlorine atom and the imido group are axially in a *trans* configuration with respect to the central metal. The Mo atom is displaced from the mean N<sub>4</sub> plane toward the imido ligand by 0.305(0) Å.



The molecular structure of [PcMo(N<sup>t</sup>Bu)Cl] (**9a**).

Reaction of 1,2,4,5-tetracyanobenzene (TCB) with  $\text{Ti}(\text{OBU})_4$  under certain conditions e.g. molar ratio 2:1 and high temperature, was found to include the four cyano groups of TCB in a cyclotetramerization process producing a higher molecular weight phthalocyanine including the pentamer,  $\text{C}_{160}\text{H}_8\text{N}_{64}\text{O}_5\text{Ti}_5$ , molecular weight = 3145.59. When this oligomer was refluxed with 2,6-diisopropyl-phenylisocyanate in DMF, the corresponding oligomer was isolated and identified to contain the imido ligand. Similarly, the reaction of TCB with  $[\text{Mo}(\text{NMe}_s)_2\text{Cl}_2(\text{dme})]$  produces a phthalocyanine pentamer having the  $[\text{Mo}(\text{NMe}_s)\text{Cl}]$  functionality. The GPC measurements of these DMF soluble oligomers showed unimodal curves and the molecular weights obtained with respect to polystyrene standards matched well with the calculated molecular weights of the three oligomers. On the basis of the spectroscopic data, it can not be excluded that the connectivity of the five PcM building blocks differs from the idealized symmetrical structure displayed below.



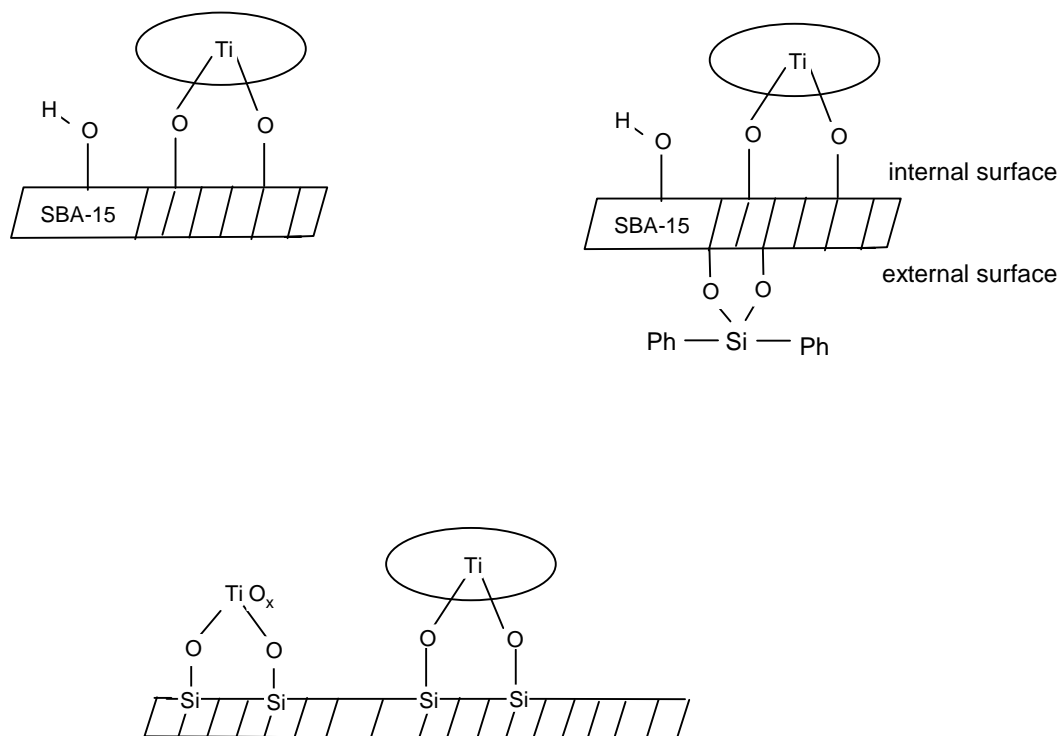
$\text{M}=[\text{TiO}]$  (**16**),  $\text{M}=[\text{Mo}(\text{NMe}_s)\text{Cl}]$  (**17**),  $\text{M}=[\text{Ti}(\text{NDip})]$  (**18**).

The time-resolved photoluminescence measurements of compounds  $[\text{PcTiO}]$  (**1**) and (**3b**) and were carried out s aiming to study the effect of replacing the axial oxo group with the ureato group in the optical properties. The observed emission bands in case of both

investigated phthalocyanines are caused by the basic structure of the phthalocyanine molecules. Otherwise the relative strength or the energetic situation of the individual signatures would have to change by variation of the axial ligands. Both samples show unusual time-decay behavior. The life time values (4-6 ns) are comparable with the values of the time-resolved fluorescence spectra of other phthalocyanines and confirm the potential of the phthalocyanines also for medical and biophysical applications, e.g. in imaging procedures, with which living organisms are examined with the help of the fluorescence spectroscopy on nanosecond time scales and as optical limiting materials.

Metal phthalocyanine modified silicas are important materials in many industrial applications. Firstly, we prepared the  $\text{TiO}_x\text{@SBA-15}$  material by impregnating titanium species in the pores of SBA-15 using TBOT as a precursor of titanium species. This method resulted in a Ti-loading of up to 2.66 wt.% titanium content. We prepared the  $\text{PcTi@SBA-15}$  and  $\text{PcTi\&TiO}_x\text{@SBA-15}$  materials by impregnation of the Pc dye selectively on the pores of SBA-15 templates depending on three factors: Firstly, the large pore size, which offers the possibility to tether sizeable and complex catalytically reactive sites within the silica framework, secondly the protolytically cleaved perfect ureato leaving group in compound **(3b)** and finally the passivation of the external surface of the templates using  $\text{Ph}_2\text{SiCl}_2$  prior to the impregnation process. The ureato ligand on the titanium atom of **(3b)** was found to react with the silanol groups of the walls of the host material. Consequently, the TiPc dye is covalently bonded to the walls of the host material SBA-15 or  $\text{TiO}_x\text{@SBA-15}$  as long as no water may induce hydrolysis of the Si-O-Ti linkage. The UV/VIS spectra of the prepared materials are in accord with a monomeric grafting of the dye in the silica templates. The TEM micrographs show small and very distributed dark contrasts from the metal-containing dye anchored on the wall surface.

No extended areas of accumulated dye molecules are found on the micrographs, which is in good accordance with the UV/VIS spectroscopic data indicating the presence of individual non-aggregated phthalocyanine molecules anchored to the pore walls. Consequently, the observed dark spots in the TEM micrographs are evenly spread over the pore walls but are not found in the pore volume.



Covalent bonding of titanium phthalocyanine onto different SBA-15 materials  
(The ring denotes to phthalocyanine macrocycle).

## 4. Experimental Work

### 4.1 Materials and Methods

- All transfer and manipulations of reagents and products were performed under an inert atmosphere of nitrogen using a vacuum atmosphere glovebox (Type MB 150 BG.II or LABMASTER 130 Braun) equipped with a gas-purifying system (< 1ppm oxygen) or on a vacuum line using standard Schlenk techniques.

- All solvents were purified and rigorously dried according to the standard techniques and stored under dry argon over 3Å or 4Å molecular sieves. Chlorine containing solvents were stored in dark bottles. Chloronaphthalene was purchased from *Acros* as a mixture of , 90% of 1-chloronaphthalene and 10% of 2-chloronaphthalene isomers, and was dried by vacuum distillation over CaH<sub>2</sub>.

- 1,2- Dicyanobenzene (PN) and 1,2,4,5- tetracyanobenzene (TCB) were sublimated under reduced pressure. The liquid arylisocyanates were distilled under reduced pressure and kept under nitrogen at 4°C. Solid arylisocyanates were crystallized and kept under nitrogen. The other organic reagents were purchased as pure grade from *Arcos* with no need for further purification. Micro filters of pore size 0.45µ were purchased from *Roth*, Germany.

- SBA-15 template was prepared according to the procedure reported in the literature having pores diameter of 200 nm.

- The following complexes were prepared according to the literature (Table 14):

Table 14: References for the Synthesis of the Complexes Used in this Work.

Compound	Ref.	Compound	Ref.
PcTiO ( <b>1</b> )	35	[W(NR) <sub>2</sub> Cl <sub>2</sub> (dme)] ( <b>10a,b</b> )	145
[Mo(N <sup>t</sup> Bu) <sub>2</sub> Cl <sub>2</sub> (dme)] ( <b>8a</b> )	143	[W(NR)Cl <sub>4</sub> ] ( <b>12a-c</b> )	144
[Mo(NMes) <sub>2</sub> Cl <sub>2</sub> (dme)] ( <b>8b</b> )	145	[Re(NR) <sub>3</sub> Cl] ( <b>14a,b</b> )	146

## **4.2 Techniques of Characterization**

For characterization and structure elucidation of the prepared compounds the following techniques and instruments were utilized:

### **UV/VIS Absorption Measurements**

UV/VIS measurements were carried out for solutions of the metal phthalocyanines in chloroform, chloronaphthalene or DMF. The spectra were recorded on UV-1601Pc, UV/VIS Spectrophotometer (Schimadzu, Japan). The following abbreviations were used to identify the intensities of the peaks: s (strong), m (medium), w (weak), sh (shoulder).

The extinction coefficient ( $\epsilon$ ) was calculated according to the following equation:

$$\epsilon = D/C.A$$

$\epsilon$  : extinction coefficient ( $\text{cm}^{-1} \text{M}^{-1}$ ).

D: The maximum absorption (without units).

C: The molar concentration of the sample (M).

A: The cross section of the cell ( $\text{cm}^{-1}$ ).

### **UV/VIS**

UV/VIS NIR spectroscopic measurements of the mesoporous materials were recorded on a Hitachi-U 310 spectrophotometer equipped with a diffuse reflectance attachment.

### **FT-IR**

IR spectra were recorded on a Bruker IFS 588 spectrometer using KBr pellets. The following abbreviations were used to identify the intensities of the peaks: vs (very strong), s (strong), m (medium), w (weak), vw (very weak), br (broad), and Sh (shoulder).  $\tilde{\nu}$  = wave-number ( $\text{cm}^{-1}$ );  $\nu$  = stretching vibration ( $\text{Hz}, \text{sec}^{-1}$ ).

### **Mass Spectra (MS)**

EI-MS (Electron Impact Mass Spectra): CH7 Mass-spectrometer, Varian MAT (450°C,  $10^{-5}$  Tor, 70 eV). ESI-MS (Electron Spray Ionization): Finnigan-Mat TSQ 700. MALDI –TOF (Matrix Associated Laser Desorption (Time Of Flight): Bruker Flex III, without addition of an energy transfer matrix. The  $m/z$  values refer to the highest peak of the isotopic pattern ratio according to the natural abundance of the isotopes.

### **Elemental Analysis (EA)**

Analysis of C, H and N elements was carried out using an Elementar, Vario EL. Combustion of the samples was carried out at 950°C.

### **Microanalysis**

Analysis of chlorine was carried out using 636 Titro-processor (Mitrohm). Analysis of sulfur was carried out using 662 Photometer (Mitrohm).

### **Atom Absorption Spectrometry (AAS)**

Determination of the metals (Ti, Mo, W and Re) was carried out using a Perkin Elmer Atom absorption spectrometer 5000. To prepare the samples, the Pc complexes were dissolved in conc. H<sub>2</sub>SO<sub>4</sub>.

### **Nuclear Magnetic Resonance (NMR)**

The <sup>1</sup>H-NMR spectra were recorded on <sup>1</sup>H-NMR: Bruker, AMX 500 (500.1 MHz). The solvent used (C<sub>6</sub>D<sub>5</sub>Br) was calibrated against TMS as standard and showed three signals at 7.2275, 7.2854, 7.5207 ppm.

### **Electron Spin Resonance (ESR)**

The ESR spectra were recorded on a Bruker ESP 300 (X band) at 9 GHz. ESR data fit and simulation program: SIMESR (Version 1.1).

### **Fluorescence Measurements**

The fluorescence spectra were recorded on a Shimadzu Spectrophotometer RF-1502. Presentation of the data was achieved with (Origin 6.0). Measurements were carried out for (10<sup>-5</sup> M) solutions in chloronaphthalene.

### **Raman Spectra (RS)**

Raman spectra were recorded on a Jobin Yvon Labram HOUR 800, Light energy 25mW, Excitation line 632 and 817 nm. The following filters were used: D1: for compounds (3a), (3b) and (3c); D0.6: for compounds (1) and (2); D2 : for compound (3d).

### **Thermal Gravimetric Analysis (TGA)**

TGA measurements were carried out using a TGA/SDTA 851, Mettler Toledo. The program of evaluation was STARe from Mettler. The heating range was from 25°C to 800°C, heating rate was 10°C/min. and slower rate from 250-400 °C (1°C/min.), weight of the sample was from 8-20 mg. The measurements were carried out under N<sub>2</sub>-atmosphere. Presentation of the data was carried out with Origin 6.0 software.

### **Differential Scanning Calorimetry (DSC)**

DSC measurements were carried out using a DSC 821 designed by Mettler. Weight of the sample was from 7-12 mg in an aluminum container. Cyclic temperature program with heating and cooling rate 10 °C/min was used. The measurements were carried out under N<sub>2</sub>-atmosphere. Program of evaluation was STARe from Mettler. Presentation of the data was carried out with (Origin 6.0) software.

### **Gel Permeation Chromatography (GPC)**

GPC measurements were carried out using a GPC unit consisting of HPLC-pump and UV/VIS spectrophotometer and knauer refractometer. The software used was derived from PSS win scientific GPC version 4.01. The columns were obtained from PSS, SDV with particle size of 10μ, and pore size of 10<sup>3</sup>, 10<sup>4</sup>, and 10<sup>6</sup> Å. Length of the columns was 60 cm.

### **Crystallographic Measurements**

We carried out about 60 attempts in the laboratory to isolate single crystals of the prepared MPcs under hard conditions, such as poor solubility and moisture sensitivity of the compounds, and only six were suitable for measurements. The crystal structure measurements and data collection were carried out by the members of the Crystal Structure Laboratory, Philipps-Universität Marburg: Prof. Dr. Massa for compound (5), Dr. K. Harms and Mrs. Geiseler for the other compounds. An IPDS-II (Stoe) diffractometer was used. Afterwards we used the program *Diamond 2.1e* to draw the molecular structures. Space groups are given according to “International Tables for Crystallography: Volume A”.

### **TEM**

High Resolution Transmission Electronmicroscope JEM-3010 (Jeol, Japan) with LaB<sub>6</sub>-cathode, double kipp- and double kipp-Kryo (LN<sub>2</sub>)-sample holder, integrated 2K x 2K CCD-camera from Gatan, USA. Point Resolution: 0.17 nm Acc. Voltage: 100-300 kV, magnification 60-1.500.000 X, Emitter: LaB<sub>6</sub>





### Growth of Single Crystals

Blue-violet needles of [PcTi=NDip] (**2**) were grown by controlled cooling of its solution in chloronaphthalene from 180°C to room temperature within 6 hours. Beautiful crystals could be also obtained by controlled cooling of the reaction mixture when the reaction is carried out in an excess of the isocyanate without solvent.

Table 15: X-ray Data Collection of [PcTi=NDip] (**2**)

Empirical formula	C <sub>44</sub> H <sub>33</sub> N <sub>9</sub> Ti
Molecular weight	735.69
Color; Habit	blue needle
Crystal size (mm <sup>3</sup> )	0.30x0.06x0.03
Crystal system	monoclinic
Space group	P2 <sub>1</sub> /n
Cell dimensions:	
a (Å)	10.9727 (13)
b (Å)	17.148 (3)
c (Å)	19.532 (2)
α (deg)	90.00
β (deg)	104.518(9)
γ (deg)	90.00
Cell formula units (Z)	4
Volume (Å <sup>3</sup> )	3557.9(9)
Temperature (K)	193
Calculated density (Mg/m <sup>3</sup> )	1.373

### 4.3.2 Preparation of N, N'-Diarylureato (phthalocyaninato) titanium (IV) (3a-d)

A mixture of [PcTiO] (**1**) (300 mg, 0.52 mmol) and the corresponding arylisocyanate (ArNCO: Ar = Ph; 4-tolyl; 2,4,6-Me<sub>3</sub>C<sub>6</sub>H<sub>2</sub> or 4-ClC<sub>6</sub>H<sub>4</sub>) (10.4 mmol, 20 fold excess) in 20 ml of chloronaphthalene was heated at 180°C for 6 hours. The color turns dark green. After

cooling, the product was precipitated by addition of 20 ml hexane. The precipitate was collected on a glass frit and washed by successive extractions from refluxing MeCN (10x50ml), refluxing toluene (10x50ml) and finally washed with pentane. The products (**3a-d**) were dried at 120°C/10<sup>-3</sup> mbar for 3 hours. The same products were obtained when the reactions, in case of liquid arylisocyanates (phenyl- and tolylisocyanates), were carried out in excess of the isocyanate without solvent. White substances, identified as the corresponding N, N'-diarylcarbodiimides (ArN=C=NAr), were detected and could be removed from the ureato-TiPcs by successive extractions from refluxing MeCN.

**Color:** generally blue-green solids      **Yield:** (~ 75%)

**Solubility:** ClN, chlorobenzene, DMF and partially in CHCl<sub>3</sub> and THF.

Table 16: Mass Spectroscopy and Analytical Data of the Ureato-TiPcs (**3a-d**)

Compound	Molecular formula (molecular weight)	m/z (found)	Elemental analysis				
				%C	%H	%N	%Ti
<b>(3a)</b>	C <sub>45</sub> H <sub>26</sub> N <sub>10</sub> OTi (770.6)	770 <sup>(M)</sup>	calcd.	70.13	3.40	18.17	6.21
		651.8 <sup>(E)</sup>	found	69.57	3.59	17.97	5.46
<b>(3b)</b>	C <sub>47</sub> H <sub>30</sub> N <sub>10</sub> OTi (798.7)	798 <sup>(M)</sup>	calcd.	70.68	3.78	17.54	5.99
		665 <sup>(E)</sup>	found	70.56	3.85	17.36	5.84
<b>(3c)</b>	C <sub>51</sub> H <sub>38</sub> N <sub>10</sub> OTi (854,8)	855 <sup>(M)</sup>	calcd.	71.66	4.48	16.39	5.60
		693 <sup>(E)</sup>	found	71.24	4.52	16.26	5.66
<b>(3d)</b>	C <sub>45</sub> H <sub>24</sub> Cl <sub>2</sub> N <sub>10</sub> O Ti (839,5)	685 <sup>(E)</sup>	calcd.	64.38	2.88	16.68	5.70
			found	64.21	3.06	16.69	5.15

(E): The fragments of the corresponding Imido-TiPc [Pc=NAr]<sup>+</sup> detected by both EI- and MALDI-TOF MS.

(M): The fragments of the ureato-TiPc, which could be detected only by MALDI-TOF MS.

Table 17: UV/VIS Data of [PcTiO] (**1**) and Ureato-TiPcs (**3a-d**) (in CHCl<sub>3</sub>, 2x10<sup>-7</sup> M)

Compound	λ max (nm)			
	Q <sub>0,0</sub>	Q <sub>1,0</sub>	Q <sub>2,0</sub>	B
[PcTiO] ( <b>1</b> )	698.5 (s)	667.0 (sh)	628.5 (m)	341.0 (m)
<b>(3a)</b>	699.0 (s)	665.5 (sh)	628.5 (m)	343.0 (m)
<b>(3b)</b>	698.5 (s)	665.5 (sh)	629.0 (m)	345.0 (m)
<b>(3c)</b>	700.5 (s)	---	627.5 (m)	343.0 (m)
<b>(3d)</b>	698.0 (s)	666.6 (sh)	628.0 (m)	342.0 (m)

- Extinction coefficient (ε) (Q<sub>0,0</sub>) of compound (**3b**) in CHCl<sub>3</sub> = 34.9x10<sup>-9</sup> cm<sup>-1</sup> M<sup>-1</sup>

Table 18: IR Data of [PcTiO] (**1**) and Ureato-TiPcs (**3a-d**)

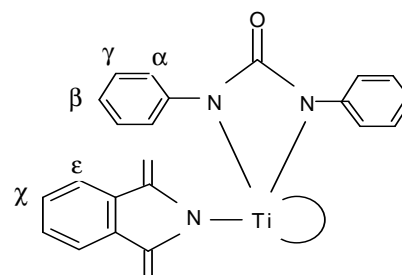
Compound	IR (KBr) $\bar{\nu}$ (cm <sup>-1</sup> )
PcTiO ( <b>1</b> )	1608(w), 1488(m), 1476(m), 1412(m), 1331(vs), 1285(m), 1162(w), 1118(s), 1068(vs), 962 (m)[v <sub>Ti=O</sub> ], 892(m), 801(m), 751(w), 730(w).
<b>(3a)</b>	<u>1690</u> (w) [v <sub>C=O</sub> ], <u>1666</u> (m), 1584(m), <u>1537</u> (w), 1488(m), <u>1450</u> (m), 1414(w), 1332(s), 1287(m), 1162(w), 1118(s), 1071(vs), <u>894</u> (w), <u>751</u> (s), <u>731</u> (vs).
<b>(3b)</b>	<u>1683</u> (m) [v <sub>C=O</sub> ], <u>1589</u> (m), <u>1503</u> (m), <u>1489</u> (m), 1414(w), 1332(vs), 1286(m), 1160(m), 1118(vs), 1069(vs), 970(s), 894(s), <u>775</u> (s), <u>751</u> (s), <u>729</u> (vs).
<b>(3c)</b>	<u>1684</u> (s)[v <sub>C=O</sub> ], <u>1502</u> (w), 1469(w), <u>1417</u> (w), 1333(s), 1287(w), <u>1259</u> (m), 1161(w), 1117(m), 1082(w), <u>1069</u> (w), 1057(m), <u>1005</u> (w), 894(w), <u>829</u> (w), <u>749</u> (m), <u>734</u> (vs).
<b>(3d)</b>	<u>1685</u> (s)[v <sub>C=O</sub> ], <u>1607</u> (w), 1539(w), 1486(s), <u>1417</u> (w), <u>1400</u> (w), 1332(s), 1286(s), 1161(m), 1118(s), 1072(s), <u>1010</u> (m), 895(m), <u>830</u> (m), <u>750</u> (m), <u>731</u> (vs).

(Underlined values in the IR data are new and not found in the spectra of PcH<sub>2</sub> or PcTiO).

<sup>1</sup>H-NMR (500 MHz, C<sub>6</sub>D<sub>5</sub>Br, 373 K) (ppm):

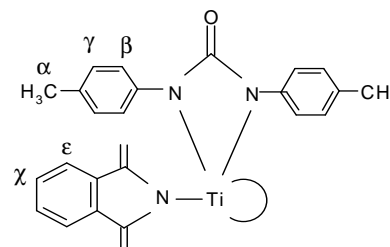
Compound (**3a**)

δ = 4.97-5.05 [m, 4 H(α)], 6.44-6.50 [m, 2H(β)], 6.52-6.60 [m, 4H(γ)], 8.21-8.32 [m, 8H(χ)], 9.50-9.60 [m, 8H(ε)].



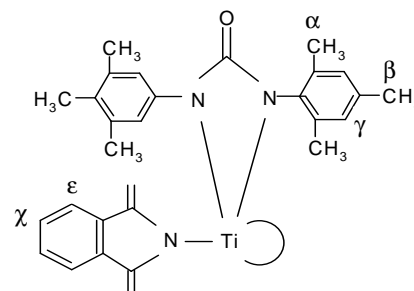
Compound (**3b**)

δ = 1.97-2.03 [s, 6H(α)], 4.95-5.03 [m, 4H(β)], 6.32-6.44 [m, 4H(γ)], 8.25-8.35 [m, 8H(χ)], 9.64-9.72 [m, 8H(ε)].



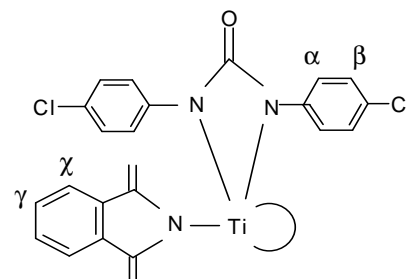
Compound (**3c**)

δ = 0.74-0.79 [s, 12H(α)], 2.03-2.07 [s, 6H(β)], 6.30 [m, 4H(γ)], 8.28-8.36 [m, 8H(χ)], 9.67-9.73 [m, 8H(ε)].



Compound (**3d**)

δ = 5.12-5.19 [m, 4 H(α)], 6.48-6.60 [m, 4H(γ)], 8.26-8.36 [m, 8H(χ)], 9.46-9.55 [m, 8H(ε)].



### Growth of Single Crystals

- Single crystals of N, N'-diphenylureato (phthalocyaninato) titanium (IV) (**3a**) were grown directly from the reaction mixture of [PcTiO] with excess phenylisocyanate without solvents.
- Dark blue prism shaped crystals, suitable for the crystallographic structure determinations of N,N'-di-4-tolylureato (phthalocyaninato) titanium (IV) (**3b**), were obtained by controlled cooling of its solution in chlorobenzene from 130°C to room temperature within 3 hours.

Table 19: Comparison of the Elemental Cells of (3a) and (3b)

<b>Crystal data</b>		
Molecular formula	C <sub>45</sub> H <sub>26</sub> N <sub>10</sub> OTi (3a)	C <sub>47</sub> H <sub>30</sub> N <sub>10</sub> OTi(3b).C <sub>6</sub> H <sub>5</sub> Cl
Molecular weight	770.6	798.6
Color	prism, dark blue	prism, dark blue
Crystal dimensions (mm <sup>3</sup> )	0.30 x 0.12 x 0.08	0.17 x 0.06 x 0.04
Crystal system	monoclinic	triclinic
Space group	P 2 <sub>1</sub> /n	P $\bar{1}$
Unit cell dimensions		
a / Å	11.8342(10)	12.3080(17)
b / Å	26.0933(19)	12.5821(14)
c / Å	12.4701(11)	16.717(2)
$\alpha$ /°	90	70.981(10)
$\beta$ /°	116.845(6)	78.757(11)
$\gamma$ /°	90	68.628(10)
Volume (Å <sup>3</sup> )	3435.7(5)	2270.6(5)
Cell formula units (Z)	4	2
D <sub>calcd</sub> /g·cm <sup>-3</sup>	1.490	1.415
Absorption $\mu$ /mm <sup>-1</sup>	0.305	0.332
<b>Data collection</b>		
Diffractometer	IPDS-II (Stoe)	
Radiation	MoK $\alpha$ graphite monochromator ( $\lambda = 0.71073$ Å)	
Temperature (K)	193	193
$\theta_{\max}$ /°	28	23
Reflections total	25798	15399
<b>Refinement</b>		
Reflections unique, >2 $\sigma$ (I)	3564	3220
Parameters	515	648
Residuals $R$ , $wR_2$ (all refl.) (observed refl.)	0.0420, 0.0914	0.0678, 0.1321
Goodness of fit $S$	0.804	0.924

### **4.3.3. Preparation of Sulfido (phthalocyaninato) titanium (IV) (4)**

#### **4.3.3.1 By reaction of (3b) with H<sub>2</sub>S gas**

Into a solution of (400 mg, 0.5 mmol) of **(3b)** in 20 ml of chloronaphthalene in a sealed teflon valve container, dry H<sub>2</sub>S gas (1 bar) was bubbled for five minutes under a cover of nitrogen gas. The container was tightly closed and the solution was stirred at 160°C for 3 hours. After cooling and removing of the gas, the product was precipitated by addition of about 10 ml of hexane. The produced bluish-green solid was collected on a glass frit and washed with MeCN (5x50 ml) and finally with pentane. The product PcTi=S (**4**) was dried at 120°C/10<sup>-3</sup> mbar for 3 hours.

#### **4.3.3.2 By reaction of PcTiO with P<sub>4</sub>S<sub>10</sub>**

A mixture of [PcTiO] (**1**) (300 mg, 0.52 mmol) and P<sub>4</sub>S<sub>10</sub> (230 mg, 0.52 mmol) in 10 ml of chloronaphthalene was heated at 160°C for 10 hours. The color turns dark green. After cooling, the product was precipitated by addition of 20 ml hexane. The precipitate was collected on a glass frit and washed by extraction from refluxing MeCN (3x50ml), refluxing toluene (3x50ml) and finally washed with pentane. The solid was dried at 120°C/10<sup>-3</sup> mbar for 1 hour. A 200 mg sample of this product (mixture of PcTiS and PcTiS<sub>2</sub>) was heated with 1 g of Ph<sub>3</sub>P to a melt (160°C) under nitrogen atmosphere for 4 hours. The blue-green mass was washed by successive extractions from refluxing MeCN (5x50 ml) and refluxing toluene (5x50 ml). The product (**4**) was finally washed with 50 ml of ether and dried at 120°C/10<sup>-3</sup> mbar for 3 hours.

**Yield:** 170 mg (57%) blue-green solid

**Solubility:** ClN, ClB, and DMF.

<b>C<sub>32</sub>H<sub>16</sub>N<sub>8</sub>S Ti</b> (592.4)	<b>EA</b>	calcd.:	C 64.87	H 2.72	N 18.91	S 5.42
		found:	C 64.60	H 3.20	N 18.44	S 4.17

**MS (EI, MT):** m/z = 592.3 (M<sup>+</sup>), 560.3 (M<sup>+</sup>-S).

**UV/VIS:** (ClN, 10<sup>-5</sup> M):

λ<sub>max</sub> (nm) = 696.0 (s) (Q<sub>0,0</sub>), 667.0 (w) (Q<sub>1,0</sub>), 635.5 (w) (Q<sub>2,0</sub>), 339.0 (s) (B).

**IR (KBr):**  $\tilde{\nu}$  (cm<sup>-1</sup>) = 1647(m), 1608(w), 1553(br), 1491(s), 1415(m), 1332(vs), 1287(m), 1160(w), 1118(vs), 1071(vs), 1053(vs), 894(s), 778(m), 751(s), 730(vs), 563(m) (ν<sub>Ti=S</sub>), 501(w), 411(vw).





Table 20: X-ray Data Collection of (5)

Molecular formula	$C_{32} H_{16} N_8 S_2 Ti$ (5)
Formula mass	624.55
Crystal description	block, black
Crystal size /mm <sup>3</sup>	0.045 × 0.03 × 0.03
Crystal system	monoclinic
Space group	P2 <sub>1</sub> /n
Unit cell	a /Å b /Å c /Å α /° β /° γ /°
	13.114(3) 9.752(2) 20.975(5) 90 100.46(2) 90
Volume /Å <sup>3</sup>	2637.9(10)
Z	4
D <sub>calcd</sub> /g·cm <sup>-3</sup>	1.573
Absorption μ /mm <sup>-1</sup>	0.524
<b>Data collection</b>	
Diffractometer	IPDS-II (Stoe)
Radiation	MoK <sub>α</sub> graphite monochromator (λ = 0.71073 Å)
Temperature /K	100(2)
θ <sub>max</sub> /°	25.00
Reflections total	16523
<b>Refinement</b>	
Reflections unique, >2σ(I)	4643, 912
Parameters	188
Residuals R, wR <sub>2</sub> (all refl.) (observed refl.)	0.444, 0.349 0.198, 0.225
Goodness of fit S	1.001
δρ (max, min) /eÅ <sup>-3</sup>	0.568, -0.947

#### **4.3.5 Preparation of 1,2-Phenylenediimino (phthalocyaninato) titanium (IV) (6)**

A mixture of **(3b)** (400 mg, 0.5 mmol) and 1,2-phenylenediamine (220 mg, 2 mmol) in 20 ml of chloronaphthalene was heated at 160°C for 2 hours. The product was precipitated by addition of 20 ml of hexane. The precipitate was collected on a glass frit and washed by successive extractions from refluxing MeCN (5x50ml), refluxing toluene (5x50ml) and finally washed with pentane. The product **(6)** was dried at 120°C/10<sup>-3</sup> mbar for 3 hours.

**Yield:** 270 mg (82%) blue-violet crystals

**Solubility:** ClN and ClB.

**C<sub>38</sub>H<sub>22</sub>N<sub>10</sub>Ti** (666.5)

**EA:** calcd.: C 68.48 H 3.33 N 21.01

found: C 67.63 H 3.35 N 20.26

**MS (EI, MT):** m/z = 666 (M<sup>+</sup>).

**UV/VIS:** (ClN, 10<sup>-5</sup> M)

$\lambda_{\max}$  (nm) = 698.5(s) (Q<sub>0,0</sub>), 668.0(sh) (Q<sub>1,0</sub>), 629.5(m) (Q<sub>2,0</sub>), 337.0(s) (B).

**IR (KBr):**  $\tilde{\nu}$  (cm<sup>-1</sup>) = 3450(m)( $\nu_{\text{NH}}$ ), 1606(w), 1491(w), 1476(w), 1414(w), 1330(s), 1283(m), 1230(w), 1160(w), 1117(s), 1074(vs), 892(m), 826(w), 748(s), 724(vs).

(Underlined values are new and not found in the spectra of PcTiO **(1)** or **(3b)**).

#### **4.3.6 Preparation of trans-Bis (triphenylsiloxy) phthalocyaninato titanium (IV) (7)**

A mixture of **(3b)** (400 mg, 0.5 mmol) and triphenylsilanol (550 mg, 2 mmol) was refluxed in 40 ml of chlorobenzene for 1 hour. After cooling, the solid was collected on a glass frit and washed with MeCN (3x50 ml), toluene (3x50ml) and finally with pentane. The product **(7)** was dried at 120°C/10<sup>-3</sup> mbar for 3 hours.

**Yield:** 620 mg (92%) dark green crystals

**Solubility:** ClN, chlorobenzene and DMF.

**C<sub>68</sub>H<sub>46</sub>N<sub>8</sub>O<sub>2</sub>Si<sub>2</sub>Ti** (1111.2)

**EA:** calcd.: C 73.50 H 4.17 N 10.08

found: C 72.75 H 4.65 N 9.50

**MS (EI, MT, ESI):** m/z = 1111 (M<sup>+</sup>).

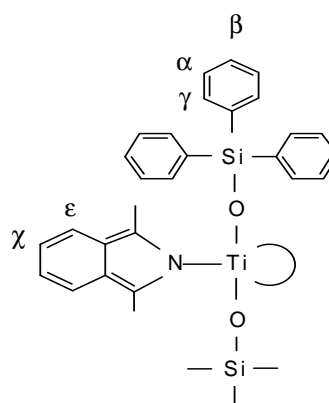
**UV/VIS:** (ClN, 10<sup>-5</sup> M)  $\lambda_{\max}$  (nm) = 741.5 (m), 698.0 (s), 663.5 (sh), 627.0 (w), 356.5 (m).

**IR (KBr):**  $\tilde{\nu}$  (cm<sup>-1</sup>) = 1590(m)( $\nu_{\text{C=C arom.}}$ ), 1429(m), 1305(s), 1104(m), 1043(s), 998(w), 971(w), 944(w), 886(vs), 821(w)( $\nu_{\text{O-Si oop}}$ ), 800(w), 766(w), 736(m), 711(m), 707(m), 697(s).

(Underlined values are new and not found in the spectra of PcTiO **(1)** or **(3b)**).

<sup>1</sup>H-NMR (500 MHz, C<sub>6</sub>D<sub>5</sub>Br, 373 K) (ppm):

δ = 5.31-5.23 [m, 12H(α)], 6.57-6.49 [m, 12H(β)],  
6.87-6.78 [m, 6H(γ)], 8.32-8.25 [m, 8H(χ)], 9.70-  
9.62 [m, 8H(ε)].



### Growth of Single Crystals

Blue needles of compound (**7**) were obtained by controlled cooling of the reaction mixture from 130 to 20°C within 3 hours. Table (8) shows some selected crystallographic data of (**7**).

Table 21: X-ray Data Collection of (**7**)

Molecular formula	C <sub>68</sub> H <sub>46</sub> N <sub>8</sub> O <sub>2</sub> Si <sub>2</sub> Ti ( <b>7</b> )	
Formula mass	1111.21	
Crystal description	prism, dark green	
Crystal size /mm <sup>3</sup>	0.38 x 0.32 x 0.27	
Crystal system	triclinic	
Space group	P $\bar{1}$	
Unit cell	a /Å	10.4160(8)
	b /Å	11.2160(8)
	c /Å	13.1495(9)
	α /°	114.124(5)
	β /°	99.452(6)
	γ /°	96.174(6)
Volume /Å <sup>3</sup>	1356.7(2)	
Z	1	
D <sub>calcd</sub> /g·cm <sup>-3</sup>	1.360	
Absorption μ /mm <sup>-1</sup>	0.259	

## 4.4 Molybdenum Phthalocyanines

### 4.4.1 Preparation of Chloro (<sup>t</sup>butylimido) phthalocyaninato molybdenum (V) (9a)

A mixture of PN (282 mg, 22 mmol) and [Mo(N<sup>t</sup>Bu)<sub>2</sub>Cl<sub>2</sub>(dme)] (**8a**) (200 mg, 5 mmol) was finely ground in a mortar under nitrogen until a homogeneous powder is obtained. The mixture was heated at melt (210°C) for 15 min. The produced dark-green solid was suspended in 50 ml of toluene and the suspension was treated with ultrasound at 70°C for 2 hours. The precipitate was collected on a glass frit and washed by successive extractions from refluxing toluene (10x50ml), refluxing MeCN (10x50ml) and finally washed with pentane. The product (**9a**) was dried at 120°C/10<sup>-3</sup> mbar for 3 hours.

**Yield:** 220mg (67%) green solid    **Solubility:** ClN, ClB, and partially in THF and toluene.

<b>C<sub>36</sub>H<sub>25</sub>ClMoN<sub>9</sub></b> (715.05)	<b>EA:</b> calcd.:	C 60.47	H 3.52	N 17.63
	found:	C 59.61	H 4.33	N 17.12

**MS(EI, MT, ESI):** m/z = 679.5 (M<sup>+</sup>-Cl)

**UV/VIS:** (ClN, 10<sup>-5</sup> M)    λ<sub>max</sub> (nm) = 871.0 (m), 729.5 (s), 328.0 (s).

**IR (KBr):**     $\tilde{\nu}$  (cm<sup>-1</sup>) = 1602(m), 1463(m), 1328(s), 1284(w), 1265((ν<sub>Mo=N-C</sub>)), 1161(w), 1115(s), 1063(m), 973(w), 893(m), 802(w), 772(w), 750(m), 728(s), 570(w).

**ESR:** (ClN/toluene 1:3, 130 K) g<sub>1</sub> = 1.989, g<sub>2</sub> = 1.987, g<sub>3</sub> = 1.977.

### Growth of Single Crystals

Blue needles of (**9a**·8H<sub>2</sub>O) were obtained by adding few drops of water to a concentrated chloronaphthalene solution and controlled cooling of the solution (160–20 °C) within 6 hours. The compound crystallizes tetragonal with Z = 2. (Table 22) shows X-ray Data Collection of (**9a**·8H<sub>2</sub>O)

Table 22: X-ray Data Collection of (**9a**.8H<sub>2</sub>O)

Molecular formula	C <sub>36</sub> H <sub>41</sub> Cl Mo N <sub>9</sub> O <sub>8</sub> .8H <sub>2</sub> O
Molecular weight	859.17
Color	plate, dark green
Crystal size (mm <sup>3</sup> )	0.18 x 0.113 x 0.01
Crystal system	tetragonal
Space group	P 4/n
Formula units	Z = 2
Unit cell dimensions	a = 13.8148(12) Å      α = 90° b = 13.8148(12) Å      β = 90° c = 10.0926(9) Å      γ = 90°
Volume (Å <sup>3</sup> )	1926.2(3)
Temperature (K)	193 (2)
Calculated density (Mg/m <sup>3</sup> )	1.481
Absorption coefficient (mm <sup>-1</sup> )	0.473
F(000)	886
R <sub>int</sub>	0.0863
θ <sub>max</sub>	24.99
Cell determination	8979 reflections, with θ = 1.5 to 26.0°.

#### **4.4.2 Preparation of Chloro (mesitylimido) phthalocyaninato molybdenum (V) (9b)**

A mixture of PN (282 mg, 22 mmol) and [Mo(NMes)<sub>2</sub>Cl<sub>2</sub>(dme)] (**8b**) (262 mg, 5 mmol) was finely ground in a mortar under nitrogen until a homogeneous powder is obtained. The mixture was heated at melt (210°C) for 15 min. The produced dark-green solid was suspended in 50 ml of toluene and the suspension was treated with ultrasound at 70°C for 2 hours. The precipitate was collected on a glass frit and washed by successive extractions from refluxing toluene (10x50ml), refluxing MeCN (10x50ml) and finally washed with pentane. The product (**9b**) was dried at 120°C/10<sup>-3</sup> mbar for 3 hours.





**Color:** generally dark green solids

**Yield:** (60-70%)

**Solubility:** ClN, ClB, DMF, and partially (~ 80%) in CH<sub>2</sub>Cl<sub>2</sub>, CHCl<sub>3</sub> and THF.

Table 23: Mass and Analytical Data of **(13a-c)**

Compound	Mol. formula (mol. weight)	m/z (found, MT)	Elemental analysis				
				% C	% H	% N	% Cl
<b>(13a)</b>	C <sub>38</sub> H <sub>19</sub> N <sub>9</sub> Cl <sub>2</sub> W (856.4)	856.9 (M <sup>+</sup> )	calcd.	53.30	2.24	14.72	8.28
		820.9 (M <sup>+</sup> -Cl)	found	53.28	2.36	14.25	9.66
		786.9 (M <sup>+</sup> -2Cl)					
<b>(13b)</b>	C <sub>39</sub> H <sub>21</sub> N <sub>9</sub> Cl <sub>2</sub> W (870.4)	870.9(M <sup>+</sup> )	calcd.	53.82	2.43	14.48	8.15
		834.9 (M <sup>+</sup> -Cl)	found	53.74	2.71	14.34	8.61
		801 (M <sup>+</sup> -2Cl)					
<b>(13c)</b>	C <sub>38</sub> H <sub>17</sub> N <sub>9</sub> Cl <sub>4</sub> W (925.3)	925.7 (M <sup>+</sup> )	calcd.	49.33	1.85	13.62	15.33
		891.9 (M <sup>+</sup> -Cl)	found	50.16	2.16	14.62	15.08
		856.8 (M <sup>+</sup> -2Cl)					

Table 24: UV/VIS Data of **(13a-c)** (ClN, 10<sup>-5</sup>M)

Compound	$\lambda_{\max}$ (nm)				
<b>(13a)</b>	871.0(w)	728.5(s)	709.5(sh)	666.0(m)	327.5(m)
<b>(13b)</b>	871.5(w)	725.5(s)	700.0(sh)	665.0(m)	320.5(m)
<b>(13c)</b>	871.0(w)	736.5(s)	708.5(sh)	639.0(m)	329.0(m)

Table 25: IR Data of **(13a-c)** (KBr pellets)

Compound	$\bar{\nu}$ (cm <sup>-1</sup> )
<b>(13a)</b>	1605(w), 1520(w), 1468(m), 1402(w), 1329(vs), 1284(m), 1160(w), 1117(s), 1065(m)( $\nu_{\text{arom. Cl}}$ ), 893(w), 750(w), 728(m), 687(w), 571(w).
<b>(13b)</b>	1606(w), 1521(m), 1468(m), 1403(w), 1362(w), 1329(s), 1285((w), 1161(w), 1118(m), 1067(m) ( $\nu_{\text{arom. Cl}}$ ), 1009(w), 893(w), 817(w), 774(w), 728(s), 638(w), 570(w).
<b>(13c)</b>	1605(w), 1561(w), 1468(m), 1434(w), 1330(vs), 1284(w), 1160(w), 1117(m), 1064(m) ( $\nu_{\text{arom. Cl}}$ ), 1010(w), 893(w), 773(w), 750, 727(s), 669(w).







**Color:** blue-black    **Solubility:** DMF

$C_{160}H_8N_{64}O_5Ti_5$  [pentamer, the proposed structure in (Figure 65) (mol. wt. =3145.59).

**EA:**            calcd.: C 61.09    N 28.49    Ti 7.61

                  found: C 60.93    N 25.46    Ti 6.81

**MS:**            MT (568.7, one unit).                    **GPC:**            (DMF, Mn= 2859);

**UV/VIS:** (DMF)  $\lambda_{max}$  (nm) =738.5 (m), 621.0 (sh), 350.5 (s).

**IR (KBr):**

$\tilde{\nu}$  ( $cm^{-1}$ ) = 2225.9(m)( $\nu_{C\equiv N}$ ), 1768.3(s), 1724.7(m), 1653(m), 1578.8(s), 1520(s),  
1437.6(s), 1308.5(m), 1241.7(s), 1193.6(s), 1080(s), 908.2(vs), 790.8(m), 765.3(s),  
719.5(m), 641.6(s), 528.6(m).

#### **4.7.2 Preparation of Polyimidomolybdenumphthalocyanine (17)**

A mixture of 1,2,4,5-tetracyanobenzene (TCB) (1g, 5.6 mmol), [Mo(NMes)<sub>2</sub>Cl<sub>2</sub>(dme)] (**8b**) (0.68 g, 1.3 mmol), urea ( 0.3 g, 5 mmol), and ammonium heptamolybdate (0.1 g) in 15 ml of chloronaphthalene was heated at reflux (~210°C) for 12 hours. After cooling, the dark product was precipitated by addition of 20 ml hexane. The precipitate was collected on a glass frit and washed by successive extractions from refluxing MeCN (10x50ml), refluxing toluene (10x50ml) and finally washed with pentane. The obtained blue-black polymer (**17**) was then dried at 120°C/10<sup>-3</sup> mbar for 3 hours.

**Color:** blue black    **Solubility:** DMF

$C_{205}H_{63}N_{64}Cl_5Mo_5$  [pentamer, the proposed structure in (Figure 65)] (mol. wt. =4079).

**EA:**            calcd.:    C 60.36    H 1.56    N 21.97    Mo 11.76

                  found:    C 53.48    H 2.71    N 23.73    Mo 10.42

**GPC:**            (DMF, Mn= 4262);

**UV/VIS:** (DMF)  $\lambda_{max}$  (nm) =731.5 (m), 605.0 (sh), 422.0, 324.5 (s), 312.5(w).

**IR (KBr):**       $\tilde{\nu}$  ( $cm^{-1}$ ) = 2223.9(s)( $\nu_{C\equiv N}$ ), 1458.3(vs), 1292.4(m), 1222.5(s), 1060.4(m),  
722.7(m), 527.3(s).

### **4.7.3 Preparation of Polyimidotitaniumphthalocyanine (18)**

A mixture of [PcTiO]<sub>5</sub> (**16**) (1g), excess (10 ml) of 2,6-diisopropyl-phenylisocyanate, and 15 ml of dry DMF was heated at reflux (~180°C) for 12 hours. After cooling, the product was precipitated by addition of 20 ml hexane. The precipitate was collected on a glass frit and washed by successive extractions from refluxing MeCN (10x50ml), refluxing toluene (10x50ml) and finally washed with pentane. The produced dark blue-green polymer (**18**) was then dried at 120°C/10<sup>-3</sup> mbar for 3 hours.

**Color:** dark blue-green      **Solubility:** DMF

C<sub>220</sub>H<sub>93</sub>N<sub>69</sub>Ti<sub>5</sub> [pentamer, the proposed structure in (Figure 65)] (mol. wt. =3941.96).

**EA:**      calcd.: C 67.03    H 2.38    N 24.52    Ti 6.07

          found: C 65.93    H 1.98    N 22.46    Ti 5.31

**GPC:**      (DMF, Mn= 3809);

**UV/VIS:** (DMF) λ<sub>max</sub> (nm) =742.0 (m), 628.5 (sh), 408.5 (w) soret, 347.0 (s).

**IR (KBr):**     $\tilde{\nu}$  (cm<sup>-1</sup>) = 2221.2(m)(ν<sub>C=N</sub>), 1748.5(s), 1723.7(m), 1653(m), 1582.8(s),  
1500.5(s), 1436.2(s), 1310.1(m), 1270.1(m), 1242.2(s), 1193.1(s), 1082(s),  
930.6(s), 906.7(vs), 791.2(m), 765.1(s), 719.3(m), 640.7(s), 529.4(m).

### **4.8 Time-resolved Photoluminescence Study of Some TiPcs**

The samples of the measured compounds were filled in capillaries of thickness 1 mm and length 5 cm under argon and tightly sealed. All samples were measured as 10<sup>-3</sup> M solution in a mixture of α- and β-CIN (90-10%) microfiltered via a teflon filter (0.45μ). Afterwards the PL measurements were carried out by the research group of Prof. Dr. W. Rühle at Physics Department, Philipps-Universität Marburg using streak-camera setup (Figures 69 a,b,c).

A femtosecond Ti: sapphire laser system generates 115 fs pulses at 810 nm with a repetition rate of 80 MHz. The light is then frequency-doubled by focusing through a BBO crystal and the solution is excited at 405 nm. The laser intensity is varied over one order of magnitude, from 1.8 to 18 mW from 1.23 to 12.33 W/cm<sup>2</sup> average powers. The sample is held at room temperature (293K). The PL signal is dispersed by a 32-cm spectrometer with a spectral resolution of ~2 nm and detected using a Hamamatsu S1 streak camera. The use of a streak camera enables to acquire the complete spectrally resolved temporal dynamics in a single experiment.

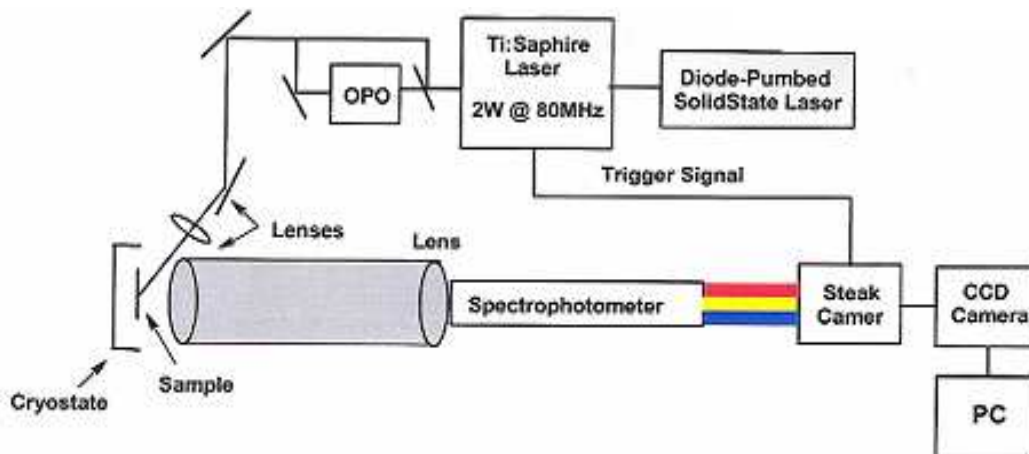


Figure 69a: Experimental design for the time-resolved PL measurements using CCD camera.

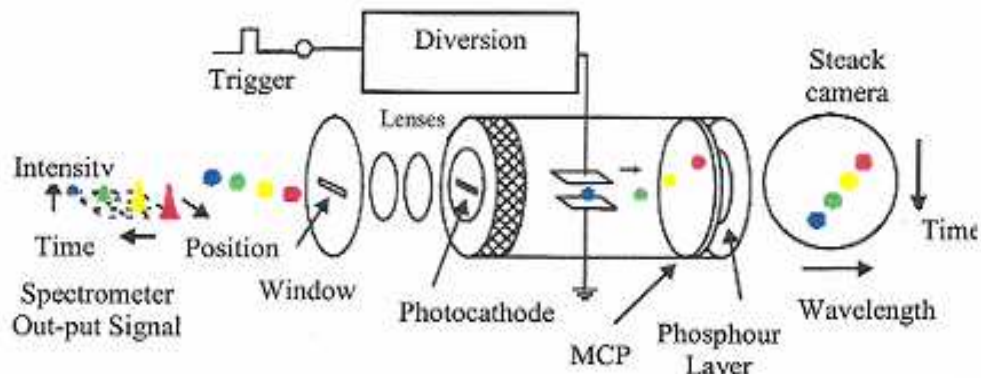


Figure 69b: Schematic design and function of the streak CCD camera.

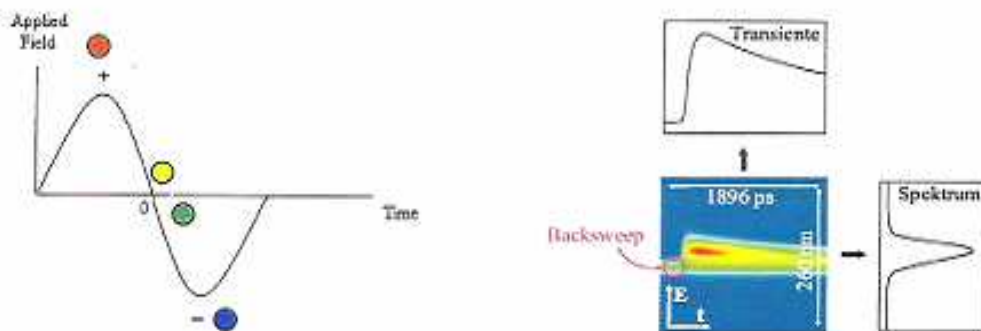


Figure 69c: The typical photo and the extracted spectrum using CCD camera.

## **4.9 Preparation of Phthalocyanine Modified Silica Materials**

The samples of SBA-15 and  $\text{TiO}_x\text{-SBA-15}$  materials were prepared for AAS as follows: The samples were weighted in gelatin capsules and dissolved in a mixture of HF (30% in  $\text{H}_2\text{O}$ ) and  $\text{H}_2\text{SO}_4$ . Afterwards, HF was evaporated at  $170^\circ\text{C}$  and then 15 ml of  $\text{H}_2\text{O}_2$  and few milligrams of lanthanum nitrate (as stabilizer) were added.

### **4.9.1 Silica ( $\text{SiO}_2$ )**

Merck ( $\text{SiO}_2$ ) for column chromatography, *silica* 60 (0.063-0.200 mm), pH = 6.5-7.05, pore volume ( $\text{N}_2$  isotherm) = 0.74-0.84 ml/g and surface area = 480-540  $\text{m}^2/\text{g}$ .

### **4.9.2 Preparation of $\text{PcTi@SiO}_2$ (Sample A)**

A solution of 200 mg of N,N'-di-4-tolylureato (phthalocyaninato) titanium (IV) (**3b**) in 30 ml of chloronaphthalene was heated at 373 K under inert atmosphere until the solution was clear. About 20 ml of this solution were filtered using a microfilter (0.45  $\mu\text{L}$ ) and then added to 100 mg of silica gel (Merck). The mixture was stirred at  $150^\circ\text{C}$  for 6 hours. The bluish-green solids were filtered and washed with refluxing chlorobenzene, toluene, MeCN, and with pentane and dried at  $120^\circ\text{C}/10^{-3}$  mbar for 2 hours.

### **4.9.3 Preparation of SBA-15**

SBA-15 was prepared by Prof M. Fröba, Justus-Liebig Universität, Gießen, Germany according to the literature.<sup>138</sup> The material was dried at  $210^\circ\text{C}/10^{-3}$  mbar for 20 hours before use. SBA-15 has surface area of  $\sim 600$   $\text{m}^2/\text{g}$ , pore diameter is  $\sim 6$  nm and  $\sim 3.7$  OH group/ $\text{nm}^2$ .

### **4.9.4 Passivation of the Surface of SBA-15**

The passivation was carried out according to the literature procedure.<sup>141</sup> Thus a mixture of 100 mg of dried SBA-15 and 0.02 ml of  $\text{Ph}_2\text{SiCl}_2$  in 10 ml of dry THF was stirred at room temperature for 1 hour. After centrifugation and decantation of the solvent, the solid was washed several times with THF and dried at  $120^\circ\text{C}/10^{-3}$  mbar for 1 hour.

#### **4.9.5 Preparation of TiO<sub>x</sub>@SBA-15**

A sample of 200 mg of the previously synthesized and dried SBA-15 was suspended in 20 ml of dry ethanol for 30 min. Afterwards 1 ml (excess) of TBOT was added and the mixture was stirred at room temperature for 24 hours. The solid was filtered and washed with dry methanol (3 x 30 ml) and finally dried at 120°C/10<sup>-3</sup> mbar for 2 hours. The solid was calcined in air at 600°C for 24 hours to give TiO<sub>x</sub>@SBA-15 (Ti = 2.66 wt%).

#### **4.9.6 Anchoring of [PcTiO] dye on SBA-15 and TiO<sub>x</sub>@SBA-15**

A solution of 200 mg of PcTiO (1) in 30 ml of chloronaphthalene was heated at 373 K until the solution was clear. About 20 ml of this solution were filtered using a microfilter (0.45 μL) and then added to 100 mg of SBA-15 or TiO<sub>x</sub>@SBA-15. The mixture was stirred at 150°C for 6 hours. The faint-blue solid was filtered and washed with refluxing chlorobenzene, toluene, MeCN, and with pentane and dried at 120°C/10<sup>-3</sup> mbar for 2 hours.

#### **4.9.7 Anchoring of Ureato-TiPc dye on SBA-15 (Samples B and C) and TiO<sub>x</sub>@SBA-15**

##### **Sample D)**

A solution of 200 mg of N,N'-di-4-tolylureato (phthalocyaninato) titanium (IV) (3b) in 30 ml of chloronaphthalene was heated at 373 K under inert atmosphere until the solution was clear. About 20 ml of this solution were filtered using a microfilter (0.45 μL) and then added to 100 mg of SBA-15 (Sample B), 100 mg of surface pasivated SBA-15 (sample C) or 100 mg of TiO<sub>x</sub>@SBA-15 (Sample D). The mixture was stirred at 150°C for 6 hours. The faint-green solid was filtered and washed with refluxing chlorobenzene, toluene, MeCN, and with pentane and dried at 120°C/10<sup>-3</sup> mbar for 2 hours.

#### **4.9.8 Anchoring of Imido-TiPc dye on SBA-15 and TiO<sub>x</sub>@SBA-15**

A solution of 200 mg of 2,6-diisopropylphenylimido (phthalocyaninato) titanium (IV) (2) in 30 ml of chloronaphthalene was heated at 373 K under inert atmosphere until the solution was clear. About 20 ml of this solution were filtered using a microfilter (0.45 μL) and then added to 100 mg of SBA-15 or PcTi&TiO<sub>x</sub>@SBA-15. The mixture was stirred at 150°C for 6 hours. The faint-green solid was filtered and washed with refluxing chlorobenzene, toluene, MeCN and pentane and dried at 120°C/10<sup>-3</sup> mbar for 2 hours.

## 5. References

- [1] Braun, A.; Tscherniac, B.; *Ber.* **1907**, *40*, 2709-2714.
- [2] Diesbach, H.; Weid, E.; *Helv. Chim. Acta* **1927**, *10*, 886-888.
- [3] Gregory, P.; *J. Porphyrins Phthalocyanins* **1999**, *3*, 468-476.
- [4] (a) Linstead, R.; Lowe, A.; *J. Chem. Soc.* **1934**, 1016-1017.  
(b) Hesse, M.; Meier, H.; Zeeh, B.; *Spektroskopische Methoden in der Organischen Chemie*. Auflage Goerge Thieme Verlag Stuttgart. New York **1991**.  
(c) Byrne, G.; Linstead, R.; Lowe, A.; *J. Chem. Soc.* **1934**, 1017-1021.  
(d) Linstead, R.; Lowe, A.; *J. Chem. Soc.* **1934**, 1022-1026.  
(e) Dent, C.; Linstead, R.; *J. Chem. Soc.* **1934**, 1027-1030.
- [5] (a) Robertson, J.; *J. Chem. Soc.* **1934**, 615-621.  
(b) Robertson, J.; Woodward, I.; *J. Chem. Soc.* **1937**, 219-232 and *J. Chem. Soc.* **1940**, 36-47.
- [6] Leznoff, C.; Lever, A.; *Phthalocyanines: Properties and Applications*, Volume 1, p. 145. VCH Publishers, New York, USA. **1989**.
- [7] (a) Turek, P.; Petit, P.; Andre, J.; Simon, J.; Even, R.; *J. Am. Chem. Soc.* **1987**, *109*, 5119-5122.  
(b) Moskalev, P.; Kirin, I.; *Russ. J. Phys. Chem.* **1972**, *46*, 1778-1781.  
(c) Andre, J.; Holczer, K.; Petit, P.; Even, R.; *Chem. Phys. Lett.* **1985**, *115*, 463-466.
- [8] Hanack, M.; Heckmann, H.; Polley, R. Chapter II. (Aromatic and Heteroaromatic Large Rings), P 718-833, in (Methods in Organic Chemistry) Houben-Weyl, Volume E9d, 4th edition, **1998**. Thieme Medical Publishers. New York.
- [9] Wagner, H. J.; Loutfy, Rafik O.; Hsiao, Cheng Kuo, J.; *Mat. Sci.*; **1982**, *17*, 2781-2791.
- [10] McKeown, N.; *Science of Synthesis*, V. 17, Capital 9, **2005**, Thieme Chemistry, Rochdale, UK.
- [11] Erk, P.; in *High Performance Pigments*. M. H. Smith, Ed; Wiley-VCH: Weinheim, **2002**, p. 103.
- [12] Kadish, K.; Smith, K.; Guillard R.; *The Porphyrin Handbook*, Vol. 20 / Phthalocyanines: Structural Characterization; Academic Press, Elsevier Science **2003**, San Diego, California, USA; and references therein.



- [13] Shannon, R. ; *Acta Crystallogr., Sect. A: Found. Crystallogr.* **1976**, 32, 751-767.
- [14] Hoard, J.; *Anuals of the New York Acad. of Sci.* **1973**, 206, 18-31.
- [15] Berezin, B.; Koifman, O.; *Usp. Khim.* **1980**, 49, 2389-2417.
- [16] Buchler, J.; Ng, D. in *The Porphyrin Handbook*. Kadish, K.; Smith, K.; Guillard, R., Eds.; Academic Press, **2000**; Vol. 3, p. 245.
- [17] Hesse, M.; Meier, H.; Zeen, B.; *Spektroskopische Methoden in der Organischen Chemie*; page 8; Georg Thieme Verlag Stuttgart **1979**.
- [18] Casstevens, M.; Samok, M.; Pflieger, J.; Prasad, N.; *J. Chem. Phys.* **1990**, 92, 2019-2024.
- [19] Van der Pol, J.; Neeleman, E.; Zwikker, W.; Nolte, R.; Drenth, W.; Aertzs, J.; *Liq. Cryst.* **1989**, 6, 577-592.
- [20] Schultz, H.; Lehmann, H.; Rein, M.; Hanack, M.; *Structure and Bonding (Berlin)* **1991**, 74, 41-146.
- [21] (a) Kuder, J.; *J. Imag. Sci.* **1988**, 32, 51-56.  
(b) Hurditch, R.; *Adv. Colour Sci. Technol.* **2001**, 4, 33.
- [22] Riou, M.; Clarisse, C.; *J. Electroanal. Chem.* **1988**, 249, 181-190.
- [23] Marks, Tobin J.; *Science* **1985**, 227, 881-889.
- [24] Collins, R. A.; Mohammed, K. A.; *J. Phys. D: Appl. Phys.* **1988**, 21, 154-161.
- [25] Kato, M.; Nishioka, Y.; Kaifu, K.; Kawamura, K.; Ohno, S.; *Appl. Phys. Lett.* **1985**, 86, 196-197.
- [26] Jidong, Z.; Fanli, L.; Haichao, H.; Jun, W.; Hong'an, Y.; Jianzhuang, J.; Donghang, Y.; Zhiyuan, W.; *Synth. Met.* **2005**, 148, 123-126.
- [27] Klofta, T.; Danzinger, J.; Lee, P.; Pankow, J.; Nebesny, K.; Armstrong, N.; *J. Phys. Chem.* **1987**, 91, 5646-5651.
- [28] Takano, S.; Enokida, T.; Kakuta, A.; Mori, Y.; *Chem. Lett.* **1984**, 2037-2040.
- [29] Henderson, B.; Dougherty, T.; *Photochem. Photobiol.* **1992**, 55, 145-157.
- [30] Taube, R.; *Zeitschrift fuer Chemie* **1963**, 3, 194.
- [31] Block, B.; Meloni, E.; *Inorg. Chem.* **1965**, 4, 111-112.
- [32] Goedken, V.; Dessy, G.; Ercolani, C., Fares, V.; Gastaldi, L.; *Inorg. Chem.* **1985**, 24, 991-995.
- [33] Law, K.; *Chem. Rev.* **1993**, 93, 449-486.
- [34] Moser, F.; Thomas, A. "*The Phthalocyanines*" CRC Press, Florida (**1983**) Vol. II.
- [35] Yao, J.; Youehara, H.; Pac, C.; *Bull. Chem. Soc. Jpn.* **1995**, 68, 1001-1005.

- [36] Hiller, W.; Straehle, J.; Kobel, W.; Hanack M.; *Z. Kristallogr.* **1982**, *159*, 173-183.
- [37] (a) Yamashita, A.; Maruno, T.; Hayashi T.; *J. Phys. Chem.* **1994**, *98*, 12695-12701.  
(b) Ghosez, P.; Cote, R.; Gastong, L.; Veilleux, G.; Denes, G.; Dodelet, J.; *Chem. Mater.* **1993**, *5*, 1581-1590.
- [38] (a) Mikhalenko, S.; Barkanova, S.; Lebedev, V.; Luk'yanets, E.; *Zh. Obshch. Khim.* **1971**, *41*, 2735-2739.  
(b) Schmid, G.; Sommerauer, M.; Geyer, M.; Hanack, M. in *Phthalocyanines, Properties And Applications*, Vol. 4 (Eds.: C. C. Leznoff, A. B. P. Lever), VCH: New York, USA. **1996**, p. 1-18.
- [39] Haisch, P.; Winter, G.; Hanack, M.; Luer, L.; Egelhaaf, H.; Oelkrug, D.; *Adv. Mater.* **1997**, *9*, 316-321.
- [40] (a) Saito, T.; Sisk, W.; Kobayashi, T.; Suzuki, S.; Iwayanagi, T.; *J. Phys. Chem.* **1993**, *97*, 8026-8031.  
(b) Hanack, M.; Schmid, G., Sommerauer M.; *Angew. Chem.* **1993**, *105*, 1540-1542 and *Angew. Chem. Int. Ed. Eng.* **1993**, *32*, 1422-1424.  
(c) Barthel, M.; Dini, D.; Vagin, S.; Hanack, M.; *Eur. J. Org. Chem.* **2002**, 3756-3762.
- [41] (a) Law, W.; Liu, R. C. W.; Jinag, J.; Dennis, K. P. Ng; *Inorg. Chim. Acta* **1997**, *256*, 147-150.  
(b) Barthel, M.; Hanack, M.; *J. Porphyrins Phthalocyanines* **2000**, *4*, 635 -638.
- [42] Mountford, P.; *Chem. Soc. Rev.* **1998**, *27*, 105-115.
- [43] Enokida, T.; Shimojima, S.; Kurata, R. (Toyo Ink Mfg. Co., Ltd., Japan). Jpn. Kokai Tokkyo Koho (1990), JP 88-334793 19881229. CAN 114:52871.
- [44] Berreau, L.; Young, V.; Keith Woo; L.; *Inorg. Chem.* **1995**, *34*, 527-529.
- [45] Gray, S.; Thorman, J.; Berreau, L.; Keith Woo; L.; *Inorg. Chem.* **1997**, *36*, 278-283.
- [46] Thorman, J.; Young, V.; Boyd, P.; Guzei, I.; Keith Woo; L.; *Inorg. Chem.* **2001**, *40*, 499-506.
- [47] Keith Woo; L.; Alan Hays, J.; Young, V.; Day, C.; Caron, C.; D'Souza, F.; Kadish, M.; *Inorg. Chem.* **1993**, *32*, 4186-4192.
- [48] (a) Guillard, R.; Ratti, C.; Tabard, A.; Richard, P.; Dubois, D.; Kadish, M.; *Inorg. Chem.* **1990**, *29*, 2532-2540.  
(b) Guillard, R.; Latour, J. M.; Lecomte, C.; Marchon, J. C.; Protas, J.; Ripoll, D.; *Inorg. Chem.* **1978**, *17*, 1228-1237.
- [49] Boerschel, V.; Straehle, J.; *Z. Naturforsch., B: Chem. Sci.* **1984**, *39b*, 1664-1667.

- [50] Edmondson, S.; Mitchell, P.; *Polyhedron* **1986**, *5*, 315-317.
- [51] Nyokong, T.; *Polyhedron* **1994**, *13*, 215-220.
- [52] Sheldon, R.; *Recueil des Travaux Chimiques des Pays-Ba* ; **1973**, *92*, 253-266.
- [53] Gorsch, M.; Homborg, H.; *Z. Anorg. Allg. Chem.* **1998**, *624*, 634-641.
- [54] Padilla, J.; Litter, M. I.; Campero, A.; *Anales de Quimica* **1993**, *89*, 177-180.
- [55] Dehnicke, K. and Straehle, J.; *Angew. Chem.* **1992**, *104*, 978-1000 and *Angew. Chem. Int. Ed. Engl.* **1992**, *31*, 955-978.
- [56] (a) Frick, K.; Verma, S.; Sundermeyer, J.; Hanack, M.; *Eur. J. Inorg. Chem.* **2000**, 1025-1030.  
(b) Ziener, U.; Hanack, M.; *Chem. Ber.* **1994**, *127*, 1681-1685.
- [57] Verma, S.; Hanack, M.; *Z. Anorg. Allg. Chem.* **2003**, *629*, 880-892.
- [58] Goeldner, M.; Hückstaedt, H.; Murray, K.; Moubaraki, B.; Homborg, H.; *Z. Anorg. Allg. Chem.* **1998**, *624*, 288-294.
- [59] (a) Eikey, R. A.; Abu-Omar, M. M.; *Coord. Chem. Rev.* **2003**, *243*, 83-124.  
(b) Kim, J. C.; Rees, W. S.; Goedken, V. L.; *Inorg. Chem.* **1995**, *34*, 2483-2486.
- [60] Berreau, L. M.; Chen, J.; Keith Woo, L.; *Inorg. Chem.* **2005**, *44*, 7304-7306.
- [61] Eikey, R. A.; Abu-Omar, M. M.; *Coord. Chem. Rev.* **2003**, *243*, 83-124.
- [62] Diebold, T.; Chevrier, B.; Weiss, R.; *Inorg. Chem.* **1979**, *18*, 1193-1198.
- [63] (a) Epstein, A.; Wild, B.; *J. Chem. Phys.* **1960**, *32*, 324-329.  
(b) Berlin, A. A.; Cherkashina, L. G.; Frankevich, E. L.; Balabanov', E. M.; Aseev, Yu. G.; CAN 61:33000 AN 1964:433000.
- [64] Marvell, C. S.; Rassweiler, J. H.; *J. Am. Chem. Soc.* **1958**, *80*, 1197-1199.
- [65] (a) Boston, D.; Bailar, J.; *Inorg. Chem* **1972**, *11*, 1578-1583.  
(b) Kreja, L.; Plewka, A.; *Electrochim. Acta* **1980**, *25*, 1283-1286.
- [66] (a) Nalwa, H.; Sinha, J.; Vasudevan, P.; *Makromolekulare Chemie*; **1981**, *182*, 811-815.  
(b) Achar, B.; Fohlen, G.; Parker, J.; *J. Polym. Sci. Polym. Lett. Ed.* **1982**, *20*, 1785-1789.
- [67] Drinkard, W; Bailar, J.; *J. Am. Chem. Soc.* **1959**, *81*, 4795-4797.
- [68] Wöhrle, D.; Preußner, E.; *Makromolekulare Chemie*; **1985**, *186*, 2189-2207.
- [69] Abd El-Ghaffar, M; Youssef, E; El-Halawany, N; Ahmed, M.; *Angew. Makromol. Chem.* **1998**, *254*, 1-9.

- [70] Abd El-Ghaffar, M; Moore, J. 3<sup>rd</sup> Arab International Conference on Polymer Science and Technology, Mansoura, Egypt, 4-7 Sept. 1995, Proceedings Vol. II, p. 613.
- [71] Block, B.; Meloni, E.; CAN 63:63533 AN 1965:463533.
- [72] Lo, Pui-Chi.; Wang, S.; Zeug, A.; Meyer, M.; Roeder, B. and Ng, D.; *Tetrahedron Lett.* **2003**, *44*, 1967-1970.
- [73] Van der Pol, J. and Zwikker, J.; *Recl. Trav. Chim. Pays-Bas* **1990**, *109*, 208-215.
- [74] Beck, J. S.; Vartuli, J. C.; Roth, W. J.; Leonowicz, M. E.; Kresge, C. T.; Schmitt, K. D.; Chu, C. T. W.; Olson, D. H.; Sheppard, E. W.; McCullen, S. B.; Higgins, J. B.; Schlenker, J.; *J. Am. Chem. Soc.* **1992**, *114*, 10834-10843.
- [75] Schulz-Ekloff, G.; Wöhrle, D.; Duffel, B., Schoonheydt, R. A.; *Microporous Mesoporous Mater.* **2002**, *51*, 91-138, and references therein.
- [76] Zhao, D.; Feng, J.; Huo, Q.; Melosh, N.; Fredrickson, G. H.; Chmelka, B. F.; Stucky, G. D.; *Science* **1998**, *279*, 548-552.
- [77] Kresge, C. T.; Leonowicz, M. E.; Roth, W. J.; Vartuli, J. C.; Beck, J. S.; *Nature* **1992**, *359*, 710-712.
- [78] Lukens, W.; Schmidt-Winkel, P.; Zhao, D.; Feng, J.; Stucky, G.; *Langmuir* **1999**, *15*, 5403-5409.
- [79] Fan, J.; Yu. C.; Wang, L.; Tu, B.; Zhao, D.; Sakamoto, Y.; Terasaki, O.; *J. Am. Chem. Soc.* **2001**, *123*, 12113-12114.
- [80] Fan, J.; Li, J.; Yu. C.; Wang, L.; Yu, C.; Tu, B.; Zhao, D.; *Chem. Commun.* **2003**, 2140-2141.
- [81] Schmidt-Winkel, P.; Yang, P.; Margolese, D.; Chmelka, B.; Stucky, G.; *Adv. Mater.* **1999**, *11*, 303-307.
- [82] Kruk, M.; Jaroniec, M.; Ko, C-H; Ryoo, R.; *Chem. Mater.* **2000**, *12*, 1961-1967.
- [83] Sutra, P.; Brunel, D.; *Chem. Commun.* **1996**, 2485-2492.
- [84] Rohfling, Y.; Wöhrle, D.; Rathousky, J.; Zukal, A.; Wark, M; *Stud. Surf. Sci. Catal.* **2002**, *142*, 1067-1074.
- [85] (a) Ortlam, A.; Wark, M.; Schulz-Ekloff, G.; Rathousky, J.; Zukal, A.; *Stud. Surf. Sci. Catal.* **1998**, *117*, 357-363.  
(b) Aguado, J.; van Grieken, R.; Lopez-Munoz, M.; Marugan, J.; *Catal. Today* **2002**, *75*, 95-102.  
(c) Segura, Y.; Cool, P.; Kustrowski, P.; Chmielarz, L.; Dziembaj, R.; Vansant, E.; *J. Phys. Chem. B* **2005**, *109*, 12071-21079.

- (d) Luan, Z.; Maes, E. M.; Paul, A. W.; Zhao, D. Czernuszewicz, R. S.; Kevan, L.; *Chem. Mater.* **1999**, *11*, 3680-3686.
- (e) Landau, M.; Vradman, L.; Wang, X.; Titelman, L.; *Microporous Mesoporous Mater.* **2005**, *78*, 117-129.
- (f) Perathoner, S.; Lanzafame, P.; Passalacqua, R.; Centi, G.; Schloegl, R.; Su, D.; *Microporous Mesoporous Mater.* **2006**, *90*, 347-361.
- (g) Calleja, G.; van Grieken, R.; Melero, J.; Iglesias, J.; *J. Mol. Catal. A: Chem.* **2002**, *182-183*, 215-225.
- (h) Wu, P.; Tatsumi, T.; Komastu, T.; Yashima, T.; *Chem. Mater.* **2002**, *14*, 1657-1664.
- (i) Brutchey, R.; Mork, B.; Sirbuly, D.; Yang, P.; Tilley, T.; *J. Mol. Catal. A* **2005**, *238*, 1-12.
- (j) Srivastava, R.; Srinivas, D.; Ratnasamy, P.; *J. Catal.* **2005**, *223*, 1-15.
- [86] Moller, K.; Bein, T.; *Chem. Mater.* **1998**, *10*, 2950-2963.
- [87] Zhao, X. S.; Lu, G. Q.; *J. Phys. Chem. B.* **1997**, *101*, 6525-6531.
- [88] Brühwiler, D.; Calzaferri, G.; *Microporous Mesoporous Mater.*, **2004**, *72*, 1-23.
- [89] Kunzmann, A.; Seifert, R.; Calzaferri, G.; *J. Phys. Chem. B* **1999**, *103*, 18-26.
- [90] Ernst, S.; Glaser, R.; Selle, M.; in Chon, H.; *Progress in Zeolites and Microporous Materials, Stud. Surf. Sci. Catal.* **1997**, *105B*, 1021-1028.
- [91] Ernst, S.; Selle, M.; *Microporous Mesoporous Mater.*, **1999**, *27*, 355-363.
- [92] Lu, X.; Wang, H.; He, R.; *J. Mol. Catal. A: Chem.* **2002**, *186*, 33-42.
- [93] Mifune, M; Shimomura, Y.; Saito, Y.; Mori, Y.; Onoda, M.; Iwado, A.; Motohashi, N.; Haginaka, J.; *Bull. Chem. Soc. Jpn* **1998**, *71*, 1825-1829.
- [94] (a) Bartels, O.; Wöhrle, D.; Caro, J.; Wark, M.; *Stud. Surf. Sci. Catal.* **2004**, *154*, 2884-2892.
- (b) Ribeiro, A.; Biazotto, J.; Serra, O.; *J. Non-Crystalline Solids* **2000**, *273*, 198-202.
- [95] Wark, M.; Ortlam, A.; Ganschow, M; Schulz-Ekloff, G.; Wöhrle, D.; *Ber. Bunsen-Ges. Phys.* **1998**, *102*, 1548-1553.
- [96] Wöhrle, D.; Suvorova, O.; Trombach, N.; Schupac, E.; Gerdes, R.; Semenov, N.; Bartels, O.; Zakurazhnov, A.; Schnurpfeil, G.; Hild, O.; Wendt, A.; *J. Porphyrins Phthalocyanines* **2001**, *5*, 381-389.
- [97] Armengol, E.; Corma, A.; Fornes, V.; Garcia, H.; Primo, J.; *App. Catal. A* **1999**, *181*, 305-312.

- [98] Ramos, R.; Peterson, P.; Johansen, P.; Lindvold, L.; Ramirez, M.; Blanco, E.; *J. Appl. Phys.* **1997**, *81*, 7728-7733.
- [99] Kimura, M.; Wada, K.; Iwashima, Y.; Ohta, K.; Hanabusa, K.; Shirai, H.; Kobayashi, N.; *Chem. Commun.* **2003**, 2504-2505.
- [100] Huc, V.; Saveyroux, M.; Bourgoïn, J.; Valin, F.; Zalczer, G.; Albouy, P.; Palacin, S.; *Langmuir* **2000**, *16*, 1770-1776.
- [101] Palomares, E.; Diaz, M.; A. Haque, S.; Torres, T. ; Durrant, J.; *Chem. Commun.* **2004**, DOI : 10.1039/b407860h.
- [102] Kadish, K. M.; Smith, K. M.; Guillard, R.; *The Porphyrin Handbook, Vol. 17 / Phthalocyanines: Properties and Materials*; Academic Press, Elsevier Science **2003**, San Diego, California, USA; and references therein.
- [103] Schneider, J.; Fanter, D.; Bauer, M.; Schomburg, C.; Wöhrle, D.; Schulz-Ekloff, G.; *Microporous Mesoporous Mater.* **2000**, *39*, 257-263.
- [104] Balkus, K. J., in Leznoff, C.; Lever, A.; *Phthalocyanines: Properties and Applications*, Volume 4, p. 287. VCH Publishers, New York, USA. **1989**.
- [105] Ganschow, M.; Wöhrle, D.; Schulz-Ekloff, G.; *J. Porphyrins Phthalocyanines* **1999**, *3*, 299-309.
- [106] Mizuguchi, J.; Rihs, J.; Karfunkel, H.; *J. Phys. Chem. B* **1995**, *99*, 16217-16227.
- [107] Namba, N.; *Phthalocyanine-Chemistry and Functions*; Shirai, Y.; Kobayashi, N.; Eds. IPC: Tokyo, **1997**, p 247.
- [108] Ottmar, M.; Hohnholz, D.; Wedel, A.; Hanack, M.; *Synth. Met.* **1999**, *105*, 145-149.
- [109] Tang, Ch.; Weidner, Ch.; Comfort, D. U.S. Patent 5409783 A 9504245, **1994**.
- [110] Spaeth, M.; Sooy, W.; *J. Phys. Chem.* **1968**, *48*, 2315-2323.
- [111] Vincett, P.; Voigt, E; Rieckhoff, K.; *J. Phys. Chem.* **1971**, *55*, 4131-4140.
- [112] Menzel, E. Roland; Popovic, Zoran D.; *Chem. Phys. Lett.* **1978**, *55*, 177-181.
- [113] Yoshino, K.; Hikida, M.; Tatsuno, K.; Kaneto, K.; Inuishi, Y.; *J. Phys. Soc. Jpn* **1973**, *34*, 441-445.
- [114] Aroca, R.; Jennings, C.; Loutfy, R.; Hor, Ah Mee.; *Mol. Biomol. Spec.* **1987**, *43(A)*, 725-730.
- [115] Huang, T. H.; Sharp, J. H.; *Chem. Phys.* **1982**, *65*, 205-206.
- [116] Yamaguchi, S.; Sasaki, Y.; *J. Phys. Chem. B* **1999**, *103*, 6835-6838.
- [117] Sakakibara, Y.; Bera, R.; Mizutani, T.; Ishida, K.; Tokumoto, M.; Tani, T.; *J. Phys. Chem. B* **2001**, *105*, 1547-1553.

- [118] Kameyama, K.; Morisu, M.; Sarake, A.; Kobuke, Y.; *Angew. Chem.*, **2005**, *117*, 4841-4844; *Angewandte Chemie, International Edition* **2005**, *44*, 4763-4766.
- [119] Sakaguchi, J.; Hasegawa, S.; Arai, S.; (Somar Corp., Japan). Eur. Pat. Appl. (1990), EP 369721 A2 19900523 Designated States R: BE, DE, FR, GB, IT, NL. Patent written in English. Application: EP 89-311744 19891114. Priority: JP 88-289624 19881115; JP 89-23249 19890201; JP 89-47571 19890228; JP 89-99196 19890419. CAN 114:33089 AN 1991:33089.
- [120] Watanabe, K.; Hayata, H.; (Konica Co., Japan). Jpn. Kokai Tokkyo Koho (2000), JKXXAF JP 2000155433 A2 20000606. Application: JP 98-330867 19981120. Priority: CAN 133:24668 AN 2000:377089.
- [121] Kim, T.; Jeong, C.; Kang, T.; (Korea Engineering Plastics Co., Ltd., S. Korea). PCT Int. Appl. (2004). Patent written in English. Application: WO 2003-KR2476 20031118. Priority: KR 7167-9 20021118. CAN 141:24537 AN 2004:453290.
- [122] Shimomura, M.; Tochihara, S.; Kubota, H.; Kimura, I.; (Canon Inc., Japan). Jpn. Kokai Tokkyo Koho (2002), JP 2002240321 A2 20020828. Application: JP 2001-42832 20010220. Priority: CAN 137:187167 AN 2002:654293
- [123] Terekhov, D. S.; Nolan, K. L. M.; MaArthur, C. R.; Lenzoff, C. C.; *J. Org. Chem.* **1996**, *61*, 3034-3040.
- [124] Keppeler, U.; Hanack, M.; *Chem. Ber.* **1986**, *119*, 3363-3381.
- [125] Iyechika, Y.; Yakushi, K.; Ikemoto, I.; Kuroda, H.; *Acta Crystallogr., Sect. B: Struct. Sci.* **1982**, *38*, 766-770.
- [126] Müller, A.; Jaegermann, W.; Enemark, J.; *Coord. Chem. Rev.* **1982**, *46*, 245-280.
- [127] (a) Barthel, M.; Dissertation at Tuebingen Universität, **2002**.  
(b) Kobayashi, N.; Muranaka, A.; Ishii, K.; *Inorg. Chem.*; **2000**, *39*, 2256-2257.
- [128] Collman, J.; Harford, S.; Franzen, S.; Eberspacher, T.; Shoemaker, R.; Woodruff, W.; *J. Am. Chem. Soc.* **1998**, *120*, 1456-1465.
- [129] Partha. B.; *J. Chem. Educ.* **2001**, *78*, 666-669.
- [130] Srivastava, T.; Fleischer, E.; *J. Am. Chem. Soc.* **1970**, *92*, 5518-5519.
- [131] Wöhrle, D.; Marose, U.; Knoop, R.; *Makromolekulare Chemie*; **1985**, *186*, 2209-2228.
- [132] Wöhrle, D.; Meyer, G.; Wahl, B.; *Makromolekulare Chemie*; **1980**, *181*, 2127-2133.
- [133] (a) Bannehr, R.; Jaeger, N.; Meyer, G.; Wöhrle, D.; *Makromolekulare Chemie* **1981**, *182*, 2633-2639.

- (b) Bannehr, R.; Meyer, D.; Wöhrle, D.; *Polym. Bull.* (Berlin) **1980**, *2*, 841.
- [134] Chen, Y.; SubRamanian, L. R.; Fujitsuka, M.; Ito, O. ; O'flaherty, S.; Blau, W. J.; Schneider, T.; Dini, D.; Hanack., M.; *Chem. Eur. J.* **2002**, *8*, 4248-4254.
- [135] Gundy, S. L.; Der Putten, V. W.; Shearer, A.; Ryder, A. G.; Ball, M.; *Physics in Medicine and Biology*, **2004**, *49*, 359-369.
- [136] Gan, Q.; Morlet-savary, S.; Wang, S.; Shen, S.; Xu, H. Yang, G; *Optics Express* **2005**, *13*: 5424-5434.
- [137] (a) Crackwell, R. F.; Gubbins, K. E.; Maddox, M.; Nicholson, D.; *Acc. Chem. Res.* **1995**, *28*, 281-284.
- (b) Thibault-Starzyk, F.; Parton, R. F.; Jacobs, P. A.; *Stud. Surf. Sci. Catal.* **1994**, *84*, 1419-1424.
- (c) Braun, I.; Schulz-Ekoloff, G.; Wöhrle, D.; *Zeolites* **1997**, *19*, 128-132.
- (d) Schomburg, C.; Wöhrle, D.; Schulz-Ekoloff, G.; *Zeolites* **1996**, *17*, 232-236.
- (e) Bockstette, M.; Wöhrle, D.; Braun, I.; Schulz-Ekoloff, G.; *Microporous Mesoporous Mater.* **1998**, *23*, 83-96.
- (f) Hoffmann, K.; Marlow, F.; Caro, J.; *Adv. Mater.* **1997**, *9*, 567-570.
- (g) Cox, S. D.; Gier, T. E.; Stucky, G. D.; Bierlein, J.; *J. Am. Chem. Soc.* **1988**, *110*, 2986-2987.
- (h) Caro, J.; Finger, G.; Kornatowski, J.; Richter-Mendau, J.; Werner, L.; Zibrowius, B.; *Adv. Mater.* **1992**, *4*, 273-276.
- (i) Ehrl, M.; deeg, F. w.; Braeuchle, C.; Franke, O.; Sobbi. A.; Schulz-Ekoloff, G.; Wöhrle, D.; *J. Phys. Chem.* **1994**, *98*, 47-52.
- (j) Ihlein, G.; Schueth, F.; Vietze, U.; Krauss, O.; Laeri, F.; *Adv. Mater.* (Weinheim, Germany) **1998**, *10*, 1117-1119.
- (k) O'Regan, B.; Graetzel, M.; *Nature* **1991**, *353*, 737-740.
- (l) Salafsky, J. S.; Lubberhuizen, W. H.; van Faassen, E.; Schropp, R. E. I.; *J. Phys. Chem. B.* **1998**, *102*, 766-769.
- (m) Hagfeldt, A.; Graetzel, M.; *Chem. Rev.* **1995**, *95*, 49-68.
- (n) Machida, S.; Horie, K.; Yamashita, T.; *Appl. Phys. Lett.* **1995**, *66*, 1240-1242.
- [138] Brieler, F. J.; Grundmann, P.; Fröba, M.; Chen, L.; Klar, P. J.; Heimbrod, W.; Krug von Nidda, H. A. ; Kurz, T. ; Loidl, A.; *J. Am. Chem. Soc.* **2004**, *126*, 797-807.



- [139] Chiker, F. Launay, F.; Nogier, J.; Bonardet, J.; *Green Chem.* **2003**, *5*, 318–322.
- [140] Ahn, W.; Lee, D.; Kim, T.; Kim, J.; Seo, G., Ryoo, R.; *Applied Catalysis A: General* **1999**, *181*, 39-40.
- [141] Rohfling, Y.; Wöhrle, D.; Wark, M.; Schulz-Ekloff, G.; Rathousky, J.; Zukal, A.; *Stud. Surf. Sci. Catal.* **2000**, *129*, 295-301.
- [142] Edwards, L. and Gouterman, M.; *J. Mol. Spec.* **1970**, *33*, 292-310.
- [143] Fox, Harold H.; Yap, Kimo B.; Robbins, J.; Cai, S.; and Schrock, R. *Inorg. Chem.* **1992**, *31*, 2287-2289.
- [144] Schrock, R.; DePue, R.; Feldman, J.; Yab, K.; Yang, D.; Davis, W.; Park, L.; DiMare, M.; Schofield, M.; Anhaus, J.; Walbrosky, E.; Evitt, E.; Krueger, C.; Betz, P.; *Organometallics* **1990**, *9*, 2262-2275.
- [145] Radius, U.; Sundermeyer, J.; Pritzkow, H.; *Chem. Ber.* **1994**, *127*, 1827-1835.
- [146] Radius, U.; Schorm, A.; Kairies, D.; Schmidt, S.; Moeller, F.; Pritzkow, H.; Sundermeyer, J.; *J. Organomet. Chem.* **2002**, *655*, 69-104.

-----